

University of Southampton Research Repository

Copyright © and Moral Rights for this thesis and, where applicable, any accompanying data are retained by the author and/or other copyright owners. A copy can be downloaded for personal non-commercial research or study, without prior permission or charge. This thesis and the accompanying data cannot be reproduced or quoted extensively from without first obtaining permission in writing from the copyright holder/s. The content of the thesis and accompanying research data (where applicable) must not be changed in any way or sold commercially in any format or medium without the formal permission of the copyright holder/s.

When referring to this thesis and any accompanying data, full bibliographic details must be given, e.g.

Thesis: Author (Year of Submission) "Full thesis title", University of Southampton, name of the University Faculty or School or Department, PhD Thesis, pagination.

Data: Author (Year) Title. URI [dataset]

University of Southampton

FACULTY OF MEDICINE

Clinical and Experimental Science

Studies on plasmid-based genetic tools for *C. muridarum*: progress towards a replicating vector
for transposon mutagenesis

by

Emma Claire Cousins

<https://orcid.org/0000-0002-6962-3797>

Thesis for the degree of Doctor of Philosophy

September 2022

University of Southampton

Abstract

Faculty of Medicine,
Clinical and Experimental Science

Doctor of Philosophy

Studies on plasmid-based genetic tools for *C. muridarum*: progress towards a replicating vector
for transposon mutagenesis

by

Emma Claire Cousins

Plasmid-based genetic tools for transposon (Tn)-mutagenesis using a 'suicide' vector approach to achieve genome saturation in *Chlamydia* are hindered by low transformation efficiencies. Progress toward achieving saturation was recently made with a self-replicating vector carrying an inducible Tn-system that facilitates Tn-transposition at the end of the developmental cycle, but this approach remains undeveloped in *C. muridarum*, and would require a stable replication-proficient vector to deliver the transposon-transposase cassette. No such vector has been identified. Identifying such a stably replicating vector in *C. muridarum* faces the additional challenge of a lower plasmid copy number (≤ 1) and a tendency for *in-vitro* plasmid loss even with positive selection using the available selectable markers.

The extent to which *in vitro* plasmid loss would inhibit the development of plasmid-based genetic tools in *C. muridarum* remained unknown due to the lack of a standardised, accurate method for measuring plasmid stability in *Chlamydia*. Development of a robust means for measuring plasmid stability was required to investigate the stability of available vectors and identify an appropriate vector backbone that is stable in *C. muridarum*. This was achieved by generating standard inocula for transformants, where every cell contained at least one plasmid, using bactericidal concentrations of chloramphenicol to kill plasmid-free cells. Both direct and indirect measures of plasmid loss were then applied in three generations of chlamydial elementary bodies passaged with and without selection.

The *E. coli*-*C. muridarum* shuttle vector pGFP::Nigg remained stable under bactericidal concentrations of chloramphenicol, which caused destabilisation of plasmid copy number when removed from the growth media. These results identified a potential mechanism for plasmid elimination, which is required in Tn-systems to reduce the likelihood of secondary transposition events. A minimal-gene vector derived from pGFP::Nigg with coding sequences *CDS5* and -6 deleted was stably maintained under penicillin selection at a higher plasmid copy number (~ 4), comparable to plasmid copy numbers reported for *C. trachomatis*.

The replication-proficient Tn-delivery vector in *C. muridarum*, pNiggHimar, was developed using pGFP::Nigg and a Tet-inducible *Himar1* Tn-system containing an erythromycin-resistance marker, and the wild type *Himar1* transposase. Inducible expression of transposase from pNiggHimar was demonstrated in *E. coli*. pNiggHimar could not be recovered in *C. muridarum* indicating weak repression of transposase expression by the Tet promoter in the "off"-state, also demonstrated with the Tet-inducible Tn-system in *C. trachomatis*. Transposition-negative constructs derived from pNiggHimar also failed to be recovered in *C. muridarum*. Together these findings suggest that a replicating Tn-system for *C. muridarum* will require a stable vector backbone with a higher plasmid copy number than pGFP::Nigg and tighter control over transposase expression.

Table of Contents

| | |
|--|--------------|
| Table of Contents | i |
| Table of Tables | vii |
| Table of Figures | ix |
| List of Accompanying Materials | xiii |
| Research Thesis: Declaration of Authorship | xxi |
| Acknowledgements | xxiii |
| Definitions and Abbreviations | xxv |
| Chapter 1 Introduction | 1 |
| 1.1 Introduction..... | 1 |
| 1.2 <i>Chlamydia</i> | 2 |
| 1.2.1 Biology | 2 |
| 1.2.2 Chlamydia-associated disease..... | 2 |
| 1.2.3 <i>Chlamydia muridarum</i> | 3 |
| 1.2.4 Mouse models of human genital tract infection..... | 4 |
| 1.3 <i>Chlamydia</i> genomics and known virulence factors..... | 6 |
| 1.4 Genetic tools for mutagenesis in <i>Chlamydia</i> ; uses and limitations | 8 |
| 1.4.1 Targeted mutagenesis in <i>Chlamydia</i> | 3 |
| 1.4.2 Genome-wide mutagenesis in <i>Chlamydia</i> : gene discovery | 7 |
| 1.5 Transposon mutagenesis in obligate intracellular bacteria..... | 9 |
| 1.5.1 Himar1/mariner transposons and their transposition..... | 10 |
| 1.5.2 Transposons as genetic tools in obligate intracellular bacteria..... | 12 |
| 1.6 Challenges for the genetic manipulation of <i>Chlamydia muridarum</i> | 15 |
| 1.6.1 Transformation with recombinant DNA..... | 15 |
| 1.6.2 Plasmid tropism..... | 17 |
| 1.6.3 In vitro plasmid loss in <i>C. muridarum</i> | 18 |
| 1.6.3.1 Plasmid maintenance in <i>Chlamydia</i> | 18 |
| 1.6.3.2 Plasmid loss on growth and development | 20 |
| 1.6.3.3 Assessment of <i>in vitro</i> plasmid loss..... | 21 |
| 1.6.3.4 Determinants of plasmid instability in <i>C. muridarum</i> | 23 |

Table of Contents

| | | |
|------------------|---|-----------|
| 1.7 | Summary and research aims..... | 24 |
| Chapter 2 | Methods..... | 27 |
| 2.1 | Bacterial strains and cell lines..... | 27 |
| 2.2 | Tissue culture..... | 28 |
| 2.3 | Microscopy..... | 29 |
| 2.4 | <i>Chlamydia</i> cell culture..... | 29 |
| 2.4.1 | Infection of tissue culture cells..... | 29 |
| 2.4.2 | Harvest of mature elementary bodies..... | 30 |
| 2.5 | Titration by X-gal staining..... | 30 |
| 2.6 | Quantifying infection efficiency..... | 31 |
| 2.6.1 | Estimating MOI using proportion of infected cells..... | 31 |
| 2.6.2 | Quantifying MOI using titres..... | 32 |
| 2.7 | <i>E. coli</i> cell culture..... | 32 |
| 2.7.1 | Luria broth-agar plate preparation..... | 32 |
| 2.7.2 | Liquid culture..... | 33 |
| 2.8 | Preparation of competent <i>E. coli</i> cells..... | 33 |
| 2.9 | Transformation..... | 33 |
| 2.9.1 | Transformation of <i>C. muridarum</i> with calcium chloride..... | 33 |
| 2.9.2 | Transformation of <i>E. coli</i> by heat shock..... | 34 |
| 2.10 | DNA extraction..... | 34 |
| 2.10.1 | Plasmid DNA..... | 34 |
| 2.10.2 | Genomic DNA..... | 35 |
| 2.11 | Quantification of DNA concentration..... | 35 |
| 2.12 | Polymerase chain reaction..... | 35 |
| 2.13 | Gel electrophoresis..... | 36 |
| 2.14 | Plasmids..... | 37 |
| 2.15 | Statistical tests..... | 37 |
| Chapter 3 | Determination of plasmid segregational stability in <i>C. muridarum</i>..... | 39 |
| 3.1 | Introduction..... | 39 |
| 3.2 | Methods..... | 42 |

| | | |
|---|--|-----------|
| 3.2.1 | Quantitative susceptibility testing in <i>C. muridarum</i> | 42 |
| 3.2.2 | Quantitative PCR | 42 |
| 3.2.3 | Preparing DNA standards for qPCR | 45 |
| 3.2.4 | Standard curve calculations for qPCR | 45 |
| 3.3 | Results | 46 |
| 3.3.1 | Characterising in vitro plasmid loss in wild type <i>C. muridarum</i> strain Nigg | 46 |
| 3.3.2 | Optimisation of real-time qPCR assays for quantifying plasmid copy number in <i>C. muridarum</i> | 49 |
| 3.3.3 | Generating standardised inocula for <i>C. muridarum</i> transformants | 53 |
| 3.3.4 | Determination of plasmid stability in Nigg P-/pGFP::Nigg..... | 57 |
| 3.4 | Discussion | 60 |
| 3.4.1 | Characterising in vitro plasmid loss in wild type <i>C. muridarum</i> | 60 |
| 3.4.2 | Optimisation of real-time qPCR assays for determination of plasmid copy number in <i>C. muridarum</i> | 60 |
| 3.4.3 | Generating standardised inocula for <i>C. muridarum</i> transformants | 61 |
| 3.4.4 | Stability of plasmid pGFP::Nigg in <i>C. muridarum</i> | 63 |
| 3.5 | Conclusions..... | 64 |
| Chapter 4 Investigating stability of plasmids to identify suitable candidates for a replication-proficient transposon-delivery vector in <i>C. muridarum</i> | | 65 |
| 4.1 | Introduction..... | 65 |
| 4.2 | Methods | 66 |
| 4.2.1 | Study design | 66 |
| 4.2.2 | Measuring plasmid segregational stability | 68 |
| 4.2.3 | Quantification of inclusion phenotypes from cell culture images..... | 68 |
| 4.2.4 | Plasmids..... | 69 |
| 4.2.4.1 | Plasmid pGFP::Nigg | 70 |
| 4.2.4.2 | Plasmid pSW2NiggCDS2 | 71 |
| 4.3 | Results | 72 |
| 4.3.1 | Generating standardised inocula of <i>C. muridarum</i> transformants..... | 72 |
| 4.3.1.1 | Plasmid copy number measured in standard inocula..... | 73 |
| 4.3.1.2 | Plasmid loss frequency measured in standard inocula..... | 74 |

Table of Contents

| | | |
|---|---|-----------|
| 4.3.2 | Stability of <i>E. coli</i> - <i>C. muridarum</i> shuttle vectors in <i>C. muridarum</i> | 77 |
| 4.3.2.1 | Changes in plasmid copy number over serial passage | 77 |
| 4.3.2.2 | Plasmid loss frequency over serial passage | 78 |
| 4.4 | Discussion..... | 85 |
| 4.4.1 | Measuring plasmid stability in <i>Chlamydia</i> | 85 |
| 4.4.2 | Generating standard inocula for <i>C. muridarum</i> transformants | 86 |
| 4.4.3 | Plasmid stability in <i>C. muridarum</i> | 87 |
| 4.5 | Conclusions | 89 |
| Chapter 5 Progress towards inducible transposon mutagenesis in <i>C. muridarum</i> | | 91 |
| 5.1 | Introduction | 91 |
| 5.2 | Methods..... | 92 |
| 5.2.1 | Quantitative susceptibility testing..... | 92 |
| 5.2.1.1 | Determination of MIC of erythromycin in <i>C. muridarum</i> | 92 |
| 5.2.1.2 | Determination of MIC to erythromycin in <i>E. coli</i> | 92 |
| 5.2.2 | Construction of an inducible, self-replicating transposon delivery vector for <i>C. muridarum</i> | 93 |
| 5.2.2.1 | Cloning strategy for the construction of pNiggHimar..... | 93 |
| 5.2.2.2 | Vector DNA preparation | 95 |
| 5.2.2.3 | Insert DNA preparation..... | 95 |
| 5.2.2.4 | DNA Ligation | 95 |
| 5.2.2.5 | Plasmid map of pRPF215 | 96 |
| 5.2.3 | Construction of transposition negative control plasmids | 98 |
| 5.2.3.1 | Cloning strategies for the construction of pNiggHimar_GFP_ΔTpase and pNiggHimar_mCh_ΔTn..... | 98 |
| 5.2.3.2 | Restriction enzyme cloning methods..... | 101 |
| 5.2.4 | Restriction endonucleases..... | 101 |
| 5.2.5 | Primers for cloning using end-point PCR | 103 |
| 5.2.6 | Immunodetection of wild type Himar1 transposase by Western blot..... | 105 |
| 5.2.6.1 | Growth curves..... | 105 |
| 5.2.6.2 | Sample preparation | 105 |

| | | |
|---------------------------|---|------------|
| 5.2.6.3 | SDS-PAGE..... | 106 |
| 5.2.6.4 | Western blot..... | 107 |
| 5.3 | Results | 108 |
| 5.3.1 | Attempts to recover ermB-resistant transposon mutants in <i>C. muridarum</i> . | 108 |
| 5.3.2 | Generating a replication-proficient transposon -delivery vector for <i>C. muridarum</i> | 114 |
| 5.3.2.1 | Phenotypic and genotypic confirmation of the <i>Himar1</i> transposon in construct pNiggHimar | 115 |
| 5.3.3 | Transformation of <i>C. muridarum</i> with a replication-proficient transposon delivery vector | 121 |
| 5.3.4 | Generating transposition-negative constructs | 123 |
| 5.3.4.1 | Genotypic confirmation of constructs pNiggHimar_GFP_ΔT _{pase} and pNiggHimar_mCh_ΔT _n | 126 |
| 5.3.5 | Inducible expression of wild type Himar1 transposase from transposon delivery vectors in <i>E. coli</i> | 129 |
| 5.3.6 | Transformation of <i>C. muridarum</i> with transposition-negative vectors..... | 135 |
| 5.4 | Discussion | 138 |
| 5.5 | Conclusions..... | 142 |
| Chapter 6 | Final discussion | 145 |
| 6.1 | Further Work..... | 149 |
| Appendix A | qPCR data | 151 |
| A.1 | Standard curves..... | 151 |
| Appendix B | Project amendment and approval | 155 |
| B.1 | Project amendment..... | 155 |
| B.2 | Confirmation of approval for amendment..... | 159 |
| List of References | | 161 |

Table of Tables

| | | |
|----------|---|-----|
| Table 1 | Vectors and their applications in the genetic manipulation of <i>C. muridarum</i> | 1 |
| Table 2 | Bacteria used in this study | 28 |
| Table 3 | Thermo-cycling conditions for end-point PCR..... | 36 |
| Table 4 | Plasmids used in this study for the genetic manipulation of <i>C. muridarum</i> | 37 |
| Table 5 | Primer and probe sequences for qPCR..... | 44 |
| Table 6 | Percentage of plasmid-free “bull’s-eye” inclusions in cell culture of wild type plasmid-bearing <i>C. muridarum</i> strain Nigg P+. | 48 |
| Table 7 | Ligation reaction with controls used for cloning experiments..... | 96 |
| Table 8 | Restriction enzymes used for cloning experiments | 102 |
| Table 9 | Primers for cloning of constructs, colony screening and sequencing | 104 |
| Table 10 | Separating gel and stacking gel recipe | 106 |
| Table 11 | Treatment regimen used for the transformation of <i>C. muridarum</i> Nigg P- with suicide transposon delivery vector pRPF215..... | 112 |

Table of Figures

| | | |
|------------|--|----|
| Figure 1-1 | Phylogeny of <i>Chlamydiaceae</i> species..... | 7 |
| Figure 1-2 | Milestones in the molecular toolkit developed for <i>C. trachomatis</i> and <i>C. muridarum</i> | 2 |
| Figure 1-3 | Transposon transposition by the 'cut and paste' mechanism mediated by <i>Himar1</i> transposase molecules. | 12 |
| Figure 1-4 | Transposons engineered as genetic tools for transposon mutagenesis of obligate intracellular bacterial pathogens. | 14 |
| Figure 1-5 | Photomicrograph of McCoy cells infected with wild type <i>C. muridarum</i> strain Nigg P+. | 22 |
| Figure 3-1 | Photomicrograph of McCoy cells infected with wild type <i>C. muridarum</i> strain Nigg P+. | 49 |
| Figure 3-2 | Standard curve plasmid DNA preparations for chromosome and plasmid real time qPCR assays. | 50 |
| Figure 3-3 | Real-time qPCR analysis of <i>C. muridarum</i> DNA standards..... | 52 |
| Figure 3-4 | Effect of serial passage on plasmid copy number in wild type <i>C. muridarum</i> strain Nigg P+..... | 53 |
| Figure 3-5 | Quantitative susceptibility testing in plasmid bearing and plasmid-cured wild type <i>C.</i> <i>muridarum</i> strain Nigg to determine the minimum inhibitory concentration of chloramphenicol..... | 55 |
| Figure 3-6 | Photomicrographs of plasmid pGFP::Nigg transformed into plasmid cured <i>C.</i> <i>muridarum</i> strain Nigg (Nigg P-) grown with and without selection with chloramphenicol at bactericidal concentrations..... | 56 |
| Figure 3-7 | Photomicrographs of Nigg P- transformed with pGFP::Nigg serially passaged three times in chloramphenicol selection..... | 57 |
| Figure 3-8 | Effect of chloramphenicol on inclusion morphology in <i>C. muridarum</i> transformant Nigg P-/pGFP::Nigg..... | 58 |

Table of Figures

| | | |
|-------------|--|-----|
| Figure 3-9 | Effect of removal of bactericidal concentrations of chloramphenicol on plasmid copy number in <i>C. muridarum</i> strain Nigg P- transformed with <i>E. coli</i> - <i>C. muridarum</i> shuttle vector pGFP::Nigg. | 59 |
| Figure 4-1 | Schematic of plasmid stability assay for <i>C. muridarum</i> strains. | 67 |
| Figure 4-2 | Plasmid map of <i>E. coli</i> - <i>C. muridarum</i> shuttle vector pGFP::Nigg..... | 70 |
| Figure 4-3 | Plasmid map of recombinant plasmid pSW2NiggCDS2 | 71 |
| Figure 4-4 | Expansion of <i>C. muridarum</i> transformants under selection with chloramphenicol. | 73 |
| Figure 4-5 | Plasmid copy number for <i>C. muridarum</i> plasmids grown under chloramphenicol | 74 |
| Figure 4-6 | Photomicrograph of plasmid-free inclusions indicating <i>in vitro</i> plasmid loss of plasmid pSW2NiggCDS2 in <i>C. muridarum</i> | 75 |
| Figure 4-7 | Effect of chloramphenicol on the proportion of plasmid-free inclusions determined for strains of <i>C. muridarum</i> | 76 |
| Figure 4-8 | Effect of changing or removing antibiotic selection on plasmid copy number in <i>C. muridarum</i> transformants. | 78 |
| Figure 4-9 | Effect of penicillin selection on plasmid-loss frequency measured <i>in vitro</i> for <i>C. muridarum</i> transformed with plasmids containing non-essential gene-deletions. | 80 |
| Figure 4-10 | Plasmid loss frequency determined for <i>C. muridarum</i> transformants over serial passage without antibiotic selection. | 82 |
| Figure 4-11 | Scatter plot showing the relationship between plasmid copy number and the frequency of plasmid-loss in <i>C. muridarum</i> | 84 |
| Figure 5-1 | Cloning strategy for the construction of replication proficient <i>E. coli</i> - <i>C. muridarum</i> transposon delivery vector pNiggHimar | 94 |
| Figure 5-2 | Plasmid map of the <i>Himar1</i> transposon in pRPF215 codon optimised for <i>Clostridium difficile</i> | 97 |
| Figure 5-3 | Cloning strategy for the construction of <i>E.coli</i> - <i>C. muridarum</i> transposon shuttle vector pNiggHimar_GFP_ΔT _{pase} | 98 |
| Figure 5-4 | Cloning strategy for the construction of <i>E.coli</i> - <i>C. muridarum</i> transposase shuttle vector pNiggHimar_mCh_ΔT _n | 100 |

| | | |
|-------------|--|-----|
| Figure 5-5 | Quantitative susceptibility testing to determine the minimum inhibitory concentration of erythromycin in <i>C. muridarum</i> Nigg | 109 |
| Figure 5-6 | Inhibition of bacterial growth for <i>E. coli</i> Q358 and GM2163 in erythromycin..... | 111 |
| Figure 5-7 | Transformation and recovery of plasmid pRPF215 in <i>C. muridarum</i> strain Nigg P-113 | |
| Figure 5-8 | Optimisation of primers to amplify the <i>Himar1</i> transposon under Tet promoter control from plasmid pRPF215..... | 115 |
| Figure 5-9 | Confirmation of the <i>gfp</i> expression from colonies selected for screening of the <i>ermB</i> -transposon..... | 116 |
| Figure 5-10 | Colony screen to confirm the presence of the <i>ermB</i> -transposon insert..... | 117 |
| Figure 5-11 | Stu1 digest of colonies that express <i>gfp</i> to confirm presence and orientation of the transposon insert in pNiggHimar | 118 |
| Figure 5-12 | Erythromycin resistance in colonies screened for presence of the <i>Himar1</i> transposon insert..... | 119 |
| Figure 5-13 | Stu1 restriction digest of pNiggHimar, colony 22. | 120 |
| Figure 5-14 | The annotated sequence of construct pNiggHimar | 121 |
| Figure 5-15 | Transformation attempts with <i>E. coli</i> - <i>C. muridarum</i> transposon delivery vector pNiggHimar..... | 122 |
| Figure 5-16 | Optimisation of primers to delete the <i>Himar1</i> ITR and <i>ermB</i> gene and primers to delete the catalytic domain of <i>Himar1</i> transposase from pNiggHimar | 124 |
| Figure 5-17 | Optimisation of primers to amplify the backbone of p2TK2 _{spec} -Nigg-mChGro(L2) adding Pfo1 sites | 125 |
| Figure 5-18 | Confirmation of plasmid size by restriction enzyme digest of transposon and transposase <i>E. coli</i> - <i>C. muridarum</i> shuttle vectors..... | 126 |
| Figure 5-19 | The annotated sequence of construct pNiggHimar_GFP_ΔT _{pase} and intermediate construct pNiggHimar_GFP_ΔT _n | 128 |
| Figure 5-20 | Sequence analysis of construct pNiggHimar_mCh_ΔT _n | 129 |
| Figure 5-21 | Growth curves of <i>E. coli</i> - <i>C. muridarum</i> transposon delivery vectors in <i>E. coli</i> Q358 after induction with ATc..... | 131 |

Table of Figures

| | | |
|-------------|---|-----|
| Figure 5-22 | Effect of ATc induction on total protein concentration in <i>E. coli</i> transformed with <i>E. coli-C. muridarum</i> transposon delivery vectors | 132 |
| Figure 5-23 | Western blot of GFP expression from <i>E. coli-C. muridarum</i> transposon delivery vectors in <i>E. coli</i> | 133 |
| Figure 5-24 | Western blot of wildtype <i>Himar1</i> transposase expression from <i>E. coli-C. muridarum</i> transposon delivery vectors in <i>E. coli</i> | 134 |
| Figure 5-25 | Transformation attempts with <i>E. coli-C. muridarum</i> transposition-negative vectors pNiggHimar_GFP_ΔTn and pNiggHimar_GFP_ΔTpase | 136 |
| Figure 5-26 | Transformation attempts with <i>E. coli-C. muridarum</i> transposition-negative vector pNiggHimar_mCh_ΔTn..... | 137 |
| Figure A-1 | Amplification plot and standard curve generated for qPCR to quantify copies of plasmids (<i>CDS2</i>) and chromosomes (<i>omcB</i>) in <i>C. muridarum</i> Nigg P+ | 151 |
| Figure A-2 | Amplification plot and standard curve generated for qPCR to quantify copies of plasmids (<i>CDS2</i>) and chromosomes (<i>omcB</i>) in Nigg P-/pGFP::Nigg..... | 152 |
| Figure A-3 | Amplification plot and standard curve generated for qPCR to quantify copies of plasmids (<i>CDS2</i>) and chromosomes (<i>omcB</i>) in Nigg P-/pGFP::Nigg..... | 153 |
| Figure A-4 | Amplification plot and standard curve generated for qPCR to quantify copies of plasmids (<i>CDS2</i>) and chromosomes (<i>omcB</i>) in Nigg P-/pSW2NiggCDS2, Nigg P-/pNiggCDS56Del and Nigg P-/pNiggCDS567Del | 154 |

List of Accompanying Materials

The data underpinning this thesis can be accessed through the following link:

<https://doi.org/10.5258/SOTON/D2425>

| | | |
|------------|--|----|
| Figure 1-1 | Phylogeny of <i>Chlamydiaceae</i> species..... | 7 |
| Figure 1-2 | Milestones in the molecular toolkit developed for <i>C. trachomatis</i> and <i>C. muridarum</i> | 2 |
| Figure 1-3 | Transposon transposition by the 'cut and paste' mechanism mediated by <i>Himar1</i> transposase molecules. | 12 |
| Figure 1-4 | Transposons engineered as genetic tools for transposon mutagenesis of obligate intracellular bacterial pathogens. | 14 |
| Figure 1-5 | Photomicrograph of McCoy cells infected with wild type <i>C. muridarum</i> strain Nigg P+. | 22 |
| Figure 3-1 | Photomicrograph of McCoy cells infected with wild type <i>C. muridarum</i> strain Nigg P+. | 49 |
| Figure 3-2 | Standard curve plasmid DNA preparations for chromosome and plasmid real time qPCR assays. | 50 |
| Figure 3-3 | Real-time qPCR analysis of <i>C. muridarum</i> DNA standards..... | 52 |
| Figure 3-4 | Effect of serial passage on plasmid copy number in wild type <i>C. muridarum</i> strain Nigg P+..... | 53 |
| Figure 3-5 | Quantitative susceptibility testing in plasmid bearing and plasmid-cured wild type <i>C.</i> <i>muridarum</i> strain Nigg to determine the minimum inhibitory concentration of chloramphenicol..... | 55 |
| Figure 3-6 | Photomicrographs of plasmid pGFP::Nigg transformed into plasmid cured <i>C.</i> <i>muridarum</i> strain Nigg (Nigg P-) grown with and without selection with chloramphenicol at bactericidal concentrations..... | 56 |
| Figure 3-7 | Photomicrographs of Nigg P- transformed with pGFP::Nigg serially passaged three times in chloramphenicol selection..... | 57 |

List of Accompanying Materials

| | | |
|-------------|--|----|
| Figure 3-8 | Effect of chloramphenicol on inclusion morphology in <i>C. muridarum</i> transformant Nigg P-/pGFP::Nigg..... | 58 |
| Figure 3-9 | Effect of removal of bactericidal concentrations of chloramphenicol on plasmid copy number in <i>C. muridarum</i> strain Nigg P- transformed with <i>E. coli</i> - <i>C. muridarum</i> shuttle vector pGFP::Nigg. | 59 |
| Figure 4-1 | Schematic of plasmid stability assay for <i>C. muridarum</i> strains. | 67 |
| Figure 4-2 | Plasmid map of <i>E. coli</i> - <i>C. muridarum</i> shuttle vector pGFP::Nigg..... | 70 |
| Figure 4-3 | Plasmid map of recombinant plasmid pSW2NiggCDS2 | 71 |
| Figure 4-4 | Expansion of <i>C. muridarum</i> transformants under selection with chloramphenicol. | 73 |
| Figure 4-5 | Plasmid copy number for <i>C. muridarum</i> plasmids grown under chloramphenicol | 74 |
| Figure 4-6 | Photomicrograph of plasmid-free inclusions indicating <i>in vitro</i> plasmid loss of plasmid pSW2NiggCDS2 in <i>C. muridarum</i> | 75 |
| Figure 4-7 | Effect of chloramphenicol on the proportion of plasmid-free inclusions determined for strains of <i>C. muridarum</i> | 76 |
| Figure 4-8 | Effect of changing or removing antibiotic selection on plasmid copy number in <i>C. muridarum</i> transformants. | 78 |
| Figure 4-9 | Effect of penicillin selection on plasmid-loss frequency measured <i>in vitro</i> for <i>C. muridarum</i> transformed with plasmids containing non-essential gene-deletions. | 80 |
| Figure 4-10 | Plasmid loss frequency determined for <i>C. muridarum</i> transformants over serial passage without antibiotic selection. | 82 |
| Figure 4-11 | Scatter plot showing the relationship between plasmid copy number and the frequency of plasmid-loss in <i>C. muridarum</i> | 84 |
| Figure 5-1 | Cloning strategy for the construction of replication proficient <i>E. coli</i> - <i>C. muridarum</i> transposon delivery vector pNiggHimar | 94 |
| Figure 5-2 | Plasmid map of the <i>Himar1</i> transposon in pRPF215 codon optimised for <i>Clostridium difficile</i> | 97 |
| Figure 5-3 | Cloning strategy for the construction of <i>E.coli</i> - <i>C. muridarum</i> transposon shuttle vector pNiggHimar_GFP_ΔTpase | 98 |

| | | |
|-------------|--|-----|
| Figure 5-4 | Cloning strategy for the construction of <i>E.coli-C. muridarum</i> transposase shuttle vector pNiggHimar_mCh_ΔTn..... | 100 |
| Figure 5-5 | Quantitative susceptibility testing to determine the minimum inhibitory concentration of erythromycin in <i>C. muridarum</i> Nigg | 109 |
| Figure 5-6 | Inhibition of bacterial growth for <i>E. coli</i> Q358 and GM2163 in erythromycin..... | 111 |
| Figure 5-7 | Transformation and recovery of plasmid pRPF215 in <i>C. muridarum</i> strain Nigg P-113 | |
| Figure 5-8 | Optimisation of primers to amplify the <i>Himar1</i> transposon under Tet promoter control from plasmid pRPF215..... | 115 |
| Figure 5-9 | Confirmation of the <i>gfp</i> expression from colonies selected for screening of the <i>ermB</i> -transposon..... | 116 |
| Figure 5-10 | Colony screen to confirm the presence of the <i>ermB</i> -transposon insert..... | 117 |
| Figure 5-11 | Stu1 digest of colonies that express <i>gfp</i> to confirm presence and orientation of the transposon insert in pNiggHimar | 118 |
| Figure 5-12 | Erythromycin resistance in colonies screened for presence of the <i>Himar1</i> transposon insert..... | 119 |
| Figure 5-13 | Stu1 restriction digest of pNiggHimar, colony 22. | 120 |
| Figure 5-14 | The annotated sequence of construct pNiggHimar | 121 |
| Figure 5-15 | Transformation attempts with <i>E. coli-C. muridarum</i> transposon delivery vector pNiggHimar..... | 122 |
| Figure 5-16 | Optimisation of primers to delete the <i>Himar1</i> ITR and <i>ermB</i> gene and primers to delete the catalytic domain of <i>Himar1</i> transposase from pNiggHimar | 124 |
| Figure 5-17 | Optimisation of primers to amplify the backbone of p2TK2 _{spec} -Nigg-mChGro(L2) adding Pfo1 sites | 125 |
| Figure 5-18 | Confirmation of plasmid size by restriction enzyme digest of transposon and transposase <i>E. coli-C. muridarum</i> shuttle vectors..... | 126 |
| Figure 5-19 | The annotated sequence of construct pNiggHimar_GFP_ΔTpase and intermediate construct pNiggHimar_GFP_ΔTn..... | 128 |
| Figure 5-20 | Sequence analysis of construct pNiggHimar_mCh_ΔTn | 129 |

List of Accompanying Materials

| | | |
|-------------|--|-----|
| Figure 5-21 | Growth curves of <i>E. coli</i> - <i>C. muridarum</i> transposon delivery vectors in <i>E. coli</i> Q358 after induction with ATc..... | 131 |
| Figure 5-22 | Effect of ATc induction on total protein concentration in <i>E. coli</i> transformed with <i>E. coli</i> - <i>C. muridarum</i> transposon delivery vectors | 132 |
| Figure 5-23 | Western blot of GFP expression from <i>E. coli</i> - <i>C. muridarum</i> transposon delivery vectors in <i>E. coli</i> | 133 |
| Figure 5-24 | Western blot of wildtype <i>Himar1</i> transposase expression from <i>E. coli</i> - <i>C. muridarum</i> transposon delivery vectors in <i>E. coli</i> | 134 |
| Figure 5-25 | Transformation attempts with <i>E. coli</i> - <i>C. muridarum</i> transposition-negative vectors pNiggHimar_GFP_ΔTn and pNiggHimar_GFP_ΔTpase | 136 |
| Figure 5-26 | Transformation attempts with <i>E. coli</i> - <i>C. muridarum</i> transposition-negative vector pNiggHimar_mCh_ΔTn..... | 137 |
| Figure 1-1 | Phylogeny of <i>Chlamydiaceae</i> species. | 7 |
| Figure 1-2 | Milestones in the molecular toolkit developed for <i>C. trachomatis</i> and <i>C. muridarum</i> | 2 |
| Figure 1-3 | Transposon transposition by the 'cut and paste' mechanism mediated by <i>Himar1</i> transposase molecules..... | 12 |
| Figure 1-4 | Transposons engineered as genetic tools for transposon mutagenesis of obligate intracellular bacterial pathogens. | 14 |
| Figure 1-5 | Photomicrograph of McCoy cells infected with wild type <i>C. muridarum</i> strain Nigg P+. | 22 |
| Figure 3-1 | Photomicrograph of McCoy cells infected with wild type <i>C. muridarum</i> strain Nigg P+. | 49 |
| Figure 3-2 | Standard curve plasmid DNA preparations for chromosome and plasmid real time qPCR assays..... | 50 |
| Figure 3-3 | Real-time qPCR analysis of <i>C. muridarum</i> DNA standards..... | 52 |
| Figure 3-4 | Effect of serial passage on plasmid copy number in wild type <i>C. muridarum</i> strain Nigg P+. | 53 |

| | | |
|-------------|---|----|
| Figure 3-5 | Quantitative susceptibility testing in plasmid bearing and plasmid-cured wild type <i>C. muridarum</i> strain Nigg to determine the minimum inhibitory concentration of chloramphenicol..... | 55 |
| Figure 3-6 | Photomicrographs of plasmid pGFP::Nigg transformed into plasmid cured <i>C. muridarum</i> strain Nigg (Nigg P-) grown with and without selection with chloramphenicol at bactericidal concentrations..... | 56 |
| Figure 3-7 | Photomicrographs of Nigg P- transformed with pGFP::Nigg serially passaged three times in chloramphenicol selection..... | 57 |
| Figure 3-8 | Effect of chloramphenicol on inclusion morphology in <i>C. muridarum</i> transformant Nigg P-/pGFP::Nigg..... | 58 |
| Figure 3-9 | Effect of removal of bactericidal concentrations of chloramphenicol on plasmid copy number in <i>C. muridarum</i> strain Nigg P- transformed with <i>E. coli</i> - <i>C. muridarum</i> shuttle vector pGFP::Nigg..... | 59 |
| Figure 4-1 | Schematic of plasmid stability assay for <i>C. muridarum</i> strains..... | 67 |
| Figure 4-2 | Plasmid map of <i>E. coli</i> - <i>C. muridarum</i> shuttle vector pGFP::Nigg..... | 70 |
| Figure 4-3 | Plasmid map of recombinant plasmid pSW2NiggCDS2..... | 71 |
| Figure 4-4 | Expansion of <i>C. muridarum</i> transformants under selection with chloramphenicol..... | 73 |
| Figure 4-5 | Plasmid copy number for <i>C. muridarum</i> plasmids grown under chloramphenicol..... | 74 |
| Figure 4-6 | Photomicrograph of plasmid-free inclusions indicating <i>in vitro</i> plasmid loss of plasmid pSW2NiggCDS2 in <i>C. muridarum</i> | 75 |
| Figure 4-7 | Effect of chloramphenicol on the proportion of plasmid-free inclusions determined for strains of <i>C. muridarum</i> | 76 |
| Figure 4-8 | Effect of changing or removing antibiotic selection on plasmid copy number in <i>C. muridarum</i> transformants..... | 78 |
| Figure 4-9 | Effect of penicillin selection on plasmid-loss frequency measured <i>in vitro</i> for <i>C. muridarum</i> transformed with plasmids containing non-essential gene-deletions..... | 80 |
| Figure 4-10 | Plasmid loss frequency determined for <i>C. muridarum</i> transformants over serial passage without antibiotic selection..... | 82 |

List of Accompanying Materials

| | | |
|-------------|---|-----|
| Figure 4-11 | Scatter plot showing the relationship between plasmid copy number and the frequency of plasmid-loss in <i>C. muridarum</i> | 84 |
| Figure 5-1 | Cloning strategy for the construction of replication proficient <i>E. coli</i> - <i>C. muridarum</i> transposon delivery vector pNiggHimar | 94 |
| Figure 5-2 | Plasmid map of the <i>Himar1</i> transposon in pRPF215 codon optimised for <i>Clostridium difficile</i> | 97 |
| Figure 5-3 | Cloning strategy for the construction of <i>E.coli</i> - <i>C. muridarum</i> transposon shuttle vector pNiggHimar_GFP_ΔT _{pase} | 98 |
| Figure 5-4 | Cloning strategy for the construction of <i>E.coli</i> - <i>C. muridarum</i> transposase shuttle vector pNiggHimar_mCh_ΔT _n | 100 |
| Figure 5-5 | Quantitative susceptibility testing to determine the minimum inhibitory concentration of erythromycin in <i>C. muridarum</i> Nigg..... | 109 |
| Figure 5-6 | Inhibition of bacterial growth for <i>E. coli</i> Q358 and GM2163 in erythromycin | 111 |
| Figure 5-7 | Transformation and recovery of plasmid pRPF215 in <i>C. muridarum</i> strain Nigg P-113 | |
| Figure 5-8 | Optimisation of primers to amplify the <i>Himar1</i> transposon under Tet promoter control from plasmid pRPF215 | 115 |
| Figure 5-9 | Confirmation of the <i>gfp</i> expression from colonies selected for screening of the <i>ermB</i> -transposon | 116 |
| Figure 5-10 | Colony screen to confirm the presence of the <i>ermB</i> -transposon insert | 117 |
| Figure 5-11 | Stu1 digest of colonies that express <i>gfp</i> to confirm presence and orientation of the transposon insert in pNiggHimar | 118 |
| Figure 5-12 | Erythromycin resistance in colonies screened for presence of the <i>Himar1</i> transposon insert | 119 |
| Figure 5-13 | Stu1 restriction digest of pNiggHimar, colony 22. | 120 |
| Figure 5-14 | The annotated sequence of construct pNiggHimar..... | 121 |
| Figure 5-15 | Transformation attempts with <i>E. coli</i> - <i>C. muridarum</i> transposon delivery vector pNiggHimar | 122 |
| Figure 5-16 | Optimisation of primers to delete the <i>Himar1</i> ITR and <i>ermB</i> gene and primers to delete the catalytic domain of <i>Himar1</i> transposase from pNiggHimar..... | 124 |

| | | |
|-------------|--|-----|
| Figure 5-17 | Optimisation of primers to amplify the backbone of p2TK2 _{spec} -Nigg-mChGro(L2) adding Pfo1 sites | 125 |
| Figure 5-18 | Confirmation of plasmid size by restriction enzyme digest of transposon and transposase <i>E. coli</i> - <i>C. muridarum</i> shuttle vectors..... | 126 |
| Figure 5-19 | The annotated sequence of construct pNiggHimar_GFP_ΔTpase and intermediate construct pNiggHimar_GFP_ΔTn..... | 128 |
| Figure 5-20 | Sequence analysis of construct pNiggHimar_mCh_ΔTn | 129 |
| Figure 5-21 | Growth curves of <i>E. coli</i> - <i>C. muridarum</i> transposon delivery vectors in <i>E. coli</i> Q358 after induction with ATc | 131 |
| Figure 5-22 | Effect of ATc induction on total protein concentration in <i>E. coli</i> transformed with <i>E. coli</i> - <i>C. muridarum</i> transposon delivery vectors | 132 |
| Figure 5-23 | Western blot of GFP expression from <i>E. coli</i> - <i>C. muridarum</i> transposon delivery vectors in <i>E. coli</i> | 133 |
| Figure 5-24 | Western blot of wildtype <i>Himar1</i> transposase expression from <i>E. coli</i> - <i>C. muridarum</i> transposon delivery vectors in <i>E. coli</i> | 134 |
| Figure 5-25 | Transformation attempts with <i>E. coli</i> - <i>C. muridarum</i> transposition-negative vectors pNiggHimar_GFP_ΔTn and pNiggHimar_GFP_ΔTpase..... | 136 |
| Figure 5-26 | Transformation attempts with <i>E. coli</i> - <i>C. muridarum</i> transposition-negative vector pNiggHimar_mCh_ΔTn | 137 |

Research Thesis: Declaration of Authorship

Print name: Emma Claire Cousins

Title of thesis: Studies on plasmid-based genetic tools for *C. muridarum*: progress towards a replicating vector for transposon mutagenesis

I declare that this thesis and the work presented in it are my own and has been generated by me as the result of my own original research.

I confirm that:

1. This work was done wholly or mainly while in candidature for a research degree at this University;
2. Where any part of this thesis has previously been submitted for a degree or any other qualification at this University or any other institution, this has been clearly stated;
3. Where I have consulted the published work of others, this is always clearly attributed;
4. Where I have quoted from the work of others, the source is always given. With the exception of such quotations, this thesis is entirely my own work;
5. I have acknowledged all main sources of help;
6. Where the thesis is based on work done by myself jointly with others, I have made clear exactly what was done by others and what I have contributed myself;
7. None of this work has been published before submission

Signature: Date:

Acknowledgements

I would like to sincerely thank my supervisors Professor Ian Clarke and Dr Colette O’neill and colleague Rachel Skilton for their commitment and support of my development as a scientist through a challenging project undertaken against the backdrop of a global pandemic and getting married. Taking on this project has been an extremely rewarding and unforgettable experience and I will take away the lessons I have learned from these incredibly dedicated and passionate scientists and hold onto them for as long as I work in science. In their own ways, they have all been an inspiration to me and I look forward to continuing research in the field.

I would also like to thank my friends and colleagues during my time spent at St George’s University of London, with special mention of Dr Tariq Sadiq, Dr Emma Harding-Esch, Dr Sebastian Fuller and Dr Achyuta Nori, who first inspired me to work in the field of sexual health research and who supported me to embark upon this journey.

To my caring and compassionate friends and colleagues at the University of Southampton, I thank for the time spent together discussing the meaning of life, the universe and everything and for their support through the more testing of times. With special mention of Emma Maytham, Dr Jay Lever and my fellow PHD students Mukhtar Ibrahim, Chloe Manning and Aiste Dijokaite for keeping things fun and whom I learned so much from both in and out of the lab.

Finally, to my loving husband and family who have always believed in me and kept me going. I couldn’t have done it without you all.

Definitions and Abbreviations

| | |
|--------|---|
| ATc | Anhydrotetracycline |
| APS | Ammonium Persulfate |
| BSA | Bovine Serum Albumin |
| CAT | Chloramphenicol acetyltransferase |
| CDS | Coding sequence |
| DMEM | Dulbecco's Modified Eagles Medium |
| DNA | Deoxyribonucleic Acid |
| EB | Elementary Bodies |
| ERM | Erythromycin |
| FCS | Foetal Calf Serum |
| FREAEM | Fluorescent Reported Allelic Exchange Mutagenesis |
| FLAEM | Floxed-Cassette Allelic Exchange Mutagenesis |
| GFP | Green Fluorescent Protein |
| HITS | High-throughput Insertion Tracking by deep Sequencing |
| HPI | Hours Post Infection |
| IS | Insertion Sequences |
| IFU | Infection Forming Units |
| IN-Seq | Insertion Sequencing |
| ITR | Inverted Terminal Repeat |
| LGV | Lymphogranuloma Venereum |
| LB | Luria Broth |
| MOI | Multiplicity of Infection |
| MOPs | 3-(N-Morpholino) propane sulfonic acid |

Definitions and Abbreviations

| | |
|-------------|--|
| ORF | Open Reading Frame |
| <i>omcB</i> | Outer Membrane Complex Protein B |
| OD | Optical Density |
| PBS | Phosphate Buffer Solution |
| PCN | Plasmid Copy Number |
| PCR | Polymerase Chain Reaction |
| PBS-t | 0.05 % Tween-20 in PBS |
| PGP | Plasmid Gene Protein |
| qPCR | Quantitative Polymerase Chain Reaction |
| RB | Reticulate Bodies |
| RSGFP | Red-Shifted Green Fluorescent Protein |
| SDS-Page | sodium dodecyl sulphate polyacrylamide gel electrophoresis |
| SPP | Species |
| SW2 | Sweden2 |
| TraDIS | Transposon Directed Insertion-site Sequencing |
| TE | Transposable Element |
| TEA | Trypsin Ethylenediaminetetraacetic acid |
| TEMED | Tetramethylethylenediamine |
| Tet | Tetracycline |
| TILLING | Targeted Induced Local Legions in Genomes |
| Tn | Transposon |
| Tn-Seq | Transposon Sequencing |
| Tpase | Transposase |
| Tris-HCL | Tris(hydroxymethyl)aminomethane hydrochloride |
| WGS | Whole Genome Sequencing |

Chapter 1 Introduction

1.1 Introduction

Chlamydia are obligate intracellular gram-negative bacterial pathogens, causing diseases of medical and veterinary significance worldwide for which there is no vaccine (Brunham and Rey-Ladino, 2005; Elwell et al., 2016). Many biological and technical challenges have limited the development of tools for the genetic manipulation of *Chlamydia* spp, which in turn has limited our understanding of *Chlamydia* biology and pathogenesis. The native mouse pathogen *Chlamydia muridarum* (*C. muridarum*) offers many advantages as a model organism for the study of chlamydial genetics. For example, *C. muridarum* strain Nigg is a well characterised available laboratory strain that poses a very low zoonotic risk with fewer restrictions to the use of antibiotics than for the primary human pathogen *C. trachomatis*. Furthermore, *C. muridarum* and *C. trachomatis* share the same overall gene content and order and *C. muridarum* infection of mice genital tracts provides a robust small animal model with which to study the human genital infection with *C. trachomatis* (Stephens et al., 1998). Despite the advantages for studying chlamydial genetics with *C. muridarum* infection models, there is a dearth of genetic tools relative to *C. trachomatis* for its' genetic manipulation.

Certain factors render *C. muridarum* less genetically tractable than *C. trachomatis*. Primarily, purification of infectious particles from host cells is required for transformation used routinely in *Chlamydia* and risks damaging the bacterial cells and is likely a contributing factor to the low transformation efficiency. In addition, plasmid replication is restricted to a host of the same genetic background, the so-called plasmid tropism barrier, which limits the universal use of plasmid-based genetic tools across different biovars, serovars and species of *Chlamydia*. Finally, *in vitro* plasmid loss in *C. muridarum*, which is observed microscopically in both the wild type plasmid-bearing strains and plasmid-cured strains transformed with currently available shuttle vectors grown in penicillin selection (Liu et al., 2014a; Song et al., 2014; Wang et al., 2014).

Plasmid-based genetic tools for transposon mutagenesis using a 'suicide' vector approach to achieve genome saturation in *Chlamydia* are hindered by low transformation efficiency. Progress toward achieving saturation was recently made with a self-replicating vector carrying an inducible transposon delivery system that facilitates transposon transposition at the end of the developmental cycle, but this approach remains undeveloped in *C. muridarum*, and would require a stable replication-proficient vector to deliver the transposon-transposase cassette. No such vector has been identified. Identifying such a stably replicating vector in *C. muridarum* faces the

Chapter 1

additional challenge of a lower plasmid copy number (≤ 1) and a tendency for *in-vitro* plasmid loss even with positive selection using the available selectable markers.

The overarching aim of this PhD is to generate a plasmid-based genetic tool for inducible transposon mutagenesis in *C. muridarum* to facilitate the identification of all essential genes for survival. This first chapter will discuss the current genetic toolkit for mutagenesis in *C. trachomatis* and *C. muridarum* and the need for new genetic tools in *C. muridarum* to investigate chlamydial gene function. It will also discuss the potential for inducible transposon mutagenesis to achieve this and the challenges for developing such capabilities in this species.

1.2 *Chlamydia*

1.2.1 *Biology*

All *Chlamydia* spp go through a complex developmental cycle changing between two distinct morphological forms recognised as the elementary body (EB) that initiates infection of host cells and the non-infectious reticulate body (RB) capable of replication. The infectious cycle is initiated when EBs attach to epithelial cells and are quickly internalised within a vacuole called an inclusion. Upon entry into the host cell, EBs initiate cell division through mitogenic signalling and begin to differentiate into RBs by binary fission at ~ 2 hours post infection (hpi) (Belland et al., 2003; Shaw et al., 2000). Movement of the inclusion is directed towards the Golgi region where it fuses with exocytic vesicles transporting the sphingolipids sphingomyelin and glucosylceramide (Fields and Hackstadt, 2002). Sphingomyelin is readily incorporated into the EB cell wall as early as 2 hpi (hpi) (Hackstadt et al., 1996) and used to evade apoptosis by the lysosomal pathway (Elwell 2016). Differentiation of EBs into RBs occurs ~ 6 hpi after which, the RBs replicate ~ 1000 fold within an expanding inclusion membrane. Differentiation of RBs back into EBs occurs at 24-36hpi in an asynchronous manner until EB release is brought about by either lysis of the eukaryotic host cell (Hybiske and Stephens, 2007) or cell extrusion (Zuck et al., 2016) to facilitate a subsequent round of infection.

1.2.2 *Chlamydia-associated disease*

Whilst the biology of chlamydial development is shared between all *Chlamydia* species, there is great diversity in disease severity and tissue tropism that separates them and consequently *Chlamydia* are responsible for causing many diseases in humans and animals. This diversity is exemplified in the human pathogen *Chlamydia trachomatis* (*C. trachomatis*), that is capable of infecting and replicating in mucosal epithelial cells to cause ocular and urogenital diseases as well as infecting lymphatic tissues to cause more systemic disease.

The strains of *C. trachomatis* have been grouped into two biovars distinguishable by their respective disease groups: trachoma, and lymphogranular venereum (LGV). Ocular infection with *C. trachomatis* serotypes A-C, causes the irreversible, but preventable, blinding disease trachoma (Harding-Esch et al., 2019). Whereas infection by *C. trachomatis* serotypes D-K and L1-L3 of the LGV biovar cause sexually transmitted diseases (van de Laar and Morr , 2007). Genital infection is predominantly asymptomatic and often goes untreated which can lead to serious complications to reproductive health in women such as pelvic inflammatory disease and tubule infertility (O'Connell and Ferone, 2016). Infection with LGV strains of *C. trachomatis* is often difficult to diagnose clinically in the early stages because of presenting symptoms that can be as innocuous as painless genital papules, but if allowed to progress, these more invasive strains can cause serious lymphadenopathies (Ceovic and Jerkovic Gulin, 2015).

The genital infection is asymptomatic in most cases and often goes undetected (Detels et al., 2011; Torrone et al., 2014). These untreated or recurrent infections are responsible for the majority of *Chlamydia*-associated morbidity (Vos et al., 2017). Access to antibiotic chemotherapy and nation-wide screening programmes to detect the asymptomatic genital infections in populations most at risk are only available in a few, typically high-economically developed, countries including the United Kingdom and the United States of America and some European countries. Furthermore, these measures have failed to reduce the incidence of *Chlamydia* genital infections (Low, 2007). There is, therefore, a need for new therapeutic targets and vaccine candidates for better prevention and treatment of *C. trachomatis* infection worldwide.

Mutagenesis approaches (e.g. use of shuttle vectors, chemical mutagenesis and transposon mutagenesis) offer a convenient means to characterise gene function in bacteria through direct genotype-phenotype associations and have been successfully deployed to identify new therapeutic targets in many different pathogenic species (Opperman et al., 2003). Mutant strains generated through these approaches are used to infect mice genital tracts *in vivo* which has led to the identification of several virulence genes.

1.2.3 *Chlamydia muridarum*

In the 1940's, the mouse adapted species of *Chlamydia* was first isolated from the lungs of mice after nasal inoculation with what was considered at the time to be the agent of clinical influenza in humans, where it caused pneumonitis (Nigg, 1942; Nigg and Eaton, 1944). The mouse agent of pneumonitis was originally designated a murine biovar of the human pathogen *Chlamydia trachomatis* (*C. trachomatis*) and called *Chlamydia trachomatis* mouse pneumonitis (MoPn) on account of its' *C. trachomatis*-like inclusion morphology and similar developmental cycle. The MoPn strain also demonstrated the ability to accumulate glycogen and sensitivity to the chemical

sulfadiazine that was characteristic of *C. trachomatis* strains isolated at the time (Barron et al., 1981; Everett et al., 1999; Skerman et al., 1980). Everett et al (1999) later re-classified MoPn as a distinct species named *Chlamydia muridarum* (*C. muridarum*) on account of genetic differences between the 16s rRNA and 23s rRNA sequences. DNA-sequence analysis has shown that the closely related human pathogen *C. trachomatis* and the mouse pathogen *C. muridarum* share the much the same overall gene order and content with ~890 open reading frames, and both species contain an extrachromosomal plasmid ~ 7,500 nucleotide base pairs in length (Read et al., 2000). As a closely related species, *C. muridarum* provides a useful model organism for investigating gene function in pathogenesis and immune response in a small animal model that can be translated to the human infection with *C. trachomatis*.

1.2.4 Mouse models of human genital tract infection

The mouse genital tract is susceptible to infection with both *C. muridarum* and *C. trachomatis* making *C. muridarum* a suitable model organism for the study of chlamydial genes and their role in human genital disease.

The development of a robust transformation system for *Chlamydia* using shuttle vectors a decade ago has enabled progress toward understanding gene functions in *Chlamydia* (Wang et al., 2011). Of particular significance is the generation of loss-of-function strains of *C. trachomatis* by mutagenesis approaches, which can be analysed both *in vitro* and *in vivo*. Molecular tools for generating loss-of-function mutant strains in *C. muridarum* lag far behind those available in *C. trachomatis*, yet there are several advantages to the use of the *C. muridarum* infection model over the use of *C. trachomatis* infection model in mice.

The principle advantage of using a *C. muridarum* infection model over a *C. trachomatis* infection model is that the mouse-native pathogen in mice better represents *C. trachomatis* infection in humans (Morré et al., 2000).

Intravaginal inoculation of mice genital tracts with *C. muridarum* was first described in 1981 (Barron et al., 1981). Intravaginal inoculation with *C. muridarum* leads to ascending infection into the upper genital tract (UGT) which can cause severe inflammatory pathologies of the mouse uterine horns and oviducts, where scarring of the fallopian tubes and oviducts causes a condition called hydrosalpinx (Liu et al., 2014b; Yu et al., 2019).

The equivalent inflammatory pathology in humans is called salpingitis. In humans, *C. trachomatis* will naturally ascend to the UGT, but studies using intravaginal inoculation in mice show that *C. trachomatis* is readily cleared in the mouse genital tract and often fails to naturally ascend and

induce the inflammatory symptoms comparable to the human infection (Gondek et al., 2012). *C. muridarum* infections of mice genital tracts are characterized by a more virulent and fast growing infection with greater bacterial loads than *C. trachomatis* infection of mice genital tracts (Williams et al., 1981), which could explain why intravaginal inoculation with *C. trachomatis* does not induce upper genital tract pathology so readily.

Alternative *C. trachomatis* infection models have been developed to induce the UGT pathology to more closely mimic the UGT pathology characteristic of human infection. These include using an innate-immune deficient mouse strain C3H/HeJ, which permits ascending infection resulting in the characteristic upper genital tract pathology after intravaginal inoculation of an L2 434/BU *C. trachomatis* strain (Sturdevant et al., 2010). Another *C. trachomatis* infection model uses transcervical inoculation which serves to circumvent the ascending infection (Gondek et al., 2012). These developments have enabled the ability to induce UGT inflammatory conditions in mice which has in turn facilitated discovery of virulence genes. For example, Sturdevant et al (2010) demonstrated that a late- clearance phenotype of increased virulence was linked to mutations in a single gene, *CT135* that encodes a putative inclusion membrane (Inc) protein using *C. trachomatis* to inoculate the cervix of C3H/HeJ mice. A separate study using transcervical inoculation enabled development of an immune-response model achieved through characterising the induction of antigen specific memory CD4⁺ T cells, demonstrating that they are essential for protection against re-infection (Gondek et al., 2012). With this immune-response model, Yang et al later demonstrated that *pgp3*, the secreted protein product of plasmid-encoded gene *CDS5*, was an essential protein for inducing UGT pathology in *C. trachomatis* infection of murine cells through a novel mechanism shown to inhibit the action of antimicrobial peptides used as part of the innate host defence to *Chlamydia* infection (Yang et al., 2020).

A number of pathogen and host genetic differences that elicit different host-pathogen interactions in mice and humans make it difficult to extend the findings from the use of infection model to the human infection (Abdelsamed et al., 2013; Morr e et al., 2000). This is exemplified by differences in the immune response to *Chlamydia* infection in mice and humans, which is indicated by differences in duration of infection, protection to re-infection and persistent infection. *C. muridarum* is cleared in ~4 weeks without antibiotic treatment, whereas *C. trachomatis* can survive in a persistent state for many months with sub-clinical inflammatory pathology in humans (Parks et al., 1997).

With these improved murine infection models, the field can begin to correlate findings between *C. muridarum* and *C. trachomatis* infection models in mice important for establishing mechanisms of pathogenesis at the molecular level to identify and test new vaccine candidates and therapeutics.

This highlights the importance of developing tools for the genetic manipulation of *C. muridarum* to produce mutant strains that can be tested in different experimental conditions both *in vitro* and *in vivo* that will be critical for better understanding host-tropisms to translate the murine investigations to the human infection.

1.3 *Chlamydia* genomics and known virulence factors

Stephens et al., (1998) first sequenced a genital *C. trachomatis* strain and identified a reduced genome of ~1 mega bases (Mb), which includes a ~7.5kb plasmid, adapted to intracellular survival with the loss of several bacterial genes no longer deemed essential. Comparative genomic analysis of genome sequences representing all *Chlamydia* show a ~40% guanine (G) + cytosine (C) content (Collingro et al., 2011). Over one hundred *C. trachomatis* genomes have been sequenced showing <2% nucleotide (nt) sequence variation which represents ~ 10 kilo bases (kb) in nt sequence variability (Harris et al., 2012; Jeffrey et al., 2010; Seth-Smith et al., 2013). The phylogenetic tree indicates that *C. muridarum* and *C. suis* are most closely related to *C. trachomatis* out of the eleven *Chlamydia* species represented on this tree (Figure 1-1). Given that *Chlamydia* share a high degree of sequence homology and genetic synteny yet are responsible for large differences in disease severity and tissue tropisms, it is not surprising that the regions of highest variability (as well as host-genetics) have been the focus of much genetic research which has successfully identified a, so far modest, number of chlamydial proteins important for pathogenesis.

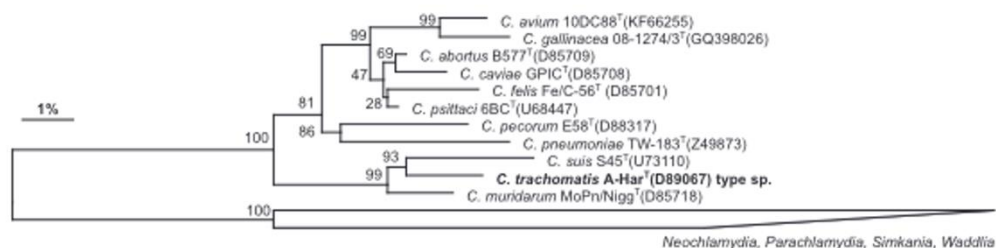


Figure 1-1 Phylogeny of *Chlamydiaceae* species.

Phylogenetic tree based on almost complete 16s rRNA genes from type strains of established *Chlamydiaceae* spp., Construction of the tree was based on the RAxML algorithm without any filter removing hypervariable positions. Bootstrap values indicate the stability of the branches based on 100 replicates. Reprinted from Systematic and Applied Microbiology, Volume 38, Issue 2, Pages 99-103, Konrad Sachse, Patrik M. Bavoil, Bernhard Kaltenboeck, Richard S. Stephens, Cho-Chou Kuo, Ramon Rosselló-Móra, Matthias Horn, Emendation of the family *Chlamydiaceae*: Proposal of a single genus, Chlamydia, to include all currently recognized species, page no. 101, Copyright (2015), with permission from Elsevier. Licence can be found via the following link <https://s100.copyright.com/CustomerAdmin/PLF.jsp?ref=f9022d00-4811-4068-82a5-63c61ea6b4b9>.

Whole genome sequencing facilitated the assignment of putative functions for 68% ORFs through *in silico* similarity searching of existing databases of bacterial genomes (Stephens et al., 1998). Of the remaining 32% ORFs, only 4% of *C. trachomatis* ORFs showed homology to hypothetical proteins in other bacteria. The predicted essential gene content of *C. trachomatis* was broadly consistent with other minimal bacterial genomes and includes homologues for tryptophan synthesis, ATP-transport, glycogen metabolism and catabolism, aerobic respiration, and genes for DNA repair, synthesis and replication (Stephens et al., 1998).

Comparative genomics has also identified several genes that encode important *Chlamydia*-specific proteins, some of those identified include the putative inclusion membrane proteins (Incs), the major outer-membrane protein (MOMP) and the chlamydial cytotoxin (Seth-Smith et al., 2009).

The inclusion membrane proteins (Incs) are important because their exposure to the host cell cytosol makes them targets for host-pathogen interactions and are therefore potential virulence determinants. Though, very few of the >50 predicted Incs in *C. trachomatis* have been functionally characterised. The Incs so far characterised as virulence determinants include the IncD-G operon which encodes a type III secretion system (T3SS) responsible for transport of effector proteins into the host cytosol (Scidmore-Carlson et al., 1999; Shaw et al., 2002), IncA responsible for homotypic

Chapter 1

fusion of intracellular inclusions (Fields et al., 2005), IncG responsible for the indirect inhibition of apoptosis (Scidmore and Hackstadt, 2001) and IncD responsible for mediating sphingolipid transport required for evading lysosomal degradation. Similarly, MOMP (encoded by the *ompA* gene) is expressed on the surface of chlamydial cells. It is also the most abundant outer membrane protein expressed in EBs. MOMP contains four variable regions (VRI-VRIV) distributed between five conserved regions. These surface-exposed variable regions of MOMP show high sensitivity for predicting the *C. trachomatis* disease biovars, however, the variation in MOMP does not associate with disease severity (Geisler et al., 2003). Nevertheless, MOMP is a leading vaccine candidate for *C. trachomatis* infection (Brunham and Rey-Ladino, 2005; Yu et al., 2012).

The translocation of chlamydia secreted (effector) proteins to the inclusion membrane or into the host cytosol are also important virulence determinants. Some examples of these include translocated actin-recruited protein (Tarp) responsible for actin polymerisation required for host-internalisation (Ghosh et al., 2020; Parrett et al., 2016), chlamydial deubiquitinating enzymes (Cdu) that are important for mediating the host immune response and apoptosis (Fischer et al., 2017) and chlamydial proteasome-like activity factor (CPAF) that targets a range of host proteins for degradation to ensure its' survival (Bauler and Hackstadt, 2014; Li et al., 2008; Yang et al., 2016; Zhong, 2009).

The functional characterisation of certain Inc and effector proteins has been relatively straight forward, owing to their predicted phenotypes that can be assayed in the laboratory and are the typical targets of newly developed tools for loss-of-function mutations in *C. trachomatis* (Han and Derré, 2017; Johnson and Fisher, 2013; Lowden et al., 2015; Mueller et al., 2017; Ouellette, 2018; Weber et al., 2015). Tools for targeted gene deletion have recently been developed for *C. trachomatis* but do not currently exist for *C. muridarum*, therefore, considered less genetically tractable. Without the means to routinely manipulate *C. muridarum* with standard molecular tools available in other free-living bacteria such as chemical mutagenesis, RNAi technologies, CRISPR/cas9 genome editing, the functional analysis of *C. muridarum* genes and the identification of the essential genes upon which survival depends remains elusive. The following section provides an overview of the molecular toolkit available for *C. muridarum* in comparison with *C. trachomatis* to highlight the importance of developing the capability for generating large-scale knock-out mutant libraries in *C. muridarum*.

1.4 Genetic tools for mutagenesis in *Chlamydia*; uses and limitations

A decade of developments in molecular tools have greatly advanced our understanding of chlamydial biology and pathogenesis by facilitating the functional analysis of chlamydial genes (Valdivia and Bastidas, 2018). These technologies predominantly relied on transforming vectors

derived from the endogenous chlamydial plasmid (Rahnama and Fields, 2018; Sixt and Valdivia, 2016). Wang et al developed the first *E.coli-Chlamydia* shuttle vector, pGFP::SW2, for the robust transformation of a genital *C. trachomatis* strain, called the Swedish new variant (nvCT) (Wang et al., 2011). Vector pGFP::SW2 was derived from the native pSW2 plasmid combined with the *E. coli* cloning vector ColE1 to facilitate both propagation and demethylation in *E. coli*, prior to transformation and maintenance in *Chlamydia*. Inclusion of the antibiotic resistance genes beta-lactamase (*bla*) and chloramphenicol acetyl transferase (*cat*), the latter of which was transcriptionally coupled to the fluorescence reporter gene green fluorescent protein (*gfp*), facilitated the recovery of transformants through selection with penicillin or chloramphenicol and identification of green fluorescent inclusions (Wang et al., 2011). This system laid the foundation for the development of molecular tools to study gene functions in *Chlamydia* spp.

There are now over 25 *C. trachomatis*-transforming vectors with a range of applications for studying chlamydial gene functions (vectors developed from 2016 onwards: Keb and Fields, 2019; LaBrie et al., 2019; Mueller et al., 2016; Ouellette, 2018; Vectors developed between 2011-2016 are reviewed by Sixt and Valdivia, 2016). By contrast, efforts to develop systems for the genetic manipulation in *C. muridarum* are much more limited and currently include only 10 transforming vectors (Campbell et al., 2014; Cortina et al., 2019; Liu et al., 2014a; Skilton et al., 2018; Song et al., 2014; Wang et al., 2014, 2019). These vectors and their applications in *C. muridarum* are listed in Table 1.

Table 1 Vectors and their applications in the genetic manipulation of *C. muridarum*

| Vector name | Vector type | Plasmid gene(s) | Selectable marker(s) | Reporter gene(s) | Application in <i>C. muridarum</i> | Reference |
|----------------|---|--|----------------------|------------------|---|-----------------------|
| pBRCM | <i>E.coli-Chlamydia</i> shuttle-vector | <i>CDS1-8</i> from pCM | <i>bla</i> | none | Characterise the properties of pCM <i>in vitro</i> | Song et al., 2014 |
| pGFP::CM | <i>E.coli-Chlamydia</i> shuttle-vector | <i>CDS1-8</i> from pCM | <i>bla, cat</i> | <i>gfp</i> | Plasmid-gene deletion | Liu et al., 2014a |
| pGFP-Luc-CM | <i>E.coli-Chlamydia</i> shuttle-vector | <i>CDS1-8</i> from pCM | <i>bla, cat</i> | <i>gfp, luc</i> | Bioluminescence imaging in live mice | Campbell et al., 2014 |
| pSW2NiggCDS2 | <i>E.coli-Chlamydia</i> shuttle-vector | <i>CDS1</i> and <i>CDS3-8</i> from pSW2. <i>CDS2</i> from pCM. | <i>bla, cat</i> | <i>gfp</i> | Plasmid-tropism | Wang et al., 2014 |
| pGFP::Nigg | <i>E.coli-Chlamydia</i> shuttle-vector | <i>CDS2-8</i> from Nigg. <i>CDS1</i> from pSW2 | <i>bla, cat</i> | <i>gfp</i> | Characterise the properties of pCM <i>in vitro</i> | Skilton et al., 2018 |
| p2TK2Spec-Nigg | <i>E.coli-Chlamydia</i> shuttle-vector | <i>CDS2-8</i> from pCM. <i>CDS1</i> from pSW2 | <i>aadA</i> | <i>mCherry</i> | Monitor RB-EB conversion <i>in vitro</i> | Cortina et al., 2019 |

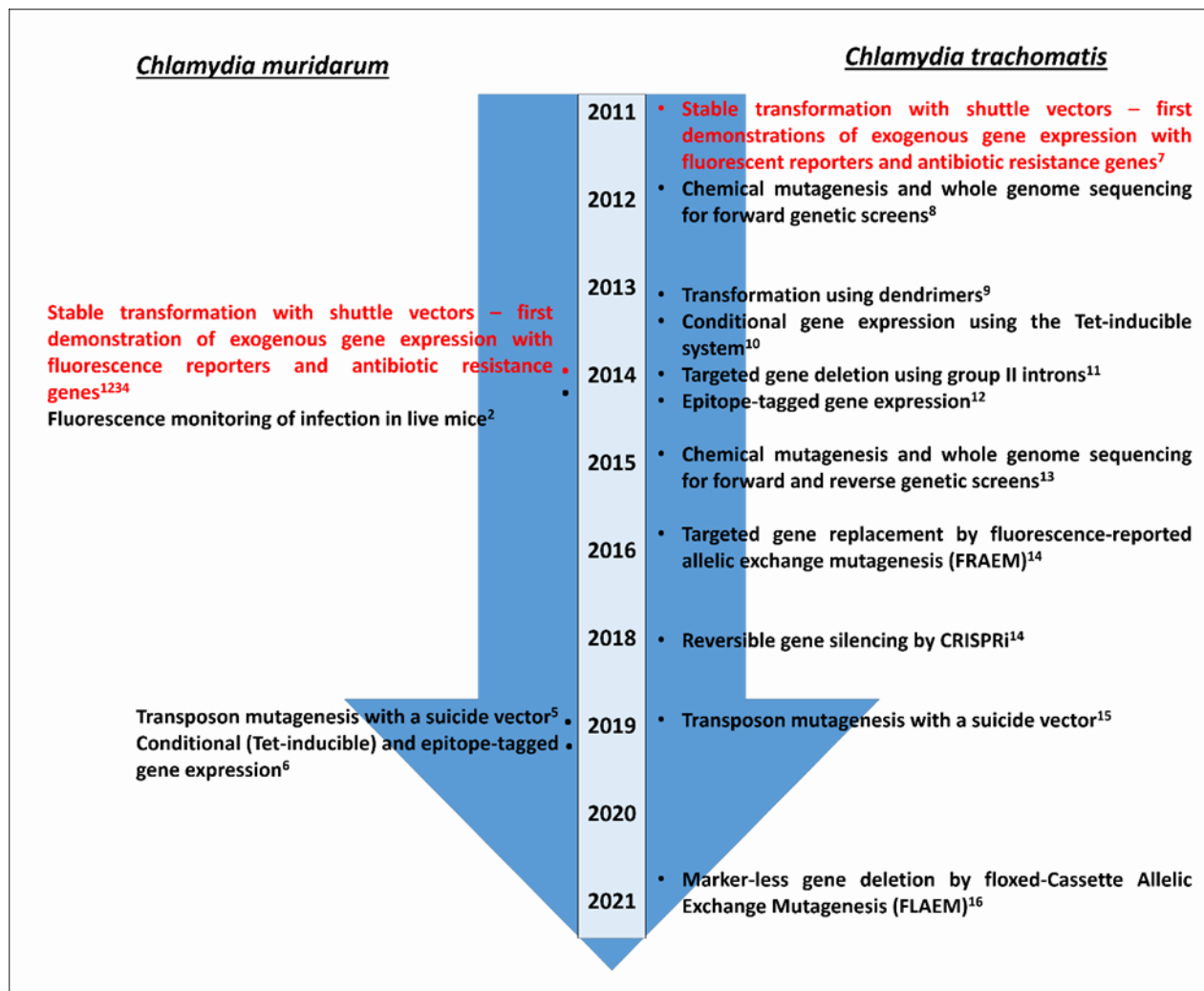
| Vector name | Vector type | Plasmid gene(s) | Selectable marker(s) | Reporter gene(s) | Application in <i>C. muridarum</i> | Reference |
|---|----------------|---|----------------------|-----------------------------|---|----------------------|
| p2TK _{Spec} Nigg mCh(Gro _{L2}) | Cloning vector | <i>CDS2-8</i> from pCM. <i>CDS1</i> from pSW2 | <i>aadA</i> | <i>mCherry</i> | Monitor RB-EB conversion <i>in vitro</i> | Cortina et al., 2019 |
| p2TK2 _{Spec} -Nigg mCh(Gro _{L2})TetTC0273-3xFLAG | Cloning vector | <i>CDS2-8</i> from pCM. <i>CDS1</i> from pSW2 | <i>aadA</i> | <i>mCherry</i> | Tet-inducible gene expression and localisation of <i>C. muridarum</i> effectors | Cortina et al., 2019 |
| p2TK2 _{Spec} -Nigg mCh(Gro _{L2})GFP(OmcA _{Cm}) | Cloning vector | <i>CDS2-8</i> from pCM. <i>CDS1</i> from pSW2 | <i>aadA</i> | <i>gfp</i> , <i>mCherry</i> | Monitor RB-EB conversion <i>in vitro</i> | Cortina et al., 2019 |
| pCMC5M | Suicide vector | none | <i>cat</i> | <i>gfp</i> | Transposon mutagenesis | Wang et al., 2019 |

Of the nine *C. muridarum* shuttle vectors, five of these were derived from the original *E. coli-Chlamydia* shuttle vector developed for *C. trachomatis*, pGFP::SW2 (Wang et al., 2011) and therefore contain the *bla* and *cat* resistance genes rendering chlamydia resistant to betalactams and chloramphenicol respectively. The recent addition of a spectinomycin resistance gene, *aadA*, to a set of cloning vectors has expanded the selection available with which to recover transformants in *C. muridarum* beyond only penicillin/ampicillin or chloramphenicol (Cortina et al., 2019). The advantages for the use of penicillin/ampicillin or chloramphenicol for this purpose in *C. muridarum* is discussed in section 1.6.

Figure 1-2 presents the key milestones in the development of molecular genetic tools for both *C. muridarum* and *C. trachomatis* highlighting the extent of the capabilities for genetic manipulation in these individual species. The use of fluorescence reporters, antibiotic resistance genes, inducible control over gene expression and epitope-tagged proteins in plasmid-based genetic tools has been well reviewed (Bastidas and Valdivia, 2016; Sixt and Valdivia, 2016). Shuttle vectors that make use of these tools have been developed for *C. muridarum*. The application of these tools in both *C. trachomatis* and *C. muridarum* offer researchers flexibility for monitoring the developmental cycle (Cortina et al., 2019; Skilton et al., 2018; Song et al., 2014) and plasmid-stability (Mueller et al., 2016), and for studying protein interactions and localisation within inclusions (Cortina et al., 2019; Weber et al., 2015).

The inclusion of at least two or more of these exogenous genes and promoter systems are essential for mutagenesis approaches that require the use of a transforming plasmid.

The focus of this PhD thesis is to develop the capabilities of a plasmid-based inducible transposon mutagenesis approach in *C. muridarum* toward achieving large-scale knock-out mutant libraries using transposons. In the following section, the use of the genetic tools will be discussed in the context of the targeted and random mutagenesis approaches currently available for *C. muridarum* and *C. trachomatis*.



Song et al., 2014¹, Campbell et al., 2014², Liu et al., 2014³, Wang et al., 2014⁴, Wang et al., 2019⁵, Cortina et al., 2019⁶, Wang Y. et al., 2011⁷, Nguyen and Valdivia., 2012⁸, Kannan et al., 2013⁹, Wickstrum et al., 2013¹⁰, Johnson and Fisher 2013¹¹, Bauler and Hackstadt., 2014¹², Kokes et al., 2015¹³, Mueller et al., 2016¹⁴, Ouelette., 2018¹⁵, LaBrie et al., 2019¹⁶, Keb and Fields., 2021¹⁷

Figure 1-2 Milestones in the molecular toolkit developed for *C. trachomatis* and *C. muridarum*

The timeline spanning the decade from 2011 to 2021 starts with the development of the first robust transformation system using an *E. coli-Chlamydia* shuttle vector and with it, the first demonstration of exogenous gene expression with the use of fluorescence reporters and antibiotic resistance genes in *Chlamydia* spp.

1.4.1 Targeted mutagenesis in *Chlamydia*

Currently there are four methods that have been developed for targeted gene knockout leading to the identification of essential genes in *C. trachomatis*. There are no such tools currently available for targeted mutagenesis of *C. muridarum*. The tools available for targeted gene deletion in *C. trachomatis* and their scope for use in *C. muridarum* will be considered in detail in the following sections.

1. Insertional mutagenesis with a mobile group II intron

The first example of targeted gene deletion in *Chlamydia* used a modified the TargeTron™ system (Johnson and Fisher, 2013). Group II introns are a class of transposable elements common to bacterial genomes, moving between genes by a unique mechanism of retro-transposition that is predominantly controlled by a self-encoded protein with the combined activities of RNA maturase, endonuclease and reverse transcriptase (Lambowitz and Zimmerly, 2004). This protein, called intron-encoded protein (IEP), aids sequence recognition of the target site. The intron contains sequences designated EBS1, EBS2 and δ guiding insertion to the corresponding IBS1, IBS2 and δ' region in the target gene. Intron insertion occurs between the IBS2 and δ' sites on the target gene.

Under normal conditions, the DNA insertion is stable, until post transcriptional RNA splicing by the IEP removes the inserted gene from mRNA which results in translation of the wild type gene and re-establishes normal gene function. Perutka et al (2004) demonstrated in *E. coli* that modifying the intron sequences at the EBS1, EBS2 and δ sites allowed for targeted recognition of any gene of interest (Perutka et al., 2004). It was further demonstrated that by removing the IEP from the intron, and instead expressing it from a conditional plasmid (in trans), that RNA splicing, and eventual restoration of the wild type gene function could be prevented. This is because the plasmid would typically be lost once transposition of the intron has occurred, and so the gene encoding for IEP would be lost with it. The addition of resistance genes within the intron, where the IEP gene once was, allows for selection of mutants and subsequent loss of the plasmid backbone. This technology called TargeTron™ (Sigma) has been adapted for targeted gene knock out in many Gram negative and positive bacteria, including that of the obligate intracellular bacterium *Ehrlichia chaffeensis*, to identify genes responsible for *in vivo* infection (Cheng et al., 2013). One of the advantages of this commercially available system is its' flexible application that can be modified for different species of bacteria.

To test the feasibility of this technology for achieving targeted gene-knockout in a *C. trachomatis* strain the chromosomal gene encoding for inclusion membrane protein A (*IncA*) was targeted because inactivation of *IncA* produces a readily identifiable phenotype characterised by non-

Chapter 1

fusogenic inclusions without affecting normal development. The TargeTron™ vector was adapted to select for stable intron insertions in *IncA* by the addition of the penicillin (*bla*) selectable marker. The penicillin resistant and *IncA*-deficient (*IncA*-) mutants were identified by microscopy, then isolated and plaque purified. The *IncA*- phenotype generated *in vitro* corresponded to that of *IncA* deficient mutants obtained from clinical samples (Johnson and Fisher, 2013). Sequencing the region of insertion verified that a stable mutation in *IncA* was caused by intron insertion causing inhibition of *IncA* production.

The system was later modified replacing the penicillin resistance marker with a spectinomycin resistance-gene marker and adapted to generate double-knock out mutant strains, causing knock out of two genes in *C. trachomatis* encoding the Anti anti-sigma factor RsbV1 and inclusion membrane protein *IncA* (Lowden et al., 2015). However, *Rsbv1* null mutants did not produce a recognisable growth phenotype relative to the wild type measured at 24 hpi by immunofluorescence in this study, where another study using plaque assays were able to identify smaller plaques in the *RsbV1* mutant indicating a role for overall fitness in *C. trachomatis* (Thompson et al., 2015). The pDFTT3 *GII(bla)* vector was adapted to investigate the role of inclusion membrane proteins responsible for chlamydial survival (Sixt et al., 2017), as well as functionally redundant chlamydial chaperone proteins (Illingworth et al., 2017), and the requirement for *TepP* (translocated early phosphoprotein) in bacterial replication and cell signalling (Carpenter et al., 2017).

These studies have demonstrated that the TargeTron™ approach to insertional mutagenesis is a relatively quick and straight forward tool to achieve stable and selectable chromosomal mutations in *C. trachomatis* but has yet to be adapted for use in *C. muridarum*. Theoretically, the TargeTron™ system has the flexibility to be adapted to target any gene for a given species but the insertion position within a gene is limited by the specific requirements for insertion of the group II intron. Identifying the correct sequence within target genes can be challenging. Another key limitation to this system, as with all transformation-dependant tools, is the low transformation efficiency of the transformation methods used. The system used in *C. trachomatis* by Johnson and Fisher (2013) had a high failure rate, producing the desired mutants in only 50% of experimental attempts. As with all plasmid-based technologies, it is likely that a low transformation efficiency of the intron-delivery vector was responsible. Finally, phenotypic analysis can be confounded by either the polar effects on the expression of genes within operons because of insertional mutagenesis or the potential for producing functional truncations.

2. Fluorescence-reported allelic exchange mutagenesis

Meuller et al., (2016) first demonstrated a system to target specific chromosomal genes for allelic exchange with a mutant version of the gene by homologous recombination in *Chlamydia*. This

technology, called Fluorescence-Reported Allelic Exchange Mutagenesis (FRAEM) was developed specifically for use in *C. trachomatis* L2 strain and its utility for targeted gene-knockout has been demonstrated in a number of studies since (Ghosh et al., 2020; Keb et al., 2018; McKuen et al., 2017; Mueller et al., 2017). Unfortunately, this technology has only been shown to work in one laboratory.

To demonstrate proof of principle, Mueller et al designed the FRAEM vector to target the *trpA* gene of the tryptophan synthase in *C. trachomatis* L2. The *trpA* gene sequence was disrupted with a *gfp-bla* cassette to enable the selection and identification of chromosomal *trpA* mutants. Two ~3kb flanking sequences were placed upstream and downstream of the open reading frame (ORF) containing the disrupted *trpA* to enable recombination with the homologous site on the chromosome. Upwards of six passages were required to facilitate allelic exchange as a mechanism for replacing the functional *trpA* gene with the disrupted gene.

To date, the pSu6 vector is the only suicide plasmid that is self-replicating in *Chlamydia*. Conditional control of plasmid maintenance in pSu6 was achieved by controlling transcription of plasmid-gene *CDS8* (also called *pgp6*) deemed essential for plasmid maintenance, by placing *CDS8* under the inducible control of the Tetracycline promoter P_{tet} . This way pSu6 would be maintained by chlamydial cells in the presence of the inducer anhydrotetracycline (ATc) for 6 or more passages required to facilitate allelic exchange as a mechanism for replacing the functional chromosomal *trpA* gene with the disrupted gene. The backbone of the suicide vector contained a different coloured fluorescence reporter (mCherry). Loss of red fluorescence from inclusions confirmed the elimination of the plasmid when transcription of *CDS8* was inhibited by removal of ATc from the growth media.

FRAEM has been used to demonstrate the role of the secreted effector TmeA (translocated membrane associated effector A) as well as Tarp in host cell invasion *in vitro* and *in vivo* respectively (Ghosh et al., 2020; McKuen et al., 2017). The FRAEM vector has only been compatible with strains with an LGV background this is most likely because of the so-called plasmid-tropism barrier (Wang et al., 2014) and this technology has yet to be developed for use in other *Chlamydia* species.

3. Floxed-cassette allelic exchange mutagenesis

The FRAEM vector was adapted to create marker-less gene deletions using a floxed cassette to lessen the polar effects of insertional mutagenesis on downstream genes (Keb et al., 2018). This technology, called Floxed-Cassette Allelic Exchange Mutagenesis (FLAEM) makes use of Cre-loxP genome editing to remove the gene cassette containing the selection marker from the chromosome after targeted insertional mutagenesis by allelic exchange.

4. CRISPR-interference (CRISPRi)

Gene silencing by CRISPR-interference technology reversibly inhibited transcription of inclusion membrane protein IncA was demonstrated in *C. trachomatis* (Ouellette, 2018). Over the last 5 years, CRISPR systems have been rapidly developed into tools that can target specific chromosomal genes and silence their expression. This technology is called CRISPR interference, or CRISPRi, is an RNA-based approach that targets the gene promoter regions in a reversible manner to inhibit transcription of a target gene with nuclease-deactivated Cas9 (dCas9). The cas9 enzyme normally functions to cause double stranded breaks in DNA at specific target sites identified by a guide RNA (gRNA) and a protospacer adjacent motif. The deactivated enzyme does not cleave double stranded DNA, instead when dCas9 is bound to the promoter it blocks transcription without altering the DNA. Choudhary et al first demonstrated the utility of CRISPRi in *E. coli*. The dcas9 and gRNA were introduced into bacteria on a plasmid and placed under control of an inducible and constitutive promoters respectively (Choudhary et al., 2015).

The feasibility of adapting CRISPRi for targeting a specific gene in *C. trachomatis* was recently published. Ouellette (2018) developed a CRISPRi vector for reversible repression of the *IncA* gene (deemed non-essential). The vector contained both deactivated-*cas9* (*dCas9*) from *Staphylococcus aureus* (*S. aureus*) under control of the inducible tetracycline promoter and gRNA from *S. aureus* controlled by the chlamydial *dnaK* promoter that is active from early phase of the developmental cycle. The gRNA was designed to target a region upstream of *IncA*. The vector backbone contained the entire native L2 plasmid sequence. Two further plasmids were constructed that isolated the *dcas9* and the gRNA on separate plasmids and were otherwise identical. All constructs contained the penicillin resistance gene *bla* to select for transformants. Plasmid-cured *C. trachomatis* strain L2 (L2P-) was first transformed with each plasmid on its' own to rule out the possibility that *IncA* repression could be caused by the constitutively expressed gRNA (small RNA) binding to *IncA* and blocking transcription. Also, to see if normal chlamydial development would be inhibited in any way by expression of dcas9. Expression of dcas9 did not negatively affect chlamydial growth and expression of gRNA on its' own did not inhibit *IncA* expression.

This novel study demonstrated proof of principle that CRISPRi is possible in *C. trachomatis*. The ability to reversibly inhibit gene transcription avoids the need for complementation using a second vector expressing the gene of interest under its native promoter. However, a key issue was that of plasmid stability in the transformed strain. This is important because without a uniform population of bacteria it may be difficult to reproduce the results obtained by CRISPRi.

Identifying candidate genes for targeted mutagenesis relies on the ability to predict gene functions based upon sequence similarity to known proteins. In addition, the functional analysis of these genes requires the isolation of clonal mutants and assays sensitive enough to identify

discrete phenotypes compared to a parent strain. In *Chlamydia*, ~20% of genes bear no homology to known proteins (Stephens et al., 1998). Furthermore, in the absence of axenic media for *Chlamydia* propagation, the only method available to isolate clonal mutants is by plaque purification which is a laborious method that takes up to a week to perform.

Methods for genome-wide mutagenesis provide the most efficient means for gene discovery by significantly reducing the overall candidate gene list and are not reliant on prior assumed knowledge of predicted function. The methods for genome-wide mutagenesis currently available in *C. trachomatis* and *C. muridarum* are discussed in the following sections with an emphasis on the capabilities for transposon mutagenesis to identify essential genes, in particular saturation mutagenesis, which is the only method that will define gene essentiality, has yet to be realised in *C. muridarum*.

1.4.2 Genome-wide mutagenesis in *Chlamydia*: gene discovery

So called “essential genes” are a group of genes that result in the death of the bacterial host upon their loss-of-function (knock-out). In addition to these core essential genes, there are broader set of genes that are essential for survival in specific environmental conditions be it at specific stages of development or in particular tissues. The identification of essential genes can provide candidates for new therapeutic targets and vaccine candidates that are desperately needed in *Chlamydia*. As mutants must be selected and propagated in eukaryotic host cells, mutating genes essential for host cell invasion and survival remains challenging. However, advances in genetic tools for generating mutant libraries by random mutagenesis techniques in *C. trachomatis* LGV strains and methods for linking genotype and phenotype has made progress towards identifying essential genes and elucidating gene functions in these pathogens.

The ability to construct libraries of knock-out mutants in *Chlamydia* spp to identify essential genes has, until recently, only been demonstrated by chemical mutagenesis using N-ethyl methyl sulfonate and N-ethyl-N-nitrosourea. Two approaches have been developed for the identification of null mutants generated by EMS and use Targeted Induced Local Lesions in Genomes (TILLING), originally developed for plant genetics, and adapted for *C. trachomatis* in 2011 (Kari et al., 2011). The two approaches are TILLING, and TILLING combined with whole genome sequencing. The former method relies on expansion of mutant pools followed the PCR amplification of a target region from the pools of genomic DNA. The amplicons are cleaved using a mismatch-specific endonuclease (CEL-1) and allow for identification of isogenic or near-isogenic pools containing the wild-type and the mutant gene of interest. The phenotypic differences between parent and mutant strains are then assessed using *in vivo* models. This approach has been used to confirm the function of TrpB predicted to be responsible for indole rescue in response to tryptophan

Chapter 1

starvation (Kari et al., 2011). This approach was adapted to isolate mutants with null mutations in predicted virulence genes including *pmpD* and several genes located in the *C. muridarum* plasticity zone (K et al., 2015; Kari et al., 2014).

Kokes et al., (2015) combined EMS mutagenesis and TILLING with whole genome sequencing (WGS) in a rifampin-resistant (*rif^r*) LGV strain of *C. trachomatis* (Kokes et al., 2015; Nguyen and Valdivia, 2012). The mutant library generated by Kokes et al, provides researchers with a library of mutant strains with nonsense mutations in 84 open reading frames that represent genes with a variety of predicted functions involved in amino acid and central metabolism, DNA repair and transcription, membrane protein transport as well as nonsense mutations in a handful of predicted Inc proteins and several proteins of unknown function (Bastidas and Valdivia, 2016). This mutant library has the added advantage that the nonsense mutations caused by the point mutations poses very limited risk of polar effects on downstream gene expression and offers a range of alternative mutations such as gain-of-function and adaptive mutations that can also be screened for.

Whole genome sequencing of the mutant library facilitated both forward and reverse genetic screens leading to the identification of several non-essential and essential genes in *C. trachomatis* Kokes et al (2015). The application of forward genetics was demonstrated through the identification of two chemically induced mutants (with identical sequences) that were unable to recruit filamentous actin (F-actin) at their inclusion membrane. Candidate genes were identified in one of these mutants based upon 12 predicted non-synonymous mutations. Linkage analysis was performed on genetic crosses of the *rif^r* mutant strain with a spectinomycin resistant strain to further refine the candidate genes to those mutations that segregate with the mutant phenotype. Subsequently, *C. trachomatis* gene *CTL0184* was identified as being responsible for failure to assemble F-actin because of the genetic association of the mutant allele with the phenotype and the lack of a detectable gene product in this mutant. Functional analysis of the mutant and complementation of the gene introduced back into the mutant and expressed using its native promoter was able to confirm the role of *CTL0184* in the recruitment of actin to the inclusion membrane and was named InaC (Inclusion membrane protein for actin assembly). Furthermore, genes associated with important biochemical pathways, such as the metabolism of glycogen and glucose, previously thought to be essential for growth were shown to be expendable in cell culture (Kokes et al., 2015).

The limitations of CEM for generating large mutant libraries include the risk of increased background mutations caused by the chemical mutagen especially with higher concentrations of EMS used which limits the ability to identify all the mutations. The application of WGS technology has made it easier to identify all CEM induced mutations by facilitating direct comparison of

whole genome sequences of mutants and reference strains. However, the method optimised by Kokes et al using N-ethyl methyl sulfonate and N-ethyl-N-nitrosourea produced an average density of 8 single nucleotide polymorphisms (SNPs) / kb, and induced predicted non-synonymous mutations in only 10% of open reading frames (Kokes et al., 2015). Lower doses of mutagen used in TILLING do, however, enable generation of clonal isolates with discrete mutant alleles that can be screened.

The main limitation for these techniques as demonstrated is the ability to map phenotypes with the genotype, especially when near-isogenic strains are compared, and gene expression and function varies between animal models in which they are tested in.

1.5 Transposon mutagenesis in obligate intracellular bacteria

In the absence of tools for the routine genetic manipulation of an organism, transposon mutagenesis promises an efficient means to interrogate whole genomes and define essential genes (Hayes, 2003). Genome-wide mutagenesis is possible because transposons insert, with little bias, into any genomic location. The success of transposon mutagenesis approaches to define essential genes depends upon the generation of saturation mutant libraries. Saturation mutagenesis requires transposons to insert at random at a high frequency to hit every gene at least once. When saturation mutagenesis is combined with high-throughput sequencing of transposon insertion sites, known as transposon-insertion-sequencing (TIS), essential genes can be identified by screening for the loss of genes that are represented in the pooled mutant library when grown in diverse test conditions (Van Opijnen and Camilli, 2013). Currently, a tool capable of generating saturation mutant libraries with transposons in *Chlamydia* does not exist.

The potential of transposons for generating saturation mutant libraries in free-living extracellular bacteria has been well established with hundreds of thousands of unique mutants generated for human pathogens such as *Salmonella typhi* (Langridge et al., 2009), *Streptococcus pneumoniae* (Van Opijnen et al., 2009), *Mycobacterium tuberculosis* (Dejesus et al., 2017) and *Clostridium difficile* (Dembek et al., 2015). However, the ability to generate saturation or near saturation mutant libraries in obligate intracellular bacterial pathogens has proven much more challenging.

The *Tc1/mariner* superfamily of transposable elements (TEs) are DNA transposons that use their own transposase (Tpase) to mobilise the TE. Their transposition does not require host specific factors for their movement between DNA molecules which allows them to function in a wide range of hosts. The *Himar1/mariner* TE, that is naturally inactive, was reconstructed from the Horn fly *Haematobia irritans* (Lampe et al., 1996) for use as a genetic tool for insertional mutagenesis of bacterial genomes and includes the obligate intracellular bacterial pathogens:

Rickettsia prowazekii (Qin et al., 2004), *Coxiella burnettii* (Beare et al., 2009) *Ehrlichia chaffeensis* (Cheng et al., 2013), and *Anaplasma phagocytophilum* (Felsheim et al., 2006). Recently, the *Himar1/mariner* transposon system was demonstrated to be functional in *Chlamydia* spp (LaBrie et al., 2019; Wang et al., 2019). Yet the ability to generate large-scale transposon mutant libraries necessary for the identification of sets of essential genes has been limited in these pathogens because of their intracellular requirements. The *Himar1* transposon and the advantages and limitations for its use as a genetic tool in obligate intracellular pathogens will be discussed next.

1.5.1 *Himar1/mariner* transposons and their transposition

Transposable elements (TEs) are DNA sequences with the ability to move within the genome by a process known as transposition. Barbara McClintock won the Nobel Prize in 1983 for her discovery of TEs in maize plants. TEs are abundant in both prokaryotes and eukaryotes and often make up large portions of a genome: 45% of the human genome (Lander et al., 2001) and 80% in maize plants (SanMiguel et al., 1996). Insertions, excisions, duplications, and translocations at the site of TE integration can cause large changes in genome size as well as disrupt normal gene functions such as activation and expression. For that reason, TE transposition within genomes is a fundamental process driving genetic variation, contributing to the speciation and evolution of all organisms. Subsequently genetic tools have been developed that engineer TEs for a variety of investigational purposes such as insertional mutagenesis for the discovery of essential genes.

In their simplest form, TEs are referred to as insertion sequences (IS) and range between 800-1500 base pairs long. IS consist of a central region that encodes the transposase enzyme (Tpase) necessary for transposition which is bordered by terminal inverted repeat (TIR) sequences roughly 10-40 base pairs (bp) in length. In a typical IS, the TIR sequences are important for Tpase binding as well as the enzymatic functions for strand cleavage and transfer. The native Tpase promoter is located upstream of Tpase overlapping the TIR region. It is noteworthy that more complex TEs require multiple binding sites to serve these functions, for example with the Tn7 family of TEs.

Transposition of transposons is by non-homologous recombination and is coordinated by a catalytic domain that sits within an RNase-H like fold of the Tpase (Richardson et al., 2006). Typically, this catalytic domain contains an arrangement of amino acids characterised by two aspartate (D) residues and one glutamate (E) residue called the DDE-motif and provides the binding sites for two metal ions. One role of these metal ions is to facilitate catalysis at this site by activating attacking nucleophiles that cleave DNA (Richardson et al., 2009). The DDE-motif is highly conserved between bacterial Tases of the *Tc1/mariner* superfamily (Polard and Chandler, 1995). Despite the high conservation of this catalytic domain between the different superfamilies' of Tases, the chemical reactions and mechanisms of transposition carried out by these domains

are highly varied. The simplest mechanism of cut-out/paste-in transposition is demonstrated in *Himar1/mariner* elements. The chemistry of this process has been well characterised and involves a series of hydrolysis and transesterification reactions for strand cleavage and joining. Figure 1-3 shows a graphical representation of the key steps in cut and paste transposition of *Himar1* mariner elements that does not result in intermediate hairpin formation.

The TIR at each end of the transposon in the donor DNA molecule are recognised by two monomers of T_pase, binding to the TIR through the conserved helix-turn-helix motif to generate a single-end complex, which activates hydrolysis and subsequent cleavage of both strands. The T_pase monomers come together to form a dimer molecule, facilitating the generation of a paired ends complex (PEC) and subsequent cleavage of the non-transferred strand followed by the transferred strand (Richardson et al., 2009). Bouuaert and Chalmers., (2017) investigated the dynamics of the PEC throughout transposition for mariner element *Hsmar1* and demonstrated that the chemical steps for transposition are carried out by a single T_pase dimer at one active site (Claeys Bouuaert and Chalmers, 2017). Cleavage is initiated by hydrolysis of the phosphodiester bonds located at the 5' ends. The PEC identifies the insertion site on the recipient DNA molecule, which in the case of mariner elements is any thiamine-adenine (TA) dinucleotide. This final excision of the transposon end exposes a free 3' hydroxyl group that attacks the phosphodiester bond on the target DNA. The 5' nick is made 3 nucleotides inside the IR sequence of the transposon but the nick at the 3' end is made at the flanking DNA-TIR junction causing the insertion site to be staggered by 3 bp and duplication of the TA at the target site during gap repair by the host.

Two key mechanisms that self-regulate T_pase expression have been described in *mariner* transposons. One mechanism involves selective pressure that causes the T_pase to acquire a dominant mutation that render them relatively inactive compared to the wild type (Lohe and Hartl, 1996). This is pertinent in light of the fact that certain T_pase mutants of *Himar1* demonstrate hyperactivity (Lampe et al., 1999). The acquisition of mutations over time that decrease T_pase activity leads to redundancy is a factor of TE ageing. These TEs become known as fossil elements. Secondly, studies have shown that expression of T_pase above a certain level will reduce the rate of transposition in a process called overproduction inhibition (Bouuaert et al., 2014).

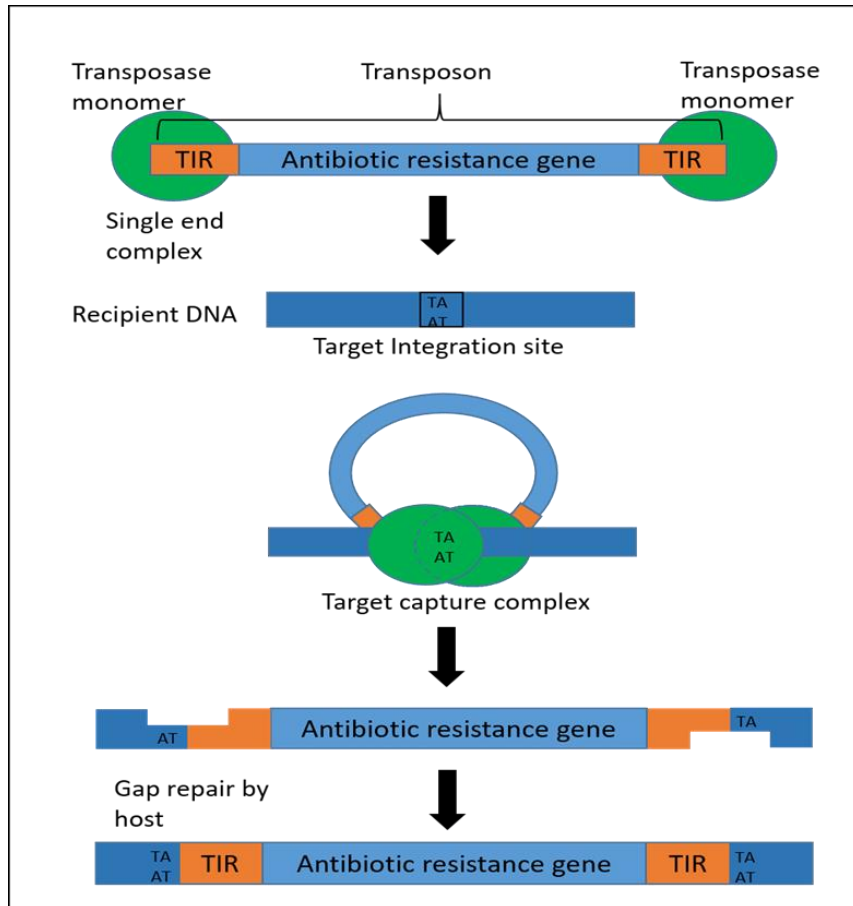


Figure 1-3 Transposon transposition by the 'cut and paste' mechanism mediated by *Himar1* transposase molecules.

Single end complexes (SEC) are formed at the transposon ends through transposase monomer binding to the terminal inverted repeats. The transposon ends are brought together through paired end formation of SEC at the target integration site, which in the case of mariner transposons is any TA dinucleotide. The catalytic domain of the transposase facilitates both double strand cleavage and insertion into the target site.

1.5.2 Transposons as genetic tools in obligate intracellular bacteria

The generation of mutant libraries by transposon mutagenesis in other obligate intracellular bacteria typically requires transformation with either a single suicide vector containing both the transposon and associated transposase as shown in figure 1-4A (Beare et al., 2009; Cheng et al., 2013; Felsheim et al., 2006), or with two separate suicide vectors as shown in Figure 1-4B. Suicide vectors are unable to replicate in their host, therefore, the transposase gene is lost along with the vector backbone after transposon transposition. This ensures that transposon insertions are stable by limiting production of transposase in the target cell after the initial transposition event. Saturation mutagenesis assays require efficient transformation with a transposon delivery vector (Naorem et al., 2018), in order to detect rare insertion events (~ 1 insertion per 10^4 - 10^6 cells)

(Thomson et al., 1999). However, transformation of suicide vectors in other species of bacteria is often inefficient at producing diverse mutant libraries (Beare et al., 2009; Cheng et al., 2013; Felsheim et al., 2006). The single suicide vector approach was used for transposon mutagenesis of *Ehrlichia Chaffeensis* and *Coxiella burnettii* resulting in a library of transposon mutants with four and thirty insertion mutations respectively, resulting in the loss of gene function (Cheng et al., 2013; Felsheim et al., 2006).

The use of suicide transposon delivery vectors transformed into both *C. trachomatis* and *C. muridarum* with calcium chloride treatment was no exception as demonstrated by the low rate of recovery of mutants even with the use of a hyperactive transposase variant known to increase efficiency of transposon transposition (LaBrie et al., 2019; Wang et al., 2019). In *Chlamydia*, transformation efficiencies are very low. Subsequently, the suicide-vector approach required numerous rounds of transformation and laborious methods for isolating mutants and was not suitable for generating saturation mutant libraries in either *C. trachomatis* or *C. muridarum*.

In free-living bacteria, transposon mutagenesis typically requires transposon mutagenesis of the linearised target DNA *in vitro* prior to transformation of the bacterial host through incubation of purified transposase mixed together with the transposon amplicon forms an extracellular DNA complex known as a transposome (Goryshin and Reznikoff, 1998; Hoffman et al., 2000). With this method, chromosomal integration of the transposon is by homologous recombination upon transformation. Whereas the use of transposomes in obligate intracellular bacteria requires transformation of the transposome into the target host prior to transposon mutagenesis (Figure 3C). Transposomes electroporated into the obligate intracellular pathogen *Rickettsiae* have shown limited success at producing diverse mutant libraries (Qin et al., 2004).

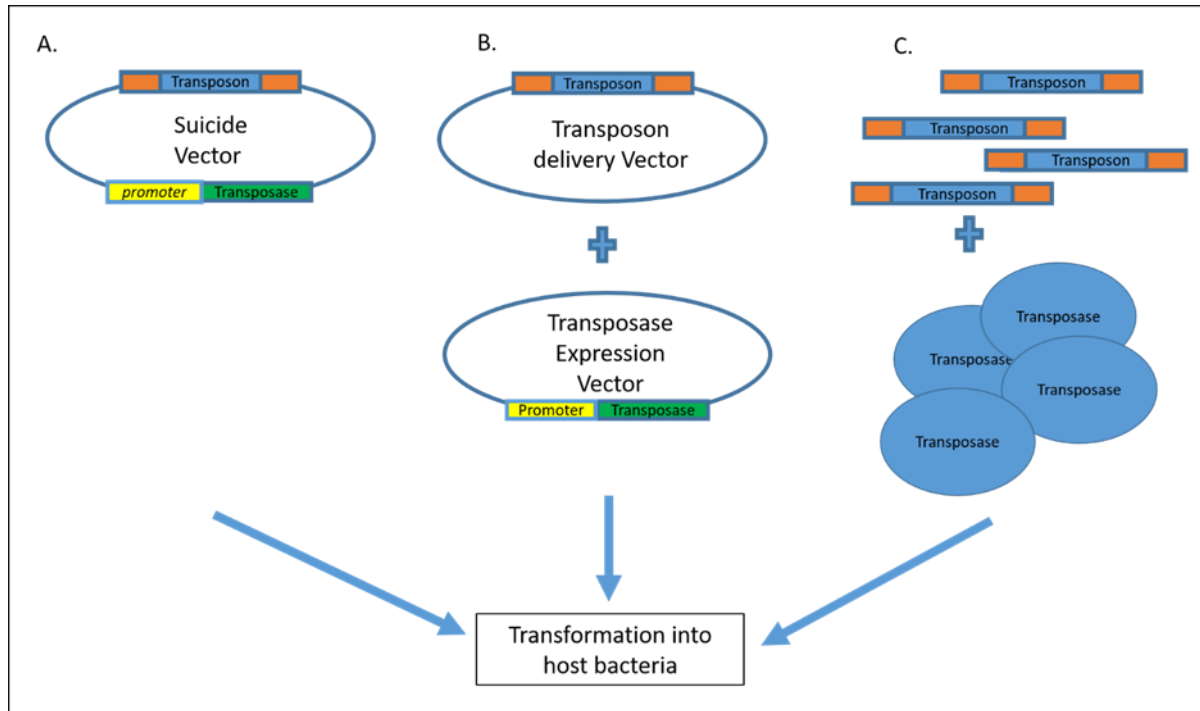


Figure 1-4 Transposons engineered as genetic tools for transposon mutagenesis of obligate intracellular bacterial pathogens.

Representation of the three transposon mutagenesis approaches used in obligate intracellular bacteria. A. A suicide vector, that is unable to replicate in the desired host, contains the transposase under control of a strong constative promoter outside of the terminal inverted repeat sequences of the transposon. B. The transposon and the transposase gene are transformed into the bacterial host on separate vectors that are unable to replicate in the chosen host. C. Purified transposon digested from a plasmid is mixed with purified transposase protein which are together transformed into the bacterial host.

An alternative approach, using an inducible transposon mutagenesis system for *C. trachomatis* was recently described (O'Neill et al., 2021; Skilton et al., 2021). It was hypothesised that a self-replicating transposon-delivery vector with control over transposase expression would enable transformants to be expanded with selection prior to transposon transposition and therefore generate large scale mutant libraries (Skilton et al., 2021).

Skilton *et al.*, (2021) attempted to construct a single plasmid vector bearing the *Himar1* transposon with the transposase under tet promoter control in *C. trachomatis*. They were unable to obtain stable transformants carrying both transposon and transposase. This was likely due to basal levels of transposase expression from the tet promoter in the uninduced state. This hypothesis was supported by the ability to obtain stable transformants bearing a single replicating

and inducible transposon delivery vector when the vector was adapted to improve repression of transposase expression with the use of a riboswitch (O'Neill et al., 2021).

Given the recent progress in *C. trachomatis*, it is reasonable to consider that an inducible transposon mutagenesis system would work in *C. muridarum*. Such a system would include stable maintenance with selection *in vitro* and inducible control over transposon transposition. The challenges for meeting these requirements in *C. muridarum* are discussed in detail in the following section. The phenomenon of *in vitro* plasmid loss is explored in relation to the use of available shuttle vectors as a genetic tool for mutagenesis in this species and forms the basis for the research questions addressed in this PhD thesis.

1.6 Challenges for the genetic manipulation of *Chlamydia muridarum*

Several technical and biological challenges have hindered the development of plasmid-based molecular tools in *C. muridarum*, considered less genetically tractable than *C. trachomatis*. In the absence of tools for the functional analysis of genes in *C. muridarum*, transposon mutagenesis offers the most efficient means to identify all essential genes for survival (Barquist et al., 2013). As discussed in the previous section, the existing suicide transposon delivery vector is not suitable for generating near-saturation mutant libraries in *C. muridarum* as evidenced by the high number of transformation attempts required to recover a mutant library with ~4% coverage of the *C. muridarum* genome (Wang et al., 2019). The current achievements in transposon mutagenesis in *C. trachomatis* and *C. muridarum* have highlighted the need for a system that is optimised for maintenance in *Chlamydia* spp and therefore conditional control over when transposon transposition and elimination of the vector backbone occur is also required. Such a system is hypothesised to substantially increase the likelihood that large-scale near-saturation mutant libraries can be generated (Skilton et al., 2021).

Development of such a system in *C. muridarum* will require an understanding of the factors that make *C. muridarum* less genetically tractable than *C. trachomatis*. The main challenges for plasmid-based tools in *C. muridarum* are low transformation efficiencies of the prevailing transformation method, limitations to the use of existing vectors because of plasmid tropism and *in vitro* plasmid-loss. These factors are discussed herein.

1.6.1 Transformation with recombinant DNA

A key limiting factor for any plasmid-based molecular tool is the ability for the bacterial host to acquire recombinant plasmid DNA also known as “competence”. The recent discovery in *C. trachomatis* of a functional homologue for a protein involved in DNA uptake in *E. coli*, ComEC,

Chapter 1

suggests that *Chlamydia* may be naturally competent (LaBrie et al., 2019), but the mechanisms of DNA uptake remain elusive. Potential gene-delivery systems for *Chlamydia* include the native plasmid or bacteriophage, however, bacteriophage have been discovered in very few species and there is no phage in *C. muridarum* (Śliwa-Dominiak et al., 2013). Thus, the development of plasmid-mediated transformation for the routine genetic manipulation of *Chlamydia* was pursued.

The first method used for transforming *Chlamydia* involved the electroporation of EBs to introduce plasmid DNA into *C. trachomatis* (Tam et al., 1994). This method failed to produce stable transformants and has not been widely adopted for use. Years later, chemical transformation using calcium chloride (CaCl₂) treatment of chlamydial EBs demonstrated robust genetic transformation of *Chlamydia* spp (Wang et al., 2011). The relative ease of the calcium chloride method and the ability to recover stable transformants led to its' widespread use for transformation of *Chlamydia* spp with recombinant DNA. However, the transformation efficiency of this transformation system is extremely low, likely because of damage caused to EBs as they are purified rendering them potentially non-infectious. In contrast, the only method of transformation that targets the RB form, using polyamidoamine (PAMAM) dendrimers, bypasses the need for transforming cell-free infectious bacteria and demonstrates high transformation efficiencies which could reflect greater natural competence of RBs (Kannan et al., 2013). However, no independent repeats of this technology have been demonstrated outside of the same laboratory. Also, transformation methods that target EBs are technically less challenging and experimental conditions are easier to reproduce because of their relative stability in an extracellular environment.

The efficiency of bacterial transformation is influenced by many factors. Calcium chloride transformation was first developed for exogenous DNA uptake in *E. coli*, upon discovery that *E. coli* contain a Ca²⁺ dependent uptake mechanism (Cohen et al., 1972). The efficiency of uptake was improved through direct means to depolarise the bacterial cell membrane potential either by heat shock or treatment with carbonyl cyanide m-chlorophenyl hydrazone (CCCP) (Panja et al., 2006). No such Ca²⁺ dependent uptake mechanism has been found in *Chlamydia*, and heat shock and CCCP treatment of CaCl₂-treated cells have to date not been investigated to improve the efficiency of calcium chloride transformation of EBs.

Studies in *C. muridarum*, but not *C. trachomatis*, have demonstrated that transforming plasmid-free strains results in higher copy numbers than the wild type plasmid (Liu et al., 2014a, 2014b). The reason for this has not been explored. *C. muridarum* naturally loses its' plasmid *in vitro* (Skilton et al., 2018), therefore, it is possible that the use of selection to enrich for transformants has improved plasmid stability and reduced the growth of plasmid-free cells leading to an overall

increase in plasmid copy numbers. It has been suggested that the use of plasmid-free strains for transformation could improve transformation efficiencies by circumventing the issue of plasmid incompatibility (Sixt and Valdivia, 2016) that results in the loss of the endogenous plasmid when shuttle vectors are used to transform *Chlamydia* (Agaisse and Derré, 2013; Wang et al., 2011).

The typical gene content of shuttle vectors includes all eight plasmid genes plus the replication of origin from the chlamydial plasmid as well as genes for antibiotic selection and fluorescence detection and replication in *E. coli*. In addition, recently engineered vectors can also include gene cassettes for mutagenesis. These vectors are nearly double the size of the native chlamydial plasmid and could be contributing to the low transformation efficiencies of these vectors in *Chlamydia* (Jones et al., 2020). Gong et al., (2013) constructed single-gene knock out vectors that replaced either *CDS5* (*pgp3*), *CDS6* (*pgp4*) or *CDS7* (*pgp5*) with a fluorescence reporter gene to demonstrate that these genes were dispensable for chlamydial growth and plasmid maintenance *in vitro*. These findings have been confirmed by other groups using shuttle vectors with plasmid-gene deletions of these genes (Wang et al., 2013b, 2013a). A complete understanding of the essential gene requirements for plasmid maintenance will be useful for restricting the size of shuttle vectors to the minimal required gene set which may improve transformation efficiency.

There are no direct means to measure transformation efficiency defined as the proportion of transformed EBs that go on to successfully replicate in *Chlamydia* (Wang et al., 2011). Therefore, in the absence of a direct measurement of transformation efficiency, the expansion of chlamydial inclusions over serial passage with antibiotics that positively select for transformants when antibiotic resistance genes are expressed from the transforming vector, can be used as an indicator of transformation efficiency. The lack of means to directly measure transformation efficiency as well as the lack of understanding of the mechanisms underlying natural competence in *Chlamydia* are significant challenges for optimising the transformation efficiency of the methods currently available.

1.6.2 Plasmid tropism

Shuttle vectors have been the primary tool for generating and testing plasmid-gene knockouts to investigate the specific functions of these genes. The applications of shuttle vectors are extremely limited due to an apparent cross-species barrier to plasmid replication, so-called plasmid tropism. This replication-barrier inhibits one species of *Chlamydia* from maintaining a vector derived from a different genetic background and is true for *C. trachomatis* plasmids from different biovars (Song et al., 2014; Wang et al., 2014). Shuttle vectors developed for *C. trachomatis* cannot therefore be used in the genetic manipulation of *C. muridarum* and vice versa. The inability to

engineer universal plasmid-based genetic tools for *Chlamydia* species places a greater emphasis on the need for enhancing the repertoire of available tools for *C. muridarum*.

1.6.3 *In vitro* plasmid loss in *C. muridarum*

The role of the chlamydial plasmid in growth and pathogenesis has been an area of increasing interest in recent years with much focus on *C. trachomatis* due to the use of a plasmid-gene as a diagnostic marker in nucleic acid amplification tests (Gaydos et al., 2003; Geelen et al., 2013; Harding-Esch et al., 2018; Masek et al., 2009), the rarity of naturally occurring plasmid-free isolates (An et al., 1992) and the use of the native plasmid in the development of plasmid-based genetic tools in clinically relevant strains (Keb and Fields, 2019; Mueller et al., 2016; Ouellette, 2018). *C. muridarum* will naturally lose its' plasmid *in vitro* (Skilton et al., 2018; Wang et al., 2014), yet in the absence of genetic tools for mutagenesis in *C. muridarum*, it is not surprising that *in vitro* plasmid loss in *C. muridarum* is not widely reported in the literature. Moreover, the few studies that have attempted to measure plasmid stability has mostly been in the context of genetic tools in *C. trachomatis*. The utility of these methods will be discussed in the next section.

Segregational stability of bacterial plasmids describes the processes responsible for stable plasmid inheritance into daughter cells upon replication. Structural stability refers to the acquisition of mutations over time and is not the focus of this research therefore segregational stability is referred to as plasmid stability throughout this thesis. For low copy number plasmids, which will include *C. muridarum*, plasmid stability is maintained through a combination of multiple systems. These typically include systems for plasmid replication, plasmid multimer resolution, active partitioning, and post segregational killing of plasmid-free cells (Sengupta and Austin, 2011). Although none of these mechanisms have been defined in *Chlamydia*.

The extent to which *in vitro* plasmid loss would inhibit the development of plasmid-based genetic tools in *C. muridarum* remains unknown due to the lack of a standardised, accurate method for measuring plasmid stability in *Chlamydia*. Given the potential for *in vitro* plasmid loss to decrease the efficiency of plasmid-based genetic tools in this species, the evidence for this phenomenon is presented in this section to highlight the need for a robust assay for measuring plasmid stability to improve the genetic tractability of this species.

1.6.3.1 Plasmid maintenance in *Chlamydia*

The mechanisms for regulating plasmid maintenance in *Chlamydia*, which include both replication and transfer, are unknown. The first sequencing of *C. trachomatis* plasmids in an LGV strain L2 (Hatt et al., 1988) and ocular strain E (Sriprakash and Macavoy, 1987), identified the origin of

replication with four 22bp tandem repeat sequences located in the intergenic region between *CDS1* and *CDS8*. These tandem repeat sequences are comprised of the following nucleotides: 5' TTTGCAACTCTTGGTGGTAGAC 3' preceded by an A-T rich sequence (Tam et al., 1992). Both *C. trachomatis* and *C. muridarum* contain four identical repeat sequences with the exception of a single SNP in the origin of replication of *C. muridarum* (Thomas et al., 1997). The high conservation of plasmid-genes shared between *C. trachomatis* and *C. muridarum* suggest that the mechanisms regulating plasmid maintenance in these species are largely homologous in nature.

The presence of repeat sequences in chlamydial plasmids suggests that plasmid replication in *Chlamydia* is controlled by binding of a replication (Rep) protein to repeat sequences, or iterons, as is the case for many theta-type replicating plasmids (Giraldo and Fernández-Tresguerres, 2004; Shintani et al., 2015). The open reading frames immediately downstream of the 22bp tandem repeat sequences are designated *CDS1* and *CDS2* have been proposed to function as Rep proteins based upon the size, sequence identity and net charge of their hypothetical protein products (Thomas et al., 1997). However, knockout of these plasmid-genes demonstrates that *CDS2* and not *CDS1* is essential for plasmid maintenance (Seth-Smith et al., 2009; Thomas et al., 1997; Wang et al., 2014). The number of repeat sequences may influence the plasmid copy number (Thomas et al., 1997). However, Seth-smith et al., (2009) showed that where loss of repeat sequence occurred, the plasmid copy number (plasmid copies per genome) was not affected.

The mechanisms that regulate high and low copy number plasmids in bacteria vary. Larger plasmids are typically maintained at low copy numbers (1-2 per cell) and require tighter control to achieve stable inheritance, whereas smaller plasmids may be present in higher numbers, which ensures their transfer to daughter cells. The plasmid copy numbers of *C. trachomatis* plasmids per genome ranges from 1-18 copies per cell (Last et al., 2014; Pickett et al., 2005). In *C. muridarum*, the wild type plasmid is maintained at a relatively low copy number at 1-4 copies per cell. Two separate studies have shown that plasmid copy number was 2-3 fold higher in transformants than the wild type strain in *C. muridarum* (Campbell et al., 2014; Liu et al., 2014a) and in *C. trachomatis*, higher plasmid copy numbers were measured during replication (Pickett et al., (2005). These variations in plasmid copies could be a result of harvesting EBs at different time-points during development (time-points ranged from 20h – 28h post infection), and the differences in the environmental conditions these strains were grown in (e.g., antibiotic selection). It could also indicate that *C. muridarum* and *C. trachomatis* plasmids are regulated by different mechanisms.

Plasmid-gene knockout studies identified five of the eight encoded plasmid genes *CDS2* (*pgp8*), *CDS3* (*pgp1*), *CDS4* (*pgp2*), and *CDS8* (*pgp6*) as essential for plasmid maintenance (Gong et al., 2013), but the exact mechanisms by which these proteins contribute to regulation of replication

and partitioning are unknown. Function of the plasmid-genes has been predicted based upon homology to known maintenance genes common to other plasmids. Of the genes shown to be essential for plasmid maintenance, *CDS2 (pgp8)* bears sequence homology to a recombinase of a phage family of proteins and is important for plasmid replication (Thomas et al., 1997), and has a role in plasmid tropism (Wang et al., 2014). *CDS3 (pgp1)* is a homologue of *E. Coli dnaB* helicase that unwinds double stranded DNA important for plasmid replication (Hatt et al., 1988). *CDS4 (pgp2)* has no known homologue, but knockout of this gene shows it is essential for plasmid maintenance (Song et al., 2013). *CDS7 (pgp5)* has homology to a plasmid partitioning protein and may also regulate chromosomal genes (Jones et al., 2020). As with *CDS4 (pgp2)*, *CDS8 (pgp6)* also has no known homologue and transcribes a protein unique to *Chlamydia* that is essential for plasmid maintenance (Gong et al., 2013; Mueller et al., 2016). Furthermore, *CDS2 (pgp8)* and *CDS7 (pgp5)* plasmid-genes encode an anti-sense RNA, which are known negative regulators of plasmid replication in a large range of bacterial species (Brantl, 2015).

1.6.3.2 Plasmid loss on growth and development

The impact of plasmid loss to *C. muridarum* growth and development has been disputed, with some studies failing to identify growth differences between plasmid-bearing and plasmid-free strains. However, plaque assays consistently show that plasmid-free *C. muridarum* produce smaller plaques at a lower frequency (Huang et al., 2015; O'Connell and Nicks, 2006; Skilton et al., 2018). In addition, O'Connell et al (2006) demonstrated that plasmid-cured *C. muridarum* showed reduced infectivity in cell culture that was overcome by centrifugation leading the authors to conclude that the plasmid is required for efficient attachment and/or uptake. A later study showed that plasmid cured *C. muridarum* had a 10-fold reduced infectivity (measured as IFU/ml) in mice genital tracts over the first ten days of infection compared to the plasmid-bearing parent, however, a difference was not observed after this time (O'Connell et al., 2007).

In attempts to reproduce the findings from previous studies, Skilton et al (2018) demonstrated growth defects in the plasmid-free *C. muridarum* using a range of methods to investigate the *in vitro* phenotypes of plasmid-free *C. muridarum*. The results of this study showed that plasmid-free *C. muridarum* produced smaller inclusions in cell culture measured by confocal microscopy, an extended eclipse period shown through comparisons of one-step growth curves, and a longer eclipse period and reduced yield measured by qPCR of the relative number of genomes over a time-course experiment *in vitro* (Skilton et al., 2018). Finally, transformation of the plasmid-free strain with a shuttle vector derived from the complete native *C. muridarum* Nigg plasmid restored the growth profile to that of the plasmid-bearing parent. The authors concluded that discrepancies between study findings were a result of either the inability to reproduce the experimental conditions or by only comparing the mature inclusion phenotypes (Skilton et al.,

2018). This evidence for the altered growth characteristics as a direct result of loss of the plasmid in *C. muridarum* indicate that the stability of transforming vectors should be an important consideration for the many mutagenesis approaches that rely on phenotypic screens to measure differences in growth and infectivity compared to a wild type parent strain.

1.6.3.3 Assessment of *in vitro* plasmid loss

C. muridarum will spontaneously lose its' plasmid *in vitro* and yield specific plasmid-loss inclusion phenotypes. One inclusion phenotype used to demonstrate plasmid loss in *C. muridarum* is the ability to stain inclusions for glycogen (O'Connell and Nicks, 2006). This is because plasmid gene *pgp4* (*CDS6*) regulates the expression of chromosomal gene *glgA* responsible for the accumulation of glycogen within chlamydial inclusions (Song et al., 2013). However, this method lacks sensitivity because a high background often makes this method difficult to distinguish between plasmid-free and plasmid-bearing inclusions.

Another plasmid-loss inclusion phenotype, specific to *C. muridarum*, is the "bull's-eye" or "donut" phenotype shown in Figure 1-5. Electron microscopy shows the bullseye to be devoid of any chlamydial cells (Skilton et al., 2018). Although not widely reported in the literature, this inclusion phenotype has been observed in the plasmid-cured *C. muridarum* strain Nigg (Nigg P-) as well as the wild type plasmid-bearing strain Nigg (Nigg P+) under antibiotic-free culture conditions (Wang et al., 2014). Skilton et al., (2018) reported a low sensitivity for detecting the bull's-eye phenotype using routine microscopy. Furthermore, this same study reported that expression of fluorescence within inclusions masks the bullseye phenotype (Skilton et al., 2018). It is likely that the low sensitivity of methods used for identifying inclusion phenotypes for detecting *in vitro* plasmid loss may explain why this phenomenon is not widely reported in the literature and highlights the need for a direct means for measuring plasmid loss in *C. muridarum* so that steps to limit plasmid loss *in vitro* can be taken.

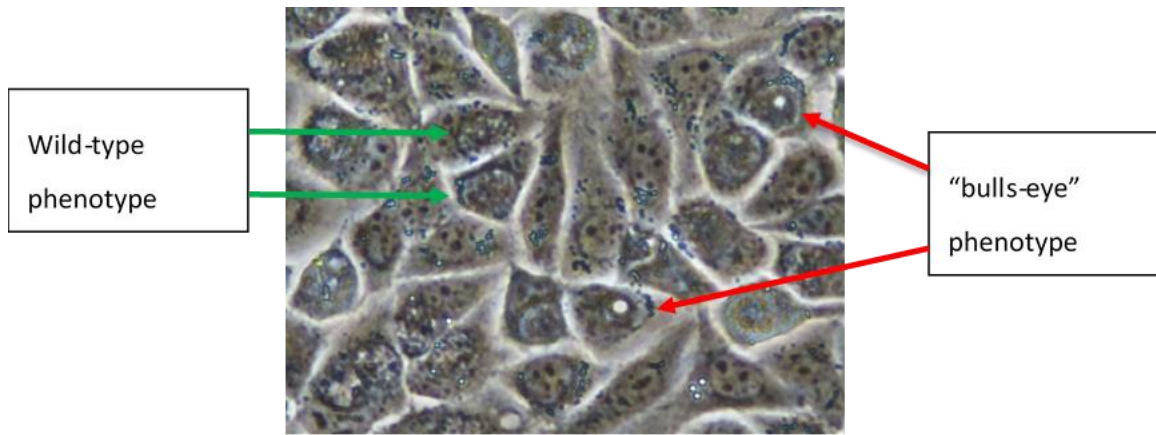


Figure 1-5 Photomicrograph of McCoy cells infected with wild type *C. muridarum* strain Nigg P+.

Cultures of wild type strain Nigg P+ imaged at 25 hpi. Inclusions displaying the plasmid-bearing wild type phenotype are indicated by green arrows and the plasmid-free phenotype are indicated by red arrows.

The use of fluorescence reporters expressed from plasmids transformed into *Chlamydia* to indicate the presence or absence of the plasmid within chlamydial inclusions is so far the only method that has been used for determining plasmid stability over serial passage in *C. trachomatis* and *C. pneumoniae*. In *C. pneumoniae*, Kensuke et al., (2018) compared the ratio of inclusions expressing GFP from the plasmid to antichlamydial lipopolysaccharide (LPS) antibody-stained inclusions. Another approach by Mueller et al., (2016) assessed the stability of a suicide vector in *C. trachomatis* by monitoring expression of GFP from the plasmid backbone and a second fluorescence reporter (mCherry) from an insertional gene cassette whereby loss of GFP over serial passage indicated loss of the vector backbone. The use of fluorescent reporters has the potential for use in *C. muridarum* to indicate plasmid-free inclusions by loss of fluorescence, however this has not yet been attempted.

The absolute quantification of plasmid copies presented as plasmid copies per genome has been investigated in *C. trachomatis* strains with relation to disease severity (Last et al., 2014), tissue tropism (Ferreira et al., 2013) and the context of investigating the effects of chemical curing agents (Pickett et al., 2005) and were measured either during the course of the developmental cycle or one-off comparisons of plasmid copies between different *C. trachomatis* strains in varied conditions. However, change in plasmid copy number over passage has not been used to assess plasmid stability in *Chlamydia*. The addition of absolute quantification of plasmid copies to phenotypic analyses has the potential to improve the sensitivity of an assay for measuring plasmid stability of transforming vectors over serial passage in *C. muridarum*. This will be explored in Chapter 3 with the aim to develop a robust plasmid stability assay for *C. muridarum*.

1.6.3.4 Determinants of plasmid instability in *C. muridarum*

Although antibiotic selection is typically used to enhance the stability of plasmids expressing antibiotic resistance genes *in vitro*, a number of studies have identified that expression of antibiotic resistance genes from a recombinant plasmid can destabilise the plasmid as a result of the stress induced by producing these proteins and the breakdown of the antibiotic itself (Silva et al., 2012).

Three independent groups have identified *in vitro* plasmid loss in *C. muridarum* when penicillin/ampicillin is used to select for shuttle vectors over serial passage (Liu et al., 2014a; Song et al., 2014; Wang et al., 2014). Wang *et al.*, (2014) identified *in vitro* plasmid loss as inclusions with a penicillin-sensitive phenotype and the absence of expression of green fluorescence in the plasmid-cured *C. muridarum* strain Nigg (Nigg P-) transformed with vector pSW2NiggCDS2 passaged in the presence of penicillin G. Vector pSW2NiggCDS2, was generated through recombination between the native *C. muridarum* strain Nigg plasmid (pCM) and *C. trachomatis* shuttle vector pGFP::SW2, resulting in a *C. trachomatis* backbone containing all eight plasmid-genes with the exception of *CDS2* which originated from pCM (Wang et al., 2014). The instability of pSW2NiggCDS2 in *C. muridarum* Nigg P- is consistent with the findings by Song *et al.*, (2014) who determined that the chlamydial backbone of the transforming shuttle vector must match the parental strain being transformed to isolate stable penicillin-resistant transformants in both *C. trachomatis* and *C. muridarum*. Finally, Liu *et al.*, (2014a) observed loss of GFP expression from inclusions after six consecutive passages with ampicillin selection when plasmid pGFP::CM, which contains the entire Nigg plasmid backbone including all eight intact plasmid-genes, was transformed into plasmid cured *C. muridarum* strain Nigg P-.

At present the only alternatives to the use of penicillin/ampicillin for the recovery and maintenance of transformants in *C. muridarum* include the antibiotic selectable markers *cat* (chloramphenicol selection) and the spectinomycin resistance marker (*aadA*) (Cortina et al., 2019; Liu et al., 2014a; Skilton et al., 2018; Song et al., 2014; Wang et al., 2014, 2019). Issues with vector segregation stability have not been reported with use of chloramphenicol or spectinomycin as an alternative to penicillin/ampicillin in *C. muridarum*, however, vector stability was not investigated in the rare cases where these antibiotics have been used.

Collectively these findings highlight the need for a robust plasmid stability assay for *C. muridarum* that can accurately determine the stability of shuttle vectors in a diverse set of conditions and to investigate the mechanisms of plasmid maintenance. This is required to identify an appropriate shuttle vector for the backbone of a self-replicating, inducible transposon mutagenesis approach in *C. muridarum*. Such an assay could provide a platform to investigate the means to destabilise

plasmids in this species and the determination of shuttle vectors that are inherently unstable in *C. muridarum* could be beneficial for a self-replicating transposon delivery vector that requires a mechanism of elimination post transposition.

1.7 Summary and research aims

Since the development of a robust transformation protocol for *Chlamydia*, the number of genetic tools with which to interrogate gene function have rapidly expanded in *C. trachomatis*. The same cannot be said of *C. muridarum*. Mutagenesis-based approaches for generating gene knock out mutants and stable chromosomal insertions in the chlamydial chromosome by methods using allelic exchange such as FRAEM and group II introns with TargeTron™ have made some progress elucidating gene functions for mutations with identifiable phenotypes in *C. trachomatis* and have yet to be adapted for use in *C. muridarum*. Furthermore, the methods for isolating mutants and performing the necessary functional analysis using *in vitro* and *in vivo* infection models remain laborious.

Unbiased genome-wide mutagenesis of bacterial genomes can generate large mutant libraries that can be used for forward and reverse genetic screens for identifying essential genes for growth or virulence and to detect new potential therapeutic and vaccine targets. All genome-wide methods require further assays to validate candidate genes identified, however, these methods are more efficient than targeted gene approaches, because they significantly reduce the number of genes that need validating. For *Chlamydia* spp chemical mutagenesis is the only validated method that bypasses the need for conventional methods that require transformation by recombinant DNA engineered as a tool for insertional gene inactivation, which is a major bottleneck for genetic approaches in obligate intracellular pathogens. This approach is as well, yet to be optimised for *C. muridarum*.

Transposon mutagenesis is the most efficient method for generating large-scale knock out mutant libraries in free-living extracellular bacteria to facilitate the discovery of essential genes through the screening for the loss of genes in the pooled mutant library in diverse conditions. The full potential of transposon mutagenesis to generate near-saturation or saturated mutant libraries has not yet been achieved in *Chlamydia*. The first vector system, using a single suicide vector, in *C. trachomatis* and *C. muridarum* generated only small numbers of unique mutants after repeated rounds of transformation (LaBrie et al., 2019; Wang et al., 2019). The limitations of this vector system to generate large numbers of mutants was likely a result of both low transformation efficiency and the inability to replicate in *Chlamydia* causing transposition to occur before replication and therefore generate single mutant clones within individual inclusions.

It is hypothesised, therefore, that the use of a replicating vector that can be stably maintained over serial passage in order to expand the number of bacterial cells that contain a transposon-delivery vector prior to transposon transposition will be able to generate large transposon mutant libraries in *Chlamydia* (O'Neill et al., 2021; Skilton et al., 2021). In *C. muridarum*, this will require a single replication-proficient vector that carries both transposon and transposase under the temporal control of an inducible promoter system. In addition, the vector will require elimination post transposon transposition in order that transposon mutants can be isolated.

The stability of potential plasmid-based genetic tools in *C. muridarum* is paramount to the success of a conditionally replicating vector for transposon mutagenesis. As discussed in this introductory chapter, *C. muridarum* will spontaneously lose its' plasmid in antibiotic-free cell culture and certain transforming vectors have been shown to be unstable in penicillin G selection over passage. The stability of the native and transforming plasmids over serial passage has only been measured by one group in *C. muridarum*, who measured the plasmid loss frequency (the proportion of plasmid-free cells) using iodine staining of inclusions; a subjective method with low sensitivity (Russell et al., 2011). Currently, no standard, sensitive and reliable assay for measuring plasmid stability exists in *Chlamydia*. To investigate the stability of available replicating vectors in *C. muridarum*, a robust assay for measuring plasmid stability will be developed. This will form the basis of the first results chapter of this thesis. The development of a plasmid stability assay will help to identify which vectors can be stably maintained in *C. muridarum* to fulfil the first requirement of a self-replicating transposon delivery vector.

As discussed previously, the ideal transposon delivery vector would contain a backbone that can be eliminated post transposon transposition to optimise stability of the transposon insertion. To address the lack of a conditional vector in *C. muridarum*, the second results chapter will investigate a means to destabilise the vector backbone by investigating the stability of vectors predicted to be less stable, because they contain either deletions of non-essential plasmid-genes or they contain mostly plasmid-genes derived from *C. trachomatis*, in selective and non-selective conditions over serial passage. The stability of potential transposon-delivery vectors over serial passage will be analysed using the plasmid stability assay developed in the course of this work.

The final results chapter aims to engineer a transposon delivery vector that can be recovered and maintained over passage in *C. muridarum* and to functionally validate the chosen transposon system in *E. coli*.

The ability to measure plasmid stability over passage *in vitro* will provide a means to test the stability of any future plasmid—based genetic tool for *C. muridarum* including the addition of new antibiotic-selectable markers as they are optimised for use in this species. An improved understanding of the plasmid-gene requirements for stable plasmid maintenance *in vitro* in *C.*

Chapter 1

muridarum will inform the design of future genetic tools for this species. Finally, the development of a replication-proficient inducible transposon-delivery vector for *C. muridarum* will provide progress towards achieving saturation mutagenesis to define essential genes in this important pathogen. Taken together, these developments improve the genetic tractability of *C. muridarum*.

The research aims, therefore, are as follows:

1. Develop a robust plasmid stability assay for *C. muridarum* to characterise the stability of replication-proficient vectors over serial passage with and without antibiotic selection in this species.
2. Investigate the stability of a range of shuttle vectors in *C. muridarum*, including those predicted to be unstable that contain non-essential plasmid-gene deletions and a *C. trachomatis*-derived backbone, to identify a minimal vector that can carry the transposon-transposase cassette, as well as a potential mechanism for plasmid elimination.
3. Engineer and functionally validate a replicative, inducible transposon delivery system in *E. coli* that can be transformed into and recovered in *C. muridarum*

Chapter 2 Methods

2.1 Bacterial strains and cell lines

McCoy cells were obtained from the National Collection of Type Cultures, Public Health England (NCTC, Public Health England, UK). The *C. muridarum* wild type plasmid-bearing strain, Nigg Atherton II, was provided and plaque-purified by Professor Kyle H Ramsey (Chicago) and referred to as Nigg P+ in this thesis. The Nigg P+ strain was originally provided by Prof. A Baron to Prof A Rank (Fox et al., 2006). Prof A. Rank provided the strain to Prof Kyle Ramsey. *C. muridarum* Nigg P+ was cured of its' plasmid with novobiocin and performed by Dr Yibing Wang as described previously (Wang et al., 2014). The plasmid-free Nigg strain referred to as Nigg P- was plaque-purified three times and the sequence verified by whole genome sequencing and PCR (Skilton et al., 2018).

Escherichia coli (*E. coli*) strains were obtained from the culture collection at the University of Southampton. Shuttle vector pGFP::Nigg was generated by Rachel Skilton as previously described (Skilton et al., 2018). Recombinant plasmid pSW2NiggCDS2 was generated by Dr Yibing Wang as previously described (Wang et al., 2014). Plasmids pNiggCDS56Del and pNiggCDS567Del containing deletions of plasmid genes *CDS5*, *CDS6* and *CDS7* were cloned from pGFP::Nigg by Dr Yibing Wang (data not published). All plasmids were transformed into *E. coli* strain DH5 α by heat shock method described in section 2.9.2 for storage and for propagation prior to de-methylation by a methyltransferase-deficient (*dam*- and *dcm*-) *E. coli* strain GM2163 as required for transformation into *Chlamydia*.

Stocks of *E. coli* transformed with *E. coli* - *C. muridarum* shuttle vectors were produced by culturing the organisms to logarithmic growth phase in liquid culture with selection specific for each vector as described in section 2.7.2. 20ml culture was pelleted and re-suspended in 4x 1ml aliquots of phosphate buffered saline (PBS) solution containing 10% sterile glycerol and stored at -70°C. When required, the stock was thawed on ice and a loop of bacteria was taken and streaked onto agar plates containing selection under a flame then incubated at 37°C overnight. Plates were then sealed and refrigerated at 4-6°C for no longer than 1 month to ensure the integrity of the antibiotics in agar. Individual colonies were selected from the streaked plates and either passaged onto new agar plates or transferred for growth in liquid culture for downstream applications.

Stocks of *C. muridarum* were produced by culturing these organisms in McCoy cells and harvested at the end of the logarithmic growth phase at 28 hpi as described in section 2.4. Purified

Chapter 2

Chlamydia EBs were suspended in 1ml PBS and mixed with 1ml 4x sugar phosphate solution (4SP) and stored at -70°C.

The bacterial strains used in this project and their relevant features are listed in Table 2.

Table 2 Bacteria used in this study

| | Features | Reference/source |
|-------------------------|--|---|
| <u><i>E. coli</i></u> | | |
| DH5α | Host for maintenance of plasmid vectors | (Hanahan et al., 1991). ThermoFisher |
| GM2163 | Methyltransferase (dcm-/dam-) deficient host | The culture collection, (University of Southampton, Prof. I Clarke) |
| Q358 | Host contains the complete Lac operon | (Karn et al., 1980). Gibco BRL |
| <u><i>Chlamydia</i></u> | | |
| Nigg Atherton II | Wild type plasmid-bearing <i>C. muridarum</i> strain | (Skilton et al., 2018). Plaque cloned by Dr Kyle Ramsey (Chicago) |

2.2 Tissue culture

McCoy cells grown to sub-confluence in a 75cm² tissue culture flask (T₇₅) in 15mL Dulbecco's Modified Eagles Media (DMEM) (1x Glutamate) supplemented with 10% foetal calf serum (FCS) were split for continuous passage twice weekly in a Class II safety cabinet. DMEM contains a red indicator dye that changes colour when contaminated (acidity increase changes red to orange), therefore, colour change was monitored to rule out contamination and increased levels of carbon dioxide. Cells were also examined for signs of abnormal growth or contamination by phase contrast microscopy.

Cells were split into two T₇₅ flasks at each passage. The fraction of cells (mL) to media (mL) was 1:12 for a two-day incubation and 1:14 for a three-day incubation. Cells were washed with 1x PBS to remove factors present in FCS that inhibit Trypsin Ethylenediaminetetraacetic acid (EDTA)

activity on cellular bonds and thus cell dissociation. Cells were then incubated at 37°C for 5 minutes with 1.5mL TE to facilitate detachment of cells from the flask and each other. DMEM + 10% FCS applied directly to detached cells aided further removal from the flask bottom. Cells were repeatedly aspirated in and out of a serological pipette placed flat against the base of the flask to separate any clumps. DMEM + 10% FCS was added to bring cell suspension to the required volume and cells were mixed well before direct transfer into the media of new T₇₅ flasks (a total of 15ml per T₇₅). Cells were then incubated at 37°C / 5% CO₂ with flasks placed flat with loosened lids to facilitate gas exchange.

For *Chlamydia* infection, the fraction of cells (mL) to media (mL) taken from a T₇₅ was 1:2 in a total of 5ml DMEM + 10% FCS for an overnight incubation at 37°C / 5% CO₂ in T₂₅ tissue culture flasks (25cm²).

2.3 Microscopy

McCoy cells and cells infected with *C. muridarum* were visualised by phase contrast microscopy using a Nikon eclipse TS100 inverted microscope accessorised with fluorescence filters. A Nikon DS-Fi1 camera fitted to the microscope was used for image capture. Cells were visualised at 20x and 40x magnification with images taken at 20x magnification for counting inclusions.

McCoy cells were routinely checked for signs of normal growth such as presence of spherical cells (dividing cells) and cellular processes extending out between cells, occasional syncytia (characteristic of McCoy cells in cell culture), and signs of contamination such as media colour change and presence of foreign entities and signs of stress such as cellular debris floating above the monolayer.

2.4 *Chlamydia* cell culture

2.4.1 Infection of tissue culture cells

All experimental procedures with *C. muridarum* were performed in a Class II safety cabinet. Bacterial inoculum was added directly to the culture media on top of McCoy cell monolayers and centrifuged at 754g for 30 minutes at 25°C to initiate entry into host cells. After centrifugation, the media was replaced with new growth media, DMEM + 10% FCS (5mL / T₂₅) containing cycloheximide (1µgml⁻¹) to arrest McCoy cell division as well as the required antibiotics for selection of transforming plasmids. Infected McCoy cells in T₂₅ flasks were incubated at 37°C / 5% CO₂.

2.4.2 Harvest of mature elementary bodies

Mature *C. muridarum* EBs harvested at 28 hpi. at the end of the logarithmic growth phase (Skilton et al., 2018) when inclusions were approximately the same size as the host cell, and movement of EBs was clearly visible by microscopy. Cells were removed from the T₂₅ flask bottom using a cell scraper. The resulting cell suspension was centrifuged at 2831g for 10 minutes at room temperature (RT) to separate the McCoy cells and bacterial cells (in pellet) from the media (supernatant). Supernatant was discarded and the pellet re-suspended in 1mL chilled 10% PBS solution. Host cell lysis was performed by vortex with glass beads for 1 minute to release EBs from cells. Cellular debris was removed by centrifugation at 233g for 5 minutes at 25°C. The supernatant containing EBs was diluted 1:1 with 4SP and stored at -70 °C.

2.5 Titration by X-gal staining

The bacterial load in harvested inoculum was quantified by titration using 5-bromo-4-chloro-3-indolyl-beta-D-galacto-pyranoside (X-gal) (ThermoFisher) stained inclusions as previously described (Skilton et al., 2007). Confluent McCoy cell layers were grown in 96 well trays (96WT) for infecting with *Chlamydia*. Monolayers in 96WT were infected with *Chlamydia* as described in section 2.4.1 with the following modifications. A series of 10-fold serial dilutions of harvested *Chlamydia* stocks were prepared in 1.5ml micro-centrifuge tubes with DMEM+10% FCS, enough for duplicates at each dilution with 100µl per well. Dilutions ranged from 10⁻¹ to 10⁻¹⁰ with one negative control well containing only media.

The infected cells were incubated at 37°C and 5% CO₂. Once *Chlamydia* inclusions had reached the plateau phase of growth in their developmental cycle, before host cell lysis, the growth media was removed, and cells washed with 1x PBS solution and then fixed with ice cold methanol for 10 minutes at -20°C. Fixed cells were then washed three times with 1x PBS for two minutes. Cells were then either incubated for 40 minutes at 37°C or refrigerated overnight at 4°C with a 1:200 dilution of *Chlamydia* genus-specific LPS monoclonal antibody Mab29 in 1x PBS (Skilton et al., 2007). Unbound primary antibody was removed with three washes with 1x PBS for two minutes. Next, cells were incubated with a 1:1000 dilution of anti-mouse IgG, heavy and light chain specific (goat) β-galactosidase conjugate (Merck) with 1x PBS for one hour at 37°C. Unbound secondary antibody was then removed with three two-minute washes with 1x PBS. X-gal stock (50mgml⁻¹) (0.05g X-gal powder dissolved in 1ml Dimethylformamide) and X-gal staining solution (potassium ferricyanide (0.016g/10ml PBS), potassium ferrocyanide (0.021g/10ml PBS), magnesium chloride 6-hydrate (0.004g/10ml PBS) was filter sterilised and stored at 4°C. *Chlamydia* binding Mab29 were then stained blue with 100µl/well of X-gal staining solution containing X-gal (1µgml⁻¹) over four hours incubated at 37°C and 5% CO₂. Inclusions in each well were viewed by phase contrast light

microscopy and counted. Wells were discounted where the number of inclusions exceeded 100-200 per field imaged at 40x magnification. Counts were converted to concentration of inclusions per 100 μ l with the assumption that one EB will form one inclusion. To calculate the number of EBs in 100 μ l, the number of inclusions were multiplied by the dilution factor for each well and then averaged across all wells at each dilution. This average inclusion count (\sim EB count) per 100 μ l was then converted to the number of inclusions per millilitre to give the final titre of infectious forming units (IFU) as IFUml⁻¹.

2.6 Quantifying infection efficiency

The efficiency of infection of host cells by chlamydial EBs - the infection-forming unit (IFU) - can be quantified by calculating the multiplicity of infection (MOI) where the MOI describes the number of infectious EBs added per cell.

Infecting a cell monolayer with an MOI=1 describes the infection of host cells with IFU at a ratio of 1:1. However, a proportion of bacterial cells will always fail to infect. The number of infectious particles that will infect and replicate within host cells is described by a Poisson distribution that demonstrates statistically the percentage of cells that will become infected with either one or more infectious particles. Statistical modelling of infection at MOI=1 predicts that approximately 60% \pm 10% cells in a monolayer will become infected, with the greatest proportion receiving one EB (S. Lanham et al., 2001). Subsequently, increasing the MOI increases the proportion of host cells which will become infected with more than one EB. As it is not possible to calculate the exact number of infectious *Chlamydia* EBs that go on to replicate within a host cell as a result of inclusion-fusion by homotypic fusion, infections were performed at MOI=1 to limit the number of cells infected with more than one EB (Hackstadt et al., 1999; Weber et al., 2016). An MOI=1 was also regarded optimal for infectivity assays to standardise assay conditions.

Two methods were deployed to calculate MOI as described below. Estimates of MOI were calculated in Chapter 3 of this study and were used to achieve a consistent infection more rapidly compared with the more accurate method for quantifying MOI that measures the number of infection-forming units (titre) with a 2–3-day delay for results. More accurate determination of MOI was used for the plasmid stability assay in chapter 4 of this study.

2.6.1 Estimating MOI using proportion of infected cells

The MOI was determined from an approximation of total infectivity measured as the percentage of infected McCoy cells. To calculate the proportion of McCoy cells that were infected, inclusions expressing GFP were imaged under UV light (with a green filter) (as described in section 2.3) and

Chapter 2

counted. Then the proportion of infected McCoy cells was determined per field from a total of McCoy cells in a T₂₅ was estimated to be 2×10^6 cells which was based on the average number of HeLa 229 cells that will form a confluent monolayer in the same volume flask. The average percentage of McCoy cells containing an inclusion was calculated from two fields imaged at 20x magnification per T₂₅ flask. The volume of inoculum was adjusted accordingly to achieve a mean proportion of $60\% \pm 10\%$ infected cells. The volume which achieved this infectivity (MOI=1) was then used for subsequent passaging of chlamydial EBs at a consistent MOI=1. The consistency of the infection was confirmed by a consistent mean proportion of infected cells at $60\% \pm 10\%$.

2.6.2 *Quantifying MOI using titres*

For accurate determination of MOI for the serial passage of *C. muridarum* strains at MOI=1 in Chapter 4, the titre (IFUml⁻¹) for each inoculum was calculated by titration, as described in section 2.5, to determine the volume of inoculum required to infect 2×10^6 McCoy cells with IFU at a 1:1 ratio.

The concentration of inclusion forming units IFUml⁻¹ was then used to determine the volume of inoculum required to infect cells at a given MOI where an MOI=1 describes a ratio of 1:1 (IFU: host cells).

2.7 *E. coli* cell culture

2.7.1 *Luria broth-agar plate preparation*

Luria broth (LB) with agar (1g tryptone, 1g sodium chloride, 2g yeast, 3g agar) was made up to 200ml in deionised water (dH₂O) and sterilised in a pressure cooker for 15 minutes at 140°C. LB was cooled to 56°C in a water bath before the addition of antibiotics to prevent denaturing at high temperatures. At 56°C LB agar is maintained in a liquid state to facilitate transfer into culture plates. The liquid LB at 56°C was supplemented with antibiotics for selection of transformants using the following final concentrations: ampicillin (50µgml⁻¹), chloramphenicol (30µgml⁻¹), erythromycin (150µgml⁻¹), and spectinomycin (50µgml⁻¹), where appropriate. 20ml LB agar was transferred to each culture plate. All plates were prepared and set in a class II cabinet to maintain sterile conditions. Any moisture was evaporated from plate lids before being sealed with parafilm to prevent environmental contamination and stored refrigerated at 4-6°C.

2.7.2 *Liquid culture*

LB (1g tryptone, 1g sodium chloride, 1g yeast) was made up to 200ml with dH₂O and sterilised in a pressure cooker for 15 minutes at 140°C then left to cool to RT. Chloramphenicol and ampicillin were added to liquid cultures at final concentrations as listed above in 2.7.1. A well isolated *E. coli* colony was selected from LB agar culture plate using a sterile loop and swirled in the liquid culture broth for a minimum of 5 seconds in sterile conditions under a flame.

2.8 Preparation of competent *E. coli* cells

LB was inoculated with a colony of the desired *E. coli* strain to be made competent and grown overnight at 37°C with shaking. 1ml overnight culture was added to 99ml LB and grown to an optical density (OD) $OD_{(600nm)} = 0.5$ with shaking at 37 °C, at which point the culture was chilled on ice for 20 minutes then centrifuged at 4°C at 5000 x g for 10 minutes. The pellet was re-suspended in 20 ml ice-cold 0.1M CaCl₂, and then incubated on ice for 30 minutes. The cell suspension was centrifuged again at 4°C at 5000 x g for 10 minutes. The pellet was re-suspended in 5ml ice-cold 0.1M CaCl₂ with 15 % glycerol, then aliquoted with 200µl transferred into microcentrifuge tubes (1ml) tubes and stored at -80 °C.

2.9 Transformation

2.9.1 *Transformation of C. muridarum with calcium chloride*

Transformation of *C. muridarum* Nigg P- was performed using the calcium chloride (CaCl₂) method developed by Wang et al (2011) with adjustments made to the volume of culture flask used for infection of transformed EBs and the experimental procedure for combining the plasmid DNA/*Chlamydia* DNA/CaCl₂ mixture to McCoy cells whereby the mixture was added to near-confluent McCoy cell monolayers in a T₂₅ culture flask at MOI = 3. For vectors with a backbone containing a spectinomycin resistance gene, *aadA*, instead of the penicillin-resistance gene, *bla*, the selection of transformants at passage 1 (T₁) and the proceeding passages up to passage 3 (T₃) was modified accordingly.

The experimental method was as follows: *Chlamydia* EBs (6×10^6 IFU) were pelleted at 14,000 x g for 2 minutes then re-suspended in 150µl CaCl₂ (10mM Tris and 50mM CaCl₂ at pH 7.4). In a separate microcentrifuge tube, 6µg plasmid DNA was diluted in 100µl CaCl₂ then mixed with the *Chlamydia* DNA in CaCl₂ in a total volume of 250 µl. This mixture was incubated at RT for 25 minutes. Culture media (DMEM + 10% FCS) was removed with a pipette from McCoy cells in two T₂₅ culture flasks and replaced with 1.5ml CaCl₂ buffer. The plasmid DNA/*Chlamydia* DNA/CaCl₂

Chapter 2

mixture was split equally across the two T₂₅ flasks and incubated at RT for 20 minutes. 5ml DMEM supplemented with 10% FCS and 1µgml⁻¹ cycloheximide was added to each T₂₅ flask which were then centrifuged at 754 x g for 30 minutes. The infected flasks were incubated for 28 hours at 37 °C and 5% CO₂ then harvested as previously described in section 2.4.2. The purified EBs were stored in an equal volume of 4SP at -80 °C. This sample was labelled T₀. Transformants were selected for through infection of McCoy cells with the entire T₀ sample split across two T₂₅ flasks and the addition of 1µgml⁻¹ cycloheximide and 10 Uml⁻¹ penicillin G or 500µgml⁻¹ spectinomycin, as per the requirements of the transforming vector, to the culture media. The infection and harvesting protocols are previously described in section 2.4. The EBs from passage 1 were harvested at 28 hpi. and labelled T₁. *Chlamydia* was passaged to passage 3 under selection. Transformants were identified using phase contrast microscopy as described in section 2.3.

2.9.2 Transformation of *E. coli* by heat shock

1µl Plasmid DNA (10ngml⁻¹) was added to 50µl competent *E. coli* cells (thawed on ice), then chilled on ice for 20-30 minutes. The cells were then heat shocked by placing in a water-bath at 42°C for 45 seconds which facilitates DNA uptake by the *E. coli* cells. Transformed *E. coli* were then chilled on ice for 5 minutes before being added to 500µl LB and incubated on a shaker for 1 hour at 37 °C to expand. The bacterial culture is centrifuged at 5000 x g for 1 minute, and the pellet re-suspended in 40µl supernatant required for spreading over one agar plate containing the necessary antibiotic selection as indicated by the resistance gene present in the plasmid DNA. Bacterial suspension was spread onto agar plates under a flame and incubated over night at 37°C to grow.

2.10 DNA extraction

2.10.1 Plasmid DNA

Each strain of *E. coli* with their respective plasmids were streaked onto LB and agar plates containing at least one of the antibiotics for selection of the plasmid. Well isolated colonies were selected and grown overnight in LB supplemented with chloramphenicol, with shaking at 37°C. 5 ml overnight culture was pelleted at 4°C for plasmid DNA extraction using the Wizard®Plus SV Miniprep DNA Purification system (Promega) or the SmartPure Plasmid Kit (Eurogentec). 50ml overnight liquid culture was pelleted at 4°C for plasmid DNA extraction using the PureYield™ Plasmid Midiprep system (Promega).

2.10.2 Genomic DNA

Whole genomic DNA (gDNA) was extracted from *C. muridarum* stocks (purified EBs stored in 4SP) for quantification of plasmid DNA and chromosomal DNA by alkali lysis of *C. muridarum* cells using ammonium hydroxide solution (2M) (ThermoFisher) to precipitate the total DNA in a method previously described for gDNA extraction of *C. trachomatis* from clinical samples and harvested *Chlamydia* EBs (Stuart Lanham et al., 2001; Pickett et al., 2005). This method is preferable over the use of a genomic DNA extraction kits because it is fast and can be used in a 96-well format for rapid and multiple sample processing. The following modifications were made: 800µl harvested EBs were centrifuged at 14,000 x g for 2 minutes. The pellet was re-suspended in 90 µl of the supernatant and then mixed with 10µl NH₄. The liquid was heated at 96°C until the pellet was dry for ~1 hour. The gDNA was re-suspended in 100µl nuclease-free water and frozen at -20°C for downstream applications.

2.11 Quantification of DNA concentration

The yield (ngµl⁻¹) of purified DNA for cloning purposes and qPCR experiments was analysed with a Nanodrop One spectrophotometer (ThermoFisher) according to manufacturer instructions.

Estimates of purity were determined spectrophotometrically by measurement of A260/A280 ratios. Plasmid quantification was automated, carried out by measurement of Absorbance A260 using a spectrophotometer.

2.12 Polymerase chain reaction

For all PCR reactions, forward and reverse primers were used at a final concentration of 10 nM. Template for one PCR reaction ranged from 10-40ng plasmid DNA. DNA was substituted for dH₂O as a negative control. Standard PCR reactions were made up to a total volume of 20µl per reaction or 50µl per reaction when performing gel extractions of the PCR product using nuclease-free water.

End –point PCR was performed on the Veriti 96 well Thermo Cycler (Applied Biosystems). Phusion Flash High-Fidelity PCR Master Mix (ThermoFisher) was used for cloning because of its high-fidelity proofreading DNA polymerase and ability to produce high yields in relatively short protocols (e.g., extension times of less than 15 seconds). This was ideal for cloning PCR where high accuracy is needed for amplification of specific sequences. BioMix™ Red (Bioline) was used for bacterial colony screen PCR and uses a heat stable Taq DNA polymerase and contains a red

Chapter 2

dye for gel visualisation. The bacterial colony screen did not require the level of accuracy of that of the qPCR or cloning PCR.

Thermo-cycling conditions for end-point PCR were as described in Table 3.

Table 3 Thermo-cycling conditions for end-point PCR

| Experiment | Polymerase Activation (1 cycle) °C / min | No. of Cycles | Denature | | Anneal | | Extend | | End cycle | | Hold °C |
|------------|---|------------------|----------|-----|--------|-----|--------|-------------------|-----------|-----|------------|
| | | | °C | sec | °C | sec | °C | sec | °C | sec | |
| 1 | 98 / 5 | 35 | 98 | 2 | 50 | 5 | 72 | 15 sec / kb | 72 | 60 | 4 |
| 2 | 94 / 5 | 35 | 94 | 30 | 55 | 30 | 72 | 15-30 sec / kb | 72 | 10 | 4 |

1. Phusion Flash protocol for a) primer optimisation b) standard PCR and c) restriction-site cloning PCR
2. BioMix™ Red (Bioline) used for bacterial colony screen PCR

2.13 Gel electrophoresis

DNA was mixed with 5 x loading buffer (total volume loaded was 10 µl for all gels except for gel extractions where 50µl was loaded) into 1% agarose (Fisher Scientific) gels (0.8% agarose gels were used for gel extraction). Agarose was dissolved in Tris acetate EDTA (TAE) buffer (40mM Tris, 20mM acetic acid, and 1mM EDTA). 0.1% SYBR™ safe DNA Gel stain (Invitrogen™) was added to visualise DNA under UV light.

2.14 Plasmids

A summary of all plasmids made and used in this project is provided in Table 4.

Table 4 Plasmids used in this study for the genetic manipulation of *C. muridarum*

| Plasmid name | Size (kb) | Antibiotic resistance gene(s) | Reference |
|--|-----------|-------------------------------------|-------------------------|
| pGFP::Nigg | 11.494 | <i>cat, bla</i> | Skilton et al., 2018 |
| pRPF215 | 9.247 | <i>cat, ermB</i> | Dembek et al., 2015 |
| pASK-IBA3c | 3 | <i>cat</i> | IBA-Lifesciences |
| P2TK2 _{Spec} -Nigg mCh(Gro)L2 | 10.433 | <i>aadA</i> | Cortina et al 2019 |
| pSW2NiggCDS2 | 11.536 | <i>cat, bla</i> | Wang et al., 2014 |
| pNiggCDS56Del | 10.364 | <i>cat, bla</i> | Generated by Dr Y. Wang |
| pNiggCDS56Del | 9.467 | <i>cat, bla</i> | Generated by Dr Y. Wang |
| pNiggHimar | 14.816 | <i>cat, bla, ermB</i> | This study |
| pNiggHimar_GFP_ΔTn | 13.813 | <i>cat, bla</i> | This study |
| pNiggHimar_mCh_ΔTn | 12.732 | <i>aadA</i> | This study |
| pNiggHimar_GFP_ΔTpase | 14.344 | <i>cat, bla, ermB</i> | This study |

2.15 Statistical tests

Statistical analyses were performed in IBM SPSS statistics 27. Shapiro-wilk test for normality were performed on the plasmid copy number data including technical repeats (n=4) presented in Figure 3-4b, also for plasmid copy number data presented in Figure 4-9 (n=6). One way ANOVA was performed on plasmid copy number data presented in Figure 3-9b (n=6). Linear regression was performed on plasmid copy number data and frequency of plasmid loss data for all strains in Figure 4-11. Tests for normality were performed on this data as part of the linear regression analysis.

Chapter 3 Determination of plasmid segregational stability in *C. muridarum*

3.1 Introduction

To develop a self-replicating transposon-delivery vector that can be expanded over serial passage for *C. muridarum* requires a vector backbone that can be stably passed under antibiotic selection and a mechanism for plasmid elimination post transposon transposition. Stable maintenance will facilitate expansion of bacterial cells containing the vector to increase the number of unique mutants generated and plasmid elimination is required to reduce the likelihood of secondary transposition events.

C. muridarum naturally loses its plasmid *in vitro* (O'Connell and Nicks, 2006; Skilton et al., 2018) and there are very limited antibiotic selection markers available for the recovery and passage of transformants (Campbell et al., 2014; Cortina et al., 2019; Liu et al., 2014a; Skilton et al., 2018; Song et al., 2014). At the time of this study, shuttle vectors containing only *bla* and/or *cat* genes conferring resistance to β -lactams and chloramphenicol acetyltransferase respectively were available. Of these two antibiotic resistance gene markers, the use of penicillin for positive selection of vectors containing *bla* demonstrated vector instability over serial passage (Liu et al., 2014a; Song et al., 2014). However, a standardised and robust means to investigate plasmid stability does not yet exist for *Chlamydia* spp. Therefore, the focus of the work presented in this chapter was to develop a robust and reproducible assay with which to investigate the stable inheritance of recombinant plasmids in this species.

Traditional assays will start with a population of cells that all contain a plasmid and measure the proportion of plasmid free cells accumulated over multiple generations, termed the plasmid loss rate (Lau et al., 2013). This is typically achieved using counter-selection of plasmid-free cells in free-living gram-negative bacteria, such as the *aph-parE* cassette in *S. typhimurium* or the *tetAR*-chlortetracycline system used in *E. coli* (Lobato-Márquez, 2020; Maloy and Nunn, 1981).

Standardised plasmid stability assays do not currently exist for obligate intracellular bacteria. In free-living bacteria, that are easily sub-cultured over multiple generations, counter-selection for plasmid-free cells provides a means to isolate the plasmid-free population making it easy to quantify the plasmid loss rate simply by plating out subcultures of cells during logarithmic growth phase onto selective and non-selective LB/agar plates to count the proportion of the plasmid-free population (Lobato-Márquez, 2020; Maloy and Nunn, 1981; S et al., 2017).

Chapter 3

Because *Chlamydia* replicate within an intracellular membrane-bound inclusion and the dividing RB form cannot be sub-cultured, it is not possible to isolate the plasmid-free population over generations of RBs during the developmental cycle with the current cell culture methods available.

With the assumption that a starting stock of *Chlamydia* could be generated that contain only plasmid-bearing cells, quantification of plasmid copy number (plasmid copies per chromosome) during logarithmic growth could provide a direct means to study plasmid loss in these microorganisms. However, this approach assumes that there is a direct relationship between the rate of plasmid loss during one developmental cycle and the proportion of EBs (the infectious forming unit) that end up plasmid-free at the end of the growth cycle. Given that plasmid-copy number in RBs has been shown to be approximately double that found in EBs (Pickett et al., 2005) the relationship between plasmid loss during logarithmic growth and over serial passage may not be straight forward and would be difficult to test experimentally and subsequently to model. Additionally, there are no alternative methods that could validate plasmid loss rate measured in RBs. This is because identifying plasmid-free inclusion phenotypes by microscopy techniques is only really feasible in the larger mature inclusions that contain EBs (O'Connell and Nicks, 2006; Skilton et al., 2018).

Mature inclusions in *C. muridarum* display a unique plasmid-free phenotype called the bullseye which describes a circular cell-free 'hole' with a defined dark boarder of chlamydial cells that is identifiable by simple phase contrast microscopy. The ability to quantify changes in the proportion of plasmid-free cells within a culture over serial passage offers another means to assess plasmid stability in *Chlamydia* alongside molecular approaches that quantify plasmid copy number. Together, therefore, these factors make the EB a preferable target for measuring plasmid stability over generations of EBs in *Chlamydia*.

There are, however, several limitations to an assay that measures plasmid stability in EBs. In this scenario one passage of EBs artificially represents one generation. As previously discussed, the relationship between plasmid loss in the RB and the number of EBs which end up plasmid-free is unknown. Furthermore, several technical issues make it difficult if not impossible to determine the proportion of plasmid-free EBs which go on to infect cells in the next passage. One such limitation is that *C. muridarum* routinely requires centrifugation onto cell monolayers to aid infection which increases the likelihood that plasmid-free cells will go on to infect at subsequent passage. Therefore, measurement of plasmid loss in mature EBs instead of over generations of RBs may reduce the accuracy of any assay.

Finally, generating a starting stock where all EBs contain a plasmid is potentially difficult because of the three selectable markers that are available for use in *C. muridarum*, plasmids are

potentially unstable in penicillin selection (Liu et al., 2014a; Song et al., 2014; Wang et al., 2014), although plasmid stability under penicillin selection has yet to be investigated in this strain. Penicillin has a bacteriostatic action on *Chlamydia* cells, which arrests EB to RB conversion and this process is reversible upon removal of the antibiotic. Therefore, there is always the chance that a proportion of plasmid free cells are passed under penicillin selection. Thus, it could be hypothesised that the use of the *bla* with penicillin is unlikely to be appropriate for use as positive selection to limit the growth of plasmid-free bacteria needed to generate standard inocula.

Chloramphenicol was demonstrated to be bactericidal at high concentrations in *C. trachomatis* by inhibiting the incorporation of sphingomyelin into the outer-membrane which is required to evade lysosomal degradation by the host cell (Scidmore et al., 1996). Therefore, it can be hypothesised that positive selection for transformants with chloramphenicol at bactericidal concentrations will maintain the plasmid at a copy number of at least one plasmid per chromosome because of effective killing of plasmid-free cells. This research, therefore, will focus on the generation of standardised inocula for *C. muridarum* transformants that consistently retain at least one plasmid copy per cell over serial passage with which to study plasmid stability and the development of a plasmid stability assay measuring plasmid loss in infectious EBs.

3.2 Methods

3.2.1 Quantitative susceptibility testing in *C. muridarum*

Susceptibility testing in *C. muridarum* was performed using an immuno-staining assay for staining and quantification of chlamydial inclusions (Skilton et al., 2007) and the method was based upon the susceptibility testing methods which use immuno-fluorescence staining of chlamydial inclusions (Black et al., 2015; Pudjiatmoko et al., 1998). Quantitative susceptibility testing to determine the minimum inhibitory concentration (MIC) of the bacterial agent chloramphenicol defined the MIC as the lowest concentration of antibiotics required to completely inhibit bacterial growth at 24 hpi.

Freshly prepared stocks of chloramphenicol (stock concentration 1mgml^{-1}) were added to 2ml DMEM + 10% FCS supplemented with $1\mu\text{g ml}^{-1}$ cycloheximide, to give a final concentration of $0.5\mu\text{gml}^{-1}$. Two-fold serial dilutions were prepared in a total volume of 2ml DMEM + 10% FCS supplemented with $1\mu\text{gml}^{-1}$ cycloheximide. Final chloramphenicol concentrations were (μgml^{-1}): 0.1, 0.3, 0.5, and 0.7. This range was chosen based upon the concentration of chloramphenicol used to select for either *C. muridarum* Nigg P- transformants with $0.4\mu\text{gml}^{-1}$ chloramphenicol (Wang et al., 2014) and *C. trachomatis* strain L2 transformants with a concentration of $0.1\mu\text{gml}^{-1}$ increasing to $0.5\mu\text{gml}^{-1}$ (Xu et al., 2013).

McCoy cells were seeded into two 96 well trays. At confluence, the two 96 well trays were infected at an MOI = 1.0 with either *C. muridarum* strain Nigg P+ or Nigg P- to accommodate duplicate experiments at each concentration of antimicrobial agent for each strain. After 30 minutes centrifugation, the media was removed from each well and replaced with 100 μl (per well) of new media that contained either cycloheximide only (control wells) or cycloheximide with the antimicrobial agent at each test concentration. Infected wells were then incubated at 37°C in 5% CO₂ for 24 hours when they were fixed with methanol for 10 minutes and immuno-stained using *Chlamydia* genus-specific LPS monoclonal antibody Mab29 followed by a β -Galactosidase conjugate and stained blue as previously described in method 2.5.

3.2.2 Quantitative PCR

The real-time quantitative PCR (qPCR) assay for quantifying chromosome and plasmid copy numbers from *C. muridarum* harvested stocks was performed as described previously for *C. trachomatis* (Pickett et al., 2005) with the following modifications. Quantities of chromosomal DNA and plasmid DNA were accurately determined for purified EBs harvested at 28 hpi using 5'-exonuclease (TaqMan) assays with unlabelled forward and reverse primers and a probe labelled

with carboxyfluorescein /carboxytetramethylrhodamine (FAM/TAMRA). Primer and probe sequences for both chromosome and plasmid assays are listed in Table 5 and were designed to amplify single copy plasmid gene *CDS2* (*orf2*) and single copy chromosomal gene outer membrane complex B (*omcB*). Due to the high conservation of gene sequences between both *C. trachomatis* and *C. muridarum* strains, the primers and probe specific for *omcB* that were optimised originally in *C. trachomatis* and were previously described (Skilton et al., 2018) were suitable for use in *C. muridarum* Nigg in this study. The primers and probe sequences for *CDS2*, however, required species-specific primers and were designed and optimised by Rachel Skilton. The primers and probes for the *C. muridarum* assay were selected from DNA sequence regions conserved between *Chlamydia* serovars. The amplified region of *CDS2* by the *C. muridarum* plasmid primers contained the entire region amplified by the *C. trachomatis* primers with the addition of 59 bp where the forward primers sharing the same binding site with a 15 bp overlap. A single copy of the *omcB* gene is located on the chromosome, therefore, the ratio of plasmid to *omcB* is equivalent to the number of plasmid copies per bacterium. The *C. muridarum* Nigg P- chromosome raw sequence data can be accessed from the European Nucleotide Archive, accession number ERS351386. The *CDS2* sequence data from plasmid pNigg can be accessed from the European Nucleotide Archive, accession number NC_002182 because plasmid pSW2NiggCDS2 is a recombinant plasmid containing *CDS2* from the wild type *C. muridarum* plasmid.

For qPCR reactions, 2.5µl of each sample (sample of gDNA was prepared as described in 2.11.2) was added to a reaction mixture containing forward primer (300nM), reverse primer (300nM), probe (250nM) and 2x SensiFAST Probe Lo-ROX mix (Bioline) made up to a total volume of 20µl. The SensiFAST master mix allows for annealing and extension at the same temperature during the same step and so reduces the length of each qPCR cycle.

Negative test control reactions contained 2.5µl of water and were performed in duplicate for every 96 well tray /batch of samples. Calibration curves were performed for each run. Samples were loaded into clear 0.1µM 96-well plates (ThermoFisher) and sealed using adhesive PCR plate seals (ThermoFisher).

Real-time PCR was performed on the viiA7 PCR platform (Applied Biosystems), with data analysis conducted using QuantStudio™ Design & Analysis software, v1.3. Fast real-time PCR cycles were performed as follows: 95°C for 5 minutes, followed by 40 cycles of 95°C for 10 seconds and 60°C for 50 seconds.

Table 5 Primer and probe sequences for qPCR

| Primer ID | Primer / Probe Name | Primer Sequence (5'-3') | Purpose | Reference |
|-----------|---------------------|--------------------------------------|--|----------------------------|
| 1 | CM_pORF2_F | GTCCTGCTTGAGAGAACGTG | | |
| 2 | CM_pORF2_R | CGTCAGACAGAAAAGAGATTATTA | Amplify <i>CDS2</i> and quantify plasmids | Designed by Rachel Skilton |
| 3 | CM_pORF2_probe | FAM-TGGCCCAATGTA CTCTTAGAGCGTG-TAMRA | | |
| 4 | CM_omcB_F | GGAGATCCTATGAACAACTCATC | | |
| 5 | CM_omcB_R | TTTCGCTTTGGTGCAGCTA | Amplify <i>omcB</i> and quantify chromosomes | (Skilton et al., 2018) |
| 6 | CM_omcB_probe | FAM-CGCCACACTAGTCACCGCGAA-TAMRA | | |

3.2.3 Preparing DNA standards for qPCR

E. coli strain DH5 α transformed with a pUC19 vector containing a 2.2 kb PstI fragment encoding the N-terminus of *omcB* from *C. trachomatis* L1 440 strain, as well as DH5 α transformed with pSW2NiggCDS2 (Wang et al., 2014) which contains *CDS2* from the native *C. muridarum* Nigg plasmid were streaked onto agar plates with ampicillin selection. Single colonies were selected and grown in liquid culture at 37 °C to late exponential phase in the presence of ampicillin (25 mgml⁻¹) selection overnight as described in section 2.7.2. Plasmid DNA was extracted and purified from overnight cultures using SmartPure plasmid kit (Eurogentec) according to the manufacturer's instructions.

Estimates of plasmid purity were obtained by measurement of A260/ A280 ratios. Plasmid quantification was carried out by the measurement of A260 using a NanoDrop One spectrophotometer (ThermoFisher).

Starting stocks at were prepared at 1 μ g for both plasmids, from which a series of 1:10 serial dilutions ranging from 10⁻¹ to 10⁻⁸, were prepared in nuclease-free water and stored frozen at -20°C.

3.2.4 Standard curve calculations for qPCR

The absolute quantity of molecules of chromosomes and plasmids were calculated from a known concentration (1000ng μ l⁻¹) and then the required length for each plasmid can be used to work out the number of molecules per microlitre. Once the number of molecules is known for the original stock, the number of molecules is determined for each dilution from 10⁻¹ to 10⁻⁸ by dividing by 10 for each in turn. The formula for calculating the number of molecules in the original stock is as follows:

$$\frac{1000 \text{ (ng)} \times (6.022 \times 10^{23})}{(\text{size of plasmid (bp)}) \times (10^9) \times (650)}$$

In the above equation, the number of moles in the original stock becomes the numerator and the denominator is the weight per mole of the plasmid. The numerator is calculated by multiplying the concentration of the original stock in 1 μ l by Avogadro's constant. The denominator is calculated by multiplying the length of the plasmid, given in nucleotide base pairs (bp), by the average molecular weight of a single DNA base pair (650gmol⁻¹). This gives the number of molecules of the target gene (either *omcB* or *CDS2*) in the original stock as represented by number of plasmid molecules and assumes a 1:1 plasmid to gene copies.

Chapter 3

To calculate the number of molecules per qPCR reaction, the number of molecules in 1µl is multiplied by 2.5 because 2.5µl of standard DNA or sample DNA is used per qPCR reaction.

The quantities of plasmid and chromosomal DNA calculated for each dilution were input into the Invia7 software to populate the standard curve used to calculate the quantities of *omcB* and *CDS2* calculated in each sample. The quantification of chromosome and plasmid copy numbers are presented as quantity means of quadruplicate experiments. All samples for *C. muridarum* Nigg P+ were run on the same plate requiring one standard curve for each plasmid and chromosome assays and using the same CT threshold values (Appendix A, Figure A-1). All samples for Nigg P-/pGFP::Nigg under chloramphenicol selection (1µgml⁻¹) were run on the same plate requiring one standard curve for each of the plasmid and chromosome assays (Figure 3-3). All samples for Nigg P-/pGFP::Nigg under penicillin selection (10Uml⁻¹) and without selection for three passages were run on the same plate requiring one standard curve for each of the plasmid and chromosome assays (Appendix A, Figure A-2).

3.3 Results

3.3.1 Characterising *in vitro* plasmid loss in wild type *C. muridarum* strain Nigg

Wild type *C. muridarum* strain Nigg carries a native plasmid that is ~7.5 kilo base (kb) pairs in length and is referred to as Nigg P+ throughout this thesis. This plasmid contains eight coding sequences (*CDS*) labelled *CDS1* – *CDS8* and an origin of replication comprised of four tandem repeats of a 22 nucleotide base pair (bp) sequence (Thomas et al., 1997). *C. muridarum* naturally loses its' plasmid *in vitro* and some recombinant plasmids have shown to be potentially unstable under penicillin selection *in vitro* ((Liu et al., 2014a; Skilton et al., 2018; Song et al., 2014; Wang et al., 2014). This presents a potential problem for genetic investigation that require homogeneous population of plasmid-bearing cells but also a potential mechanism for destabilising the plasmid in this strain.

The plasmid loss frequency in *C. muridarum*, which measures the proportion of plasmid-free cells per generation (in this case per passage), has previously been measured by iodine staining of glycogen accumulation, a plasmid-dependent process, within inclusions (O'Connell and Nicks, 2006; Russell et al., 2011). However, this method has poor reproducibility and sensitivity. Therefore, a more accurate method for measuring stability in *C. muridarum* is needed. Thus, the feasibility of quantifying the proportion of plasmid-free inclusions in tissue culture using the bullseye phenotype to distinguish plasmid-free from wild type plasmid-bearing inclusions was investigated in the wild type plasmid-bearing strain Nigg P+. In addition, plasmid copy number was determined for inocula harvested at each passage by qPCR.

Accurate measurement of plasmid loss phenotypes over passage requires a consistent infectivity at a low MOI to control for the number of EBs that infect individual host cells and therefore maintain accuracy when counting inclusions. MOI=1 represents a high level of infection not too toxic to host cells and is the optimal concentration to achieve one inclusion per cell in ~60% infected cells. Infecting at high MOI increases the proportion of cells infected with more than one EB, which is masked by inclusion fusion of multiple inclusions in one cell. Therefore, MOI needed to be low (≤ 1) so that most inclusions represent infection with one EB to make counting infected cells more accurate in infectivity assays.

Titration by immuno-staining as previously described is the most accurate method for quantifying the number of stable EBs in a inoculum harvested at each passage (Skilton et al., 2007). However, this method is lengthy and time consuming as it allows for only one passage and one titration experiment per week. Therefore, a rapid means to achieve a consistent infection over passage was necessary for preliminary experiments to optimise a plasmid stability assay in *C. muridarum*.

To achieve a consistent infection at low MOI, the volume of inoculum of Nigg P+ used to infect McCoy cell monolayers at each subsequent passage were determined based upon the proportion of infected cells measured in the previous passage and adjusted up or down until a consistent infectivity of 60% \pm 10% infected cells was achieved using the same volume of inocula to infect one T₂₅ culture flask at each passage.

Consistent infectivity for three serial passages was achieved from the 8th passage using 5 μ l harvested Inocula with 56%, 69% and 57% infected cells (highlighted in bold in Table 6), assuming approximately equal numbers of *Chlamydia* cells for measurement of plasmid loss at each passage. Once a consistent infectivity was achieved at MOI=1 in wild type strain Nigg P+, the mean proportion of inclusions with a bullseye phenotype was measured from two fields of view imaged at 24 hpi. Bullseye phenotype inclusions were identified in 5-12% of inclusions (Table 6) at passage 8, 9 and 10, concordant with frequencies of plasmid loss identified using iodine staining of inclusions ($\leq 14\%$) (Russell et al., 2011).

Table 6 Percentage of plasmid-free “bulls-eye” inclusions in cell culture of wild type plasmid-bearing *C. muridarum* strain Nigg P+.

| Passage | Volume of inoculum used to infect one T ₂₅ (μl) | Infected McCoy cells (%) | Bullseye phenotype (%) (n=2) |
|-----------|--|--------------------------|------------------------------|
| 1 | 10 | 70 | n/a |
| 2 | 50 | 80 | n/a |
| 3 | 20 | 95 | n/a |
| 4 | 5 | 46 | n/a |
| 5 | 20 | 49 | n/a |
| 6 | 25 | 65 | n/a |
| 7 | 10 | 74 | n/a |
| 8 | 5 | 56 | 12, 7 |
| 9 | 5 | 69 | 6, 7 |
| 10 | 5 | 57 | 8, 5 |

For the wild type strain, Nigg P+, that is grown without positive selection for the plasmid in cell culture, inclusions will contain a reasonable degree of cell-to-cell heterogeneity due to plasmid-loss during replication. However, plasmid loss from individual chlamydial cells in cell culture cannot be assessed using microscopy techniques and assessment of inclusion phenotypes because analysis of inclusion phenotypes can only provide an indirect measure of the proportion of plasmid-free bacterial cells. This is responsible in part for the low sensitivity of such techniques that aim to quantify plasmid-free inclusions. In addition, the bullseye inclusion phenotype was difficult to distinguish from wild type inclusions by phase contrast microscopy which is likely to result in poor sensitivity of such a method. This was a result of the unequal distribution of EBs as shown in Figure 3-1. This issue may be overcome for recombinant plasmids that express fluorescent reporter proteins that make distinguishing plasmid-free (no fluorescence) from plasmid-bearing inclusions (fluorescent) easier. However, this method is likely to be highly insensitive if the plasmid-free population are still able to survive within inclusions. For example, if the antibiotic agent has bacteriostatic action such as penicillin. In this instance, inclusions may

potentially exhibit both green fluorescence and the bullseye phenotype. Indeed, fluorescence has been shown to mask the bullseye phenotype in cell culture (Skilton et al., 2018). Given the lack of sensitivity for screening for inclusion phenotypes, a more accurate means to determine the proportion of plasmid-free *C. muridarum* in cell culture is also needed.

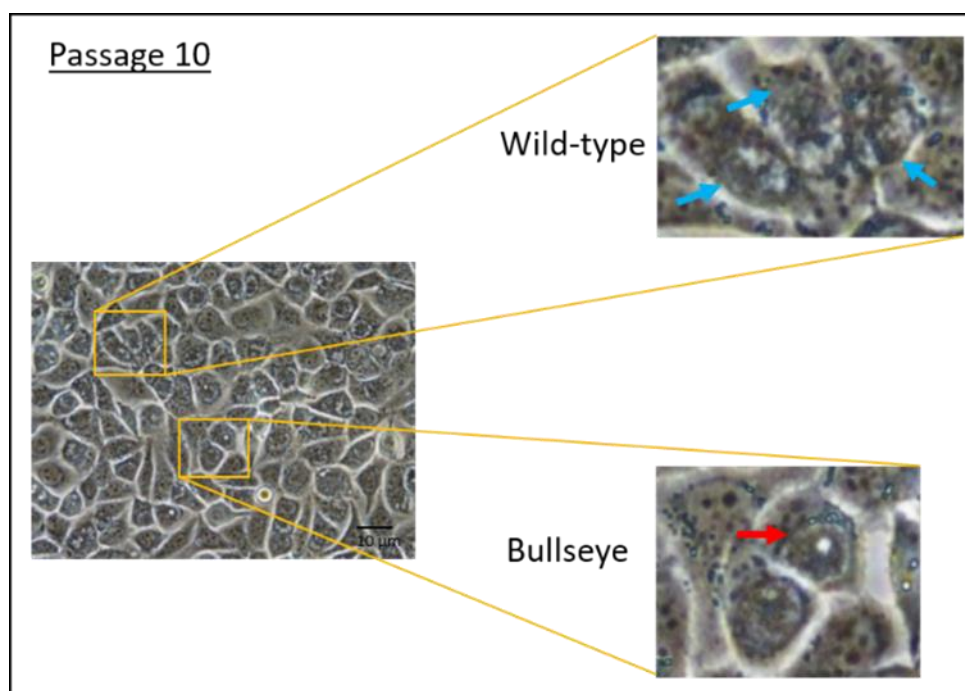


Figure 3-1 Photomicrograph of McCoy cells infected with wild type *C. muridarum* strain Nigg P+.

Images taken at 24 hpi. Wild type plasmid-bearing inclusions are indicated with a blue arrow and demonstrate a varied distribution of elementary bodies (EBs). Plasmid-free “bullseye” inclusions are indicated with a red arrow and are demonstrated by a circular region absent of EBs (Skilton et al., 2018).

3.3.2 Optimisation of real-time qPCR assays for quantifying plasmid copy number in *C. muridarum*

The most direct and potentially accurate method for quantifying plasmid loss is to quantify the relative plasmid copy number (absolute plasmids per chromosome) in the purified EB population, a proportion of which are used for onward passage. Given the high sensitivity of qPCR which theoretically can detect as few as 10 molecules per reaction, this technique provides the most direct, accurate and reproducible means to quantify plasmid loss over serial passage.

Genomic DNA was extracted from purified EBs using ammonium solution as previously described (method 2.11.2). This simple method reduced the workload and has been widely adopted (Stuart Lanham et al., 2001; Pickett et al., 2005). It also ensures that the total DNA content of cells was

retained for quantitative analysis of both plasmid and chromosome copies by qPCR from the same sample.

The qPCR assay has been optimised in *C. trachomatis* and *C. pneumoniae* species as previously described (Pickett et al., 2005). Primers and probe sequences were designed to target single copy plasmid gene *CDS2* and chromosomal gene *omcB*. The chromosome qPCR assay targeting the *omcB* gene has also been adapted for *C. muridarum* and previously described therefore the same primers and probe were used for this work (Skilton et al., 2018). Due to the lack of sequence similarity between the *C. trachomatis*, *C. pneumoniae* and *C. muridarum* plasmids, separate primers, and probe, specific for *C. muridarum* were required that targeted plasmid gene *CDS2*. Primers were designed to amplify the same region as the *C. trachomatis* plasmid assay primers with the addition of 59 bp. Sequences are provided in Table 5. Plasmid DNA was linearised by single-site cuts made by restriction enzyme digest and run on 1% agarose gels to check the size and quality of each plasmid preparation (Figure 3-2). Serial dilutions of recombinant plasmids harbouring either *CDS2* or the N-terminus of *omcB* were prepared and were used to produce amplification plots and standard curves as described in method 3.2.3 and 3.2.4. An example of the amplification plot and standard curves are shown in Figure 3-3. The slope of the curve was used to determine the efficiency of the plasmid and chromosome PCR, which for the experiment shown in Figure 3-3 were 0.987 and 0.996 respectively.

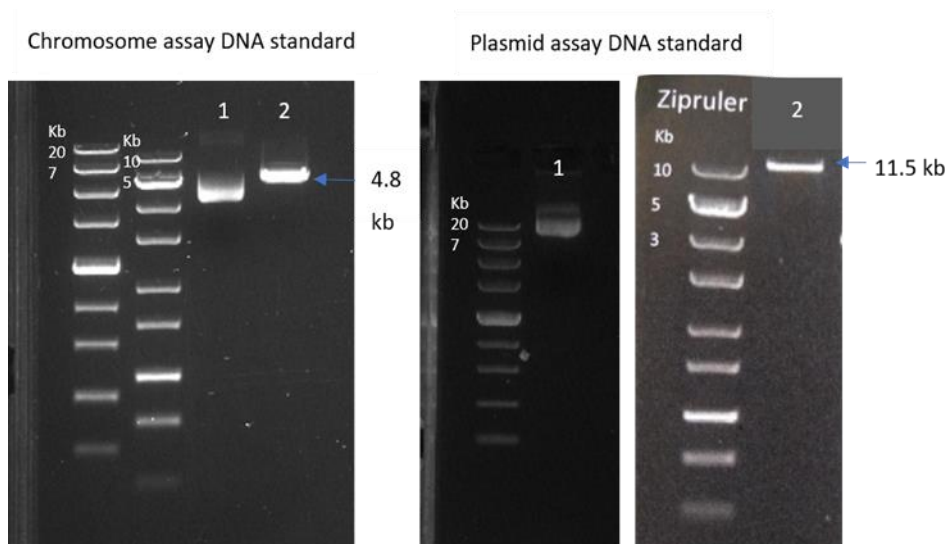


Figure 3-2 Standard curve plasmid DNA preparations for chromosome and plasmid real time qPCR assays.

Plasmid pSRP1A, 4.8 kb (chromosome DNA standard), and pSW2NiggCDS2, 11.5 kb (plasmid DNA standard) were linearised by restriction digest using *NdeI* and *SacI* enzymes respectively. Undigested DNA was loaded into well 1 and digested DNA was loaded into well 2. 300 ng and 188 ng were loaded into each well for pSRP1A and pSW2NiggCDS2 respectively.

Plasmid copy number was determined by qPCR in triplicate repeat measurements for inocula harvested at passages 8, 9 and 10 as previously described. The plasmid was relatively stable over passage in wild type *C. muridarum* strain Nigg P+ (Figure 3-4). These results demonstrate a very low median copy number over three passages 0.5 (0.2) (median (interquartile range) of triplicate technical repeat measurements) at passage 8, 0.7 (0.7) at passage 9 and 0.3 (0.2) at passage 10, which is on average is approximately 0.5-fold lower than reported in the literature for this strain (Liu et al., 2014a). A plasmid copy number this low indicates high cell to cell heterogeneity in the wild type plasmid-bearing strain Nigg P+, with roughly 50% cells missing a plasmid at each passage. Such a high degree of plasmid loss most likely indicates plasmid loss early in development which would allow for expansion of the plasmid-free population over time or else it could indicate a significant loss event sometime during development. These data suggest that recombinant plasmids passaged without selection in *C. muridarum* may also show high cell to cell heterogeneity.

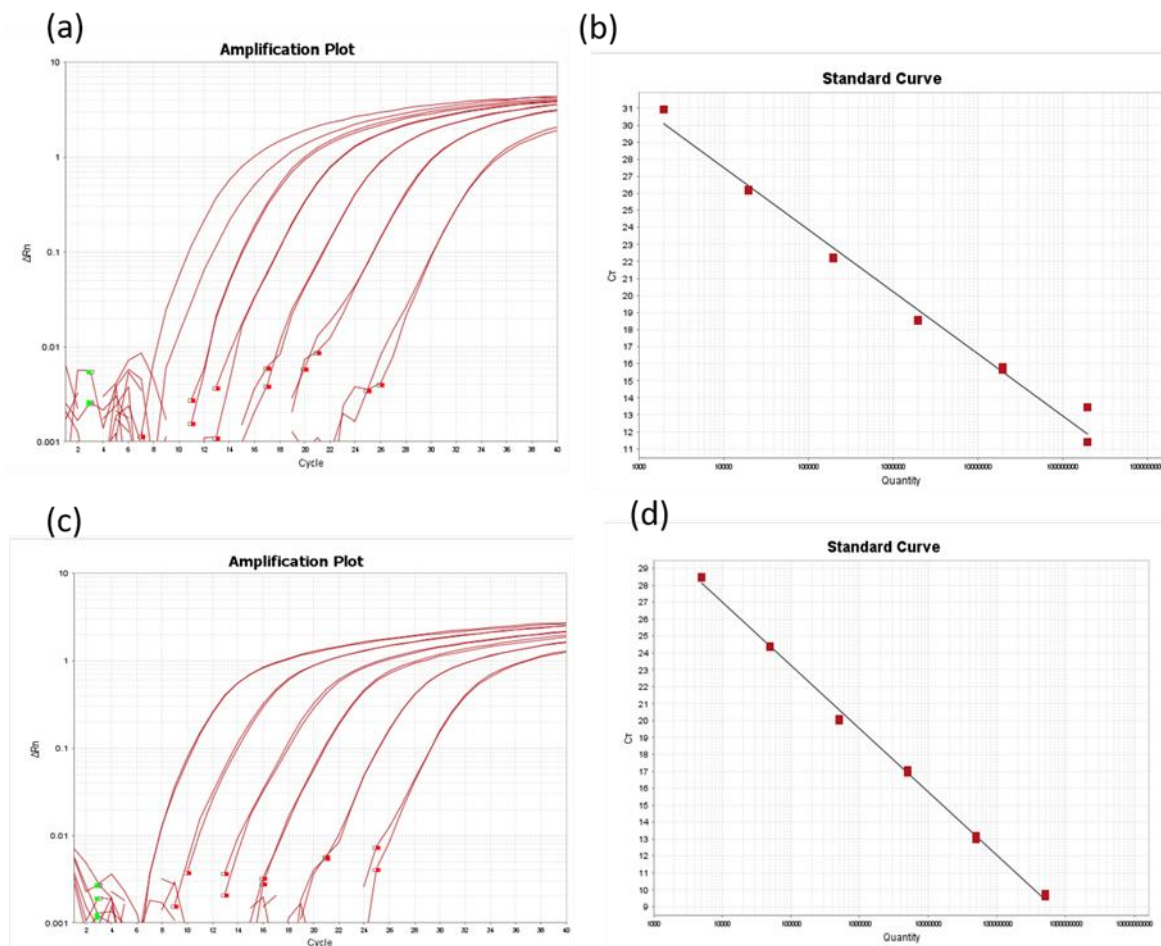


Figure 3-3 Real-time qPCR analysis of *C. muridarum* DNA standards

(a) Amplification plot of *C. muridarum* CDS2 (plasmid) assay using the pSW2NigCDS2 standard. (b) Standard curve derived from (a). (c) Amplification plot of the *C. muridarum* omcB assay using the pSRP1A standard. (d) Standard curve derived from (c). Serial, tenfold dilutions of purified plasmid DNA from 10^{-3} to 10^{-8} were used as template. At 10^{-3} pSW2NigCDS2 is equivalent to 2×10^8 DNA molecules per 2.5 μ l reaction, and 10^{-3} pSRP1A is equivalent to 5×10^8 DNA molecules per reaction. The amplification plots shown were generated for quantification of plasmids and chromosomes for Nigg P- transformed with shuttle vector pGFP::Nigg grown under chloramphenicol ($1 \mu\text{gml}^{-1}$). These plots illustrate the change in fluorescence as the cycle number increases for each concentration of template DNA used. The quantification cycle (Cq) for each reaction is the cycle number at which a fixed threshold value of relative fluorescence is reached. The quantity of DNA molecules was calculated for samples using the Cq set for standard curves. Standard reactions were performed in duplicate.

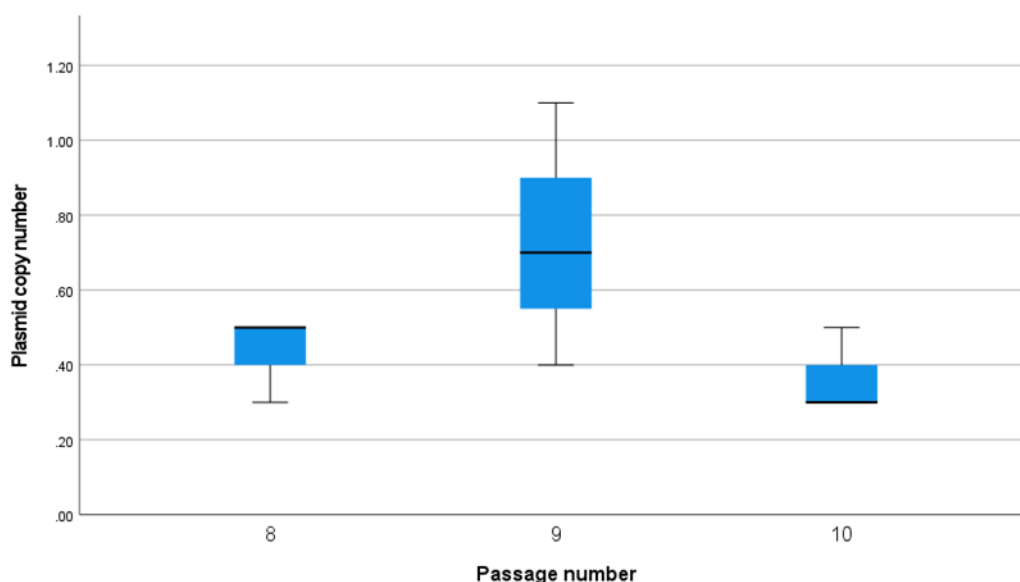


Figure 3-4 Effect of serial passage on plasmid copy number in wild type *C. muridarum* strain Nigg P+.

Wild type strain Nigg P+ bearing the native plasmid was passed three times at a MOI=1.0. Cultures were harvested at 28 hpi for determination of plasmid copy number by qPCR targeting the single copy chromosomal gene *omcB* and single copy plasmid-gene *CDS2* for amplification and quantification. Box plots show one passaging experiment with three technical repeat measurements at each passage.

3.3.3 Generating standardised inocula for *C. muridarum* transformants

Chloramphenicol used at bactericidal concentrations was hypothesised to reduce cell-to-cell heterogeneity in cell cultures by killing plasmid-free bacteria. Given that the efficacy of antibiotics to inhibit chlamydial growth is affected by the MOI used to infect host cells (Suchland et al., 2003), it was necessary to determine the appropriate concentration of chloramphenicol for use in the 'plasmid stability' assay that require infection at an MOI=1. Chloramphenicol is a protein synthesis inhibitor and used at high concentrations ($>10\mu\text{gml}^{-1}$) can cause adverse effects on McCoy cells by reducing ATP production (Li et al., 2010). Therefore, a concentration was required that allowed the expansion of *C. muridarum* transformants in cell culture as well as maintain a healthy monolayer of McCoy cells.

The MIC for this antimicrobial agent has yet to be determined for *C. muridarum* infected at MOI=1. Only two studies have used chloramphenicol for the selection of transformants in *C. muridarum*. Transformants of *C. muridarum* were grown in $0.4\mu\text{gml}^{-1}$ at an unspecified MOI (Wang et al., 2014). A more recent study used $0.5\mu\text{g ml}^{-1}$ chloramphenicol with *C. muridarum* at

Chapter 3

low MOI (Wang et al., 2019). However, neither study reported MIC for *C. muridarum* strains at these MOI.

McCoy cells seeded into 96-well trays were infected with EBs of strain Nigg P+ and Nigg P- at MOI=1. Media supplemented with cycloheximide ($1\mu\text{gml}^{-1}$) only and cycloheximide plus chloramphenicol at final concentrations of 0.1, 0.3, 0.5, 0.7 (μgml^{-1}) were added to infected cells in duplicate wells for incubation for 24 hours (method 3.2.1). At 24 hpi cells were fixed in methanol and inclusions were incubated with *Chlamydia* genus-specific lipopolysaccharide (LPS) monoclonal antibody Mab29 and using a secondary β -Galactosidase conjugate allowing for inclusions to be stained blue with X-gal staining solution (method described in section 2.5).

The generally accepted definition of bactericidal is a >99% reduction in viable bacterial density in a 18 to 24 hour period (Pankey and Sabath, 2004). In this study, the MIC was defined as complete inhibition of growth. No inclusions were visible under $0.5\mu\text{gml}^{-1}$ chloramphenicol or higher concentrations for either strain, whereas <4 inclusions were visible under $0.3\mu\text{gml}^{-1}$ per well (Figure 3-5). The plasmid-bearing and plasmid-free wild type strains, Nigg P+ and Nigg P- respectively, were grown under $0.4\mu\text{gml}^{-1}$ to see if complete growth inhibition occurred at this concentration, used in published studies (Wang et al., 2019). No inclusions were found to grow and therefore $0.4\mu\text{gml}^{-1}$ was determined to be the breakpoint MIC for chloramphenicol in these strains.

Because a minimum bactericidal assay was not performed, a higher concentration of $1\mu\text{gml}^{-1}$ was chosen to match bactericidal concentrations of chloramphenicol reported for other *Chlamydia* spp (Black et al., 2015). Under this concentration, the transformed strain of *C. muridarum* Nigg P-/pGFP::Nigg grew normally demonstrated by typical expansion over passage after transformation, requiring only a few passages, with no visible signs of stress to McCoy cells observed by phase contrast microscopy during live infection (Figure 3-6). Therefore, all future experiments presented in this chapter for measuring plasmid stability in Nigg P-/pGFP::Nigg were carried out using chloramphenicol at a final concentration of $1\mu\text{gml}^{-1}$.

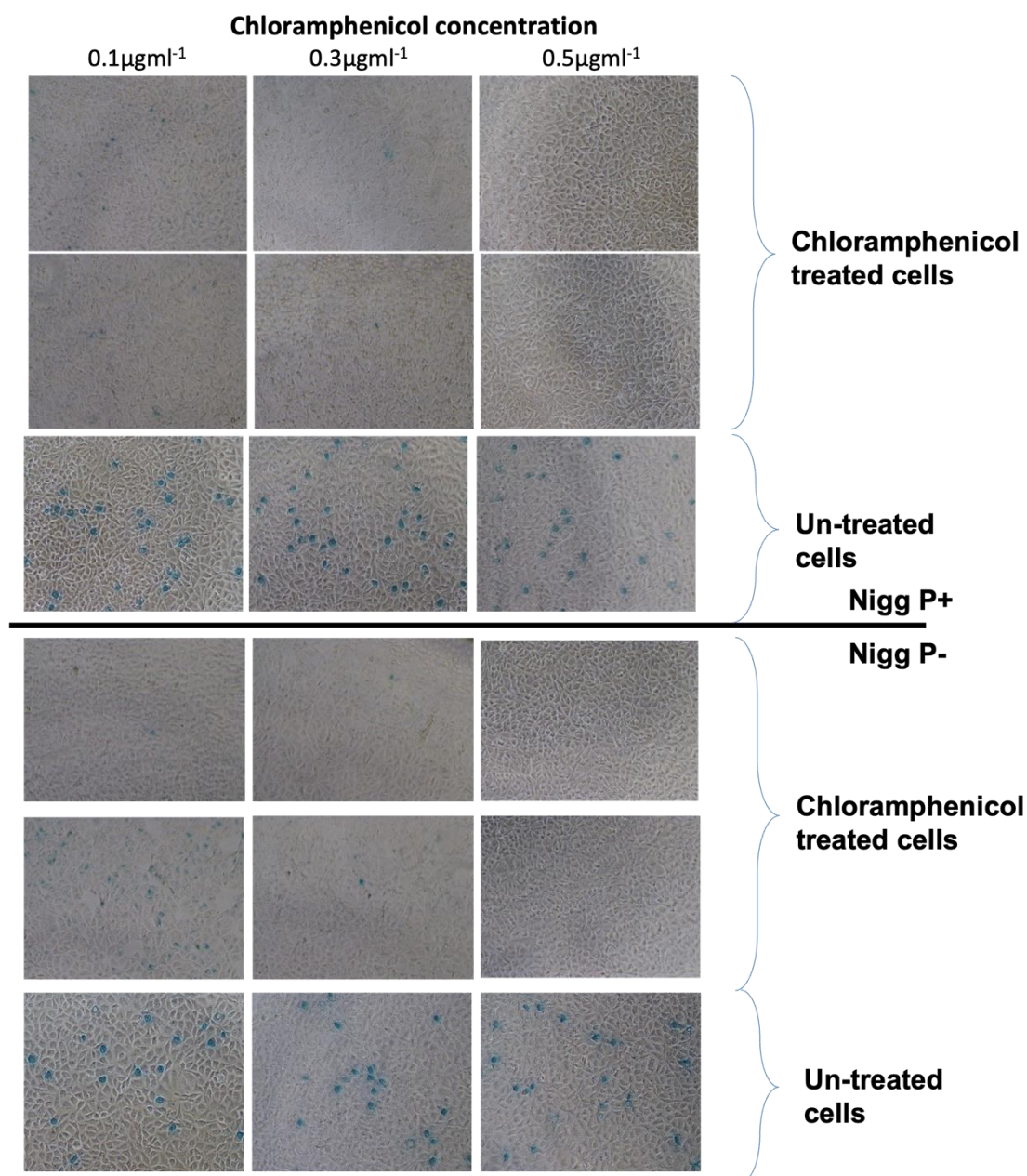


Figure 3-5 Quantitative susceptibility testing in plasmid bearing and plasmid-cured wild type *C. muridarum* strain Nigg to determine the minimum inhibitory concentration of chloramphenicol

96 well trays were seeded with each strain at MOI=1 in duplicate wells and incubated at 37°C with 5% CO₂. At 24 hpi, cells were fixed with methanol and immuno-stained using antibodies against Chlamydia genus specific LPS and a secondary β -Galactosidase antibody then stained blue with X-gal staining solution as previously described (Skilton et al., 2007). The MIC was defined as the concentration of bacterial agent which completely inhibited growth at 24 hpi. No inclusions were visible at 0.5 μgml^{-1} for either strain.

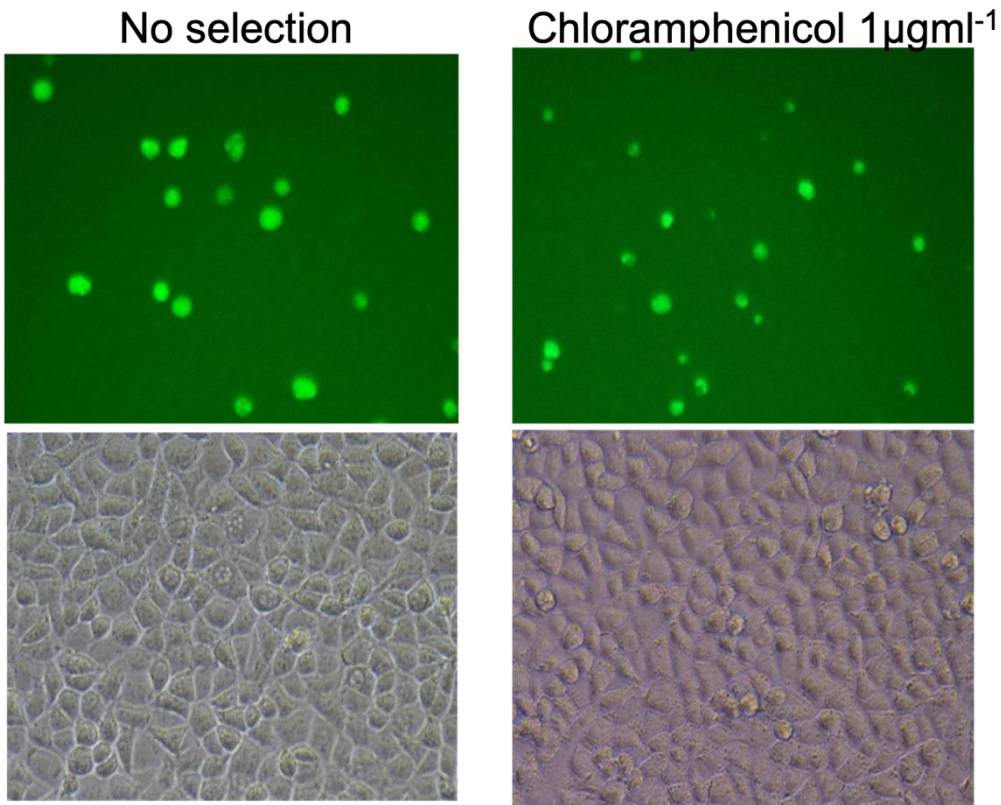


Figure 3-6 Photomicrographs of plasmid pGFP::Nigg transformed into plasmid cured *C. muridarum* strain Nigg (Nigg P-) grown with and without selection with chloramphenicol at bactericidal concentrations.

Wells of McCoy cells seeded into T₂₅ tissue culture flasks were infected with recombinant plasmid pGFP::Nigg transformed into plasmid cured *C. muridarum* strain Nigg P- (Nigg P-/pGFP::Nigg) at an MOI=1. Cultures were grown either with or without media supplemented with 1 µgml⁻¹ chloramphenicol and imaged at 24 hours post infection. Inclusions were identified through green fluorescence from expression of the green fluorescent protein from plasmid pGFP::Nigg. Inclusion size at 24 hpi were comparable with or without selection.

3.3.4 Determination of plasmid stability in Nigg P-/pGFP::Nigg

To determine the plasmid copy number over serial passage in chloramphenicol for shuttle vector pGFP::Nigg transformed into Nigg P- (Nigg P-/pGFP::Nigg), Nigg P-/pGFP::Nigg was serially passaged until a consistent infectivity was achieved for three consecutive passages under chloramphenicol selection at a final concentration of $1 \mu\text{gml}^{-1}$. This had the effect of selecting only plasmid-bearing *Chlamydia* shown by the presence of inclusions that all expressed GFP (Figure 3-7), confirming that each EB that successfully infected a cell contained a plasmid. However, the morphology and size of inclusions grown under chloramphenicol selection was diverse showing evidence of enlarged aberrant RBs like a penicillin-sensitive phenotype (Figure 3-8). These results suggest that chloramphenicol used at this high concentration is toxic to *Chlamydia* cells and has affected normal conversion of EBs to RBs in some cells.

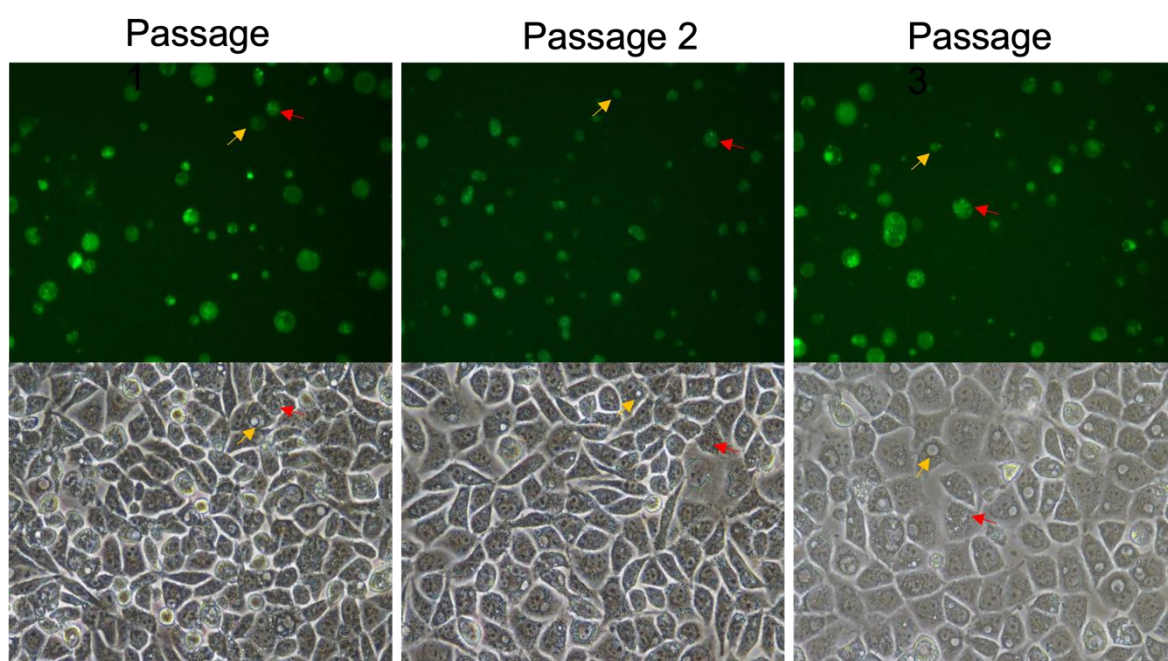


Figure 3-7 Photomicrographs of Nigg P- transformed with pGFP::Nigg serially passaged three times in chloramphenicol selection.

C. muridarum Nigg P- transformed with pGFP::Nigg was passaged three times at MOI=1 under selection with chloramphenicol ($1 \mu\text{gml}^{-1}$). A single field of view is shown visualised under blue (top row) and white light (bottom row) taken at each passage at 24 hpi. Inclusions containing plasmid-bearing *Chlamydia* express green fluorescent protein and are green. Normal inclusions are indicated by yellow arrows. Abnormal inclusion phenotypes are indicated by red arrows and show enlarged aberrant cells or inclusions that contain only a few moving cells.

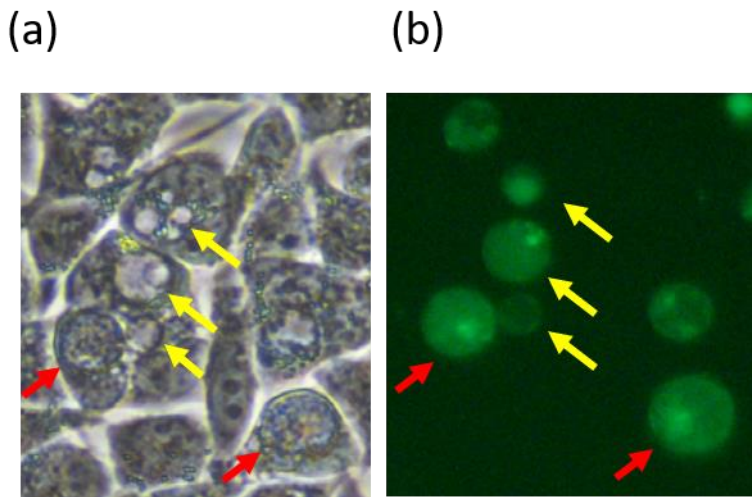


Figure 3-8 Effect of chloramphenicol on inclusion morphology in *C. muridarum* transformant Nigg P-/pGFP::Nigg

Photomicrographs depicting the diverse inclusion morphology of Nigg P-/pGFP::Nigg grown with chloramphenicol ($1\mu\text{gml}^{-1}$) selection. (a) Inclusion morphology was visualised under phase contrast (b) The corresponding GFP expression in these same inclusions was visualised as shown in image (a). Red arrows highlight the wild type inclusion phenotype and yellow arrows indicate, translucent 'atypical' inclusion phenotypes containing enlarged aberrant RBs.

The plasmid copy numbers determined for each culture of Nigg P-/pGFP::Nigg under $1\mu\text{gml}^{-1}$ chloramphenicol selection at passage 1, 2 and 3 (as imaged in Figure 3-7), were 1.18, 0.7 and 0.8 respectively (Figure 3-9a). Mean copy number of these three passages was 0.9 ± 0.14 (mean \pm SD). These data show that positive selection under chloramphenicol selection at $1\mu\text{gml}^{-1}$ increased the copy number closer to ~ 1 on average.

With a starting inocula containing approximately 1 plasmid copy per chromosome (the equivalent of one plasmid per infectious EB), the stability of plasmid pGFP::Nigg could be investigated under changing culture conditions, either by removal of antibacterial agent from the culture media or by addition of penicillin selection to the culture media. To investigate the effect of changing selection or removing chloramphenicol selection on plasmid copy number, equal volumes of inocula harvested at passage 3 under chloramphenicol selection was passaged for a further three serial passages either with penicillin or without selection as before. Plasmid copy number (median (interquartile range)) significantly decreased from 0.87 (0.38) at passage 3 under chloramphenicol selection, to 0.03 (0.03) under penicillin and to 0.01 (0.01) without antibiotic selection determined by One Way Anova ($n=6$) ($p<0.001$) (Figure 3-9b). These data suggest that removal of

chloramphenicol caused the destabilisation of the plasmid which was unable to recover over serial passage either under penicillin selection or no antibiotic selection.

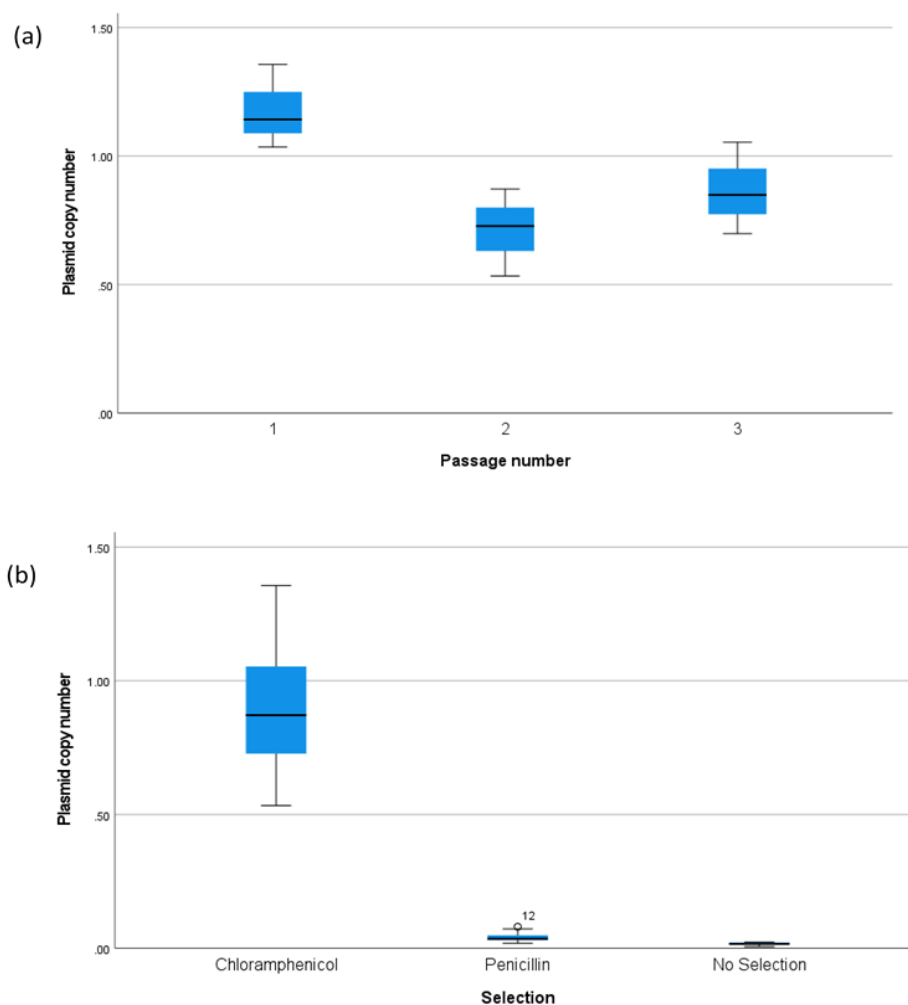


Figure 3-9 Effect of removal of bactericidal concentrations of chloramphenicol on plasmid copy number in *C. muridarum* strain Nigg P- transformed with *E. coli*-*C. muridarum* shuttle vector pGFP::Nigg.

C. muridarum strain Nigg P- transformed with plasmid pGFP::Nigg was serially passaged three times in chloramphenicol selection ($1\mu\text{gml}^{-1}$) at MOI=1.0. Equal volumes of inocula from passage three was then serially passaged either in penicillin G (10Uml^{-1}) or without selection. Plasmid copy number (ratio of gene copies, *CDS2:omcB*) was determined by qPCR in EBs harvested at 28 hpi at each passage. (a) box plot showing the median plasmid copy number of three technical repeats taken from one passaging experiment. (b) Box plots showing plasmid copy number in EBs harvested from three passages from two passaging experiments in selection with chloramphenicol and penicillin, and without selection (n=6) (One way ANOVA, $p < 0.001$).

3.4 Discussion

3.4.1 *Characterising in vitro plasmid loss in wild type C. muridarum*

Plasmid loss frequency over serial passage in wild type *C. muridarum* strain Nigg P+ was <12% at every passage measured by phenotypic analysis of the proportion of bullseye inclusions in cell cultures. This was concordant with <14% measured by iodine staining of plasmid-bearing inclusions (Russell et al., 2011). Counting inclusion phenotypes can only provide an indirect measure of plasmid-loss because the unit counted is the inclusion and not individual *Chlamydia* cells which makes such methods less sensitive than molecular methods that can directly quantify the plasmid copy number in a sample. Adding to this issue of sensitivity, the bullseye phenotype was difficult to distinguish from normal inclusions in cell cultures of the wild type strain Nigg P+ because the distribution of EBs within inclusions was not always even leaving empty 'holes' that were indistinguishable from bullseye inclusions. For recombinant plasmids containing fluorescent reporters expressed from the plasmid, the distinction between fluorescent and non-fluorescent inclusions is easier to identify and therefore to quantify. Therefore, the proportion of non-fluorescent inclusions in cell cultures are likely to be more accurate for transformants with recombinant plasmids containing fluorescent reporter genes.

3.4.2 *Optimisation of real-time qPCR assays for determination of plasmid copy number in C. muridarum*

Without the ability to isolate and quantify the proportion of plasmid-free *Chlamydia* cells over generations, qPCR used to quantify the relative plasmid copy number of absolute plasmid copies per chromosome can provide an accurate and sensitive technique to determine plasmid-loss frequency at each passage. Such assays have been developed for both *C. trachomatis* and *C. pneumoniae* and showed a high analytical sensitivity and specificity but have yet to be developed for *C. muridarum* (Pickett et al., 2005).

The qPCR assay for determination of absolute copy numbers of single copy plasmid-gene *CDS2* and *omcB* (plasmid and chromosome genes respectively) developed for *C. trachomatis* was adapted for *C. muridarum* using species specific primers. Chromosome assay primers used were previously published for the quantification of chromosomal gene, *omcB*, and used identical priming sites in the *omcB* gene to those optimised for *C. trachomatis* L1 strain (Skilton et al., 2018). However, species specific primers were required for *C. muridarum* plasmid gene *CDS2*. The same *CDS2* region amplified by *C. trachomatis* plasmid assay primers was also amplified by the *C. muridarum* primers with the addition of 59 bp. A species-specific probe was designed to maintain specificity; however, analytical sensitivity and specificity assays were not carried out. *In-silico*

analysis confirmed the specificity of the *C. muridarum* plasmid gene primers against plasmid sequences for shuttle vectors pGFP::SW2 and pGFP::L1 that contain the native plasmids from *C. trachomatis* serovar SW2 and L1 respectively. The *C. trachomatis* and *C. pneumoniae* assays had a sensitivity of 10 and 10-100 copies per reaction for chromosome and plasmid assays respectively (Pickett et al., 2005), this is four orders of magnitude lower than the minimum number of chromosomes added per reaction in this work of 10^{-6} copies determined by titration for each sample.

Alkali lysis of EBs was performed using ammonia in the same manner as for the *C. trachomatis* and *C. pneumoniae* assays (Pickett et al., 2005). This method was adapted from the original method with the addition of heating the sample to remove the ammonia which could affect the sensitivity of the qPCR assay (Stuart Lanham et al., 2001).

The effect of DNA supercoiling on the efficiency of the qPCR assay was determined to be negligible in previous studies in *C. trachomatis* and *C. pneumoniae* (Pickett et al., 2005). The efficiency of the *C. muridarum* qPCR plasmid and chromosome assays calculated from the slope was consistently >0.98 , which falls within the accepted range as stated by MIQE guidelines (minimum information for publication of quantitative real-time qPCR) (SA et al., 2009). Plasmid standards were used to generate calibration curves for every PCR plate to ensure accuracy in quantification of relative fluorescence in unknowns.

3.4.3 Generating standardised inocula for *C. muridarum* transformants

The first requirement for the plasmid stability assay was to generate a standard inocula comprised of only plasmid-bearing cells for reproducibility and standardisation. Of the two antibiotics available for use as positive selection for recombinant plasmids in *C. muridarum* at the time, chloramphenicol and penicillin (Liu et al., 2014a; Skilton et al., 2018; Song et al., 2014; Wang et al., 2014), it was hypothesised that chloramphenicol used at bactericidal concentrations would kill plasmid-free bacteria and maintain a plasmid copy number of 1 over passage.

Lipid-soluble chloramphenicol will readily diffuse across bacterial membranes where, once inside the bacterial cytosol, it reversibly binds to the L16 protein of the 50S subunit of bacterial ribosomes. This prevents the transfer of amino acids to growing peptide chains therefore inhibiting protein synthesis serving to block transcription and translation of bacterial genes (Schwarz et al., 2004). This reversible action is generally bacteriostatic; however, chloramphenicol will have bactericidal action at high concentrations or when used against highly susceptible organisms (Black et al., 2015; Hackstadt et al., 1996; Suchland et al., 2003).

Chapter 3

A bactericidal mechanism of action has been demonstrated in *Chlamydia*, using a very high concentration of chloramphenicol at $200\mu\text{gml}^{-1}$ (Scidmore et al., 1996). This study investigated the effect of chloramphenicol on the ability of EBs of *C. trachomatis* LGV-434, serotype L2 strain to enter the exocytic pathway as defined by the ability to acquire endogenously synthesized sphingomyelin from C6- NBD-ceramide. Incorporation of sphingomyelin into the EB cell wall is a process required for evasion of lysosomal degradation by the host and is therefore required for intracellular survival (Elwell 2016). Chloramphenicol used at this very high concentration ($200\mu\text{gml}^{-1}$) inhibited the attachment and entry of EBs, as well as the ability for EBs to sufficiently adapt the inclusion membrane during development through acquisition of sphingomyelin, leading to bacterial cell death (Scidmore et al., 1996).

Given that plasmid-free (non-fluorescent) inclusions have been identified under penicillin (Wang et al., 2014) as well as failure to recover transformants under penicillin selection beyond six passages (Liu et al., 2014a; Song et al., 2014), it was hypothesised that serial passage in penicillin would decrease plasmid stability.

To test these hypotheses, first the minimum inhibitory concentration (MIC) of chloramphenicol was determined. Large variation exists in the standardisation of techniques that define if an antibacterial agent is bacteriostatic or bactericidal. Therefore, species and even strain specific definitions exist for specific antibacterial agents (Pankey and Sabath, 2004). Currently there are no standardised guidelines for antimicrobial susceptibility testing in *Chlamydia spp* and a variety of methods have been adopted for determination of minimum inhibitory concentration (MIC) and minimum bactericidal concentration (MBC) using immuno-fluorescence staining of chlamydial inclusions (Black et al., 2015; Pudjiatmoko et al., 1998). Typically, quantitative susceptibility testing requires preparation of a series of 2-fold dilutions of the test antibacterial agent in a liquid culture medium which is inoculated with a standard number of microorganisms in a minimum of duplicate wells, and incubated at 35°C – 37°C for ~ 18 – 24 h (Black et al., 2015; Pankey and Sabath, 2004; Suchland et al., 2003). Determining an end-point for MIC determination using immuno-fluorescence staining of chlamydial inclusions has shown to be highly subjective (Suchland et al., 2003). The method adopted in this study potentially avoided these pitfalls by using a β -Galactosidase conjugate instead of a fluorescent conjugate and setting the endpoint as complete inhibition of growth as opposed to $>90\%$ inclusions with altered size and morphology. This method facilitates observation of stained inclusions using standard phase contrast microscopy and therefore counts across the entire well can be made as opposed to individual fields, which could provide more accurate assessment of cell counts and confirmation of complete growth inhibition (Skilton et al., 2007).

The concentration that achieved complete inhibition of inclusion development was $0.5\mu\text{gml}^{-1}$ consistent with the MIC for chloramphenicol determined for plasmid-free *C. trachomatis* L2 strain (L2R) infected at $\text{MOI}=0.1$ was $0.05\mu\text{gml}^{-1}$ (Xu et al., 2013) but slightly higher than concentrations of chloramphenicol used in recent genetic studies in *C. muridarum* of $0.4\mu\text{gml}^{-1}$ (Wang et al., 2019). However, complete inhibition of inclusion formation was also observed at $0.4\mu\text{gml}^{-1}$.

The minimum bactericidal concentration has been defined as the lowest concentration of antimicrobial that prevented inclusion formation after a single freeze–thaw passage without antimicrobial agent present with a $>99.9\%$ reduction in viable bacterial density in an 18–24-h period (Pankey and Sabath, 2004). An onward passage was not performed in this work. In the absence of performing an extra passage of sub-cultured cells to determine the MBC, a higher concentration of $1\mu\text{gml}^{-1}$ was chosen for preliminary experiments with the transformant Nigg P-/pGFP::Nigg. Under this concentration, this strain of *C. muridarum* grew normally as demonstrated by a normal developmental cycle (inclusions were approximately as large as the host cell at 28 hpi) and expansion over passage after transformation.

A preliminary experiment was conducted passaging Nigg P-/pGFP::Nigg for three consecutive passages under $1\mu\text{gml}^{-1}$ chloramphenicol selection. Estimates of infectivity were determined for cultures by quantifying the proportion of infected cells from images taken in duplicate at 24 hpi. These estimates were then used to infect at $\text{MOI}=1$ (equal to approximately 60% infected cells) to maintain a high level of infection not too toxic to host cells and to facilitate infection of host cells with one EB for most cells infected. Mean plasmid copy number for all three passages was 0.9 ± 0.14 (mean \pm SD), close to 1 plasmid per chromosome. Furthermore, all inclusions expressed GFP shown demonstrated by phase contrast microscopy. Thus, confirming that chloramphenicol is bactericidal at this concentration for the transformed strain and that a standardised inocula, where every cell contained a plasmid, can be generated using this agent at bactericidal concentrations.

3.4.4 Stability of plasmid pGFP::Nigg in *C. muridarum*

To test the hypothesis that stability of the plasmid would decrease over serial passage under penicillin selection, inocula at passage 3 containing only plasmid-bearing *Chlamydia* were then grown using either penicillin or no antibiotic selection in the growth media. In both conditions, with and without penicillin selection, the plasmid copy number decreased significantly from the first passage either with or without penicillin selection and was maintained at this low level over two further passages. These data suggest that upon removal of chloramphenicol selection after three consecutive passages, and therefore without adequate positive selection for the plasmid,

the number of plasmid-bearing cells is reduced to such an extent that the plasmid-bearing population cannot recover over serial passage even under positive selection.

Moreover, these data showed that significant plasmid loss occurred when chloramphenicol selection used at bactericidal concentrations was removed or changed to penicillin selection and there was no difference between plasmid copy number in cultures passaged either with or without penicillin selection over three passages. These data suggest that the collapse in plasmid copy number was caused by the stress placed upon the chlamydial cells through continuous passage under chloramphenicol selection at high concentrations and then a sudden change in conditions. Furthermore, given that there was no difference between plasmid copy number passaged under penicillin selection and when selection was removed all together, these data also show that penicillin selection fails to inhibit the growth of plasmid-free cells.

3.5 Conclusions

This research focussed on the optimisation of a plasmid stability assay for *C. muridarum* transformants starting with the generation of standardised inocula using chloramphenicol at bactericidal concentrations. The purpose of this was to inform the choice of vector backbone for engineering a self-replicating transposon delivery vector that could be stably passaged in *C. muridarum* and potentially eliminated.

Chloramphenicol at $1\mu\text{gml}^{-1}$ is bactericidal in other *Chlamydia* spp (Black et al., 2015). Preliminary experiments with Nigg P-/pGFP::Nigg demonstrated that a plasmid copy number close to 1 was maintained over passage under $1\mu\text{gml}^{-1}$ chloramphenicol selection. In addition, all inclusions showed expression of *gfp*. Together these findings demonstrate that $1\mu\text{gml}^{-1}$ is bactericidal to *C. muridarum* at an MOI=1.0 and will therefore inhibit the growth of plasmid-free *C. muridarum*. This is necessary for generating a homogenous starting inocula for experiments assessing plasmid stability.

Once a reproducible inocula was generated, plasmid stability was investigated under alternative culture conditions by either removing antibiotic selection or changing selection to penicillin in the growth media. However, changing or removing chloramphenicol selection at $1\mu\text{gml}^{-1}$ from the growth media resulted in complete collapse in plasmid copy number from the first passage onwards. These findings demonstrate that chloramphenicol used at bactericidal concentrations is likely to be very toxic to chlamydial cells, so much so that, the plasmid-bearing population are unable to recover over serial passage upon its removal. Together these data represent a means to stably maintain the plasmid at a copy number of ~ 1 per cell as well as a novel mechanism to eliminate the plasmid from *C. muridarum*.

Chapter 4 Investigating stability of plasmids to identify suitable candidates for a replication-proficient transposon-delivery vector in *C. muridarum*

4.1 Introduction

Developing plasmid-based tools for *C. muridarum* faces significant challenges which includes low transformation efficiency, a low plasmid copy number (PCN) and *in vitro* plasmid-loss. So, to develop a stably replicating vector system for transposon mutagenesis in *C. muridarum* required a means to investigate plasmid stability in available replicating plasmids to identify an appropriate vector backbone that is stably maintained over passage in cell culture.

Historically, categorisation of plasmid-genes as essential or not-essential for plasmid maintenance in *Chlamydia* was based upon the ability to recover and “stably” maintain transformants over serial passage (Gong et al., 2013; Liu et al., 2014a; Song et al., 2013). Three independent laboratories applied this criterion to plasmids with either whole gene deletions, nonsense mutations or gene replacements for each plasmid gene for either *C. trachomatis* or *C. muridarum* (Gong et al., 2013; Liu et al., 2014a; Song et al., 2013). Fluorescent reporter genes expressed from plasmids were used to identify plasmid-bearing *Chlamydia* within inclusions. Only transformants carrying deletions of plasmid genes *CDS1* (*pgp7*), *-5* (*pgp3*), *-6* (*pgp4*), and *-7* (*pgp5*) were recovered and passaged up to five or six times under selection with ampicillin to enrich for fluorescent cells and were plaque cloned. Subsequently, these genes were considered not essential for plasmid maintenance. However, direct measurement of plasmid loss without selection was not assessed for these mutants therefore a role, albeit not “essential”, in plasmid maintenance cannot be excluded based on these findings alone.

The aim of the work in this chapter was to identify an appropriate vector for the backbone of a self-replicating transposon-delivery vector that can be stably maintained in plasmid-cured *C. muridarum* strain Nigg. The objectives therefore were to investigate plasmid stability in a range of available vectors to determine the minimal gene-set that could be adapted to carry the largest gene cassettes without compromising transformation efficiency and plasmid maintenance. The available shuttle vectors included pGFP:Nigg and recombinant plasmid pSW2NiggCDS2 which contain all eight plasmid genes, and plasmid-gene deletion mutants; pNiggCDS56Del and plasmid pNiggCDS567Del with a combination of the possible deletion of genes *CDS5*, *-6*, and *-7* constructed by Dr Yibing Wang.

4.2 Methods

4.2.1 Study design

It was shown that chloramphenicol used at bactericidal concentration ($1\mu\text{gml}^{-1}$) can be used to generate a standardised inoculum of plasmid cured Nigg P- transformed with plasmid pGFP::Nigg in the previous chapter. Therefore, the assay design first generates a standardised inoculum under chloramphenicol selection from which to investigate the effect of changing selection conditions on PCN and the frequency of plasmid loss (proportion of plasmid-free cells in the total population) over generations of EBs.

The assay is comprised of two treatment arms (Figure 4-1). Starting inocula is serially passaged three times in T₂₅ culture flasks with DMEM supplemented with either chloramphenicol ($1\mu\text{gml}^{-1}$) and cycloheximide ($1\mu\text{gml}^{-1}$) (arm 1) or DMEM supplemented with cycloheximide ($1\mu\text{gml}^{-1}$) without antibiotic selection (arm 2). Inocula harvested at passage 3 (P3) in each treatment arm was passaged a further three times (P4-P6) and grown in DMEM supplemented with either cycloheximide ($1\mu\text{gml}^{-1}$) only or with the addition of penicillin G (10Uml^{-1}). *Chlamydia* EBs were harvested at 28 hpi (hpi) at the end of exponential growth. Harvested inocula at each passage represents individual samples. A schematic of the assay design is shown in Figure 4-1.

In the previous chapter, estimates of infectivity were made to determine the volume of inocula required to infect at an MOI=1. So, for better precision, the concentration of infection forming units (IFU ml^{-1}) was quantified for all samples by immunostaining as previously described (Skilton et al., 2007) and the titre was used to calculate the volume required to infect McCoy cells at MOI=1 (method 2.6.2).

Cell cultures were imaged by phase contrast microscopy at 24 hpi then harvested at 28 hpi and stored 1:1 in sugar phosphate solution and frozen at -70°C . Samples were thawed once for titration experiments, a second time for subsequent passage, and one final time for extraction of genomic DNA.

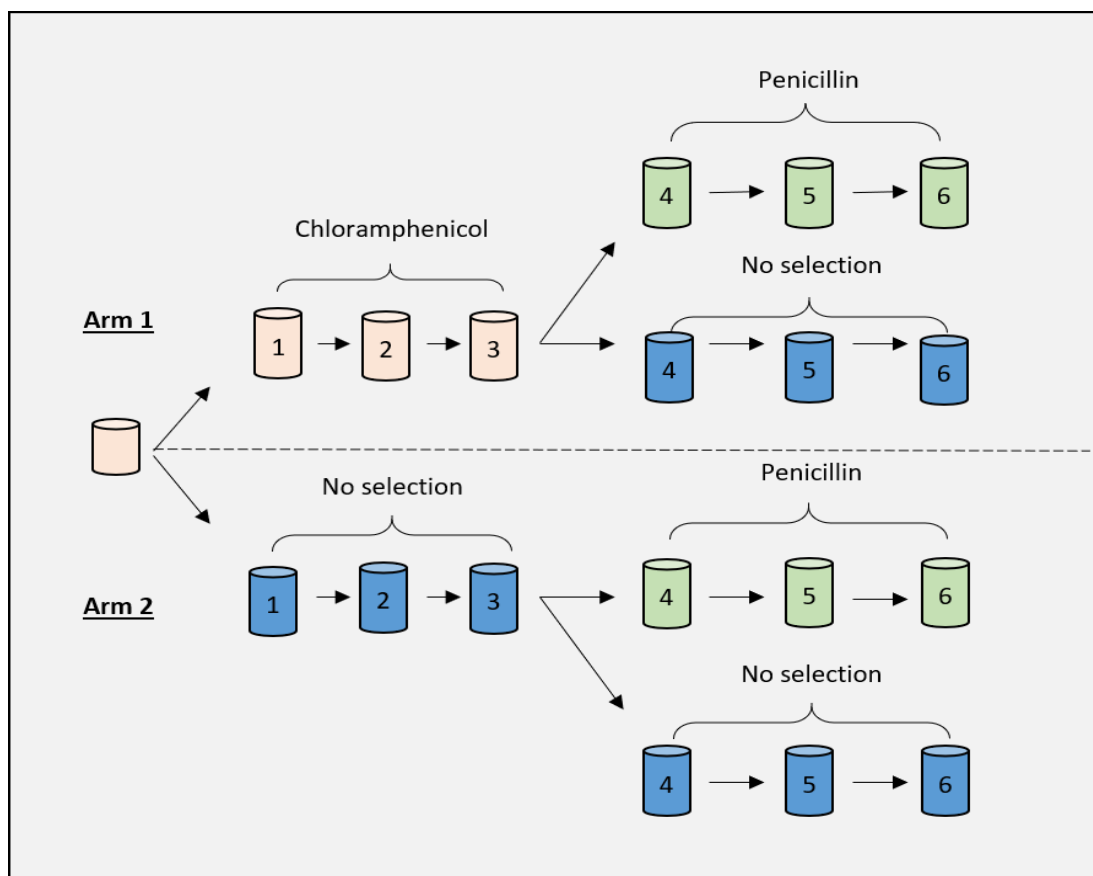


Figure 4-1 Schematic of plasmid stability assay for *C. muridarum* strains.

A starting inoculum of transformed *C. muridarum* Nigg P- was serially passaged three times (P1-3) either with (orange) or without (blue) selection with chloramphenicol. Inocula harvested at P3 was passaged three times either with or without selection with penicillin. Bacteria were harvested from cultures in one T25 culture flask at 28 hpi and stored in 4SP at -70°C . Harvested EBs at each passage represent individual samples numbered 1-6. The concentration of infectious forming units (IFU ml^{-1}) were calculated for each sample by titration by *Chlamydia* binding genus-specific LPS monoclonal antibody (Mab29) which were stained with X-gal (Skilton et al., 2007). Titres were used to calculate the volume required to infect a T25 culture at $\text{MOI}=1$ at each passage. Plasmid copy number (*CDS2: omcB*) ratios were determined for samples at P3 and P6 by qPCR. The proportion of non-fluorescent inclusions (plasmid-free *Chlamydia*) in the total population for each culture was determined from two fields imaged for each culture flask.

4.2.2 *Measuring plasmid segregational stability*

Plasmid-loss was measured by two independent methods. First, phenotypic analysis was performed on images of cell cultures at each passage to quantify the frequency of plasmid loss as a proxy for the rate of plasmid loss, by quantifying the proportion of plasmid-free inclusions in the total population identified by the absence of GFP expressed *in trans* (method 4.2.3).

Second, the total genomic DNA was extracted (method 2.10.2) from samples at passage 3 and 6 only for determination of PCN (absolute plasmid copies per chromosome) by qPCR protocol optimised in chapter 3 which used primer pairs to target single copy genes located on the chromosome (*omcB*) and on the plasmid (*CDS2*) (method 3.2.2). Quadruplicate technical repeats were performed for each sample and the DNA standards were run in duplicate. All samples for Nigg P-/pGFP::Nigg were run on the same plate requiring one standard curve for both the plasmid and chromosome assays (Appendix A, Figure A-3). All samples for Nigg P-/pSW2NiggCDS2, Nigg P-/pNiggCDS56Del and Nigg P-/pNiggCDS567Del were run on the same plate requiring one standard curve for both assays (Appendix A, Figure A-4).

It was hypothesised that the sensitivity of the plasmid stability assay to detect changes in plasmid loss over each passage would be greatest when comparisons were made at the highest passage (generation) number under each specified condition (chloramphenicol, penicillin selection or no selection). Subsequently comparisons of PCN for treatment arm 1 were made between P3 under chloramphenicol selection and P6 under penicillin selection or without selection.

A standardised inocula is indicated by a mean PCN of 1 and a visible fluorescent signal within all inclusions. Hence, plasmid loss is indicated by a decrease in PCN and an increase in the proportion of inclusions that lack a fluorescent signal over serial passage.

4.2.3 *Quantification of inclusion phenotypes from cell culture images*

For all images of *C. muridarum* transformants that fluoresced green in cell culture, the total number of inclusions within a McCoy cell monolayer was automatically quantified using Image J™ software version 1.53k. Images were converted into black and white and then to 8-bit resolution. The minimum and maximum threshold was set from 20 to 255 respectively with a dark background selected. To allow the software to detect individual inclusions that were so close in proximity that they did not appear as separate inclusions, the watershed function was selected to add a separating line of 1 pixel in diameter between each inclusion. The pixel size was set to 700-10,000 for analysing particles (a particle is the same as one inclusion in this instance) that fell within this range. The ability of this size range to detect all mature inclusions was verified by

manual counts of the same images, performed for two images. The circularity was set from 0.1 to 1.00 where 0.0 is a straight line and 1 is a complete circle.

4.2.4 Plasmids

Plasmid pSW2NiggCDS2 contains gene *CDS2* derived from the native *C. muridarum* plasmid, pCM, as a result of recombination between *C. trachomatis* plasmid pGFP::SW2 and pCM (Wang et al., 2014). Plasmid pGFP::Nigg was derived from *C. trachomatis* shuttle vector pGFP::SW2 and the native *C. muridarum* plasmid pCM (Skilton et al., 2018). Plasmids pSW2NiggCDS2 and pGFP::Nigg both contain all eight plasmid genes.

Plasmids pNiggCDS56Del and pNiggCDS567Del were derived from shuttle vector pGFP::Nigg and contain deletions of plasmid genes *CDS5* and *CDS6* (pNiggCDS56Del) and *CDS5*, *CDS6* and *CDS7* (pNiggCDS567Del). Deletion of plasmid genes was performed by Dr Yibing Wang and achieved using PCR cloning technique to amplify the plasmid pGFP::Nigg from the *PacI* site located in the intergenic region between *CDS4* and *CDS5* through to the intergenic region between *CDS7* and *CDS6* (for pNiggCDS56Del) or *CDS7* and *CDS8* (pNiggCDS567Del) adding the *PacI* restriction site to the other end of the PCR product for ligation of *PacI* sticky ends.

For all vectors described above, plasmid gene *CDS1* is truncated, used as a cloning site for the *E. coli* plasmid containing an *E. coli* (ColE1) origin of replication as well as the chloramphenicol acetyltransferase gene transcriptionally coupled to a gene encoding the green fluorescent protein (GFP), and the β -lactamase gene.

4.2.4.1 Plasmid pGFP::Nigg

Plasmid pGFP::Nigg was previously described by Skilton *et al.*, (2018) and provided by Professor Ian Clarke (University of Southampton). Plasmid pGFP::Nigg was constructed from the recombinant plasmid pSW2NiggCDS2 (Wang *et al.*, 2014), (see plasmid map for pSW2NiggCDS2 below, Figure 4-2) by replacing *CDS2-8* from *C. trachomatis* plasmid pSW2 with *CDS2-8* from the native *C. muridarum* plasmid (pCM) using primers to amplify the donor fragment from pCM. The forward primer was homologous to the 26 nt downstream of the existing *SpeI* unique site in *CDS2* (pCM) and the reverse primer added a unique *MluI* site 48 nt from the start codon of *CDS1* (pCM) to ligate the truncated *CDS1* from pSW2 with the start of *CDS1* in pCM. Plasmid pGFP::Nigg also contains *bla* and the transcriptionally coupled *gfpcat* gene cassette under the control of constitutive promoter's *bla* and *Neisseria* constitutive promoter *MCIP* respectively.

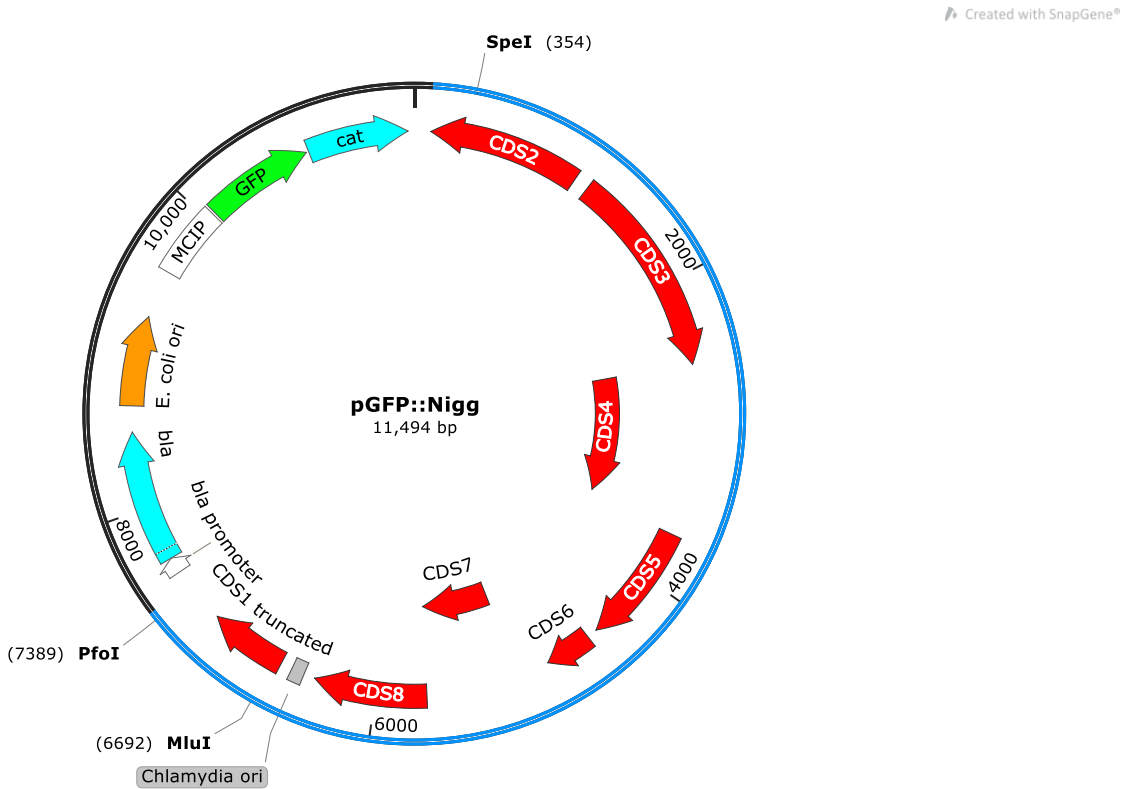


Figure 4-2 Plasmid map of *E. coli*- *C. muridarum* shuttle vector pGFP::Nigg

Plasmid pGFP::Nigg contains all coding sequences (*CDS1-8*) as purple arrows orientated in the direction of transcription. The origin of replication from *C. muridarum* Nigg plasmid, pCM, is located upstream of a truncated *CDS1*. The origin of replication from *E. coli* plasmid ColE1, facilitates plasmid propagation at high copy number in *E. coli*, and is located downstream of the *bla* resistance gene conferring resistance to ampicillin/penicillin. *Neisseria* promoter MCIP drives expression of a GFPCAT fusion protein.

4.2.4.2 Plasmid pSW2NiggCDS2

Plasmid pSW2NiggCDS2 was previously described by Wang *et al.*, (2014). Plasmid pSW2NiggCDS2 was recovered from wild type *C. muridarum* Nigg P+ transformed with plasmid pGFP::SW2 from the *C. trachomatis* nvCT strain. Plasmid pSW2NiggCDS2 contains only *CDS2* from pCM, replacing the entire *CDS2* sequence from pGFP::SW2 (Wang *et al.*, 2011) (Figure 4-3).

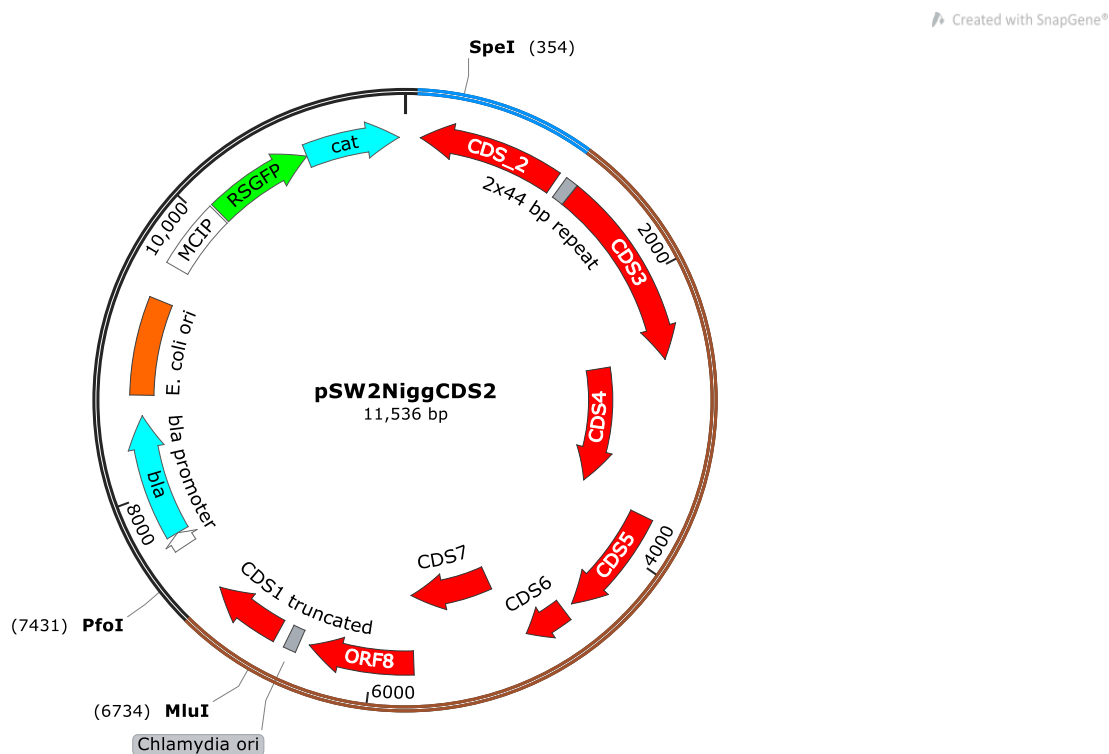


Figure 4-3 Plasmid map of recombinant plasmid pSW2NiggCDS2

Plasmid pSW2NiggCDS2 contains all coding sequences from *C. trachomatis* plasmid pSW2, indicated by red arrows orientated in the direction of transcription, except for *CDS2* from *C. muridarum* plasmid pGFP::Nigg. The beta lactamase resistance gene as well as the transcriptionally coupled green fluorescent protein and chloramphenicol resistance gene are also represented by purple arrows in the direction of their transcription. The *Chlamydia* origin of replication is located upstream of the truncated *CDS1*. A unique 44bp tandem repeat sequence is located at the transcriptional start site of *CDS2* (Wang *et al.*, 2014).

4.3 Results

4.3.1 *Generating standardised inocula of C. muridarum transformants*

Traditional approaches for measuring plasmid stability measure the frequency of plasmid loss over multiple generations from a starting population where all bacterial cells contain a plasmid (Lau et al., 2013). In the previous chapter, a standardised inoculum of plasmid-cured (P-) *C. muridarum* strain Nigg transformed with plasmid pGFP::Nigg (Nigg P-/pGFP::Nigg) was generated using positive selection with chloramphenicol at the bactericidal concentration of $1\mu\text{gml}^{-1}$ to kill plasmid-free progeny over three passages. This approach was applied to cultures of Nigg P- transformed with pSW2NiggCDS2, pNiggCDS56Del and pNiggCDS567Del to generate standardised inocula for each strain.

Transformants were initially recovered using penicillin selection as previously described (Wang et al., 2011) and then expanded under chloramphenicol ($1\mu\text{gml}^{-1}$) selection. Plasmid pSW2NiggCDS2 expanded over three passages, but not to the same extent as pGFP::Nigg. Three attempts to expand transformants of pNiggCDS56Del and pNiggCDS567Del beyond P2 were unsuccessful demonstrated by the absence of mature inclusions in McCoy cells at 24 hpi (Figure 4-4). These findings suggest that under high chloramphenicol concentration ($1\mu\text{gml}^{-1}$) plasmid pSW2NiggCDS2 and plasmid-gene-deletion mutants pNiggCDS56Del and pNiggCDS567Del are less stable than plasmid pGFP::Nigg which contains the complete native *C. muridarum* plasmid. These findings suggest that overall, the plasmid copy number and therefore gene dosage was not sufficient for CAT expression to sustain inclusions for these plasmids.

So, the concentration of chloramphenicol was reduced to the MIC of $0.4\mu\text{gml}^{-1}$, as determined in the previous chapter, which facilitated the expansion of transformants Nigg P-/pNiggCDS56Del, Nigg P-/pNiggCDS567Del and Nigg P-/pSW2NiggCDS2. Inocula for each strain including the strain Nigg P-/pGFP::Nigg were subsequently passaged three times in $0.4\mu\text{g ml}^{-1}$ chloramphenicol through treatment arm 1. PCN was determined from inocula harvested at P3 and the frequency of plasmid loss was determined from photomicrographs of each culture to determine whether a standardised inocula ($\text{PCN} \geq 1$) was generated under these conditions for these plasmids.

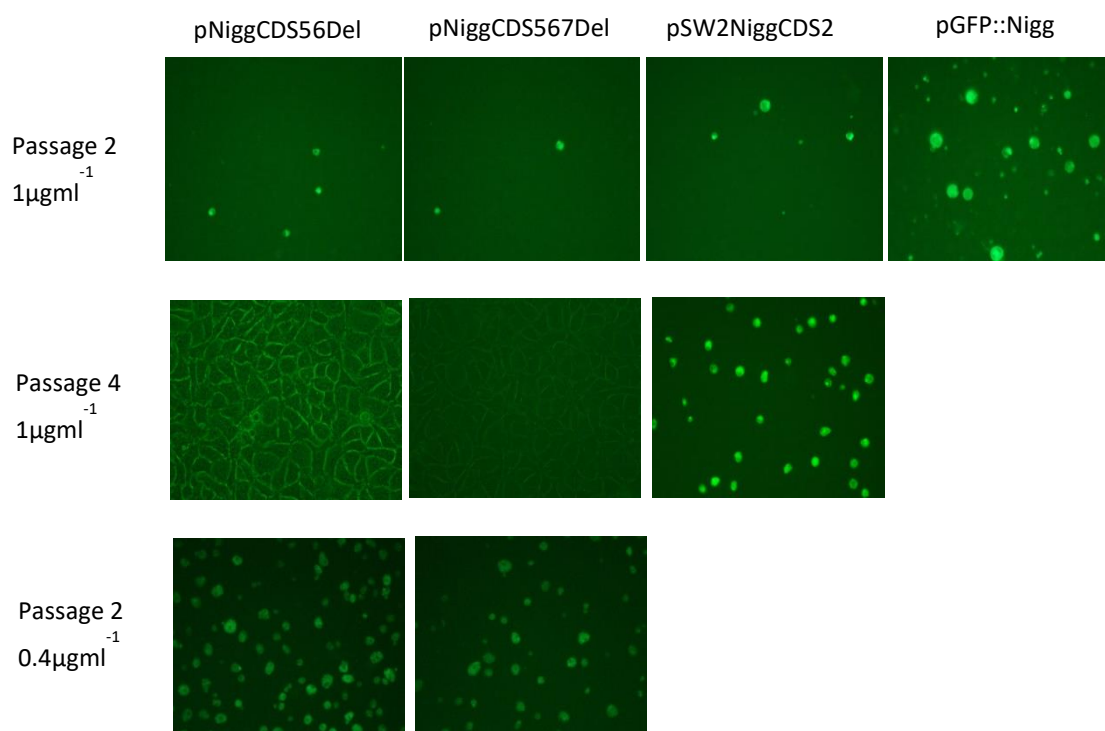


Figure 4-4 Expansion of *C. muridarum* transformants under selection with chloramphenicol.

The plasmid cured *C. muridarum* strain Nigg (Nigg P-) was transformed with recombinant plasmid pSW2NiggCDS2 and deletion mutants pNiggCDS56Del and pNiggCDS567Del a total of four passages were performed. Infected McCoy cells were imaged at 24 hpi. Strain Nigg P-/pSW2NiggCDS2 successfully expanded over four passages, whereas the absence of any inclusions at passage 4 for both deletion mutant strains indicated failure to expand under selection with $1\mu\text{gml}^{-1}$ chloramphenicol. Successful expansion of plasmid-gene deletion mutant strains is shown at passage 2 under subinhibitory concentrations of chloramphenicol.

4.3.1.1 Plasmid copy number measured in standard inocula

For strains Nigg P-/pSW2NiggCDS2, Nigg P-/pNiggCDS56Del and Nigg P-/pNiggCDS567Del the PCN was ≥ 1 at third passage (P3) indicating that, despite the sub-inhibitory concentration of chloramphenicol used, a standardised inocula was generated for these strains (Figure 4-5). In contrast, standard inoculum was not generated under sub-inhibitory concentrations of chloramphenicol for strain Nigg P-/pGFP::Nigg, which averaged a PCN of ≤ 0.5 representing a greater heterogeneity in the inocula (Figure 4-5). When a sub-inhibitory concentration of

chloramphenicol was used ($0.4\mu\text{gml}^{-1}$), the expansion of plasmid-free cells was not limited, therefore, it is possible to achieve a plasmid copy number (ratio *CDS2*: *omcB*), below 1. These findings show that sequence differences between the plasmids are responsible for the variation in plasmid copy number.

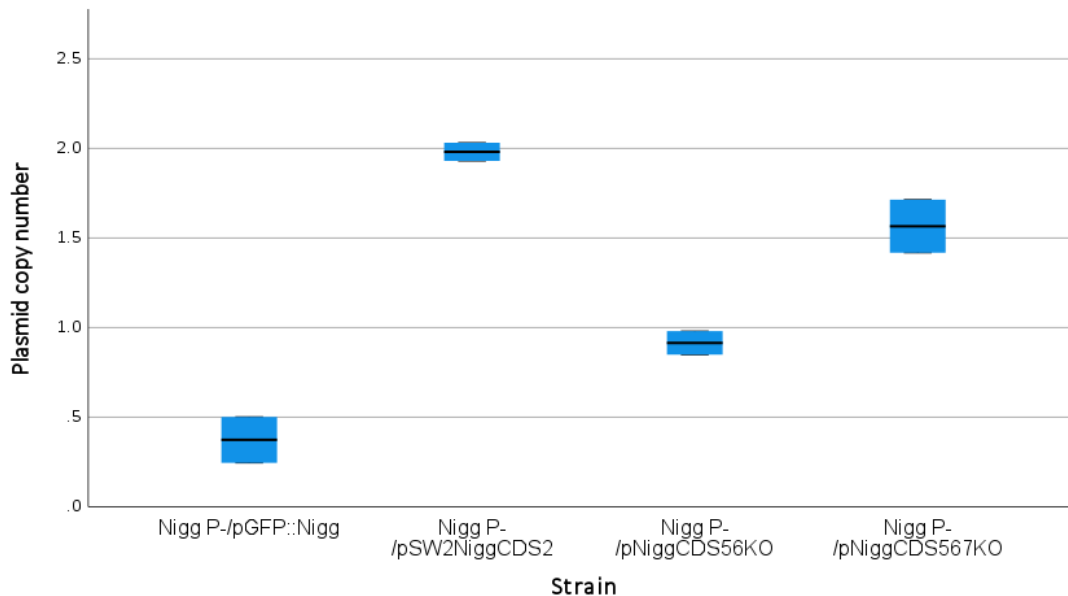


Figure 4-5 Plasmid copy number for *C. muridarum* plasmids grown under chloramphenicol selection.

Box plot of duplicate experiments showing the plasmid copy number (ratio of plasmid and chromosomal genes *CDS2* : *omcB* respectively) determined by qPCR for *C. muridarum* strains grown after three passages under $0.4\mu\text{gml}^{-1}$ chloramphenicol selection.

4.3.1.2 Plasmid loss frequency measured in standard inocula

The heterogeneity of the sample was also assessed by quantifying the proportion of inclusions without a fluorescent signal, indicating that *Chlamydia* cells within the inclusion are plasmid-free, from two fields of view that were imaged for each T_{25} culture ($n=2$) at each passage. An example of plasmid-free inclusions in cell culture of Nigg P-/pSW2NiggCDS2 without selection are shown in Figure 4-6.

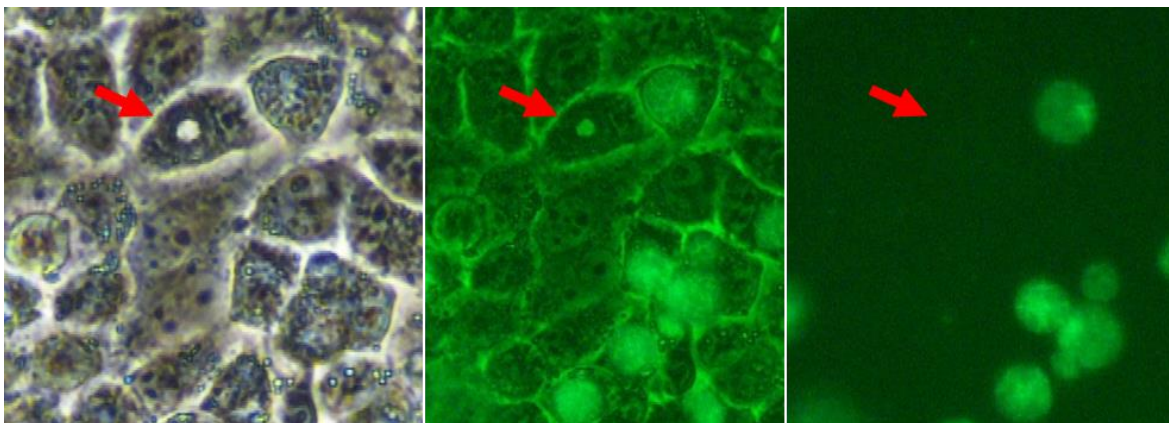


Figure 4-6 Photomicrograph of plasmid-free inclusions indicating *in vitro* plasmid loss of plasmid pSW2NiggCDS2 in *C. muridarum*

Inclusions of *C. muridarum* Nigg P- transformed with pSW2NiggCDS2 infected at MOI=1 were imaged at 24 hpi and show loss of plasmid pSW2NiggCDS2 *in vitro* without selection as indicated by the loss of green fluorescence from inclusions (arrowed).

A heterogeneous sample in the inocula for Nigg P-/pGFP::Nigg at P3 under chloramphenicol selection was previously evidenced by a plasmid copy number <1 , therefore, a proportion of plasmid free inclusions were expected to be visible in cell cultures. However, the mean proportion of plasmid-free inclusions was 0%. In comparison, a small proportion of plasmid-free inclusions (1-2%) were identified in cultures of Nigg P-/pSW2NiggCDS2, Nigg P-/pNiggCDS56Del and Nigg P-/pNiggCDS567Del under $0.4\mu\text{gml}^{-1}$ chloramphenicol selection at P3 (Figure 4-7). These data suggest that a degree of cell-to-cell heterogeneity exists in inocula generated under these conditions for all of the strains and is likely to be underestimated as a result of the low sensitivity of this approach for measuring plasmid loss.

Without selection, plasmid loss frequency was ≥ 2 -fold higher in the cultures at P3 for both strain Nigg P-/pGFP::Nigg and Nigg P-/pSW2NiggCDS2, indicating that these plasmids are less stable in the absence of selection. However, there was little difference in plasmid loss frequency measured in cultures of plasmid-gene deletion mutants of Nigg P-/pNiggCDS56Del and Nigg P-/pNiggCDS567Del after three serial passages regardless of the presence or absence of positive selection with chloramphenicol suggesting that these plasmids are inherently unstable. This is concordant with the inability to expand either plasmid-gene deletion mutant under higher concentrations of chloramphenicol.

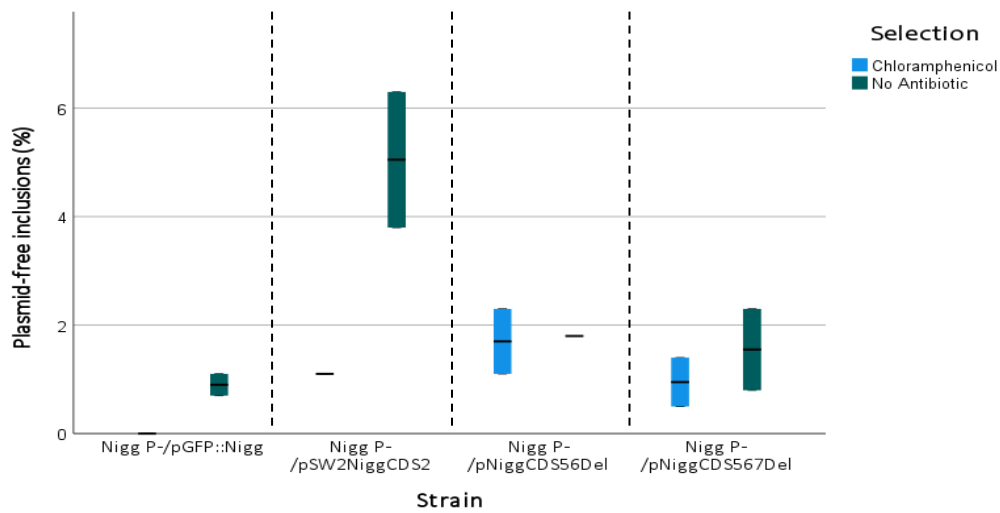


Figure 4-7 Effect of chloramphenicol on the proportion of plasmid-free inclusions determined for strains of *C. muridarum*.

Box plots showing the proportion of plasmid-free inclusions for strains of *C. muridarum* measured from the third passage with or without selection with sub-inhibitory concentration of chloramphenicol ($0.4\mu\text{gml}^{-1}$). Passage experiments were performed in duplicate. The proportion of plasmid-free inclusions was quantified from two fields of view per culture, taken at 40 x magnification at 24 hpi. Inclusions were classified as plasmid-free that did not fluoresce green.

4.3.2 Stability of *E. coli*-*C. muridarum* shuttle vectors in *C. muridarum*

4.3.2.1 Changes in plasmid copy number over serial passage

Standardised inoculum generated with chloramphenicol selection for each transformant was passaged a further three times both with and without penicillin selection as described in method 4.2.1. The random distribution model predicts the scenario where if plasmid loss occurs and the growth of plasmid-free cells is unrestricted by antibiotic selection, the proportion of plasmid-free cells can outgrow the plasmid-bearing population over generations (Million-Weaver and Camps, 2014). So, it was reasoned that a change in PCN is more likely to be detected when a comparison is made between PCN measured in both the EBs in the standardised inocula (P3) and from the progeny harvested at the final passage either with or without penicillin selection (P6).

For plasmid pGFP::Nigg, PCN remained stable over three passages (P3-P6) at ~0.5 copies demonstrating plasmid loss regardless of selection with or without penicillin, suggesting that *C. muridarum* maintains tight regulatory control over copy number, typical of low copy number plasmids. A lower plasmid copy number (<1) was expected given that PCN under bactericidal concentrations was 0.9 copies per cell (chapter 3 results 3.3.4). In comparison, PCN was at least 2-fold higher for all other transformants in any condition tested. A standardised inocula of Nigg P-/pSW2NiggCDS2 contained, on average, 1.98 plasmids per cell, decreasing by ~2-fold to 0.92 copies per cell after three passages upon removal of selection from the growth media. These results suggest that plasmid pSW2NiggCDS2 is less stable than plasmid pGFP::Nigg in *C. muridarum*.

For Nigg P-/pNiggCDS56Del, the standardised inocula contained 0.9 copies per cell, which increased to 2.9 under penicillin selection and to 1.9 upon removal of selection (Figure 4-8). The same trend was observed for strain Nigg P-/pNiggCDS567Del when median PCN increased from 1.6 to 3.7 under penicillin selection. However, the median PCN did not increase, but instead was maintained at 1.6 copies per cell when selection was removed, which suggests a role for plasmid gene *CDS7* in the regulation of PCN in *C. muridarum*.

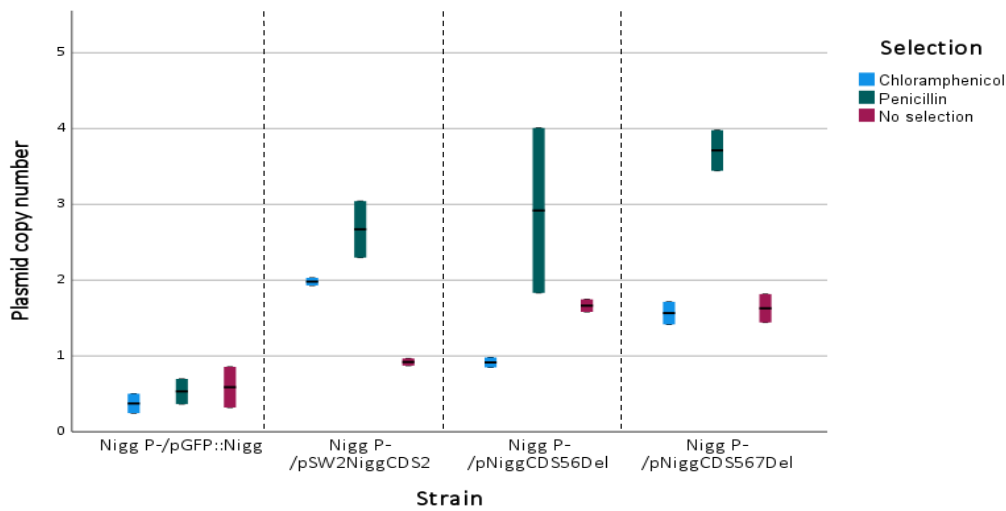


Figure 4-8 Effect of changing or removing antibiotic selection on plasmid copy number in *C. muridarum* transformants.

Box plots comparing the plasmid copy number for strains of *C. muridarum* measured after three passages in chloramphenicol selection ($0.4\mu\text{gml}^{-1}$), followed by three passages either without selection or with penicillin (10Uml^{-1}). Passage experiments were performed in duplicate. The plasmid copy number ratio (gene copy ratio *CDS2:omcB*) was determined by qPCR from gDNA purified from harvested chlamydial EBs at 28 hpi at the third passage in each condition.

4.3.2.2 Plasmid loss frequency over serial passage

To investigate plasmid stability further in these strains, quantification of the frequency of plasmid loss (the proportion of plasmid-free cells) was determined from images of mature inclusions for all transformants (method 4.2.3).

Figure 4-9 shows the plasmid loss frequencies measured from cultures from three passages and two passaging experiments combined, with selection ($n=6$) and without penicillin selection ($n=6$). Plasmid loss frequency for Nigg P-/pGFP::Nigg was low in both cultures grown under penicillin selection at 4.10% (6.22%) (median (interquartile range)) and without selection at 3.46% (2.92%). Given that the mean plasmid copy number was ~ 0.5 measured in these same cultures, indicating that on average 50% inclusions were plasmid-free, these results demonstrate that quantification of plasmid-loss using mature inclusion phenotypes as a proxy for *Chlamydia* cells within an inclusion is a much less sensitive a method for determining plasmid loss than using qPCR to determine PCN.

For plasmid pSW2NiggCDS2, that was shown to be less stable than pGFP::Nigg by measurement of PCN, the median frequency of plasmid loss was 2-fold greater at 9.34% (7.24%) with penicillin selection and 9.33% (5.43%) without selection (Figure 4-9). These data further demonstrate that plasmid pSW2NiggCDS2 is less stable than pGFP::Nigg over passage. The same pattern was observed in cultures of the plasmid-gene deletion mutant Nigg P-/pNiggCDS567Del, that also demonstrated higher median plasmid loss frequencies both with penicillin selection at 6.77% (5.71%) and without penicillin selection at 6.58% (7.76%). The range of the data was notably greater in these two plasmids, compared with those of pGFP::Nigg and pNiggCDS56Del, as demonstrated by the length of the whiskers on the box plots. This suggests that there was greater variability in the plasmid loss frequency measured in these cultures, which is concordant with a more heterogeneous sample.

The plasmid loss frequencies determined for plasmid-gene deletion mutant pNiggCDS56Del were 2.50% (0.84%) with penicillin selection and 0% (2.46%) without selection. These were closer to the frequencies observed to the parent strain pGFP::Nigg. These data further suggest that *CDS7* alone has a role in plasmid maintenance.

The data for each strain both with or without penicillin selection as represented in Figure 4-9 were not normally distributed as determined by Shapiro-Wilk test for normality and visual inspection of box plots. The skewed distribution is likely to indicate the inherent lack of sensitivity and variability that comes with quantifying plasmid loss based upon inclusion phenotypes with the current method. The sensitivity and variability could both be improved if the inclusions across the entire culture flask could be quantified as opposed to randomly sampling two fields of view in a T25 cell culture flask. However, this would be extremely laborious and time consuming.

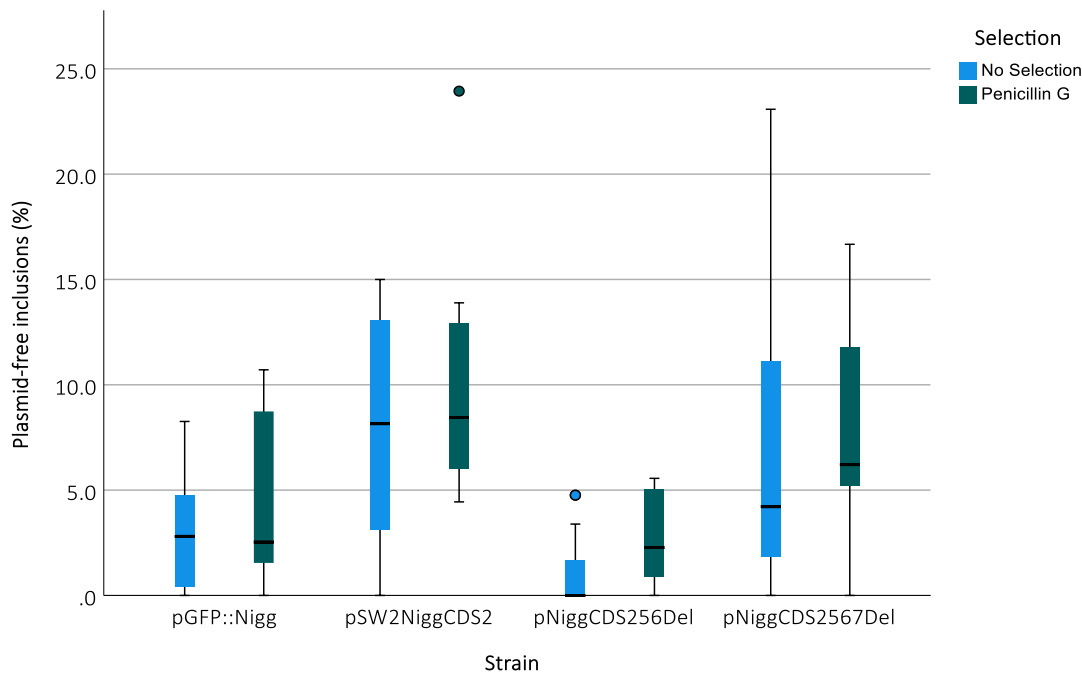


Figure 4-9 Effect of penicillin selection on plasmid-loss frequency measured *in vitro* for *C. muridarum* transformed with plasmids containing non-essential gene-deletions.

Box plots showing the proportion of plasmid-free inclusions for strains of *C. muridarum* measured from cell cultures either without selection or with penicillin (10Uml^{-1}) ($n=6$). The proportion of plasmid-free inclusions was quantified from two fields of view per culture, taken at 40 x magnification at 24 hpi. Inclusions were classified as plasmid-free that did not fluoresce green. A plasmid-free phenotype in mature inclusions was identified by loss of green fluorescence.

The frequency of plasmid loss was also quantified for each strain serially passaged six times without antibiotic selection (treatment arm 2 cultures). In this instance, the frequency of plasmid loss was consistently low (<4%) over six consecutive passages without antibiotic selection for both plasmid pNiggCDS56Del and the parent plasmid pGFP::Nigg (Figure 4-10). These findings were concordant with plasmid loss frequencies measured both with and without penicillin selection over three passages for these same plasmids in treatment arm 1. Furthermore, the mean frequency of plasmid loss for plasmid pNiggCDS567Del increased from $4.5\% \pm 1.55\%$ (mean \pm sem) at P1 to $12.32\% \pm 3.2\%$ at P6 (Figure 4-10), consistent with the plasmid loss frequencies measured for this strain in treatment arm 1 when passaged with penicillin selection. Together, these findings support the following hypothesis that *CDS7* has a role in regulating plasmid copy number in *Chlamydia*.

When Nigg P-/pSW2NiggCDS2 was serially passaged six times without antibiotic selection, the mean frequency of plasmid loss decreased from $19.88\% \pm 8.82\%$ at P1 to $3.35\% \pm 1.92\%$ at P2, then steadily increased to $11.02\% \pm 1.15\%$ at P6. These findings support the hypothesis that plasmids with a *C. trachomatis* backbone such as pSW2NiggCDS2 are less stable over passage in *C. muridarum* than plasmids containing the native *C. muridarum* backbone, and supports the plasmid copy number data for this strain.

It was notable that the proportion of plasmid-free inclusions was high for cultures of pSW2NiggCDS2 in the first passage without selection. This was because plasmid free inclusions were observed in cultures where the total number of inclusions was very low at <6 inclusions per field of view at passage 1 only. The total number of inclusions was also very low for Nigg P-/pGFP::Nigg at P1, however, no plasmid-free inclusions were observed for this strain at this passage. The relatively low number of chlamydial cells that went on to infect McCoy cells at P1 was reflected in a decrease in the concentration of infectious forming units (IFUml⁻¹) between the starting inocula under selection with chloramphenicol and the inocula harvest at P1 without selection for both strains. This was supported by IFU data showing that the concentration of infectious EBs decreased in cultures of Nigg P-/pGFP::Nigg from 8.85 IFUml⁻¹ (Log10) to 8.4 IFUml⁻¹ (Log10), and from 8.45 IFUml⁻¹ (Log10) to 7.15 IFUml⁻¹ (Log10) for Nigg P-/pSW2NiggCDS2 in the starting inocula and then P1 inocula harvested. These data suggest that serial passage of plasmids under chloramphenicol has an adverse effect on IFU for larger plasmids.

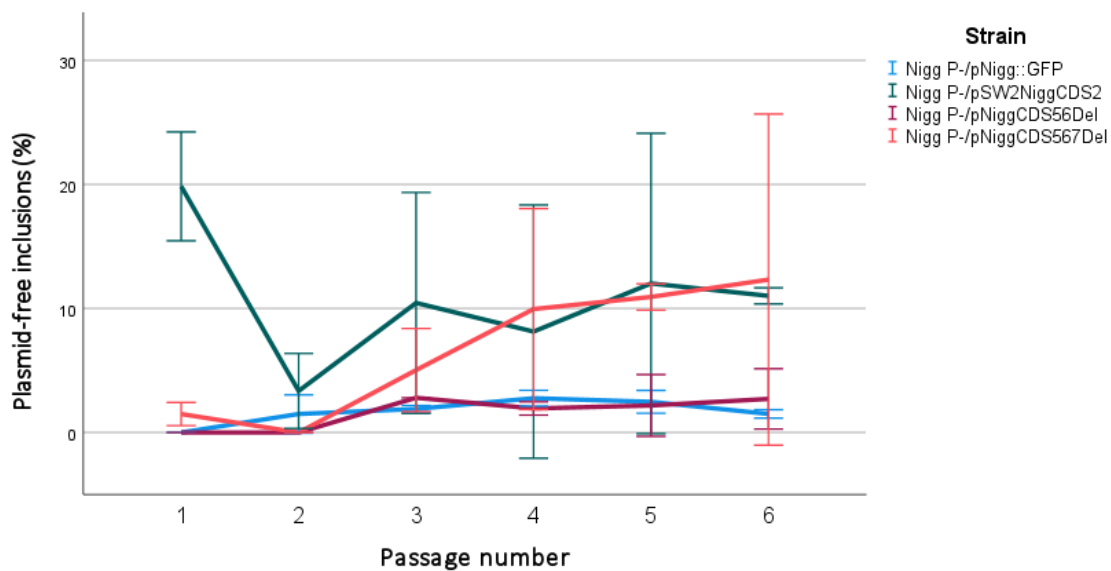


Figure 4-10 Plasmid loss frequency determined for *C. muridarum* transformants over serial passage without antibiotic selection.

Inocula containing Nigg P- transformed with either pNiggCDS56Del, pNiggCDS567Del, and their parent plasmid pGFP::Nigg as well as the recombinant plasmid pSW2NiggCDS2 were serially passaged six times at MOI=1.0 without antibiotic selection in the growth media. Inclusions were quantified from two fields of view taken at 40x magnification per culture at 24 hpi. Each datapoint represents the mean of biological replicates (n=4) error bars represent 95% CI. A plasmid-free phenotype in mature inclusions was identified by the absence of GFP expression. Plasmid loss frequency (proportion of plasmid-free inclusions) was determined at every passage.

To investigate the relationship between PCN and the plasmid loss frequency, and to see if the former could be used to predict the latter, linear regression analysis was performed. Linearity was established by visual inspection of a scatterplot with the independent variable, PCN, on the x-axis and the dependent variable, plasmid loss frequency (percentage of plasmid-free inclusions), on the y-axis (Figure 4-11). There was independence of residuals as assessed by Durbin-Watson statistic of 1.135. Visual inspection of a plot of standardised residuals versus standardised predicted values confirmed homoscedasticity of the data. Residuals were normally distributed as assessed by visual inspection of histogram and normal probability plots.

The slope coefficient was not statistically significant ($p=0.114$) demonstrating that there is no true linear relationship between plasmid copy number and the frequency of plasmid loss (percentage of plasmid-free inclusions). This is not surprising given that less stable plasmids pSW2NiggCDS2, pNiggCDS56Del and pNiggCDS567Del demonstrated much higher PCN in all conditions compared to plasmid pGFP::Nigg and shows therefore that the plasmid distribution is masked by mean PCN. This is consistent with some studies that have similarly found that PCN was not correlated with increased plasmid stability (Standley et al., 2019).

When the biological replicates for plasmid pSW2NiggCDS2 at third passage without selection, represented as green circles, were treated as outliers, and removed from the analysis, the assumptions for linear regression were still met and the slope coefficient became significant ($p=0.022$) with a positive linear relationship. These datapoints represent the only example in the dataset for all four plasmids where PCN decreased over passage. This analysis showed that a predicted increase in plasmid loss frequency of 1.6% (0.2-2.9 95% CI) for every increase in PCN of 1. However, given that the study is designed to investigate the stability of plasmids where stability is unknown, it would not be appropriate to remove these datapoints from the analysis. Overall, these findings suggest that this study design requires the interpretation of plasmid stability to consider the analysis of PCN and plasmid-loss frequency separately.

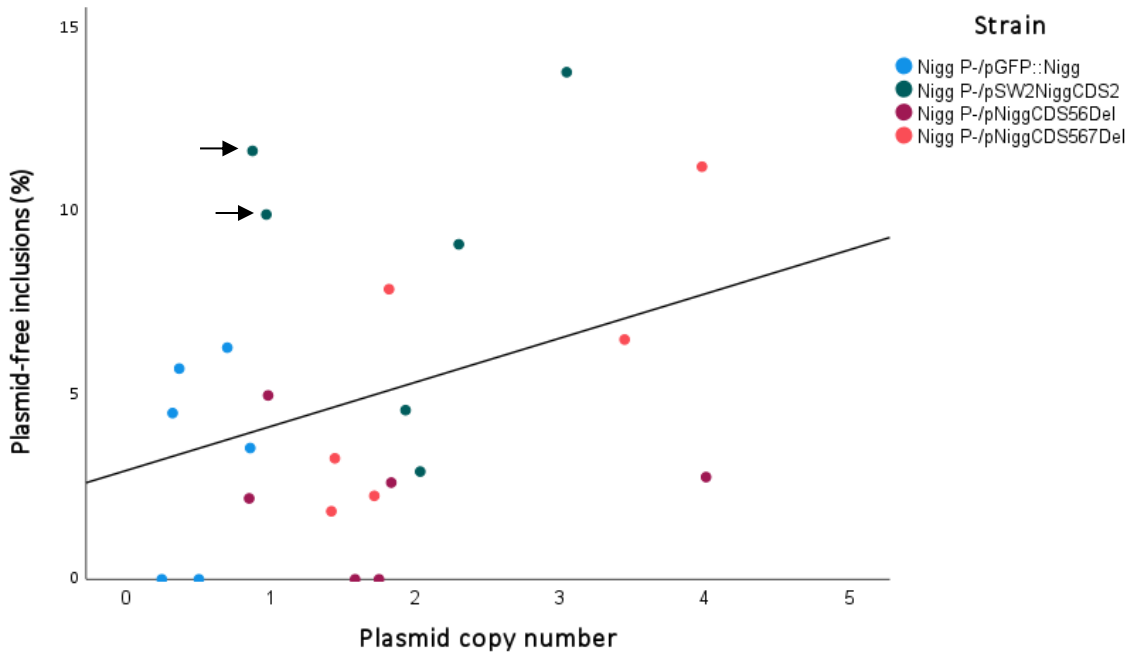


Figure 4-11 Scatter plot showing the relationship between plasmid copy number and the frequency of plasmid-loss in *C. muridarum*

Transformants of *C. muridarum* strain Nigg P- carrying plasmids pGFP::Nigg, pSW2NiggCDS2, pNiggCDS56Del and pNiggCDS567Del were serially passaged three times with chloramphenicol selection ($0.4\mu\text{gml}^{-1}$) in the growth media. Inocula harvested at third passage was then serially passaged a further three times either with or without penicillin G selection (10Uml^{-1}) in the growth media. Plasmid copy number (PCN) and plasmid loss frequency (proportion of plasmid-free inclusions) were determined from cultures at third passage in each condition for two biological replicates. The mean PCN (*CDS2* : *omcB*) of the total population was determined by qPCR with quadruplicate technical repeats and plasmid loss frequency (mean proportion of plasmid-free inclusions that did not express GFP) were quantified from images of two fields of view taken at 40 x magnification at 24 hpi. Biological replicates for plasmid pSW2NiggCDS2 at P6 without selection are indicated by arrows. The mean linear line of best fit is shown. Linear regression analysis demonstrated that there was no true linear relationship between PCN and plasmid loss frequency for *C. muridarum* transformants ($p=0.114$).

4.4 Discussion

4.4.1 *Measuring plasmid stability in Chlamydia*

No standardised method for measuring plasmid stability in *Chlamydia* exist. Plasmid stability has been quantified as ratios of red-shifted GFP-expressing-inclusions to antichlamydial lipopolysaccharide (LPS) antibody-stained inclusions in strains of *C. pneumoniae* (Shima et al., 2018). In *C. muridarum*, plasmid loss frequency has been measured quantifying the proportion of plasmid-free inclusions that negatively stain for glycogen using iodine (Liu et al., 2014a; O'Connell and Nicks, 2006; Russell et al., 2011; Wang et al., 2014). However, interpretation of such an approach is subjective and lacks sensitivity (Skilton et al., 2018). Therefore, it was expected that any method that relies on the quantification of inclusion phenotypes as a proxy for plasmid loss within individual cells would be less sensitive than a molecular method that directly quantifies the PCN.

In free-living bacteria traditional plating techniques using selection and fluorescent reporters are used to measure plasmid loss frequency, however, such approaches have been shown to be inherently biased (Jahn et al., 2014). To improve the accuracy of estimation of PCN, several direct quantitative methods for estimation of mean PCN in the total population of bacteria have been developed that use gel or capillary electrophoresis, liquid chromatography, and real-time qPCR (qPCR) (Dell'anno et al., 1998; Projan et al., 1983). In this study, both indirect and direct measures of plasmid loss were adopted.

A novel approach directly measured plasmid loss in *C. muridarum* through quantification of PCN (*CDS2: omcB*) by qPCR, comparing PCN in a standardised inocula compared with the PCN in cultures of 3rd generation progeny to assess stability through change in PCN over three generations of EBs. This required a method for generating a standard inocula for *C. muridarum* transformants and provided a robust and reproducible means to measure plasmid stability in *C. muridarum* that could be easily adapted for other *Chlamydia* spp.

A second novel approach indirectly measured plasmid loss frequency over three passages (generations) in *C. muridarum* through quantification of the proportion of mature plasmid-free inclusions indicated by absence of expression of GFP. The bullseye phenotype, indicative of plasmid-free inclusions, was not used because this phenotype was frequently observed in conjunction with expression of GFP within an inclusion and therefore the *Chlamydia* within these inclusions were heterogeneous. Typically, a mean PCN of 1 is thought to indicate stable segregational stability, however, when PCN is estimated for the total population of bacteria, as it was in this study, it has been shown that the mean PCN will mask plasmid-free cells by ignoring

the variation in distribution between cells (Million-Weaver and Camps, 2014). This was observed for all strains, where plasmid-free inclusions were observed in cultures with PCN ≤ 1 .

As expected, the visual quantification of plasmid-free inclusions was less sensitive than direct measurement of PCN for each culture at detecting plasmid loss, particularly for within-strain comparisons. Furthermore, linear regression analysis showed that plasmid copy number could not be used to predict plasmid loss frequency, which is not surprising given that less stable plasmids had higher copy numbers than the control plasmid and the mean PCN of the total population is known to mask the true plasmid distribution which is variable between cells (Million-Weaver and Camps, 2014). The classic distribution model describes a correlation between an increase in PCN and an increase in plasmid stability (Werbowsky et al., 2017). But these models are simulated on high copy number plasmids which do not rely upon active partitioning systems which are more typical of low copy number plasmids for their segregational stability.

Despite this, the two approaches provided complimentary information and the overall conclusions that could be derived from both methods were not contradictory. These findings suggest that the interpretation of these approaches should be made separately. Understanding the relationship between changes in PCN in *C. muridarum* and how they relate to plasmid stability in cell culture could benefit from using a more sensitive technique that determines PCN at the single cell level. Such an approach has been developed in *Pseudomonas putida* which isolated plasmid-free from plasmid-bearing cells that did not or did express a fluorescent reporter protein respectively using flow cytometry, and applied digital droplet PCR to the sub-populations of cells to determine PCN (Jahn et al., 2014).

4.4.2 Generating standard inocula for *C. muridarum* transformants

The generation of a standardised inocula for *C. muridarum* transformants was necessary for a robust and reproducible means to investigate plasmid stability through the quantification of the frequency of plasmid loss or changes in PCN measured over three generations of EBs. The use of chloramphenicol at bactericidal concentrations was successful at killing plasmid-free cells resulting in the desired plasmid copy number of approximately 1 for shuttle vector pGFP::Nigg as demonstrated in the previous chapter. Given that plasmid genes *CDS5*, *-6* and *-7* are inessential for plasmid maintenance it was surprising that only plasmids pGFP::Nigg and pSW2NiggCDS2 that contain the complete set of plasmid-genes were able to expand under chloramphenicol selection at a concentration of $1\mu\text{gml}^{-1}$ and demonstrated that plasmids pNiggCDS56Del and pNiggCDS567Del were inherently unstable in these test conditions. Liu et al (2014a) demonstrated that plasmid genes *CDS5* and *-6* act as positive and negative regulators for expression of some of the same chromosomal genes, which led the authors to hypothesise that plasmid genes may

regulate chromosomal gene expression in response to changes in the environment.

Chloramphenicol disturbs chromosomal replication because this process is dependent on *de novo* protein synthesis (Clewell, 1972). So, the inability for these plasmids to expand under high concentrations of the protein synthesis inhibitor suggests that the chromosomal genes under regulatory control by both *CDS5* and *-6* are essential for survival.

The sub-inhibitory concentration of chloramphenicol at $0.4\mu\text{gml}^{-1}$ has previously been used for the recovery of *C. trachomatis* and *C. muridarum* transformants and this concentration was determined to be the MIC for *C. muridarum* strain Nigg at MOI=1 in the previous chapter (LaBrie et al., 2019; Wang et al., 2019; Xu et al., 2013). It was expected therefore that the plasmid-gene-deletion mutants would expand under selection at sub-inhibitory concentrations, which they did. However, the ability to limit the growth of the plasmid-free population of bacteria using sub-inhibitory concentrations of chloramphenicol to generate a standardised inoculum for each strain was unknown. A standardised inocula was considered optimal for a starting inocula to measure plasmid stability to reduce the heterogeneity in the inocula generated for each strain. Plasmid copy number was ≥ 1 for all plasmids, except for pGFP::Nigg. Therefore, the criteria for generating a standardised inocula was met for all strains excluding the parent plasmid pGFP::Nigg, which has such a minimal PCN, only killing of plasmid-free cells would enable the possibility of PCN of ≥ 1 . However, this criterion is imperfect and does not guarantee that all cells will contain a plasmid. This is because mean PCN is measured across the whole population and therefore does not represent the variation in the distribution of plasmids between cells. It was not surprising therefore that the frequency of plasmid loss, measured as the proportion of plasmid-free mature inclusions in these same cultures ranged from 0- 4% for all strains at P3 under sub-inhibitory concentrations of chloramphenicol.

4.4.3 Plasmid stability in *C. muridarum*

The mechanisms for plasmid maintenance are unknown in *Chlamydia*, however, given the low plasmid copy number obtained for all transforming plasmids (<4) it is likely that tight regulatory control is maintained by several processes typical of low copy number plasmids which include control of active partitioning, replication, and plasmid copy number. It was not surprising therefore that PCN, albeit very low (<1) was stably maintained in the control strain pGFP::Nigg, which contains the complete native *C. muridarum* plasmid, regardless of a change in selection to penicillin or removal of antibiotic selection from the media. The mean PCN measured for all plasmids in this study ranged from 0.32- 4.01 copies per cell, these findings are consistent with a range of 1-4 copies per cell quantified in plasmids pGFP::CM, which is very similar to pGFP::Nigg, and its derivatives containing single gene deletions of *CDS5*, *-6* and *-7* in *C. muridarum* by qPCR

Chapter 4

(Liu et al., 2014a). However, they are lower than PCN reported for *C. trachomatis* strains which range between 4 and 10 copies per chromosome (Pickett et al., 2005).

Plasmid pSW2NiggCDS2 has been described as stably maintained in *C. muridarum* (Weinmaier et al., 2015), however, this conclusion was based upon the simple ability to recover transformants and maintain the plasmid over six passages under selection with ampicillin in the growth media (Wang et al., 2014). It was hypothesised that plasmid pSW2NiggCDS2 would be less stable than plasmid pGFP::Nigg on account of the *C. trachomatis* backbone because the plasmid sequence variation has been shown to directly impact the ability for a plasmid to replicate and be maintained in its' original host (Song et al., 2014; Wang et al., 2014). This process may only be dependent upon *CDS2*, but other genes including *CDS3*, *-4* and *-8* are also essential for plasmid maintenance may also play a role in plasmid tropism (Gong et al., 2013; Liu et al., 2014a; Song et al., 2014; Wang et al., 2014).

A mean PCN of 1 or above is regarded as being indicative of stable maintenance because every daughter cell has inherited at least one plasmid. Under positive selection, the mean PCN was at least 2 copies per cell for plasmid pSW2NiggCDS2, suggesting that this plasmid was stable. However, the mean plasmid-loss frequency measured over three passages in cultures with and without penicillin selection were equally high at ~10%, which was 3-fold higher than cultures of pGFP::Nigg. Given that an increase in PCN did not correlate with a decrease in plasmid loss frequency, there is not enough evidence to conclude that the increased PCN under penicillin selection is indicative of a stable plasmid. In fact, in some studies, increases in plasmid copy number, as a result of loss of regulation of copy number control, were associated with increased instability (Million-Weaver and Camps, 2014; Tomizawa and Som, 1984). It is reasonable to suggest that sequence variation in plasmid genes introduced by a non-native recombinant plasmid could alter the control mechanisms in a species.

The mean PCN decreased by 2-fold upon removal of selection for plasmid pSW2NiggCDS2, and the plasmid loss frequency increased over six serial passages without selection. In comparison, both PCN and plasmid loss frequency were stable for plasmid pGFP::Nigg regardless of selection. Together these data strongly suggest that plasmid pSW2NiggCDS2 is unstable without positive selection in *C. muridarum*, and that sequence variations in the essential plasmid-genes other than *CDS2* are responsible. Therefore, this shuttle vector is not appropriate for a stably replicating transposon delivery vector in *C. muridarum*.

Plasmid instability was also indicated for plasmid pNiggCDS567Del. Plasmids pGFP::Nigg, pNiggCDS56Del and pNiggCDS567Del are identical except for deletion of plasmid genes *CDS5*, *-6* and *-7*. Therefore, differences in plasmid stability between these plasmids can be explained by these deleted genes. The mean PCN was higher (≥ 1) in plasmids pNiggCDS56Del and plasmid

pNiggCDS567Del compared with the parent plasmid pGFP::Nigg in any condition. When positive selection was changed to penicillin G in the growth media, the mean PCN remained the same or increased for all plasmids. When selection was removed however, a different effect on PCN was observed between these plasmids. PCN increased by 2-fold in plasmid pNiggCDS56Del whereas PCN failed to increase for plasmid pNiggCDS567Del and was instead unchanged over three passages. This data could suggest a positive regulatory role for *CDS7* in regulation of plasmid copy number, but it also suggests that the antisense RNA for this gene (if it is transcribed in *C. muridarum*) does not play a regulatory role in plasmid maintenance, because antisense RNAs typically act as negative regulators in control of plasmid copy number (Brantl, 2015, 2014, 2002). Plasmid gene *CDS7* has been shown to be a negative regulator to suppress expression of some chromosomal genes, therefore, these findings suggest that this protein may act as both activator and repressor. This capability is true for a few known bacterial proteins such as transcriptional activator CAP and bacteriophage lambda repressor (Alberts et al., 2002).

When plasmid pNiggCDS567Del was passaged six times without selection, the plasmid loss frequency increased from 0-12%, whereas it stayed the same at <4% for both plasmids pGFP::Nigg and pNiggCDS56Del. Furthermore, the mean plasmid loss frequency over three passages with and without penicillin selection were comparably high with those measured in plasmid pSW2NiggCDS2 at ~12%, and well above those measured in plasmid pGFP::Nigg and pNiggCDS56Del at ~4%. The frequency of plasmid loss also increased over six passages without selection in this strain, whereas plasmid pGFP::Nigg and plasmid pNiggCDS56Del stayed stable over passage. These data show that plasmid gene *CDS7* is very likely to have a role in plasmid maintenance which directly conflicts with published data that state that *CDS7* is not essential for plasmid maintenance (Gong et al., 2013; Liu et al., 2014a). This discrepancy can be explained by the differences between the methods used to assess whether a gene has a role in plasmid maintenance. These are the ability to transform and passage transformants under positive selection compared with quantitative measurement of plasmid loss over serial passage both with and without selection. However, it is not clear whether the effect of deletion of three plasmid genes in tandem or *CDS7* on its' own are responsible for these observations. So, further investigation is required to demonstrate a role of *CDS7* in plasmid maintenance, starting with testing the single gene knock out mutant using this same approach.

4.5 Conclusions

The aim of the work presented in this chapter was to identify an appropriate vector that can be stably passaged in *C. muridarum* for the backbone of a transposon delivery vector to allow for its' expansion in cell culture prior to induction of transposition. This study demonstrated how two

Chapter 4

novel methods can be used to measure plasmid stability in *C. muridarum*: 1 change in mean PCN over serial passage, measured by quantitative real-time PCR of plasmid and chromosomal genes and plasmid loss frequency measured as lack of GFP expression over serial passage. However, further work is needed to optimise these methods for other strains and species of *Chlamydia*. Plasmid pGFP::*Nigg*, which contains the complete native *C. muridarum* plasmid was the most stable in any condition and was therefore determined to be the most appropriate candidate for the backbone of a stably replicating transposon delivery vector. Plasmid pSW2*NiggCDS2* was previously considered stable based upon a non-quantitative assessment of plasmid stability but was shown to be unstable in *C. muridarum* demonstrating that plasmid genes other than *CDS2* may have a role in plasmid tropism. In addition, plasmid-gene *CDS7* was shown to have a role in plasmid copy number control and plasmid maintenance contrary to previous research that classified this gene as not-essential for plasmid maintenance. These findings demonstrate the importance of having robust and sensitive quantitative methods for determining plasmid stability in *Chlamydia*.

Chapter 5 Progress towards inducible transposon mutagenesis in *C. muridarum*

5.1 Introduction

Suicide vectors engineered as transposon delivery vectors are consistently unreliable tools for generating saturation or near-saturation mutant libraries, where every gene contains at least one transposon insertion, in *C. muridarum*, *C. trachomatis* or indeed any other obligate intracellular bacterial species (Beare et al., 2009; Cheng et al., 2013; Felsheim et al., 2006; LaBrie et al., 2019; Wang et al., 2019). The suicide vector approach, by design, limits the number of unique mutants which can be generated in *Chlamydia* by initiating transposon transposition and loss of the plasmid in the transformed EB. This generates single-mutant clones within individual inclusions hence the low efficiency of transformation estimated to be approximately 1 in 10^6 becomes an even greater limiting factor for the ability to generate large numbers of unique mutants using this approach (Jones et al., 2020). For these reasons, transposon mutagenesis based on the suicide vector approach does not generate near-saturation mutant libraries which is required to identify all essential genes (Cain et al., 2020). Therefore, it was hypothesised that the generation of near-saturation mutant libraries may be possible with the expansion of the transformant population carrying a transposon delivery vector prior to the induction of transposon transposition (Skilton et al., 2021). Having demonstrated that *E. coli*-*C. muridarum* shuttle vector pGFP::Nigg was stable over passage in *C. muridarum*, the aim of this chapter was to engineer an inducible, self-replicating transposon delivery vector using pGFP::Nigg, which can be stably passaged and expanded prior to induction of transposon transposition, and to recover transformants in *C. muridarum*.

5.2 Methods

5.2.1 *Quantitative susceptibility testing*

Quantitative susceptibility testing was performed to determine the minimum inhibitory concentration (MIC) of antimicrobial agent erythromycin in both *C. muridarum* and *E. coli*. The MIC was defined as the lowest concentration of antibiotics required to completely inhibit bacterial growth. The immuno-staining assay used to determine the MIC in *C. muridarum* in chapter was adapted to minimise the 2–3-day delay in results by replacing identification of immune-stained inclusions with the use of phase contrast and UV light microscopy to visualise inclusions at 24 hpi. Determination of MIC in *E. coli* was made using a crude solid-phase assay by preparing LB agar plates containing the calculated concentration of antimicrobial agent which were then seeded with subcultures of *E. coli* in liquid medium, either streaked or spread, and growth of bacteria was confirmed after 24 hours incubation at 37°C. Assays are described in full below.

5.2.1.1 *Determination of MIC of erythromycin in C. muridarum*

Freshly prepared stocks of erythromycin (stock concentration 1mgml⁻¹) were added to 2ml DMEM/10% FCS supplemented with 1µgml⁻¹ cycloheximide, to give a final concentration of 0.5µgml⁻¹. Two-fold serial dilutions were prepared in a total volume of 2ml DMEM + 10% FCS supplemented with 1µgml⁻¹ cycloheximide. Final erythromycin concentrations were 0.5, 0.25, 0.125, 0.06 and 0.03 (µgml⁻¹).

For determination of the MIC of erythromycin, McCoy cells were seeded into T₂₅ tissue culture flasks. At confluence, flasks were infected at an MOI=1.0 with either *C. muridarum* strain Nigg P- or Nigg P-/pGFP::Nigg to accommodate duplicate experiments at each concentration of antimicrobial agent and an untreated (control) flask for each strain. After 30 minutes centrifugation, the media was removed and replaced with new media that contained either cycloheximide only (control wells) or cycloheximide with the antimicrobial agent at each test concentration. Infected wells were then incubated at 37°C in 5% CO₂ and imaged at 24 hpi under 40 x magnification by phase contrast. The MIC was determined to be the concentration of erythromycin that completely inhibited inclusion formation at 24 hpi.

5.2.1.2 *Determination of MIC to erythromycin in E. coli*

A crude solid phase assay was used to determine the MIC erythromycin for *E. coli* strains DH5α, GM2163 and Q358 to select for *E. coli* transformants carrying vectors containing erythromycin

resistance gene, *ermB*. A wide concentration range was chosen based upon wide ranging, and high MICs reported in early studies using *E. coli* (Andreumont et al., 1986). From a starting stock of 1mgml^{-1} , erythromycin was added to 20ml LB agar to obtain the following final concentrations: 10, 20, 50, 100, 125, 150, and 500 ($\mu\text{g ml}^{-1}$). The *E. coli* strains were streaked onto LB agar supplemented with erythromycin at the calculated concentrations and onto LB agar without antibiotics. Plates were incubated over night at 37°C in a warm room then a visual inspection of plates for bacterial growth was performed.

5.2.2 Construction of an inducible, self-replicating transposon delivery vector for *C. muridarum*

5.2.2.1 Cloning strategy for the construction of pNiggHimar

Construction of a self-replicating, inducible transposon delivery vector identified as pNiggHimar (Figure 5-1), combined the complete pGFP::Nigg plasmid with a PCR amplicon (3297 nt) amplified from transposon delivery vector pRPF215 which was engineered for transposon mutagenesis in *Clostridium difficile* (*C. diff*) (Dembek et al., 2015). The PCR amplicon from pRPF215 contained the *Himar1* transposon with an erythromycin resistance gene *ermB* located in between *Himar1* inverted repeat sequences as well as the wild type *Himar1* mariner transposase (1047 nt) under the control of an inducible Tet promoter system. PCR of the *Himar1* transposon-containing fragment was performed using primers 7-8: Transposon_F2 and Transposon_R2, adding Pfo1 restriction sites to 5' and 3' ends of the PCR fragment. The PCR fragment was cloned into the unique Pfo1 site located 249 nt upstream of the start codon of *bla* and 227 nt downstream of the stop codon of truncated *CDS1*, to insert outside of any coding regions in pGFP::Nigg. The cloning methods are described in detail in the following sections.

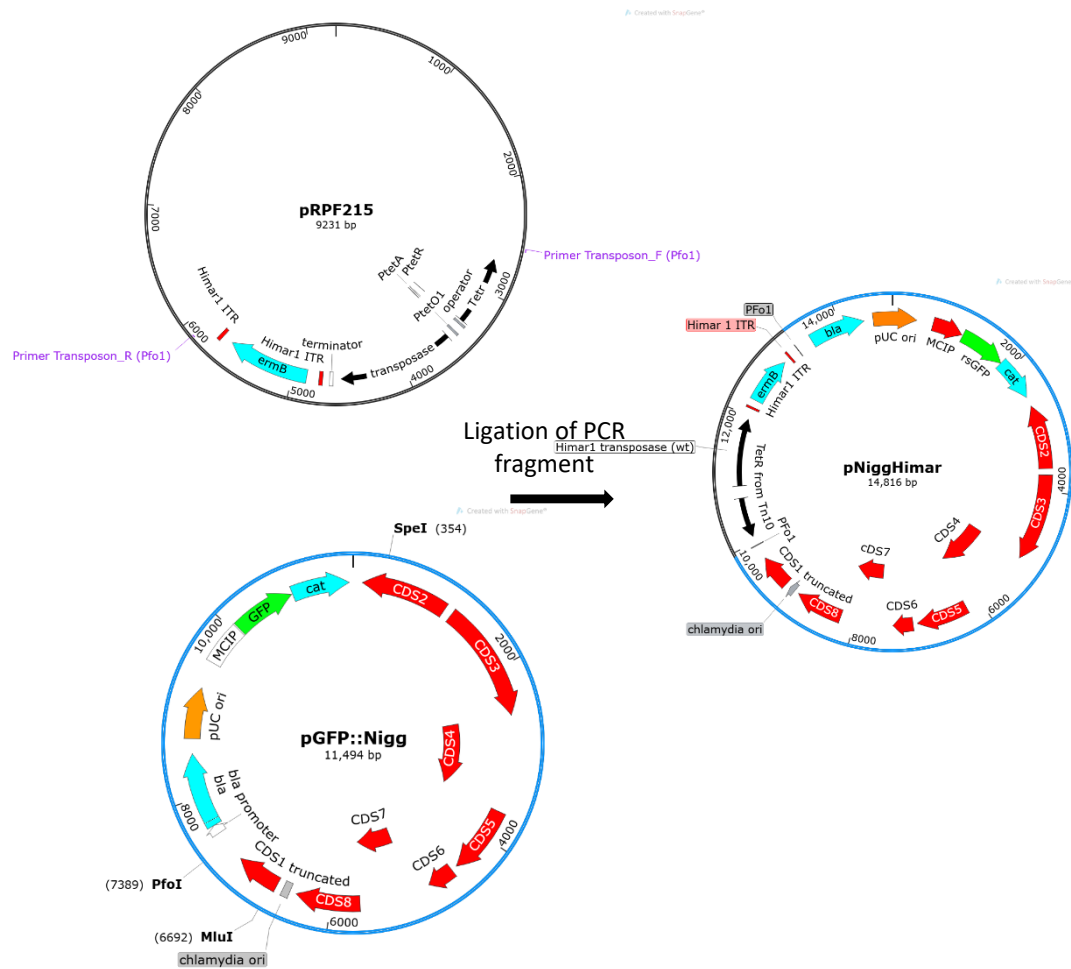


Figure 5-1 Cloning strategy for the construction of replication proficient *E. coli-C. muridarum* transposon delivery vector pNiggHimar

An amplicon (3297 nt) containing the *Himar1* transposon under *tet* promoter control from plasmid pRPF215 was cloned into the unique Pfo1 site on *E. coli-C. muridarum* shuttle vector pGFP::Nigg to generate a single, self-replicating transposon delivery vector for *C. muridarum*. Primers for end point PCR are indicated in purple text. The unique Pfo1 site is situated in a non-coding region between the antibiotic resistance gene *bla* and the first coding sequence (*CDS1*) on the *C. muridarum* plasmid backbone.

5.2.2.2 Vector DNA preparation

Vector DNA (plasmid pGFP::Nigg) was linearised by restriction enzyme digestion with Pfo1 (Table 8) followed by de-phosphorylation to remove 5'-phosphate groups from each molecule end to prevent self-ligation. De-phosphorylation was performed using alkaline phosphatase and alkaline phosphatase buffer 10x (Promega) made up to 10µl with dH₂O, added to a 50µl enzyme digest. Alkaline phosphatase was activated at 37°C for 30 minutes followed by deactivation at 56°C for 15 minutes. Once dephosphorylated, the linearised DNA was purified using the Wizard® DNA clean up kit (Promega) and the amplicon size confirmed on a 1% agarose gel. The undigested vector was loaded to demonstrate the size difference between the supercoiled and linearised plasmid DNA. Purified vector DNA was analysed on a spectrophotometer (Nanodrop, ThermoFisher) to calculate the concentration stored at -20°C ready for ligation.

5.2.2.3 Insert DNA preparation

Next, the ~3kb transposon (insert), was PCR amplified from the original parent vector, pRPF215 using primers 7 and 8 (Table 9) to add Pfo1 restriction sites to each end to allow for ligation to the Pfo1 sticky ends of the linearised vector backbone. The High-Fidelity Phusion Flash PCR protocol (method 2.12, Table 3) was optimised with 2mM magnesium chloride and three 50µl reactions performed. PCR product was run on a 0.8% agarose gel at 90 V for 65 minutes and bands visualised on a blue light transilluminator. The PCR product was excised from the gel, pooled into one 1.5ml microcentrifuge tube, and dissolved at 55°C in a water-bath with equal amounts of membrane binding solution. The DNA was purified using the Wizard® SV Gel and PCR purification system (Promega) and concentration analysed on a spectrophotometer (NanoDrop, ThermoFisher). 2µg insert DNA was digested with the appropriate restriction endonuclease to remove the flanking polymerase-binding sequence. The DNA was purified a second time and eluted in dH₂O. The cleaned product was confirmed on a gel and stored at -20°C ready for ligation.

5.2.2.4 DNA Ligation

The concentration of insert DNA was mixed with 10ng vector DNA at a molar ratio of three to one and/or six to one respectively, in separate ligation reactions, to favour ligation between insert with vector molecules as opposed to the self-ligation of vector molecules. The DNA was incubated with T4 DNA ligase and rapid ligation buffer (2x) in a 10µl reaction for 15 minutes at room temperature. DH5α competent cells (50 µl) were transformed with the total ligation reaction (10 µl) and plated onto selective LB agar plates relevant to the specific markers carried on the DNA insert, then incubated over night at 37°C. Three control reactions were performed to control for

background of undigested or self-ligated vector DNA. Ligation reactions and the controls used for each ligation reaction are described in Table 7.

Table 7 Ligation reaction with controls used for cloning experiments

| | Ligation reaction | Control reactions | | |
|-------------------|-------------------|-------------------|---|---|
| | 1 | 2 | 3 | 4 |
| Vector DNA | ✓ | ✓ | ✓ | ✓ |
| De-phosphorylated | ✓ | ✗ | ✓ | ✗ |
| Insert DNA | ✓ | ✗ | ✗ | ✗ |
| DNA ligase | ✓ | ✓ | ✓ | ✗ |

2 – Shows the efficiency of digestion of the vector by the amount of background of vector template DNA carried over.

3 – Shows the efficiency of dephosphorylation, because if dephosphorylation was efficient, self-ligation should not occur even in the presence of DNA ligase.

4 – When the original vector is used to transform *E. coli*, this control serves as a transformation control.

5.2.2.5 Plasmid map of pRPF215

Plasmid pRPF215 (Figure 5-2), previously described by Dembek et al., (2015), was purchased from Addgene (Addgene plasmid # 106377). Divergent promoters, each with a single overlapping operator sequence, control expression of the tet repressor TetR and the wild type *Himar1* transposase. The promoter P_{tet}, which regulates tetracycline resistance gene *tetA*, controls expression of the transposase gene. The ITR repeat sequences recognised by transposase contain the erythromycin resistance gene *ermB* for selection of transposon mutants with erythromycin.

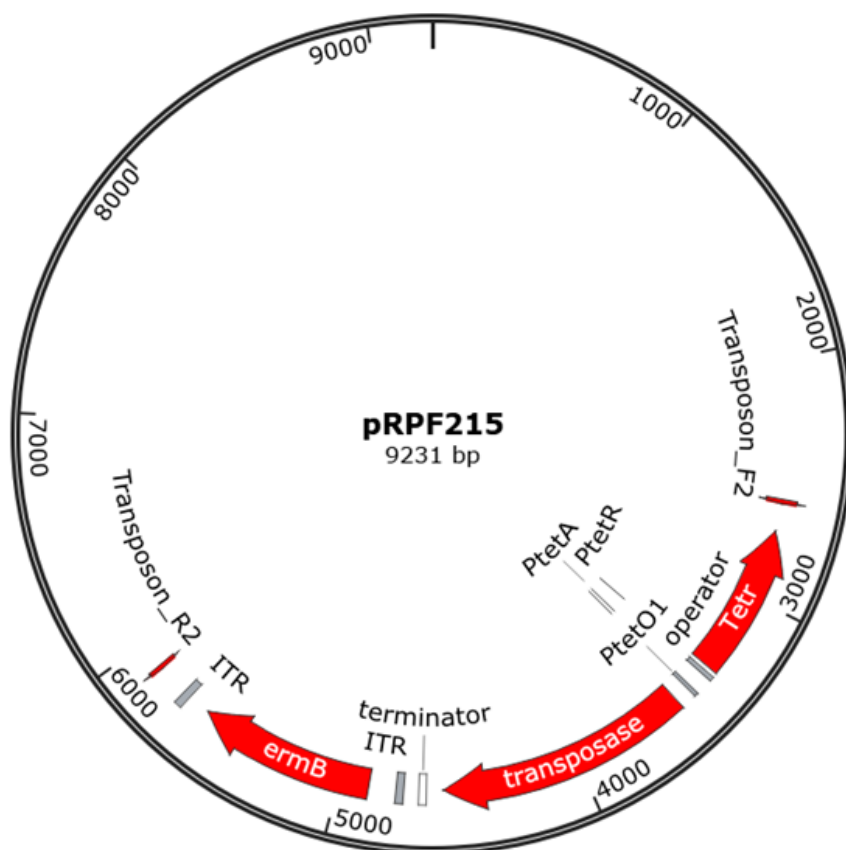


Figure 5-2 Plasmid map of the *Himar1* transposon in pRPF215 codon optimised for *Clostridium difficile*.

Plasmid pRPF215 contains the erythromycin resistance gene (*ermB*) in between two *Himar1* inverted terminal repeat sequences (ITR). Upstream of the transposon, is the *Himar1* (wild type) transposase under control of the *tetA* promoter, Ptet, and tetO1 operator sequence. Divergent tet promoter controls expression of TetR which encodes the repressor protein. The primers: Transposon_F2 and Transposon_R2 used to PCR amplify the transposon fragment from pRPF215 are shown by red arrows.

5.2.3 Construction of transposition negative control plasmids

5.2.3.1 Cloning strategies for the construction of pNiggHimar_GFP_ΔTpase and pNiggHimar_mCh_ΔTn

The transposition negative-control plasmids, pNiggHimar_GFP_ΔTpase, and pNiggHimar_mCh_ΔTn were constructed to determine whether premature transposition of the transposon could be causing failure to recover transformants with pNiggHimar.

Plasmid pNiggHimar_GFP_ΔTpase was constructed by deleting the catalytic domain of the *Himar1* transposase on plasmid pNiggHimar by PCR amplification using primers 13 and 14 (Table 9). The resulting plasmid retains the functional *ermB* marker in between the two *Himar1* ITR sequences, however, the transposase should be unable to perform cut and paste transposition of the transposon into the chromosome (Figure 5-3).

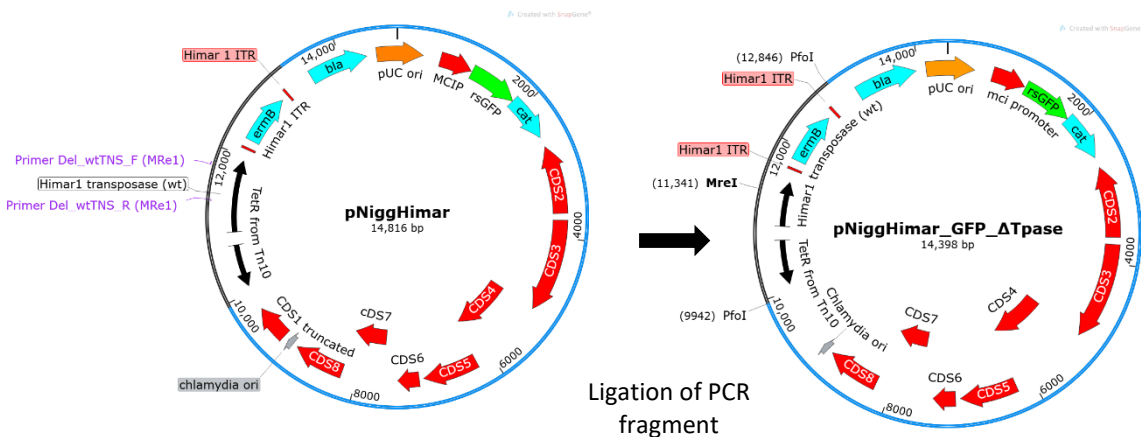


Figure 5-3 Cloning strategy for the construction of *E.coli*-*C. muridarum* transposon shuttle vector pNiggHimar_GFP_ΔTpase

The catalytic domain of the wild type *Himar1* transposase on plasmid pNiggHimar was removed by PCR. Primers, highlighted in purple, added MRe1 restriction sites to each end of the PCR amplicon. The overhang of MRe1 sites were ligated to generate plasmid pNiggHimar_GFP_ΔTpase, a transposition-negative control plasmid.

In addition to pNiggHimar_GFP_ΔTpase, an *ermB*-transposon-negative plasmid, pNiggHimar_mCh_ΔTn was generated as a separate transposition-negative control. An intermediate plasmid, pNiggHimar_GFP_ΔTn, was first constructed by deleting the *ermB* marker and both *Himar1* ITR sequences on plasmid pNiggHimar, by PCR amplification using primers 11 and 12 (Table 9). The resulting plasmid retains the functional *Himar1* transposase gene but does not provide the transposon gene template for transposition on the same vector (Figure 5-4).

To distinguish transformants carrying the *ermB*-transposon-negative plasmid in a co-infection with pNiggHimar_GFP_ΔTpase, the backbone of pNiggHimar_GFP_ΔTn was replaced with the entire p2TK_{Spec}-Nigg-mCh(Gro)L2 plasmid to generate pNiggHimar_mCh_ΔTn. This plasmid was designed such that it contains the same plasmid genes (*CDS1-8*) as pNiggHimar_GFP_ΔTpase but instead, contains the mCherry fluorescent reporter and the spectinomycin resistance gene *aadA* to facilitate selection of double transformants with spectinomycin and penicillin G and their identification with both red and green fluorescence respectively.

To construct pNiggHimar_mCh_ΔTn, primers 15 and 16 (Table 9) were used to add Pfo1 sites to plasmid p2TK-Spec-Nigg-mCh(Gro)L2 (Cortina et al., 2019) at position 10,079 nt between *CDS8* on the pNigg backbone and the *incDEFG* promoter. Next, the *ermB*-negative transposon from pNiggHimar_GFP_ΔTn was digested with Pfo1 and ligated to the amplicon containing p2TK-Spec-Nigg-mCh(GroL2) to generate pNiggHimar_mCh_ΔTn. The cloning methods are described in detail in the following sections.

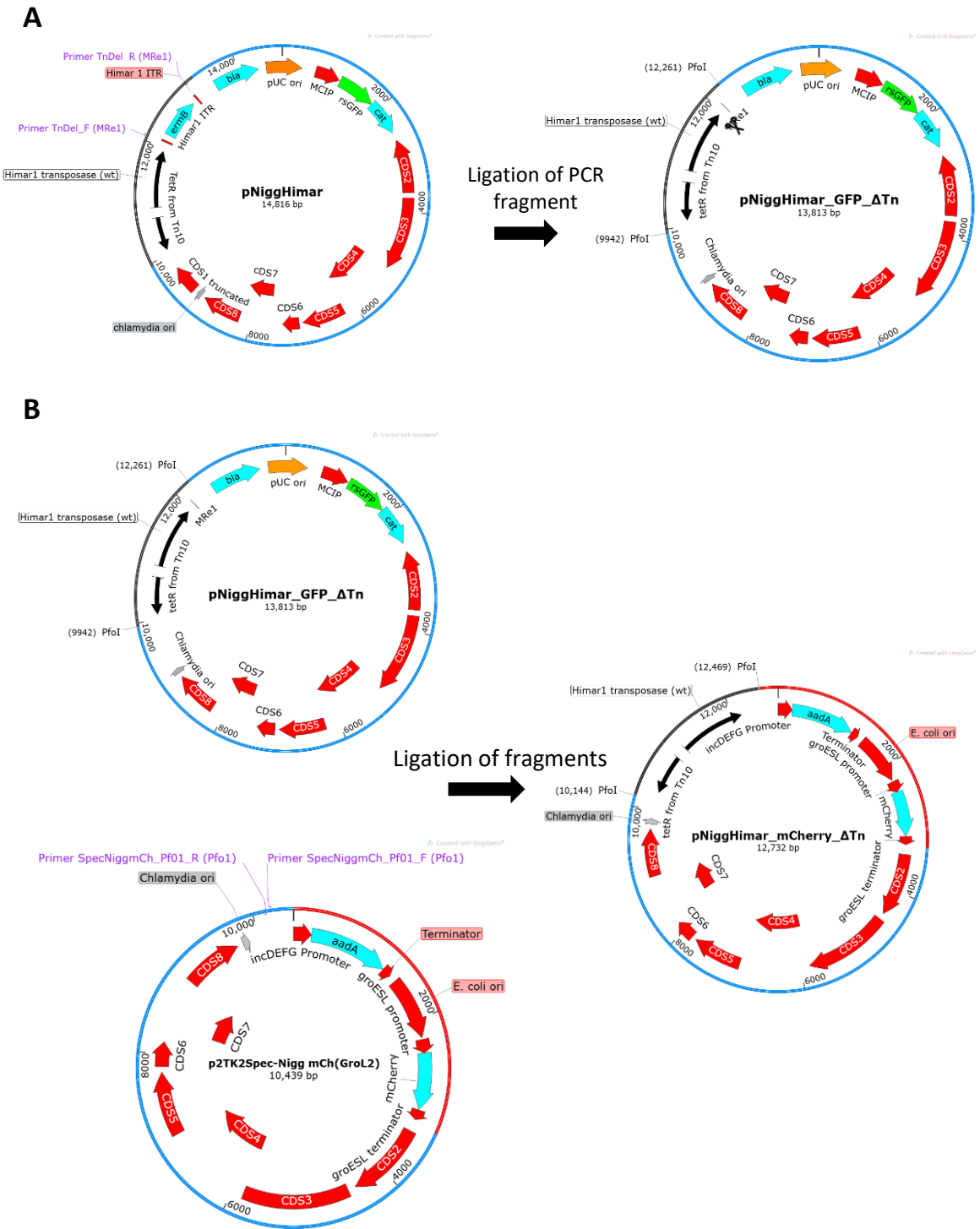


Figure 5-4 Cloning strategy for the construction of *E.coli-C. muridarum* transposase shuttle vector pNiggHimar_mCh_ΔTn

The *ermB*-transposon was deleted from plasmid pNiggHimar by end point PCR using primers, highlighted purple, adding MRe1 restriction sites to each end allowing for self-ligation to generate intermediate plasmid pNiggHimar_GFP_ΔTn (A). To generate pNiggHimar_mCh_ΔTn, the wild type *Himar1* transposase under tet promoter control was digested from pNiggHimar_GFP_ΔTn and cloned into plasmid p2TK2_{spec}-NiggmCh(Gro)L2 at the Pfo1 site added by PCR using primers highlighted purple (B).

5.2.3.2 Restriction enzyme cloning methods

The generation of pNiggHimar_GFP_ΔTn and intermediate plasmid pNiggHimar_GFP_ΔT_{pase} required amplification of the vector removing the ITR sequences containing the *ermB* gene, and in a separate experiment removal of the catalytic domain of the transposase, as described. The primers used for these purposes were designed to add MRe1 restriction sites onto the amplicon ends for self-ligation of each PCR product. To do this, amplicons were purified using the Wizard[®] DNA clean up kit (Promega) and the Mre1 sticky ends were digested with restriction endonuclease MRe1 as described in section 5.2.4. Ligation reactions were performed as previously described with the following modification. Only vector DNA was added to each reaction and a dephosphorylation step was not required because the aim was to achieve self-ligation of the amplicon. Controls for the efficiency of dephosphorylation and transformation (the latter using the parent plasmid) were performed as described in Table 7.

Generation of plasmid pNiggHimar_mCh_ΔTn first required restriction enzyme (Pfo1) digestion of the *Himar1* transposon-transposase cassette from pNiggHimar_GFP_ΔTn. This became the 'insert DNA'. The vector DNA was prepared by using primers designed to amplify all of plasmid p2TK2_{spec}-Nigg-mChGro(L2).and to add Pfo1 restriction sites to the fragment ends. Restriction endonuclease Pfo1 was used for digestion of the purified amplicon to reveal the Pfo1 restriction site 'stick ends' and was then dephosphorylated as previously described (method 5.2.2.2) to facilitate ligation to the insert DNA. Ligation of the vector and insert were performed as previously described in method 5.2.2.4 (Table 7) to generate plasmid pNiggHimar_mCh_ΔTn.

5.2.4 Restriction endonucleases

Digestion of plasmid DNA was performed using five units of restriction enzyme to digest up to 2 μg of DNA and incubated for 1 hour per μg at 37°C as per manufacturer's instructions. The restriction endonuclease enzymes used in this project are listed in Table 8.

Table 8 Restriction enzymes used for cloning experiments

| Restriction enzyme | | | |
|---------------------------------|--------------------------|----------------|--|
| (restriction site 5'-3') | Buffer | Company | Use of restriction site |
| Pfo1 T [^] CCNGGA | Buffer Tango (10x) | ThermoFisher™ | <ul style="list-style-type: none"> • Restriction site added to ends of pNiggHimar insert • Restriction site added to p2TK-Spec-Nigg-mCh(GroL2) between <i>CDS8</i> and <i>IncDEFG</i> promoter • Confirm size of pGFP::<i>Nigg</i> and pNiggHimar_GFP_ΔTn |
| Stu1 AGG [^] CCT | Cutsmart Buffer (10x) | NEB | <ul style="list-style-type: none"> • Confirm size of pNiggHimar |
| MRe1 CG [^] CCGGCG | Buffer G (10x) | Promega | <ul style="list-style-type: none"> • Confirm size of pNiggHimar_GFP_ΔT_{pase} |
| SpeI A [^] CTAGT | Buffer B (10x)) | Promega | <ul style="list-style-type: none"> • Confirmation of pNiggHimar_mCh_ΔTn |

5.2.5 *Primers for cloning using end-point PCR*

Primers (Eurogentec) were designed to amplify plasmid and genomic DNA and to add nucleotides for cloning with restriction enzymes. Primers contained a minimum of 18 bp homologous to the target sequence. Where possible, primers contained G or C residues at the 3' end to optimise binding to target sequence. The melting temperature (T_m) difference between primer pairs did not exceed 5°C with a total GC content of between 40-60%. Where possible, primers did not contain a run of >4 of the same nucleotides to reduce primer dimer formation. Primer pairs were analysed *in silico* (Lasergene) for potential non-specific binding in the target sequence and primer dimerization. The optimal T_m of all primer pairs was determined by PCR for a range of temperatures with a 5°C incremental increase spanning the predicted T_m .

The sequencing of PCR products was performed by MGH CCIB DNA Core. Primer specifications were as follows: primers were designed with 18 - 23 bp homology to the target sequence ~50 bp upstream of the target sequence. The predicted T_m was between 55-60°C with a GC content between 40 and 60%. Microcentrifuge tubes (0.5ml) containing either the PCR product at 10ng μ l⁻¹ and individual primers at 3.2pmol μ l⁻¹ were prepared for sequencing. The product band size was checked on a 1% agarose gel. A list of all primers used for PCR cloning and sequencing reactions in this project are presented in Table 9.

Table 9 Primers for cloning of constructs, colony screening and sequencing

| Primer | | | |
|---------------|--------------------|--|--|
| ID | Primer Name | Primer Sequence (5'-3') | Purpose |
| 7 | Transposon_F2 | TTTTTT-TCCGGG-ACACCTCTTTTTGACTTTA | Amplify <i>Himar1</i> transposon system from plasmid pRPF215 and add Pfo1 restriction sites to fragment ends |
| 8 | Transposon_R2 | TTTTTT-TCCGGG-AGTCCCCATGCGCTCCATCAA | |
| 9 | Ori_R | GCGGCGAGCGGTATCAGC | Amplify the <i>ermB</i> -transposon in pNiggHimar for a PCR screen |
| 10 | Erm_del_R | GGAGGAAATAATTCTATGAGTCGC | |
| 11 | TnDel_F1 | ATATAT-CGCCGGCG-CATCTTTTTATTTAGGGATTTCTCAC | Delete ITR and <i>ermB</i> transposon from pNiggHimar adding MRe1 restriction sites to fragment ends |
| 12 | TnDel_R1 | ATATAT-CGCCGGCG-GTTACCAGTGTGCTGGAATTC | |
| 13 | Del_wtTNS_F | ATATAT-CGCCGGCG-TTTAGTGATTTAAAAAGAATGTT | Delete catalytic domain from wild type <i>Himar1</i> transposase, adding MRe1 restriction sites to fragment ends |
| 14 | Del_wtTNS_R | ATATAT-CGCCGGCG-GTGTATTCTTGTTAATAATTGT | |
| 15 | SpecNiggmCh_Pf01_F | ATATAT-TCCGGG-AAGTTGTTTCAGAGGCATC | Add Pfo1 restriction site to plasmid p2TK2-Spec-NiggmCh(Gro)L2 |
| 16 | SpecNiggmCh_Pf01_R | ATATAT-TCCGGG-AAGATTCGCTGTGGTCAAG | |
| 17 | SeqTnDel_F | TCTTTAGAGATTCTGGAT | Sequence the region of <i>ermB</i> -transposon deletion and transposase in pNiggHimar_mCh_ΔTn |
| 18 | SeqTnDel_R | ATCCCTTGGTCAATCTAT | |

5.2.6 Immunodetection of wild type *Himar1* transposase by Western blot

The detection of the wild type *Himar1* transposase protein by Western blot was performed as previously described by Skilton et al (2021) with the following modifications. Liquid cultures of *E. coli* Q358 transformed with plasmids pNiggHimar and pNiggHimar_GFP_ΔTpase were incubated either with or without induction with ATc for four hours. Western blots using antisera against the *Himar1* transposase were performed on samples taken at induction (T0), 1 hour (T1) and 2 hours (T2) post induction to demonstrate the activity of the wild type *Himar1* transposase cloned from plasmid pRPF215 (codon optimised for *C. diff*) in *E. coli*. Plasmid pGFP::Nigg, which does not contain the *Himar1* transposon under tet promoter control and is the parent plasmid for pNiggHimar, was used as a negative control. Blots were performed to detect expression of GFP from the same cultures for each of these plasmids to act as a positive control for the expression of genes carried on the plasmid.

5.2.6.1 Growth curves

E. coli strain Q358 transformed with pNiggHimar, pNiggHimar_GFP_ΔTpase and pGFP::Nigg was grown on LB agar supplemented with chloramphenicol overnight at 37 °C, 5% CO₂. One well-isolated colony of Q358/pRPF215 was selected and added to liquid LB supplemented with chloramphenicol (30µgml⁻¹) and incubated at 37°C overnight with shaking to reach an OD_(600nm) = 2.0. The host strain Q358 was grown in the same conditions overnight in LB without antibiotics, as it has no natural resistance to antibiotics. Two sub-cultures of Q358/pRPF215 overnight culture (1%) in 100ml liquid LB supplemented with chloramphenicol (30µgml⁻¹), and two sub-cultures of Q358 overnight culture without antibiotic selection were incubated at 37°C with shaking. Optical density measurements were taken using a spectrophotometer at regular 15-minute intervals until an OD_(600nm) = 0.5 was reached indicating the start of logarithmic growth phase. At this point, transposase expression was induced by adding 200ngml⁻¹ ATc to the Q358 subculture and to one of the Q358/pRPF215 sub-cultures as per manufacturer's instructions (ThermoFisher). This sample was labelled T0. The OD_(600nm) was measured every hour for four hours T1-T4 for each culture.

5.2.6.2 Sample preparation

For Western blot analysis, samples were thawed on ice and sonicated for 30 sec pausing for 10-20 sec and sonicated for a further 30 sec at an amplitude of 3 (microns) The protein concentration (µgml⁻¹) in cell lysates were determined by Pierce BCA protein assay kit (ThermoFisher) according to manufacturer's instructions then stored frozen at -20°C. Cell lysates stored in PBS were thawed on ice and 10 µl sample (either neat, or diluted at a 1:2 ratio in ice-cold PBS) was mixed with 4 µl

sample buffer containing (125 mM Tris-HCl pH 6.8, 4% (w/v) SDS, 20% (w/v) glycerol, 10% (w/v) β -mercaptoethanol, 10 μ g bromophenol blue) and then evaporated by boiling at 100 °C in a water bath for 5 minutes.

5.2.6.3 SDS-PAGE

Proteins were separated by 12% Tris-Glycine-SDS polyacrylamide gel electrophoresis (SDS-PAGE), hand-cast using the following method. Resolving gel solution and stacking gel solution were prepared as shown in Table 10 for one gel cassette (Bio-Rad). Resolving gel solution polymerised in between two glass panels held in place in the gel cassette for 45-60 minutes at RT made air-tight with isopropanol. Stacking gel was transferred onto the resolving gel using a pipette and a 10-well comb was placed into the gel to polymerise for 45 minutes at RT.

Table 10 Separating gel and stacking gel recipe

| | Separating gel | Stacking gel |
|-----------------------|----------------|---------------|
| | 12% | 4% |
| 30% acrylamide | 1.5 ml | 225 μ l |
| 0.5M Tris-HCL, pH 6.8 | - | 1,000 μ l |
| 1.5M Tris-HCL, pH 8.8 | 1.9 ml | - |
| 10% SDS | 100 μ l | 40 μ l |
| UHQ H ₂ O | 1,500 μ l | 675 μ l |
| TEMED | 5 μ l | 2 μ l |
| 10% APS | 20 μ l | 10 μ l |

5.2.6.4 Western blot

Samples (20 μ l) were run on polyacrylamide gels at 200V for 1 hour against a pre-stained protein ladder (5 μ l) (ThermoFisher) in 1x SDS running buffer (21.6g glycine, 4.5g Tris, 1.5g SDS, 0.15L UHQ H₂O).

Transfer membranes, polyvinylidene difluoride (PVDF) Immobilon membrane (EMD Millipore), were activated with 100% methanol prior to transfer. Proteins were transferred for 7 minutes at 25V in Pierce Fast Semi-Dry Buffer (ThermoFisher) using a Pierce Fast Semi-Dry Blotter. Transfer efficiency was checked by staining residual protein in gels post-transfer by incubation with a protein gel stain (0.5g Brilliant blue (Fisher, Reso), 50ml acetic acid, 100ml isopropanol, 350ml H₂O) with rocking for 5 minutes. Excess stain was removed by a series of washes with de-staining solution (50ml acetic acid, 100ml isopropanol, 350ml H₂O) which included washes in de-stain for 10 minutes then 4 x 5 minutes. Transfer membranes were then blocked in 10% milk/ 0.05 % Tween-20 in PBS (PBS-t) at 4°C, overnight or for 1 hour at RT with rocking, before incubation with primary antibody in 1 % milk/PBS-T solution for 1 hour, with rocking. Anti-GFP polyclonal antibody (Sigma-Aldrich) or primary mouse polyclonal antisera to purified *Himar1* transposase (Akerley BJ & Lampe DJ., 2002), neither conjugated to HRP, were used at dilutions of 1:4000 and 1:5000 respectively. Un-bound primary antibodies were washed from membranes for 3 x 5 min in PBS-t, with rocking. Membranes were incubated with secondary antibody (Bio-Rad): either goat-derived anti-mouse Horse Radish Peroxidase (HRP)-labelled IgG (for anti-GFP binding) or goat-derived anti-rabbit HRP-labelled IgG (for anti-*Himar1* transposase binding) were used at 1:2000 dilutions in 5 ml 1 % milk/PBS-T for 1 h at RT, with rocking. Membranes were washed another 3 x 5 minutes in PBS-T, with rocking, then hydrated with Pierce enhanced chemiluminescent (ECL) substrate (ThermoFisher). Photographic films were exposed to membranes prior to development and fixing using ECL western blotting reagents (ThermoFisher) in a dark room.

5.3 Results

5.3.1 Attempts to recover *ermB*-resistant transposon mutants in *C. muridarum*

A stably replicating transposon delivery vector that can be expanded in cell culture prior to transposition requires inducible control over transposase expression (Skilton et al., 2021). The inducible tet promoter system is the only system currently used for the conditional expression of genes in *Chlamydia* (Cortina et al., 2019; Keb and Fields, 2019; Mueller et al., 2016; Wickstrum et al., 2013). Plasmid pRPF215 is a transposon delivery vector codon optimised for *C. diff* and contains the *Himar1* transposon containing an erythromycin antibiotic resistance gene (*ermB*) under tet promoter control (plasmid map is shown in method 5.2.2.5). For these reasons plasmid pRPF215 provides a potentially suitable inducible transposon mutagenesis system that could be adapted for use in *Chlamydia*.

The inducible system was previously untested in *E. coli* (Dembek et al., 2015), which is typically required to demonstrate the functionality of the gene features carried on a vector prior to their transformation into *Chlamydia*. So, before this transposon system was used to clone a transposon delivery vector suitable for stable passage in *C. muridarum*, attempts were made at transforming *C. muridarum* with pRPF215 directly. This was necessary to optimise the conditions for selecting for potential *ermB*-resistant transposon mutants in *C. muridarum* and to demonstrate functionality of the system in *Chlamydia*. Functionality of the components on a vector carrying the inducible transposon cloned from pRPF215 were also verified in *E. coli*, the results of which are described in the results sections that follow this one.

Plasmid pRPF215 lacks the origin of replication required for replication in *Chlamydia* (Dembek et al., 2015), and instead contains an *E. coli* origin of replication, and as such would be an example of a suicide vector in *Chlamydia*. Recovery of transposon mutants in *C. muridarum* generated with a suicide vector that was first propagated and demethylated in *E. coli* has been recently achieved (Wang et al., 2019). Therefore, it was hypothesised that it would be possible to transform and recover transposon mutants in *C. muridarum* using plasmid pRPF215 directly.

Selection conditions using erythromycin were optimised in *C. muridarum*. First, therefore approval for the use of erythromycin resistance gene *ermB* in *C. muridarum* was obtained (see Appendix B for the application and approval for use of the *ermB* resistance gene in the genetic modification of *C. muridarum*) because erythromycin is used in the treatment of *C. trachomatis* infections in the UK (Nwokolo et al., 2016). Quantitative susceptibility testing for erythromycin in *C. muridarum* was performed as described in method 5.2.1.1. Two-fold serial dilutions were prepared from a starting stock at 0.5 µg ml⁻¹. In the absence of MIC data for *C. muridarum*, the

concentration range was chosen based upon the MIC of erythromycin determined for *C. trachomatis* serovar D ($0.25\mu\text{gml}^{-1}$) (Suchland et al., 2003). The minimum concentration which inhibited inclusion formation in the plasmid-cured wild type strain Nigg P- and for Nigg P- transformed with *E. coli*-*C. muridarum* shuttle vector pGFP::Nigg occurred at $0.125\mu\text{gml}^{-1}$ in the growth media (Figure 5-5). Therefore, a concentration of $0.125\mu\text{gml}^{-1}$ was used to optimise a protocol for the recovery of *ermB*-resistant transposon mutants in *C. muridarum*.

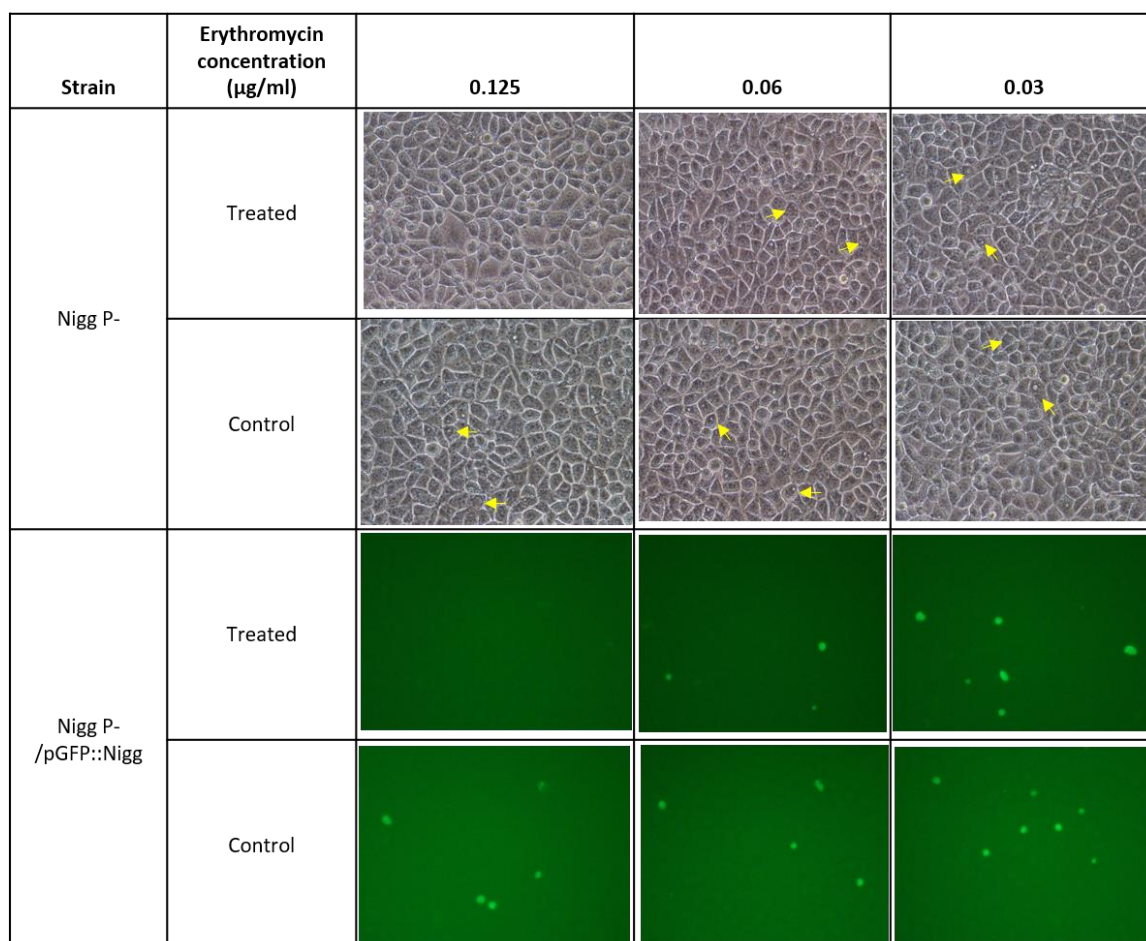


Figure 5-5 Quantitative susceptibility testing to determine the minimum inhibitory concentration of erythromycin in *C. muridarum* Nigg

Culture flasks (T_{25}) of McCoy cells were infected with Nigg P- and Nigg P- /pGFP::Nigg at $\text{MOI}=1$ in duplicate wells and incubated at 37°C with $5\% \text{CO}_2$. Serial dilutions (1:2) of erythromycin were prepared and added to the growth media (DMEM) (treated cells) after centrifugation of *Chlamydia* onto McCoy cells. Untreated cells (control) were grown without antibiotic selection in the media. At 24 hpi, cells were imaged at 40x magnification under UV light. The MIC was defined as the concentration of bacterial agent which completely inhibited growth at 24 hpi. No inclusions were visible at $0.125\mu\text{gml}^{-1}$ for either strain. Yellow arrows indicate inclusions.

Chapter 5

Plasmid pRPF215 contains the *cat* gene conferring resistance to chloramphenicol, therefore propagation of this plasmid in *E. coli* DH5 α and demethylation in *E. coli* GM2163, which is required prior to transformation into *Chlamydia*, was performed under selection with chloramphenicol in the liquid media and LB agar. So, to verify erythromycin resistance in *E. coli* transformants carrying plasmids containing the *ermB*-transposon, a crude solid phase assay for determining the MIC erythromycin in *E. coli* strains (used for propagation of vectors in preparation for transformation into *Chlamydia*) was performed as described in method 5.2.1.2. An appropriate concentration of erythromycin that would inhibit growth of erythromycin-sensitive *E. coli* that did not carry the *ermB* gene on a plasmid was performed by spreading or streaking a loop of *E. coli* stored in glycerol across LB agar supplemented with calculated concentrations of erythromycin. Complete inhibition of bacterial growth occurred at 150 μgml^{-1} and 125 μgml^{-1} for strains DH5 α and Q358 respectively, therefore LB agar supplemented with 150 μgml^{-1} of erythromycin was used for confirmation of erythromycin resistance conferred by the *ermB*-transposon in transformants in these host strains (Figure 5-6). Unexpectedly, *E. coli* GM2163 was resistant up to 250 μgml^{-1} erythromycin as genotypes for the strains tested do not indicate natural resistance to erythromycin.

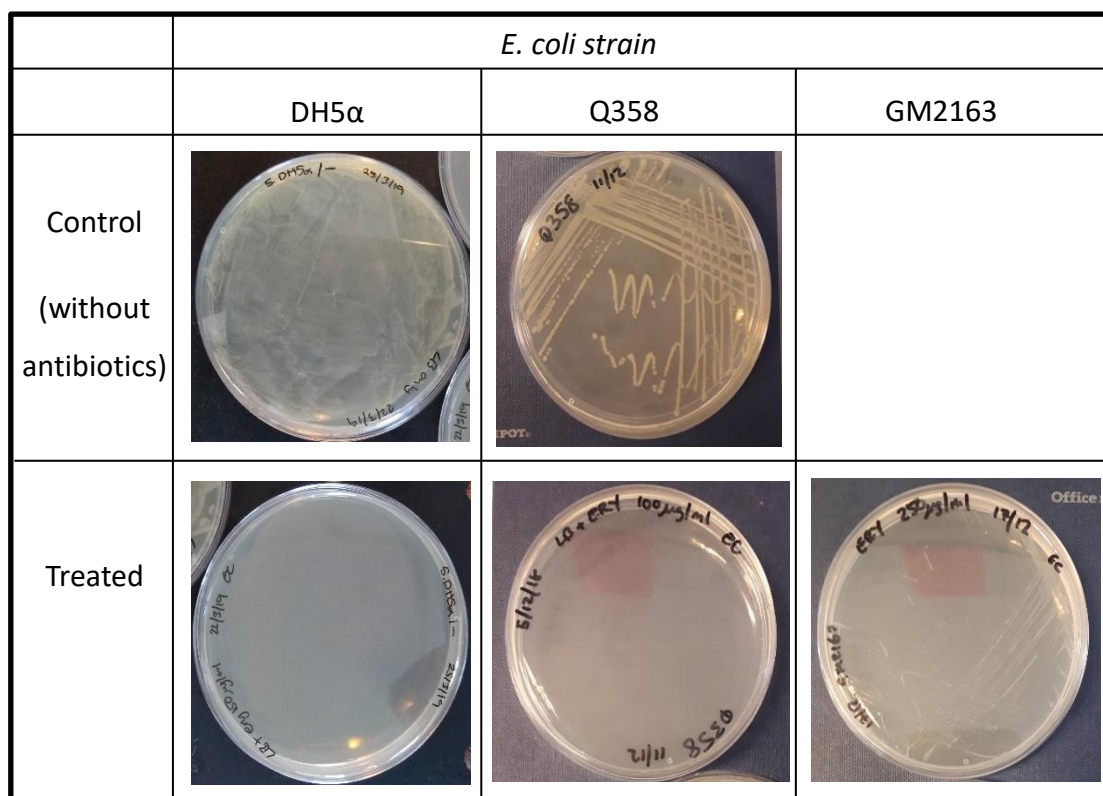


Figure 5-6 Inhibition of bacterial growth for *E. coli* Q358 and GM2163 in erythromycin

A crude solid phase assay was used to determine the MIC erythromycin for *E. coli* strains DH5 α , Q358 and GM2163. Concentrations of erythromycin tested were 10, 20, 50, 100, 125, 150 and 500 (μgml^{-1}) in 20 ml LB agar. *E. coli* were streaked or spread onto LB agar supplemented with erythromycin at the calculated concentrations (treated) and onto LB agar without antibiotics (control). Colony growth was completely inhibited at 150 μgml^{-1} and 100 μgml^{-1} for *E. coli* DH5 α and Q358 respectively. *E. coli* GM2163 was resistant up to 250 μgml^{-1} .

At the time of conception, no protocol existed for the induction of transposition and the recovery of transposon mutants in *Chlamydia*. Also, no protocol existed using erythromycin for the recovery of transformants in *Chlamydia*. Therefore, two treatment regimens were designed based upon the standard protocol for the transformation and recovery of transformants in *Chlamydia* (Wang et al., 2011). The standard transformation protocol typically excludes antibiotic selection from the growth media overlaid onto transformed cells at T0, then antibiotic selection is introduced to select for transformants in the first passage (T1) (method 2.9.1). This protocol was adapted as follows. Strategy 1 included the addition of the inducer ATc and erythromycin (0.125 μgml^{-1}) in the growth media overlaid onto transformed cells at T0. Erythromycin selection was then added to the growth media for three consecutive passages (T1-T3). Strategy 2 included ATc only at T0 and then erythromycin selection in all consecutive passages (T1-T3). Plasmid Nigg P-/pGFP::Nigg was used as a transformation control following the transformation protocol using

penicillin at T1. There was no available transposon-plasmid to serve as a transposon mutagenesis control. Three transformation attempts were made using each method described (Table 11).

Table 11 Treatment regimen used for the transformation of *C. muridarum* Nigg P- with suicide transposon delivery vector pRPF215

| | Regimen 1 | | Regimen 2 | | 3 (Transformation control using pGFP::Nigg) |
|---------|-------------------|--|-------------------|--|--|
| Passage | ATc (10 ng/ml) | Erythromycin (0.125 µg ml ⁻¹) | ATc (10 ng/ml) | Erythromycin (0.125 µg ml ⁻¹) | Penicillin (10 U/ml) |
| T0 | ✓ | ✓ | ✓ | ✗ | ✗ |
| T1 | ✗ | ✓ | ✗ | ✓ | ✓ |
| T2 | ✗ | ✓ | ✗ | ✓ | ✓ |
| T3 | ✗ | ✓ | ✗ | ✓ | ✓ |

Identifying potential transposon mutants was challenging due to the absence of fluorescent reporter gene from plasmid pRPF215. Identification of mutants was therefore based upon the observation of a mature inclusion-like structure; a membrane-bound vacuole, containing visible movement of small round EB-like structures situated next to the cell nucleus. When ATc and erythromycin were used at T0, inclusion-like structures were visibly seen in McCoy cells which contained a single large, circular dark structure that moved rigorously within the constraints of the vacuole membrane. An example of this is arrowed at T4 and T5 for regimen 1 in Figure 5-7. These were unlikely to be transposon mutants because despite the absence of a plasmid, *Chlamydia* cells should still be able to replicate inside the inclusion and produce many hundreds of visibly moving EBs. For this reason, the lack of movement seen in the inclusion-like structures observed under the treatment regimen 2 indicate that these are also unlikely to be transposon mutants. Successful transformation was demonstrated at T2 on each transformation attempts for the control strain by visible inclusions that fluoresced green.

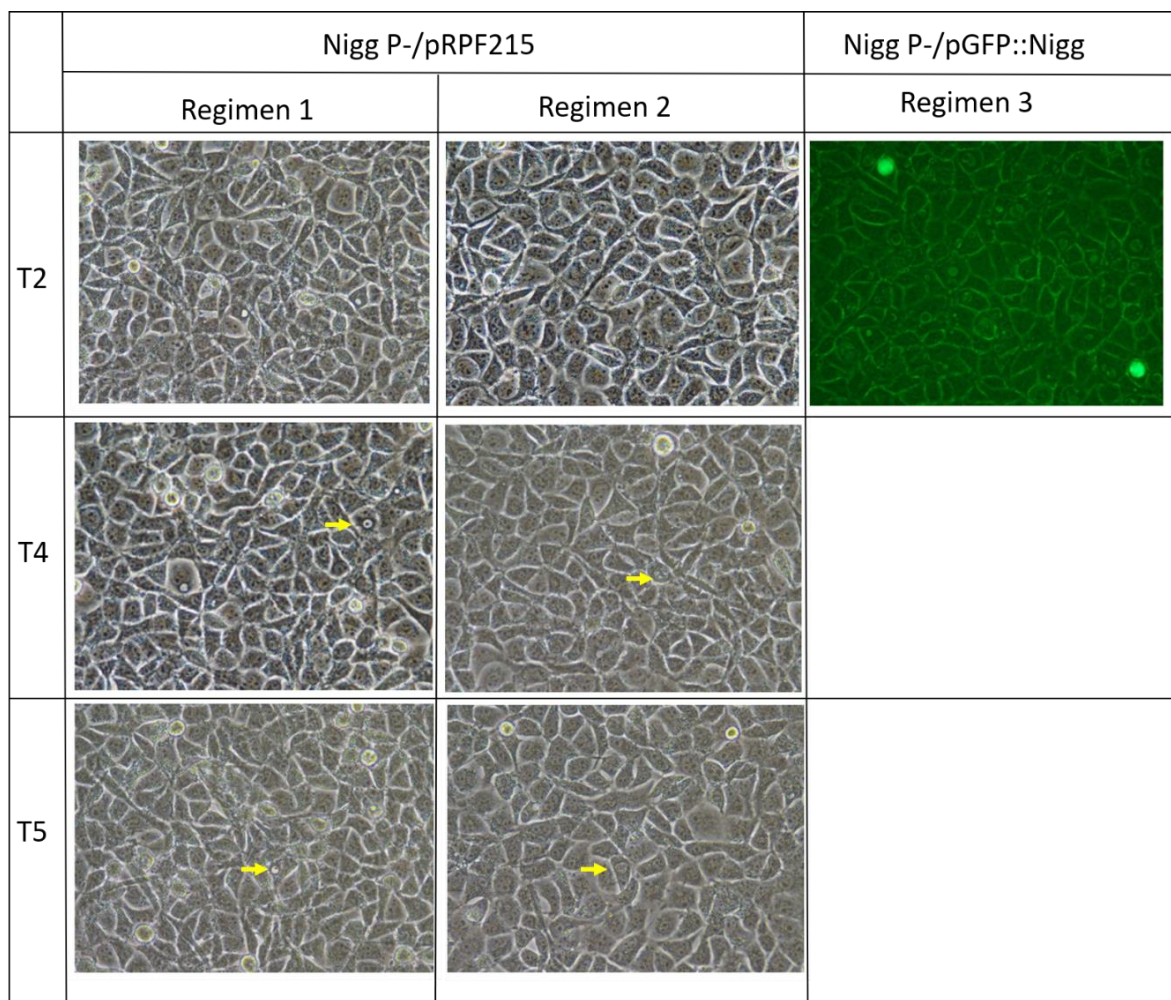


Figure 5-7 Transformation and recovery of plasmid pRPF215 in *C. muridarum* strain Nigg P-

Transformation of plasmid-cured *C. muridarum* strain Nigg (Nigg P-) with the suicide vector pRPF215 (codon optimised for *Clostridium difficile*) was attempted three times using a different plasmid preparation each time. Plasmid pGFP::Nigg was used as the transformation control with penicillin introduced into the growth media at T1. Inclusions fluoresced green due to expression of GFP fluorescent reporter genes from these respective plasmids. Regimen 1 included ATc induction and erythromycin selection at T0 with selection and for all onward passages. Regiment 2 included ATc induction at T0 without selection with erythromycin selection from T1 onwards. Regimen 3 included penicillin selection from T1 onwards.

5.3.2 **Generating a replication-proficient transposon -delivery vector for *C. muridarum***

The *Himar1* transposon had very recently been shown to be functional in *C. muridarum* and *C. trachomatis*, however, to achieve saturation mutagenesis, inducible control over transposition was required for a stably replicating vector that can be expanded prior to the induction of transposon mutagenesis. Therefore, the *Himar1* transposon under tet promoter control was cloned from plasmid pRPF215 into plasmid pGFP::Nigg, that was previously shown to stably passage in *C. muridarum* (Chapter 3 and 4 of this thesis). The resulting *E. coli*-*C. muridarum* transposon delivery vector was called pNiggHimar and the cloning strategy is described in method 5.2.2.1 of this chapter.

The level of expression of the transposase will be a limiting factor for the number of transposon mutants generated. Lampe et al demonstrated that the wild type mariner transposase has a low transposition efficiency that would not be optimal for interrogating larger genomes (Lampe et al., 1999). For this reason, the hyperactive transposase mutant, *C9*, was developed to improve the transposition efficiency for genetic applications. However, whilst demonstrating the functionality of the hyperactive transposase in *E. coli*, an inhibitory effect on transposition was observed caused by the over-expression of transposase in a process called “overproduction inhibition”. Given that *C. muridarum* has a relatively small genome compared to other prokaryotes, and the potential for overproduction inhibition caused by the hyperactive form of *Himar1* transposase, the wild type form has been chosen.

Primers 7 and 8 (method 5.2.5, Table 9) were designed to PCR amplify the *ermB* transposon and the wild type transposase gene under tet promoter control from plasmid pRPF215 and add Pfo1 restriction sites to each fragment end. The annealing temperature was optimised by temperature gradient with the addition of either MgCl₂ (2mM) or DMSO to the master mix (Phusion Flash) (Figure 5-8). The greatest yield was obtained with the addition of MgCl₂ to the master mix at 50°C therefore these conditions were chosen for end point PCR. Amplicons were excised from gels for purification of DNA for cloning into plasmid pGFP::Nigg.

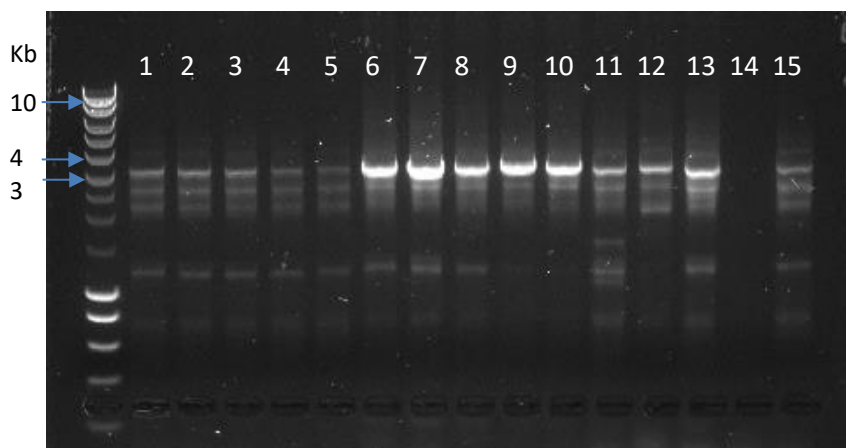


Figure 5-8 Optimisation of primers to amplify the *Himar1* transposon under Tet promoter control from plasmid pRPF215

Primers 7 and 8 were tested at the following temperatures: 45°C, 50°C, 55°C, 60°C and 65°C without the addition of MgCl₂ or DMSO (wells 1-5) or with the addition of MgCl₂ (2mM) (wells 6-10) and DMSO (wells 11-15), to amplify the *Himar1* transposon carrying the erythromycin antibiotic resistance gene *ermB* under Tet promoter control from plasmid pRPF215. Primers produced the largest yield at the expected band size (3,312 bp) with the addition of MgCl₂ at 50°C.

The ligation reaction was performed as described in method 5.2.2.4 to generate an inducible replication-proficient transposon delivery vector called pNiggHimar. Colonies were streaked onto LB agar supplemented with chloramphenicol (*cat* is present on the backbone, pGFP::*Nigg*).

5.3.2.1 Phenotypic and genotypic confirmation of the *Himar1* transposon in construct pNiggHimar

To discern which colonies contained undigested vector template pGFP::*Nigg* and the desired construct pNiggHimar, 29 colonies were screened for the presence of the *Himar1* transposon insert by PCR and streaked onto LB agar supplemented with erythromycin to confirm the presence of the *ermB*-carrying transposon.

Bacterial colony screening was performed as a quick means to identify colonies that likely contain the *Himar1* transposon insert. A single colony was selected using a loop under a flame and re-streaked onto LB agar supplemented with chloramphenicol and, separately, erythromycin, before being placed directly into the PCR tube. Phenotypic confirmation of an active *gfp* marker was shown in all 29 colonies that were selected and culture purified from the ligation plate onto a new plate with chloramphenicol selection (Figure 5-9).

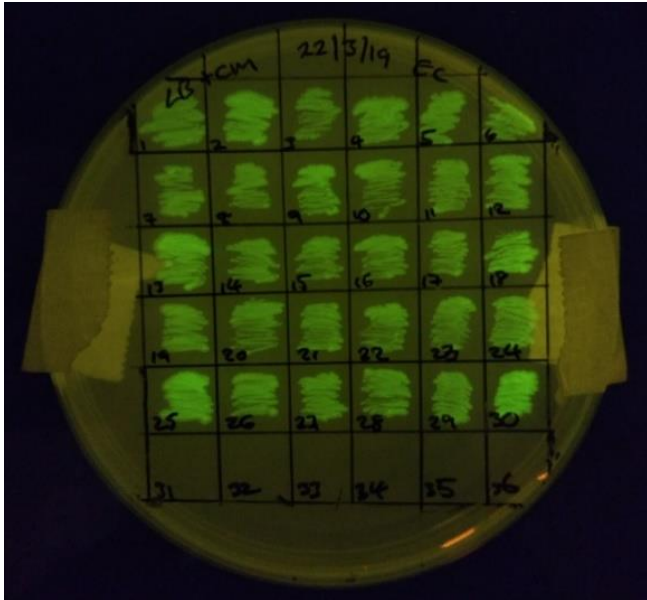


Figure 5-9 Confirmation of the *gfp* expression from colonies selected for screening of the *ermB*-transposon

The functional fluorescent reporter gene *gfp* expressed from the backbone of construct pNiggHimar in *E. coli* DH5 α was demonstrated for 30 colonies of DH5 α /pNiggHimar selected from chloramphenicol selective plates of the ligation experiment using UV light.

Primers 9 and 10 were designed to amplify the transposon from pNiggHimar with one primer specific for the vector backbone on pGFP::Nigg and the other primer specific for the *Himar1* transposon insert to produce a 2,155 bp amplicon. Amplicons at the correct size at 2,155 bp were observed for 11 out of the 29 colonies (Figure 5-10). Given that the plasmid DNA was not purified from the bacteria and instead were directly added to the PCR reaction, a degree of non-specific binding was expected. As expected, evidence of non-specific binding was present in most reactions producing amplicons of ~600 bp, much smaller than the target sequence of 2.1 kb. An internal positive control was not performed therefore PCR inhibition could not be ruled out for the colonies that failed to amplify a product at the desired size. Interpretation of whether the *Himar1* transposon was present in these colonies also required confirmation of erythromycin resistance and restriction endonuclease digest to size the plasmids present.

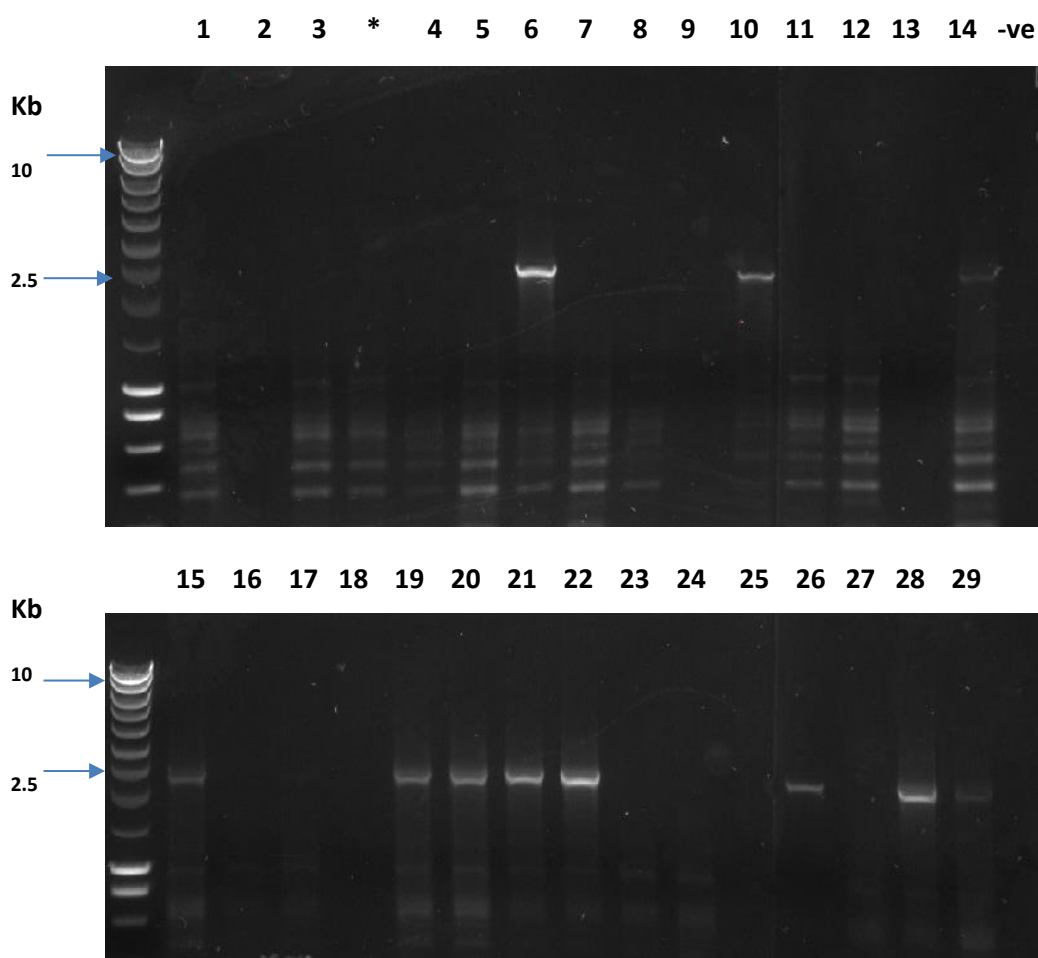


Figure 5-10 Colony screen to confirm the presence of the *ermB*-transposon insert

Bacterial colony screen of 29 chloramphenicol-resistant clones to identify the presence of the *Himar1* transposon cloned into vector pGFP::Nigg by PCR to produce an amplicon of 2,155 bp using primers specific for the *ermB* gene. A negative (-ve) control (water) was performed as indicated. Sample 3 was tested twice indicated by an Asterix.

In the absence of an internal positive control in the PCR screen, restriction enzyme digestion was performed to confirm the results of the PCR screen and the orientation of the transposon insert. A selection of colonies that were positive for the insert (colonies 6, 21, 22) and some that were negative for the insert (colonies 5 and 13) were digested with restriction enzyme *Stu1*. Overnight cultures were prepared for the selected colonies and plasmid DNA was extracted and purified for digestion. The two *Stu1* restriction sites in the vector backbone and single site in the insert sequence produce two amplicons of 3,556 and 7,938bp when no insert is present. Three amplicons were produced if the insert was present at 4,205 bp, 6,774 bp and 3,556 bp or 3,504 bp, 7,442 bp and 3,556 bp depending on insert orientation. *Stu1* digestion confirmed that colonies

6, 21, and 22 contained the insert and that colonies 5 and 13 were missing the insert (Figure 5-11).

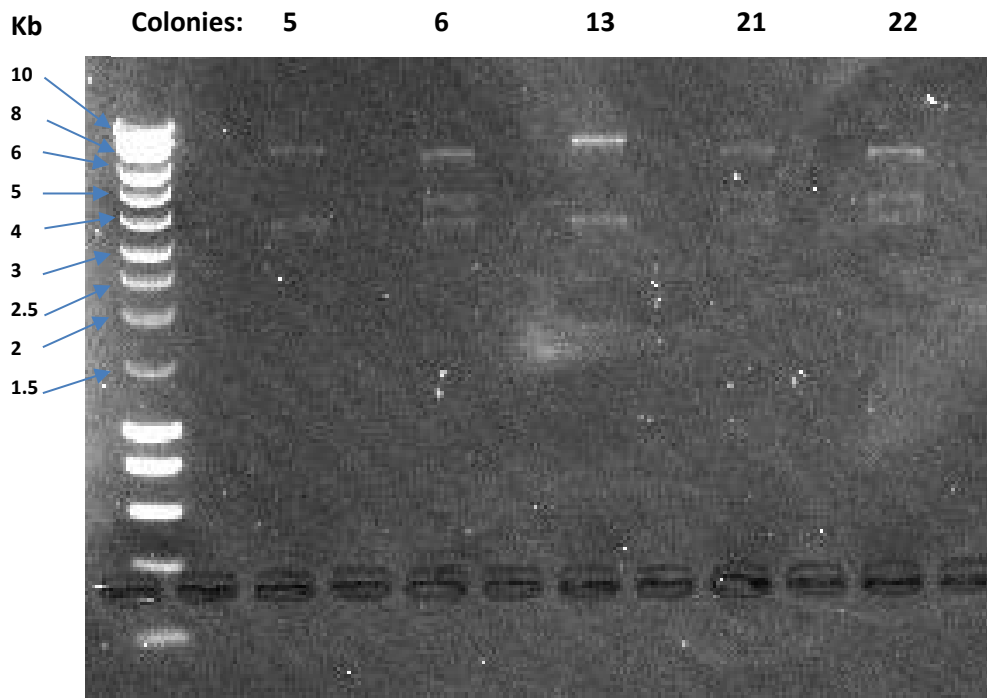


Figure 5-11 *Stu1* digest of colonies that express *gfp* to confirm presence and orientation of the transposon insert in pNiggHimar

Stu1 digest of purified colonies that express *gfp* to confirm presence and orientation of the transposon insert in the cloned transposon delivery vector. The two *Stu1* restriction sites in the vector backbone and single site in the insert sequence produce two amplicons of 3,556 and 7,938 bp when no insert is present. Three amplicons were produced if the insert was present at 4,205 bp, 6,774 bp and 3,556 bp or 3,504 bp, 7,442 bp and 3,556 bp depending on insert orientation. *Stu1* digestion confirmed that colonies 6, 21, and 22 contained the insert.

Finally, erythromycin resistance conferred by the *ermB* gene present on the insert was confirmed for colonies 6, 21, 22, and sensitivity was confirmed in colony 13, concordant with PCR and digest results (Figure 5-12). However, colony 5 was erythromycin resistant demonstrating that the two amplicons seen in the *Stu1* digest for colony 5 were three amplicons with the insert ligated to the vector in the opposite orientation but the resolution of the gel was unable to discern between amplicons of sizes 3,556 bp and 3,504 bp.

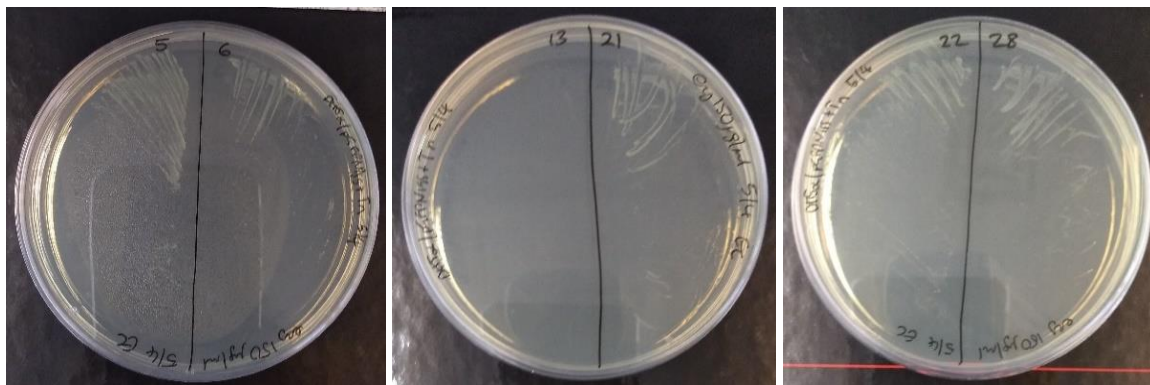


Figure 5-12 Erythromycin resistance in colonies screened for presence of the *Himar1* transposon insert

Confirmation of the *ermB*-transposon present on the vector insert was confirmed for colonies identified as likely to contain the insert by a screening PCR. Single colonies were streaked onto one half of an LB agar plate supplemented with erythromycin ($150\mu\text{gml}^{-1}$). All colonies were erythromycin resistant except for colony no. 13 confirming the results of a PCR screen which did not identify the insert by PCR in this colony.

Colony 22 was chosen for propagation and purification of the transposon delivery vector pNigHimar for *Chlamydia* transformation because all the genotypic and phenotypic requirements were met: it was chloramphenicol and erythromycin resistant, expressed *gfp*, and the plasmid was the correct size confirmed by restriction digest (Figure 5-13). Subsequently the plasmid DNA from this clone was purified and commercially sequenced by Source Bioscience for the final confirmation of the pNigHimar vector sequence.

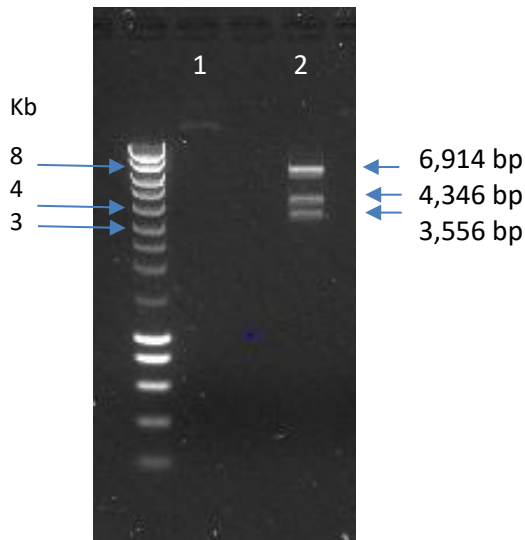


Figure 5-13 Stu1 restriction digest of pNiggHimar, colony 22.

Restriction digest of plasmid pNiggHimar (14,816 bp) using Stu1 endonuclease (5U) to produce three fragments at 6,914 bp, 4,346 bp and 3,556 bp. Undigested and digested plasmid DNA were loaded into well 1 and 2 respectively of a 1% agarose gel. A 10 kb DNA ladder (5 μ l) was used to size the digested bands.

Sequencing of plasmid pNiggHimar revealed a correct sequence matching the pGFP::Nigg backbone (blue DNA sequence) and the *Himar1* transposon under tet promoter control cloned from plasmid pRPF215 (black DNA sequence) (Figure 5-14). Subsequently, this clone was propagated in *E. coli* DH5 α and demethylated in *E. coli* GM2163 ready for transformation into *C. muridarum*.

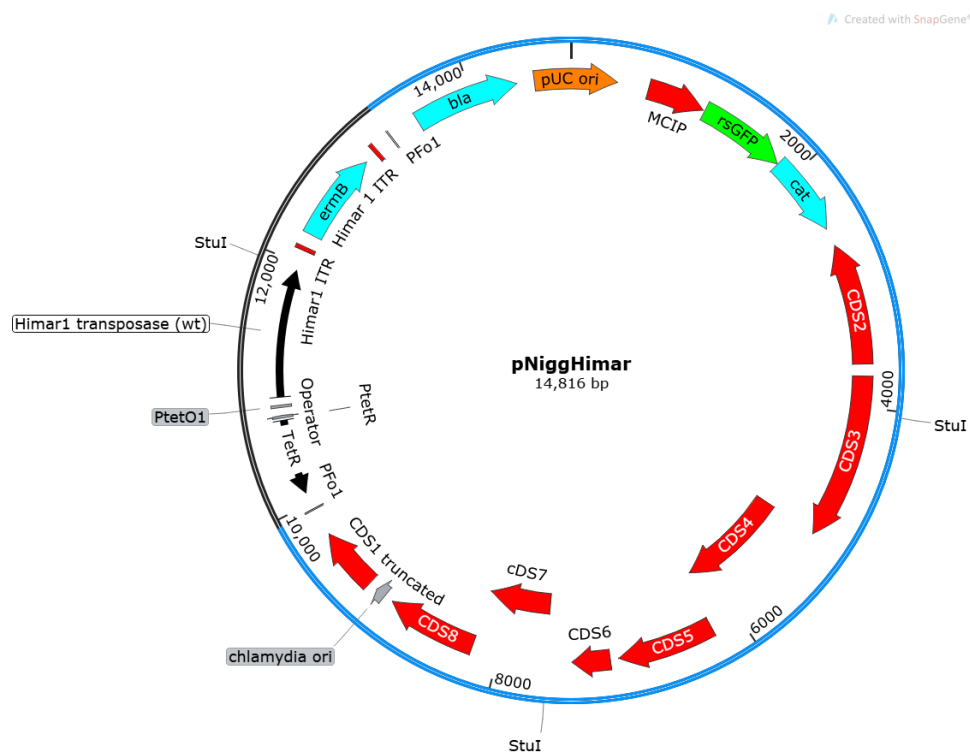


Figure 5-14 The annotated sequence of construct pNiggHimar

Colony 22 of pNiggHimar was sequenced and annotated as follows: chlamydial plasmid genes (red), antibiotic resistance genes (light blue), green fluorescent reporter gene (green), *Himar1* inverted terminal repeat sequences (red) and wild type *Himar1* transposase and regulatory components (black). Restriction endonuclease Pfo1 sites and Stu1 sites are indicated.

5.3.3 Transformation of *C. muridarum* with a replication-proficient transposon delivery vector

Three attempts were made at transforming plasmid-cured *C. muridarum* Nigg P- with pNiggHimar. Plasmid DNA was propagated in *E. coli* GM2163 (dam-/dcm-) and purified to generate new plasmid stocks for each transformation attempt. Assuming that transposase expression was inhibited by exclusion of the ATc inducer, antibiotic selection with erythromycin was not required for expansion of the transformants carrying pNiggHimar. Instead, expansion of transformants was attempted with the addition of penicillin selection added to the growth media at T1 and for all subsequent passages because plasmid pGFP::Nigg was shown to be stable under selection with penicillin in chapter 4 of this thesis. Plasmid pGFP::Nigg was used as a transformation control and penicillin selection was added to the growth media at T1. Transformants carrying plasmid pGFP::Nigg were successfully recovered at T2 at every attempt, whereas all attempts to recover transformants carrying pNiggHimar failed (Figure 5-15). It was reasoned therefore that premature

transposition caused by basal expression of transposase was likely to cause lethal mutations resulting in the failure to recover transformants.

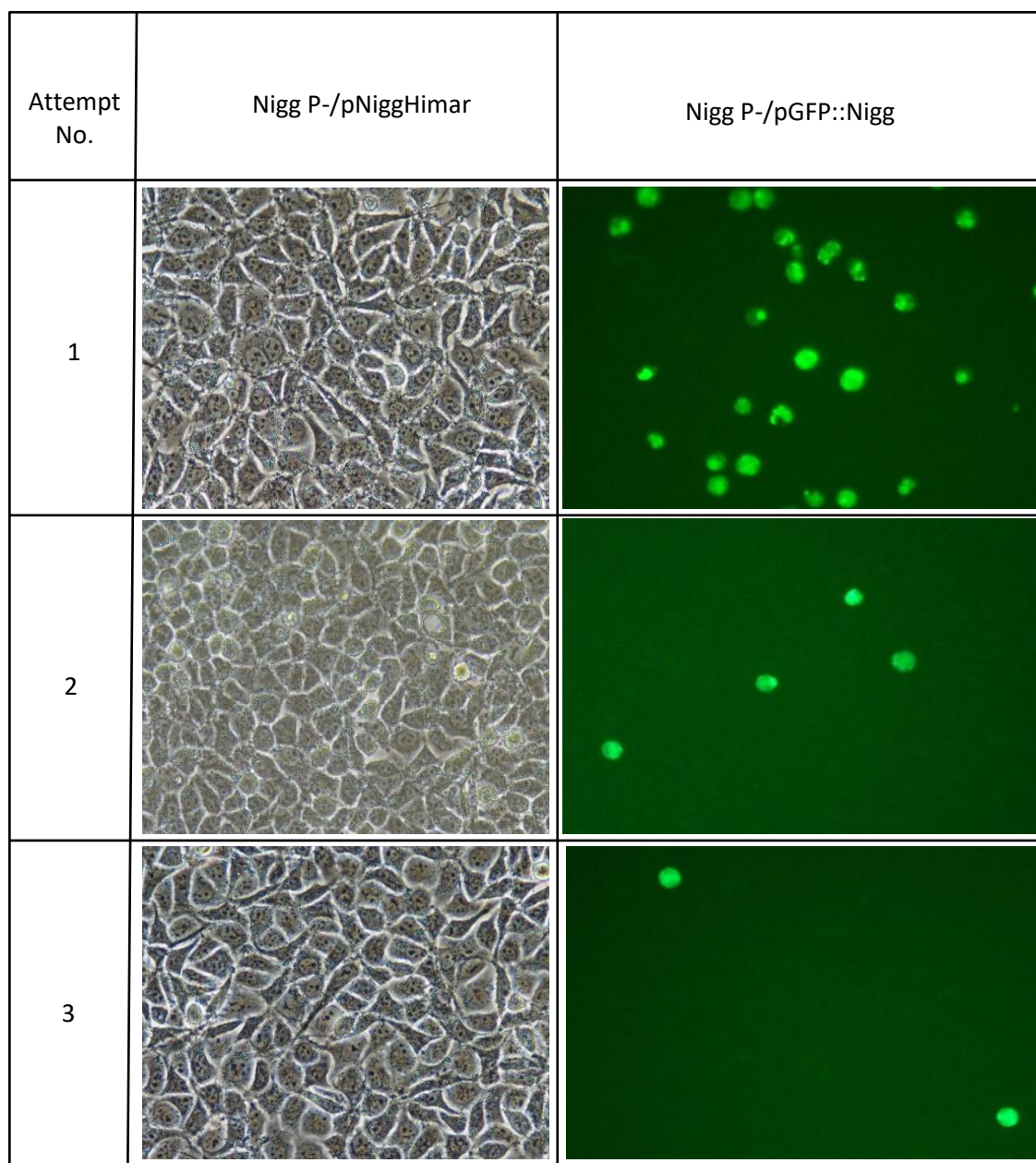


Figure 5-15 Transformation attempts with *E. coli*-*C. muridarum* transposon delivery vector pNiggHimar

Transformation of plasmid-cured Nigg (Nigg P-) with transposon delivery vector pNiggHimar was attempted three times using a different plasmid preparation each time. Plasmid pGFP::Nigg was used as the transformation control with penicillin introduced into the growth media at T1. Inclusions fluoresced green due to expression of *gfp* fluorescent reporter genes from these respective plasmids. The fluorescent reporter gene and plasmid backbone of Plasmids pGFP::Nigg and pNiggHimar are identical except for the *Himar1* transposon under tet promoter control cloned from plasmid pRPF215 into pNiggHimar.

5.3.4 *Generating transposition-negative constructs*

To test the hypothesis that the tet promoter is leaky, causing premature transposition of the transposon, transposition-negative plasmids were generated by isolating the active wild type *Himar1* transposase and the *Himar1* transposon on separate plasmids. Each plasmid, called pNiggHimar_GFP_ΔTn and pNiggHimar_mCh_ΔTpase, contained a different coloured fluorescent reporter gene, the green fluorescence reporter GFP and the red fluorescent reporter mCherry, as well as different selectable antibiotic resistance gene markers, *cat* and *aadA* conferring resistance to chloramphenicol and spectinomycin respectively. The recovery of both transposition-negative plasmids would indicate that premature transposition was likely to be the cause for the failure to recover transformants carrying pNiggHimar.

The cloning strategies and method for plasmid pNiggHimar_GFP_ΔTn and plasmid pNiggHimar_mCh_ΔTpase are described in method 5.2.3 of this chapter.

Plasmid pNiggHimar_GFP_ΔTn was generated by deletion of the *Himar1* ITR region containing the *ermB* antibiotic resistance gene by PCR cloning using primers 11 and 12 (Table 9). These primers were designed to add MRe1 restriction sites to the amplicon ends to facilitate self-ligation at the new reduced size.

Plasmid pNiggHimar_mCh_ΔTpase required two cloning steps. The first involved deletion of the catalytic domain of the transposase by PCR from pNiggHimar to generate an intermediate plasmid pNiggHimar_GFP_ΔTpase using primers 13 and 14 (Table 9). These primers were designed to add MRe1 restriction sites to the amplicon ends to facilitate self-ligation at the new reduced size in the same manner as for generation of pNiggHimar_GFP_ΔTn.

Plasmid pNiggHimar was used as the template DNA at either 10ng or 1 ng for optimisation of both primer pairs (11 and 12, and 13 and 14) by temperature gradient (Figure 5-16). Primers 9 and 10 amplified a product at the correct size at all temperatures tested (55°C, 60°C and 65°C) using both 1 ng and 10 ng of plasmid template DNA. Whereas primers 11 and 12 amplified a product with a greater yield at 55°C, 60°C than at 65°C. Some small faint bands were seen for primers 9 and 10 that were likely to be the result of primer dimer. However, the separation between the amplicon and the primer dimers was significant as not to be a concern for excising the desired band from the DNA gel and the bands were extremely faint, and nearly non-existent 55°C. Therefore, further optimisation was not required and the optimal annealing temperature for amplification of both the transposon and the transposase was determined to be 55°C.

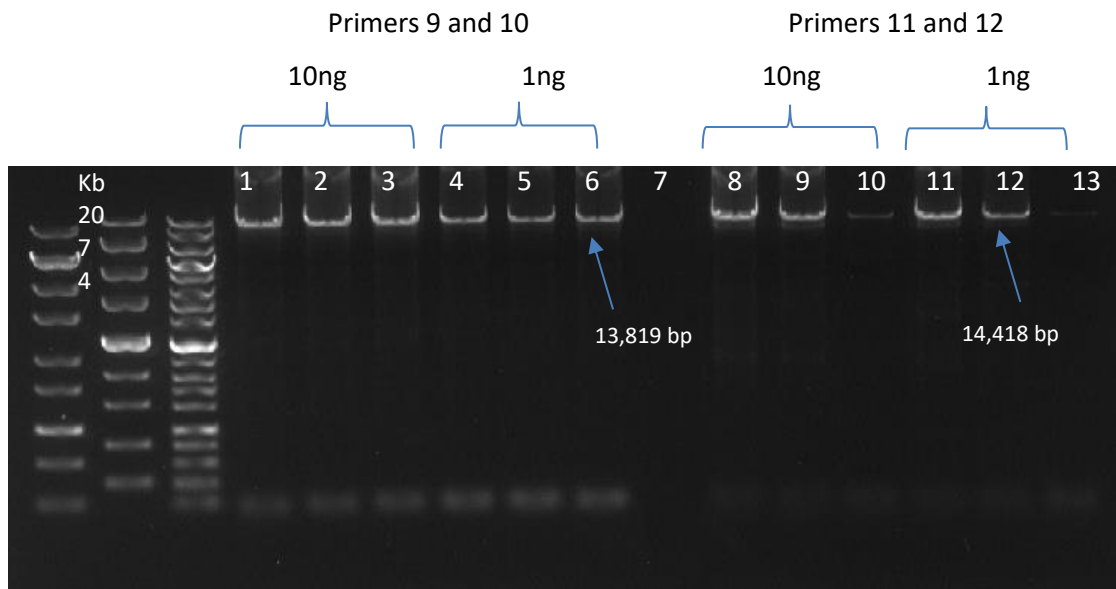


Figure 5-16 Optimisation of primers to delete the *Himar1* ITR and *ermB* gene and primers to delete the catalytic domain of *Himar1* transposase from pNiggHimar

Primers were tested at the following temperatures: 55°C, 60°C and 65°C with either 1 ng or 10 ng of plasmid template DNA (pNiggHimar). Primers 11 and 12 were designed to delete the *Himar* transposon, which included the *Himar1* ITR regions containing the erythromycin antibiotic resistance gene *ermB*, whereas primers 13 and 14 were designed to delete the catalytic domain of the *Himar1* transposase. A negative (water) control was loaded into well 7. Primers produced the strongest band at the expected band size (14,418 bp) at 55°C for primers 11 and 12. Primers produced the same strength bands regardless of annealing temperature for primers 9 and 10. A 10 kb ladder (5µl) was loaded into well 1, a 20 kb ladder (5µl) was loaded into well 2 and both 10 and 20 kb ladder were loaded into the third well for sizing of amplicons.

Ligation reactions for plasmid pNiggHimar_GFP_ΔT_{pase} and pNiggHimar_GFP_ΔT_n were performed without the dephosphorylation step to facilitate self-ligation of overhanging Mre1 restriction sites added to the PCR amplicon ends.

The second cloning step to generate pNiggHimar_mCh_ΔT_{pase} from pNiggHimar_GFP_ΔT_{pase} required digestion of the transposon cassette now containing the truncated transposase gene from pNiggHimar_GFP_ΔT_{pase} and cloning this into vector p2TK2_{spec}-NiggmCh(Gro)L2.

Primers 15 and 16 (Table 9) were designed to amplify the backbone of p2TK2_{spec}-NiggmCh(Gro)L2 and the annealing temperature for these primers was optimised using temperatures 50°C, 55°C, 60°C and 65°C (Figure 5-17). Primers produced the strongest band at the expected band size (10,369 bp) at 60°C, however, some non-specific binding did occur represented by very faint

bands at the bottom of the gel and at ~500 bp for all temperatures above 50°C. The small amount of non-specific binding was ignored based upon the good separation and the strength of the band at the correct size and further optimisation for this PCR experiment was not considered necessary. Therefore, the annealing temperature of 65°C was chosen for amplification of the p2TK2_{spec}-NiggmCh(Gro)L2 backbone using primers 15 and 16.

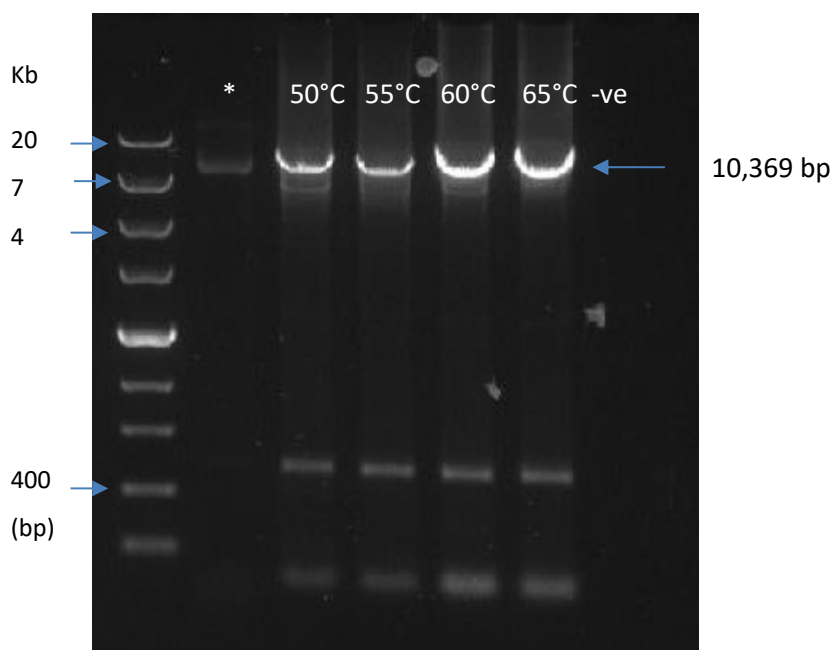


Figure 5-17 Optimisation of primers to amplify the backbone of p2TK2_{spec}-Nigg-mChGro(L2) adding Pfo1 sites

Primers 15 and 16 were tested at the following temperatures: 50°C, 55°C, 60°C and 65°C (wells 2-5) to amplify the backbone of plasmid p2TK2_{spec}NiggmChGro(L2). Some of well 2 sample drifted into well 1 marked with an asterisk. A negative (water) control was loaded into the final well. Primers produced the strongest band at the expected band size (10,369 bp) at 60°C.

Ligation of p2TK2_{spec}-Nigg-mChGro(L2) and the *Himar1* transposon cassette with deletion of the *Himar* ITR and *ermB* gene (Δ Tn) insert was performed as described in method 5.2.3.2.

5.3.4.1 Genotypic confirmation of constructs pNiggHimar_GFP_ΔTpase and pNiggHimar_mCh_ΔTn

The size of plasmids pNiggHimar_GFP_ΔTpase and pNiggHimar_mCh_ΔTn were checked by restriction digestion with restriction endonucleases Pfo1 and Spe1 respectively to produce the desired fragment sizes of 11,494 bp and 2,904 bp (pNiggHimar_GFP_ΔTpase) and 7,302 bp and 5,430 bp (colony 5 of pNiggHimar_mCh_ΔTn) respectively (Figure 5-18).

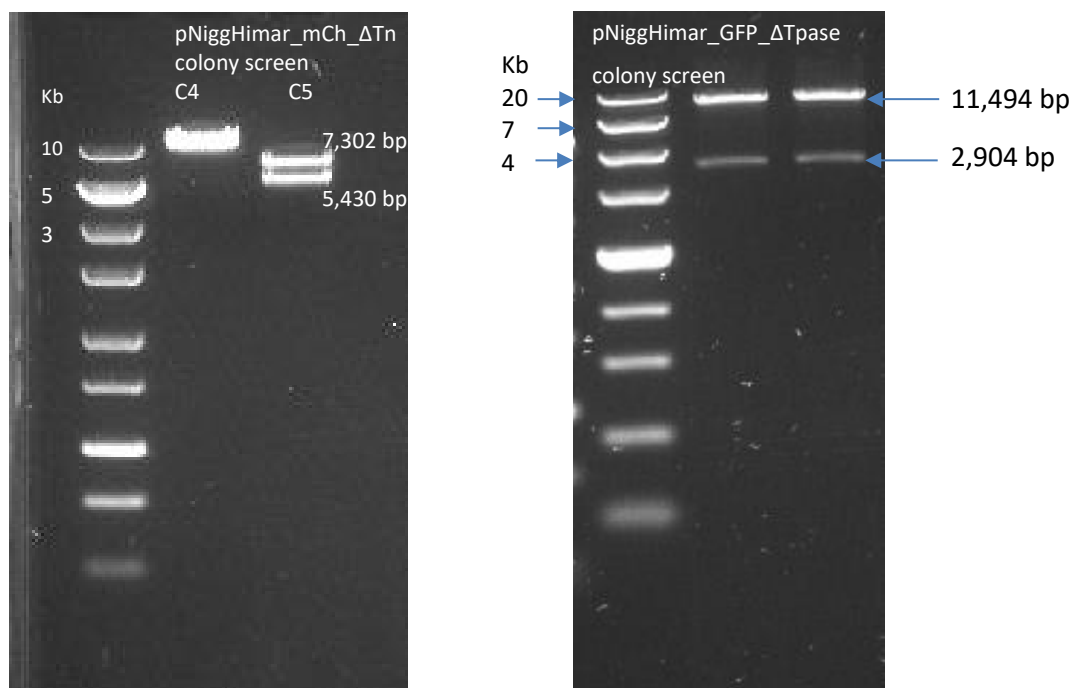


Figure 5-18 Confirmation of plasmid size by restriction enzyme digest of transposon and transposase *E. coli*-*C. muridarum* shuttle vectors

Plasmid pNiggHimar_GFP_ΔTpase and pNiggHimar_mCh_ΔTn were digested with restriction endonucleases to produce the desired fragment sizes of 11,494 bp and 2,904 bp (pNiggHimar_GFP_ΔTpase) using Pfo1 and 7,302 bp and 5,430 bp (colony 5 of pNiggHimar_mCh_ΔTn) using Spe1, confirmed against DNA ladders.

The cloned constructs were verified by sequencing. The entirety of pNiggHimar_GFP_ΔTpase and pNiggHimar_GFP_ΔTn plasmids were sequenced (Figure 5-19). Whereas, for plasmid pNiggHimar_mCh_ΔTn, sequencing primers 17 and 18 were designed to sequence only the *Himar1* transposon system insert. The correct sequence was confirmed in pNiggHimar_GFP_ΔTpase and pNiggHimar_GFP_ΔTn. However, one substitution (marked SNP) and two frameshift mutations (deletions) located within the transposase enzyme were identified on plasmid pNiggHimar_mCh_ΔTn as shown in the forward sequence (Figure 5-20). The first deletion is at the start of residue 76, the A/T substitution is at the start of residue 82 and the second deletion is at the start of residue 97. None of these residues resides within the catalytic domain responsible for transposase binding to *Himar1* ITR sequences, however, the deletion at the start of residue 76 causes a frameshift and severe truncation of the transposase enzyme by introducing a premature stop codon at the 79th residue. Therefore, the transposase enzyme will be inactive when expressed from plasmid pNiggHimar_mCh_ΔTn.

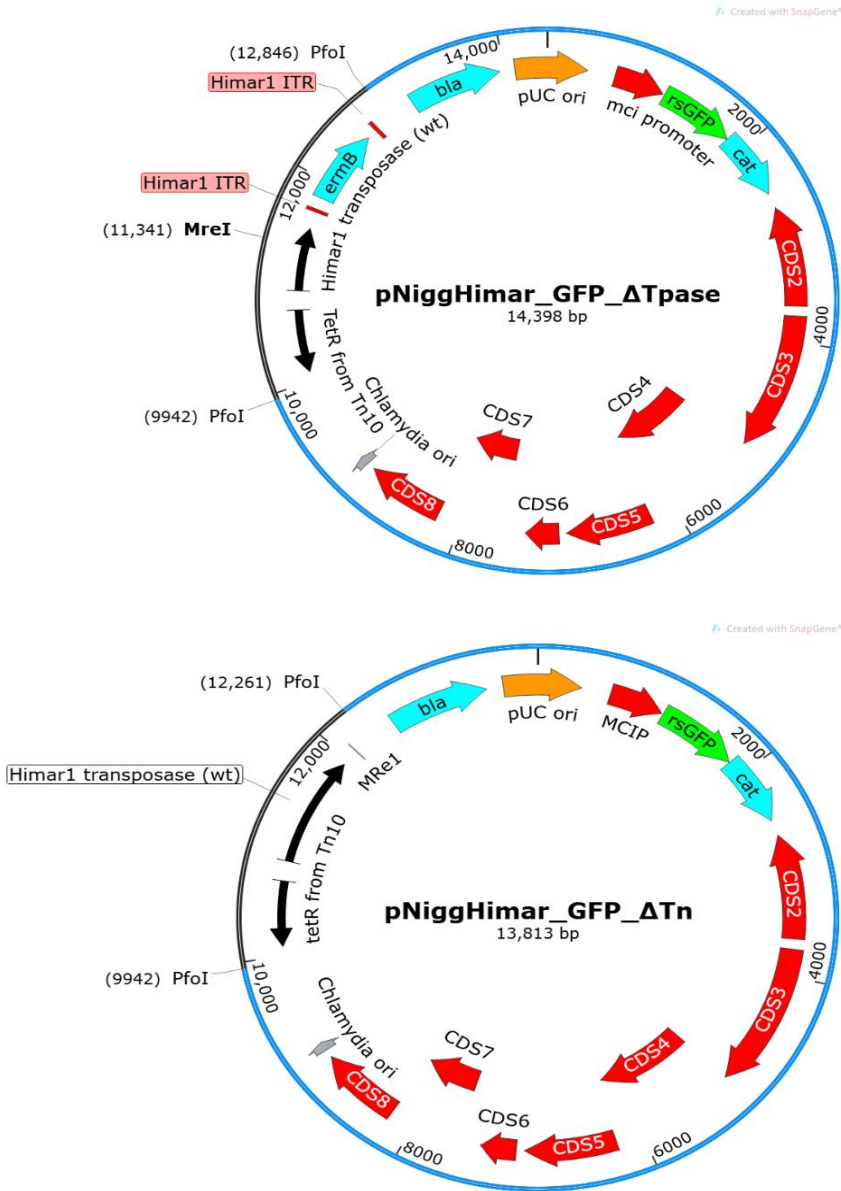


Figure 5-19 The annotated sequence of construct pNiggHimar_GFP_ΔTpase and intermediate construct pNiggHimar_GFP_ΔTn

Plasmid constructs pNiggHimar_GFP_ΔTpase and intermediate construct pNiggHimar_GFP_ΔTn were sequenced and annotated as follows: plasmid genes (red), antibiotic resistance genes (light blue), green fluorescent reporter gene (green), *Himar1* inverted terminal repeat sequences (red) and wild type *Himar1* transposase and regulatory components (black). Restriction endonuclease Pfo1 sites and Stu1 sites are indicated. Plasmid pNiggHimar_GFP_ΔTpase is missing the catalytic domain of the wild type *Himar1* transposase and plasmid pNiggHimar_GFP_ΔTn is missing the *Himar1* ITR regions flanking the *ermB* erythromycin resistance gene. The Mre1 sites added by PCR cloning primer pairs 11 and 12 (pNiggHimar_GFP_ΔTpase) and 9 and 10 (pNiggHimar_GFP_ΔTn) are indicated.

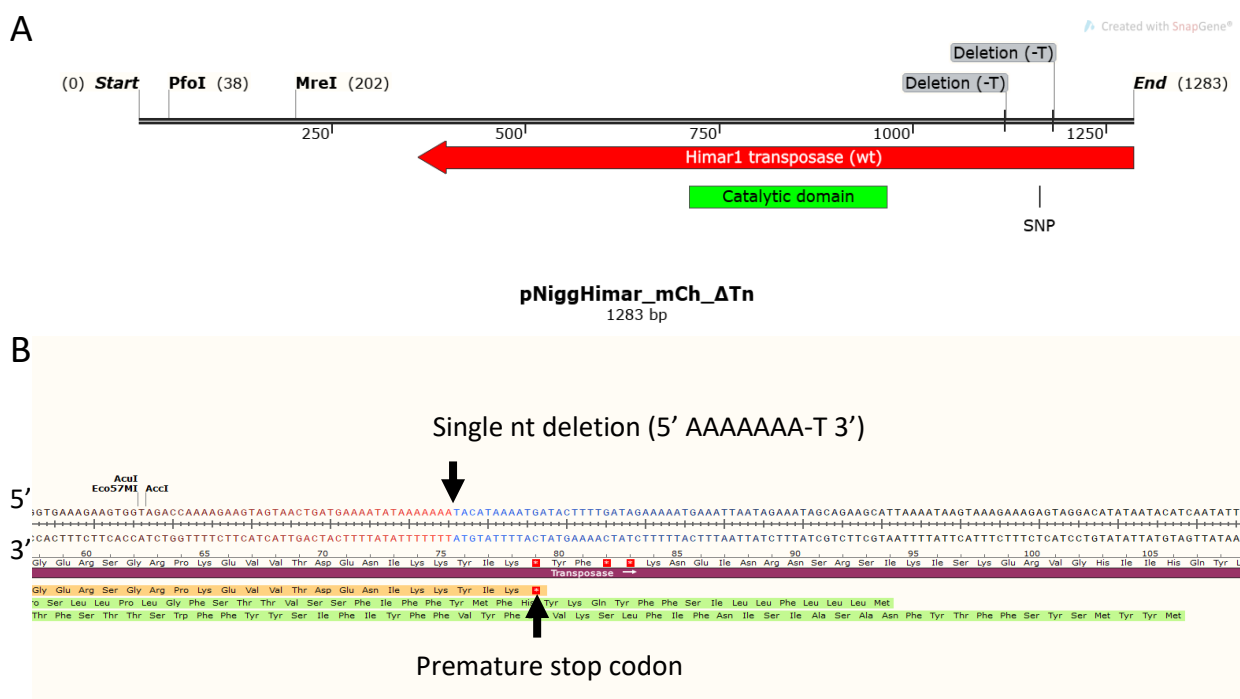


Figure 5-20 Sequence analysis of construct pNiggHimar_mCh_ΔTn

The sequence from primer SeqTnDel_F was annotated showing the restriction endonuclease site for MRE1 in place of the *Himar1 ermB*-carrying transposon. (A) The *Himar1* transposase gene contained three SNPs. One T/A substitution (marked SNP) and two deletions in proximity of each other. The first deletion is at the start of residue 76, a T/A substitution is at the start of residue 82 and the second deletion is at the start of residue 97, all outside of the catalytic domain of the transposase enzyme. (B) The deletion of a single nucleotide base results in a frameshift causing truncation of the transposase enzyme at the 79th residue. The nucleotides highlighted in blue represent the altered sequence downstream of the deletion indicated by an arrow.

5.3.5 Inducible expression of wild type *Himar1* transposase from transposon delivery vectors in *E. coli*

The wild type *Himar1* transposase under tet promoter control was cloned from plasmid pRPF215 into *E. coli*-*C. muridarum* shuttle vector pGFP::Nigg to generate pNiggHimar. The tet repressor regulates transposase expression through binding to the tetracycline promoter and the system was codon optimised for *C. diff* (Dembek et al., 2015). At the conception of this study, the inducible transposon system from plasmid pRPF215 had not been shown to work in an *E. coli* model system nor *Chlamydia*. The expression of exogenous genes in *E. coli* is typically used as a good indicator that they will be expressed in *Chlamydia* due to the sequence homology between sigma factors of the major RNA polymerase in both *E. coli* and *Chlamydia* (Shen et al., 2004). As

such, expression of exogenous genes is first demonstrated in an *E. coli* model organism prior to transformation of *Chlamydia* as routine practice. Therefore, it was necessary to verify that transposase was inducible and expressed from cloned transposon delivery vector pNiggHimar. Transposase expression was induced with ATc in *E. coli* Q358 transformed with pNiggHimar and samples were taken at multiple timepoints during a four-hour induction period as described in method section 5.2.6.1 of this chapter for immunodetection of transposase expression, and measurements of optical density.

Cultures of *E. coli* Q358 were transformed with the transposon delivery vector pNiggHimar, the transposition-negative plasmid pNiggHimar_GFP_ΔTpase and the parent plasmid pGFP::Nigg and were grown either in the presence or absence of the inducer (ATc) at a final concentration of 200 ng/ml as per the manufacturer's instructions (ThermoFisher). Induction was started when cultures reached an $OD_{(600nm)} = 0.5$ and single measurements were taken at 1, 2 and 4 hours post induction (Figure 5-21). The un-transformed host strain Q358 grew exponentially over the induction period reaching an $OD = 2.0$. The transformed strains did not reach $OD_{(600nm)} = 2.0$ over the same time suggesting that the expression of plasmid genes placed an added metabolic burden to the host which slowed its' rate of growth.

Cultures grown under the presence of the inducer had lower growth rate compared to uninduced cultures for all transformed strains. Changes in the growth rate between induced and uninduced cultures were only apparent from two hours post induction onwards. The largest difference was observed for pNiggHimar at 4 hpi with uninduced cultures reaching an $OD_{(600nm)} = 1.8$ compared to $OD_{(600nm)} = 1.6$ in the induced culture. The smallest difference in growth rate was observed between induced and uninduced cultures of plasmid pGFP::Nigg that does not contain the *Himar1* transposon system suggesting that transposase expression in the induced cultures placed an added burden to the growth of the host strain.

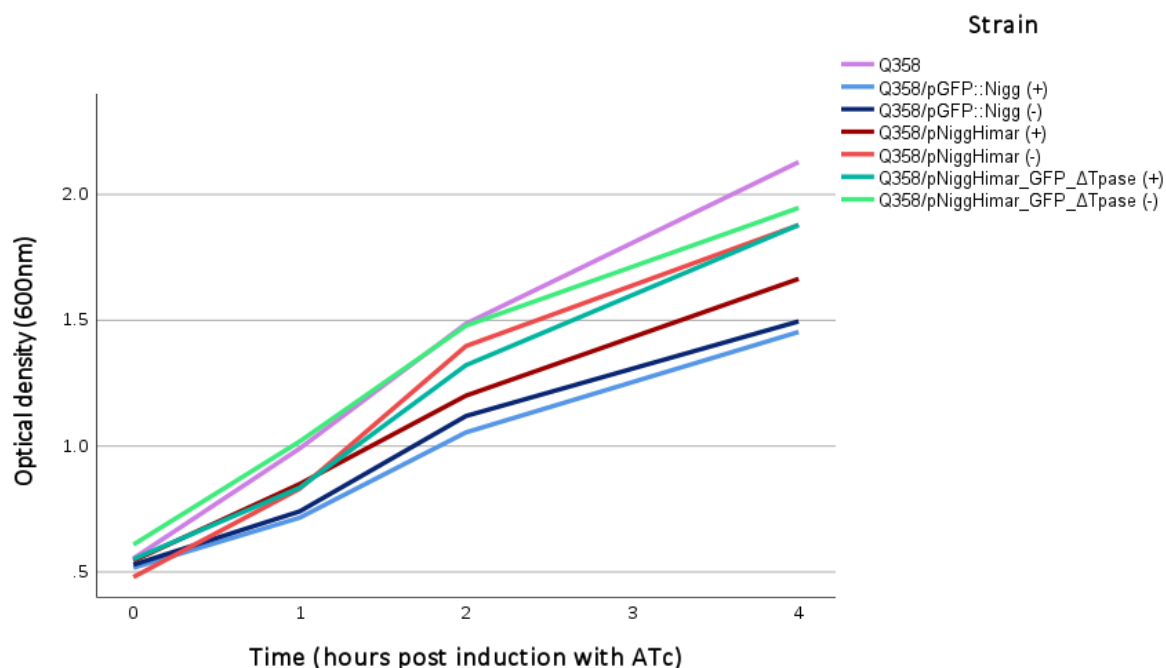


Figure 5-21 Growth curves of *E. coli*-*C. muridarum* transposon delivery vectors in *E. coli* Q358 after induction with ATc

E. coli Q358 was transformed with plasmid pGFP::Nigg and the transposon delivery vector pNiggHimar and its' derivative, the transposon vector pNiggHimar_GFP_ΔTpase. Liquid cultures for each strain were separated into two separate cultures, one was induced with ATc (+) one was not (-). Single OD_(600nm) measurements were taken at the time of induction (0h), and 1, 2 and 4 hours post induction.

Samples were taken from these same cultures at 0.5, 1.5 and 2.5 hours post induction to quantify the change in total protein concentration over the induction period (method 5.2.6.2). This was necessary to make a judgement about how much total protein was in each sample probed for expression of transposase. There were large discrepancies between the total protein concentration measured in cultures for each strain and between induced and uninduced cultures for each strain except for the control plasmid pGFP::Nigg which demonstrated similar increase in total protein concentration at all timepoints for both the induced and uninduced cultures. Samples were taken at 0h (time of induction), 1 and 2 hours post induction for immunodetection of transposase expression, and a sample at 2.5 hours post induction was analysed for immunodetection of GFP expression. The amount of protein loaded into each well for the western blots was extrapolated from the graph represented in Figure 5-22. Since the aim was simply to demonstrate that transposase was expressed in transposon delivery vector pNiggHimar, and because it was not known whether expression of transposase enzyme was transient or not, or what the limits of detection would be using such an old antiserum (~30 years old), it was not

considered essential to add equal amounts of protein for each strain into each well for the purposes of this experiment.

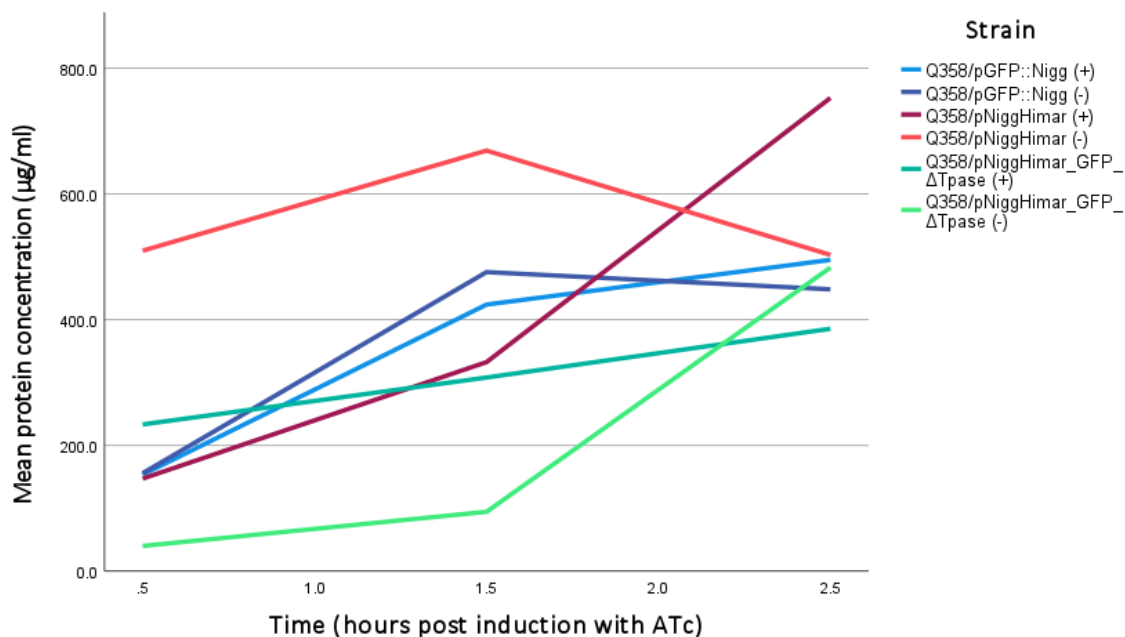


Figure 5-22 Effect of ATc induction on total protein concentration in *E. coli* transformed with *E. coli*-*C. muridarum* transposon delivery vectors

Cultures of *E. coli* Q358 transformed with transposon delivery vector pNiggHimar, and its' transposition-negative derivative plasmid pNiggHimar_GFP_ΔTpase were grown both in the presence of the inducer ATc (+) or absence of ATc (-) for four hours. Samples were taken at 0.5 hpi, 1.5 hpi and 2.5 hpi. The total protein content was extracted from cells by lysis with sonication and total protein concentration was quantified against a known concentration of BSA.

A very small and finite amount of the antiserum raised against the transposase was kindly donated Professor David Lampe (Duquesne University, USA), with 3µl available for use in this experiment only. Used at a 1:5000 dilution in 1% powdered milk solution (10ml), this was enough for one protein gel. To potentially extend the use of such a limited amount of antiserum, an experiment using antisera to GFP was performed to see how many times the primary antibody could be potentially re-used whilst maintaining the same or similar level of sensitivity. Strong bands were visualised for three reuses. Based upon these findings it was hypothesised that three uses of the transposase antiserum would be possible. Therefore, transposase expression from three timepoints was investigated for each strain with one gel per timepoint, measuring T0 (time of induction), 1 hour post induction (T1) and 2 hours post induction (T2).

To test whether the wild type transposase enzyme was actively expressed from the transposon delivery vector pNiggHimar, a Western blot to probe for transposase expression was performed for plasmids pNiggHimar and plasmid pNiggHimar_GFP_ΔTpase in *E. coli* with the parent plasmid pGFP::Nigg used as a transposase-negative control. GFP expression from each plasmid was used as a positive control and tested in the same cultures from samples taken at 2.5 hours post induction. The plasmid-free *E. coli* Q358 host was used as a GFP-negative control. The method for these experiments is described in method section 5.2.6.

GFP expression was confirmed for all plasmids of both induced and uninduced cultures confirming that the plasmids were present and constitutive expression of exogenous genes carried on each plasmid vector were being transcribed and translated into protein (Figure 5-23).

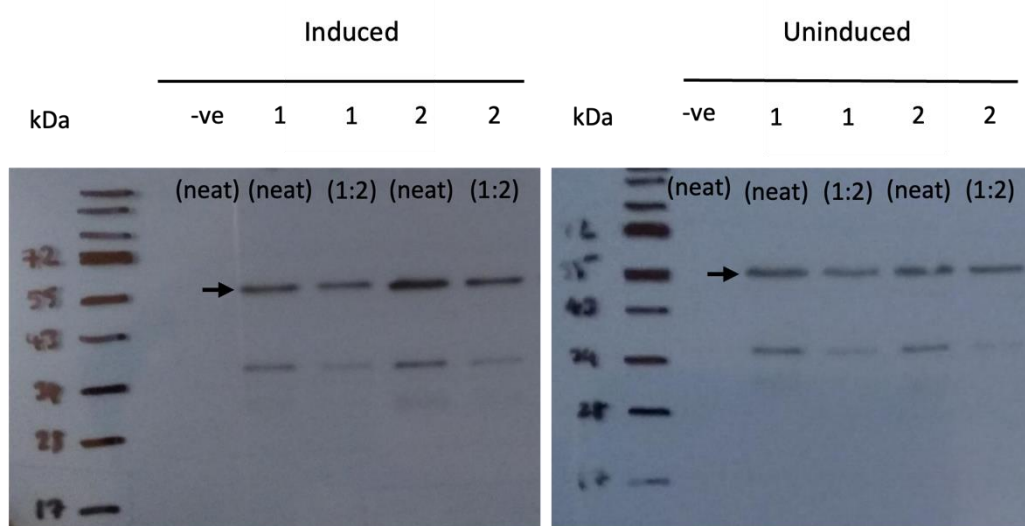


Figure 5-23 Western blot of GFP expression from *E. coli*-*C. muridarum* transposon delivery vectors in *E. coli*

Cultures of *E. coli* Q358 transformed with transposon delivery vector pNiggHimar (1), and its' transposition-negative derivative plasmid pNiggHimar_GFP_ΔTpase (2) were grown both in the presence of the inducer ATc (induced) or absence of ATc (uninduced) for four hours. The untransformed host *E. coli* Q358 was grown without induction with ATc in the same manner and used as a negative control. Samples (10 μ l) taken at 2.5 hours post induction were loaded into wells neat or diluted in PBS (1:2). Anti-GFP was used to probe the transfer membrane to show expression of GFP from both plasmids. The expected molecular weight for the GFPCAT fusion protein (arrowed) is \sim 57 kDa.

Transposase expression was seen in cultures of plasmid pNiggHimar at 1 and 2 hours post induction, with no expression detected in the uninduced cultures for the same time-points (Figure 5-24). The total protein concentration was higher in the uninduced cultures. No expression was detected for plasmid pNiggHimar_GFP_ΔTpase, which was identical to plasmid pNiggHimar except for the active site of the transposase. The total protein concentration for the 1-hour timepoint was very similar to that of the induced culture of plasmid pNiggHimar, in which transposase expression was detected, therefore failure to detect expression in the induced cultures for pNiggHimar_GFP_ΔTpase is not likely to be due to poor sensitivity of the antiserum. The exact binding site of the antibody was unknown; however, it was predicted that truncation of the transposase protein would be unlikely to completely inhibit antibody binding. This hypothesis was not supported by the lack of transposase expression in the induced culture for pNiggHimar_GFP_ΔTpase.

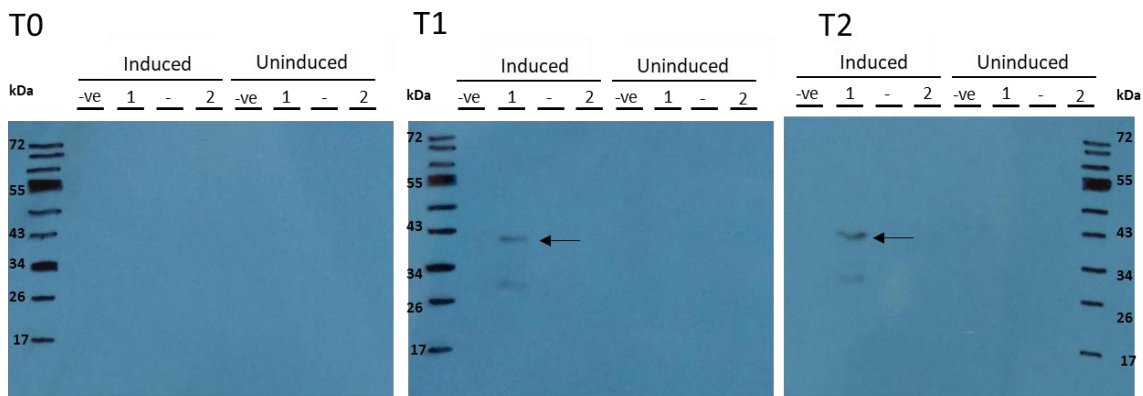


Figure 5-24 Western blot of wildtype *Himar1* transposase expression from *E. coli*-*C. muridarum* transposon delivery vectors in *E. coli*

E. coli Q358 transformed with the following plasmids: pGFP::Nigg (the parent plasmid and negative control lacking the *Himar1* transposon system), pNiggHimar (1) and pNiggHimar_GFP_ΔTpase (2) were grown in liquid culture and induced with ATc (T0). Samples were taken at 1h (T1), and 2h (T2) post induction as indicated. Samples were separated by 12% SDS-PAGE and expression of the wildtype *Himar1* transposase was detected with polyclonal antisera by Western blot. Transposase binding is indicated at 40.7 kDa by an arrow.

5.3.6 Transformation of *C. muridarum* with transposition-negative vectors

Three attempts were made at transforming plasmid-cured *C. muridarum* Nigg P- with pNiggHimar_GFP_ΔTpase (Figure 5-25) as well as both transposon-deletion plasmids pNiggHimar_GFP_ΔTn and pNiggHimar_mCh_ΔTn (Figure 5-26). Plasmid pNiggHimar_GFP_ΔTn was also used to transform *C. muridarum* representing a functional transposase-only *E. coli*-*C. muridarum* shuttle vector because sequence analysis of pNiggHimar_mCh_ΔTn revealed that the translated transposase enzyme was likely to be inactive on this plasmid. Plasmid DNA was purified from *E. coli* (method 2.10.1) to generate new plasmid stocks for each transformation attempt. The transposon is stable in plasmid pNiggHimar_GFP_ΔTpase due to the removal of the catalytic domain of the transposase which is responsible for transposition. Therefore, expansion of transformants carrying pNiggHimar_GFP_ΔTpase was attempted with the addition of penicillin selection added to the growth media at T1 and for all subsequent passages as described in method 2.9.1. The parent plasmid pGFP::Nigg was used as a transformation control for pNiggHimar_GFP_ΔTpase and passaged under selection with penicillin in the same manner. Transformants carrying plasmid pGFP::Nigg were successfully recovered at T2 at every attempt, whereas all attempts to recover transformants carrying pNiggHimar_GFP_ΔTpase failed (Figure 5-25).

A different replicating plasmid backbone, derived from plasmid p2TK2_{spec}-NiggmCh(Gro)L2, was used to generate plasmid pNiggHimar_mCh_ΔTn and contained the spectinomycin antibiotic resistance marker *aadA* and the red fluorescent reporter gene mCherry. Therefore, recovery of transformants was performed as described in method 2.9.1 with the following modifications. Spectinomycin (500 ug/ml) was added to the growth media at T0 at 16 hpi and plasmid p2TK2_{spec}-NiggmCh(Gro)L2 was used as the transformation control. Three attempts were made at transforming *C. muridarum* with pNiggHimar_mCh_ΔTn and recovering transformants which were unsuccessful, when the control plasmid was readily recovered in *C. muridarum* at T2 at every attempt (Figure 5-26).

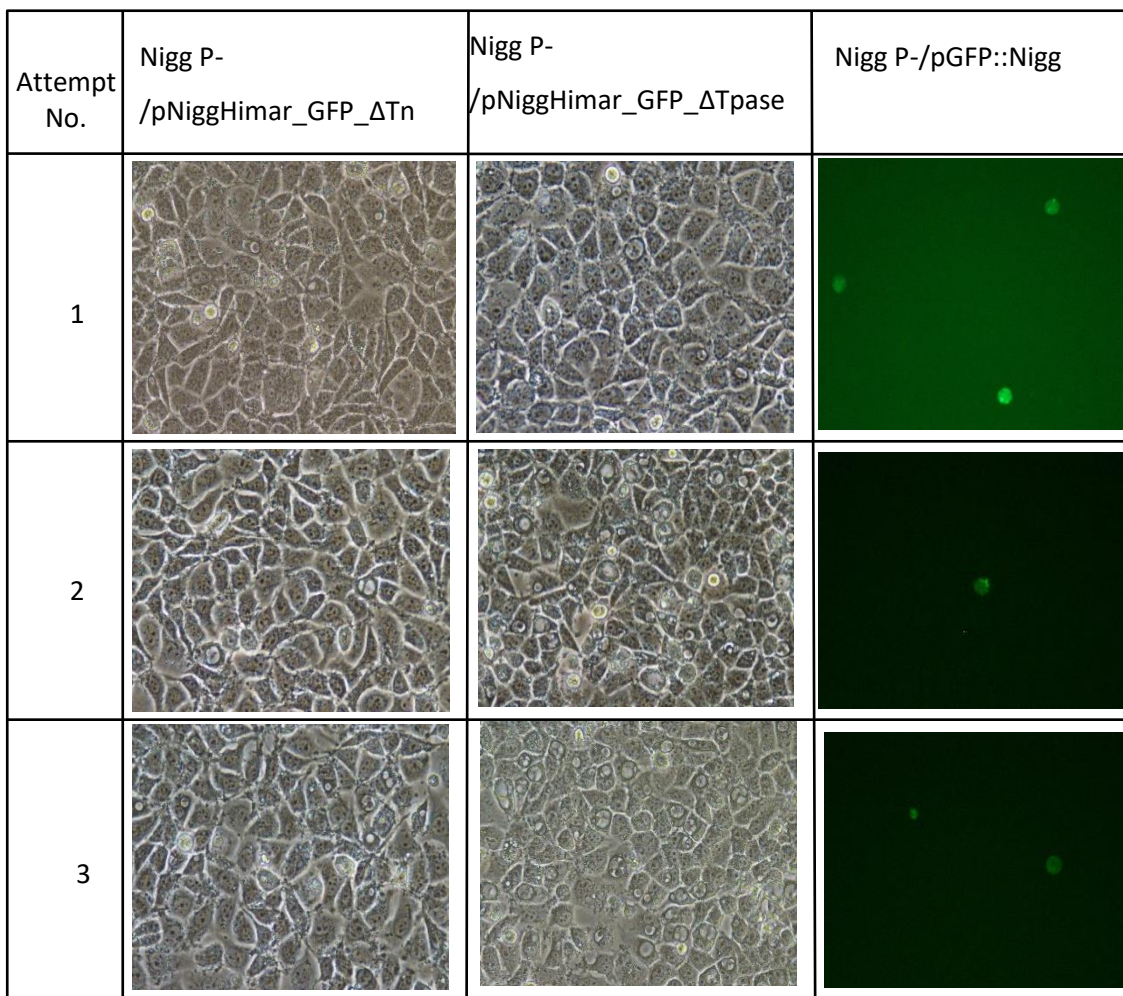


Figure 5-25 Transformation attempts with *E. coli-C. muridarum* transposition-negative vectors pNiggHimar_GFP_ΔTn and pNiggHimar_GFP_ΔTpase

Transformation of plasmid-cured Nigg (Nigg P-) with plasmids pNiggHimar_GFP_ΔTn and pNiggHimar_GFP_ΔTpase was attempted three times using a different plasmid preparation each time. Plasmid pGFP::Nigg was used as transformation control. Penicillin was introduced into the growth media at T1. Inclusions green for Nigg P-/pGFP::Nigg transformants due to expression of GFP from the plasmid. The fluorescent reporter gene and plasmid backbone of both pNiggHimar_GFP_ΔTn and pNiggHimar_GFP_ΔTpase vectors are the same as the control plasmid pGFP::Nigg.

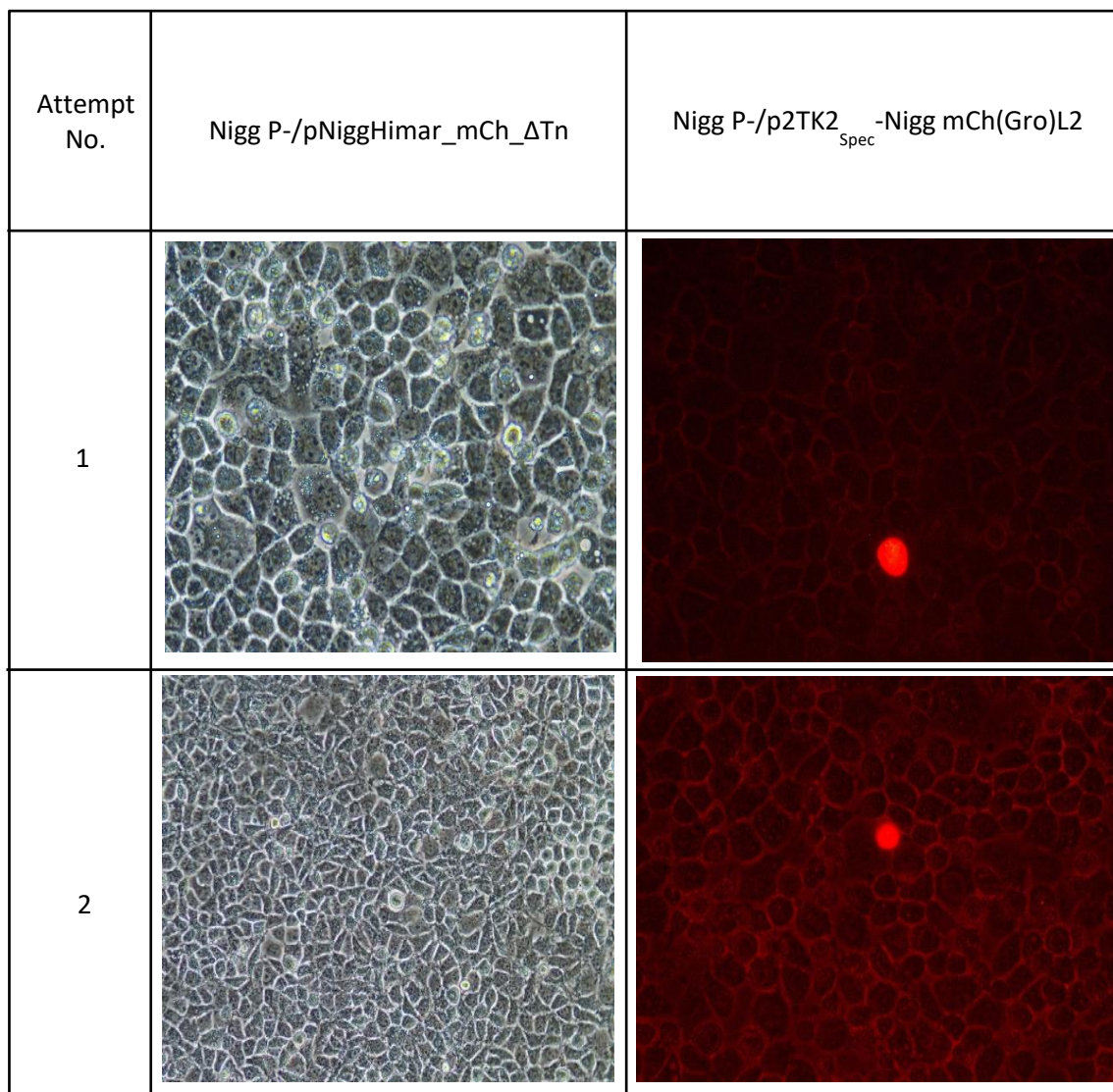


Figure 5-26 Transformation attempts with *E. coli*-*C. muridarum* transposition-negative vector pNiggHimar_mCh_ΔTn

Transformation of plasmid-cured Nigg (Nigg P-) with plasmid pNiggHimar_mCh_ΔTn was attempted three times using a different plasmid preparation each time. Plasmid p2TK2_{spec}-NiggmCh(Gro)L2 was used as transformation control with spectinomycin (500μgml⁻¹) introduced into the growth media at 16 hpi at T0. Inclusions fluoresced red for Nigg P-/ p2TK2_{spec}-NiggmCh(Gro)L2 transformants due to expression of the mCherry fluorescent reporter genes from the plasmid backbone, which is the same for pNiggHimar_mCh_ΔTn and p2TK2_{spec}-NiggmCh(Gro)L2.

5.4 Discussion

An inducible transposon mutagenesis approach does not yet exist for *C. muridarum*. The first demonstration of a tool, using the suicide vector approach, for transposon mutagenesis in *C. trachomatis* and adapted for use in *C. muridarum*, was achieved very recently (LaBrie et al., 2019; Wang et al., 2019). The use of suicide vectors is most common for transposon mutagenesis in bacterial species because they offer the most efficient means to reduce the likelihood of the occurrence of secondary transposition events by eliminating the transposase along with the plasmid once transposition has occurred. The *Himar1* transposase facilitates transposition by a cut and paste mechanism and therefore a secondary transposition event could cause mutations because of errors in DNA repair. It is also likely to increase the chance of lethal mutation by 'jumping' into essential genes.

Suicide vector pCMC5M was developed for transposon mutagenesis in *C. muridarum* with *Himar1* ITR sequences flanking transcriptionally fused GFP-*cat* genes that translate into green fluorescent protein and chloramphenicol acetyl transferase to identify and select transposon mutants using chloramphenicol selection in cell culture (Wang et al., 2019). The backbone of pCMC5M is missing the *Chlamydia* origin of replication to ensure that the transposase gene on the plasmid is not passed onto daughter cells after transposition. Although only small numbers of unique mutants can be generated using the suicide vector approach, this was the first demonstration of a functional transposase engineered as a genetic tool in *C. muridarum*.

An inducible transposon system required control of transposase expression using a promoter system that would be functional in *C. muridarum* as well as a stable, replication-proficient plasmid backbone. The transposon system on plasmid pRPF215 was developed for transposon mutagenesis in *C. diff* (Dembek et al., 2015). This system was engineered to provide regulatory control over transposition using the inducible Tet promoter system. This system is the only inducible system that has been shown to be functional with a high degree of control in *Chlamydia* (Wickstrum et al., 2013). Therefore, the complete transposon system from plasmid pRPF215 was chosen as the basis for developing an inducible transposon mutagenesis approach in *C. muridarum*. In addition, the stably replicating vector pGFP::Nigg was chosen as the backbone resulting in the construction of vector pNiggHimar.

At the time of conception, the functionality of the transposon system from plasmid pRPF215 had not been demonstrated either in an *E. coli* model system nor *Chlamydia*. Certain sigma factors of the major RNA polymerase in *Chlamydia* and *E. coli* share high sequence homology that facilitate *E. coli* RNA polymerase recognition of chlamydial promoters (Shen et al., 2004), so if transposase is expressed in the *E. coli* system it was considered highly likely that these genes would also be

expressed in *C. muridarum*. Hence why the expression of exogenous genes in *E. coli* is typically used as a good indicator that they will be expressed in *Chlamydia*. This step was also necessary because the transposon system was codon optimised for *C. diff*. Given the recent and successful application of this system adapted for use in *C. trachomatis* (Skilton et al., 2021) it was not surprising therefore that functionality of the Tet-system to induce transposase expression was successfully demonstrated in *E. coli*.

Attempts were also made to transform plasmid-cured *C. muridarum* Nigg P- using vector pRPF215 and to recover transposon mutants to demonstrate that this inducible system is functional in *Chlamydia*. The transposon on plasmid pRPF215 contains an erythromycin antibiotic resistance gene *ermB*. For simplicity in cloning the transposon delivery vector pNiggHimar, the *ermB* marker was not replaced with a typical selectable marker used in *C. muridarum*. Instead, approval for the use of the *ermB* marker in *C. muridarum* was obtained. This was necessary because of the use of erythromycin in the treatment of *C. trachomatis* infection (Nwokolo et al., 2016). However, under the category 2 regulations under which *C. muridarum* is handled in the laboratory setting, as well as the minimal risk of transmission to humans, approval was readily given. This provided the opportunity to demonstrate the feasibility of using *ermB* as a selectable marker in *C. muridarum*. Consequently, optimisation of selection conditions using erythromycin in both *E. coli* and *Chlamydia* were required. Prior to transforming *Chlamydia*, plasmid DNA is typically propagated using *E. coli* DH5 α followed by demethylation in an appropriate strain deficient of *dcm* and *dam* methylases, such as GM2163. Therefore, the breakpoint for erythromycin was first determined for *E. coli* DH5 α and GM2163 which have no known natural resistance to erythromycin and additionally *E. coli* Q358 as an alternative strain available for use with no known resistance to erythromycin.

The ideal assay would have employed either liquid turbidity or Kirby-Bour disc diffusion methods which are used routinely in research and clinical settings respectively (Alagumaruthanayagam et al., 2009). The main limitation to the use of solid phase assays is the formation of concentration gradients within the set plates and the time delay for results is often long (2-3 days). For the purposes of this study, a crude solid phase assay that could be performed quickly was used to simply demonstrate that the *ermB* gene was functional prior to transformation into *Chlamydia* therefore more accurate determination of susceptibility was not deemed necessary.

The approximate MIC for erythromycin in DH5 α and Q358 was determined to be 150 μgml^{-1} . Thus, 150 μgml^{-1} erythromycin was used to select for DH5 α and Q358 transformants with all vectors containing the *Himar1 ermB*-transposon. GM2163 demonstrated high natural resistance to erythromycin and grew on LB agar supplemented with 500 μgml^{-1} . This was unexpected because there is no reported evidence of erythromycin resistance in GM2163, and the genotype does not

contain the main erythromycin resistance genes such as the 23s rRNA methylase genes *erm(T)*, *erm(TR)*, and *erm(AX)* or *erm(A)*. It is possible that other mechanisms of erythromycin resistance are present in GM2163 such as the non-specific efflux-pump mediated antibiotic resistance that has been shown to be responsible for erythromycin resistance in other *E. coli* strains (Li et al., 2015). Therefore, erythromycin resistance was confirmed in plasmids purified from DH5 α on LB agar supplemented with erythromycin at 150 μgml^{-1} with further genotypic verification of the correct plasmid with a restriction digest in plasmid DNA purified from *E. coli* GM2163 prior to transformation into *Chlamydia*.

No standard protocol existed for the use of erythromycin for the recovery of transposon mutants in *C. muridarum* at the time the study design was conceived. For the recovery of chloramphenicol-resistant transposon mutants generated using suicide vector pCMC5M, Wang et al (2019) adapted the standard protocol used for the transformation and recovery of *Chlamydia* by adding chloramphenicol to the growth media used for transformed cells at T0. Therefore, addition of erythromycin selection was included both at T0 and starting from the first passage (T1).

Erythromycin, like chloramphenicol, is a protein synthesis inhibitor which targets the 50S subunit of the ribosome and is known to be bactericidal particularly at high concentrations. The *erm* genes, which can be both inducible or constitutively expressed, encode methylases which can render bacteria resistant to erythromycin through methylation of the binding-site on the ribosome (Desjardins et al., 2004). The *ermB* gene in plasmid pRPF215 was constitutively expressed and, in isolation, has been shown to function in *E. coli* (Heap et al., 2009) therefore it was reasonable to hypothesise that the *ermB* marker would be functional in *C. muridarum* for the selection of *ermB*-transposon mutants.

The suicide vector approach dictates that any markers or reporter genes contained on the backbone cannot be used to identify and select for transformants because of loss of the plasmid post transposition. To resolve this issue, suicide vector pCMC5M, engineered for transposon mutagenesis in *C. muridarum*, ensured that the fluorescent reporter GFP was coupled with antibiotic resistance gene *cat* and therefore transposed together to facilitate the identification and selection of transposon mutants (Wang et al., 2019). A key limitation in the attempt to recover *ermB*-resistant transposon mutants was the lack of a fluorescent reporter gene in the transposon itself to aid in their identification in cell culture. Identifying any potential transposon mutant was particularly challenging as it required the traditional inclusion phenotyping approach using microscopy but without the use of fluorescent reporters. Also, without a transposon mutagenesis control, the inclusion phenotypes of transposon mutants were not known. Also, transposon mutagenesis is random and the impact of knock out of most chlamydial genes on inclusion phenotype is not known.

A key criterion to identify mature inclusions is the visual confirmation of movement of EBs within the inclusion membrane. Potential transposon mutants of Nigg P-/pRPF215 were seen in cultures at fourth passage under erythromycin selection, indicated by a round EB-like structure that had significant movement within an inclusion-like membrane. The same phenotype was observed at passage 5 under selection with erythromycin. Typically, mature inclusions contain up to one thousand EBs so the appearance of only one moving EB-like structure was not confirmatory of a transposon mutant. Whole genome sequencing of the DNA harvested from these cultures or sequencing the transposon-*C. muridarum* insert junction would have confirmed this, however, the demonstration of an inducible transposase system in *E. coli* in this study and the demonstration of a functional *Himar1* transposase in *C. muridarum* by Wang *et al.*, (2019) was considered sufficient that this system would be inducible in *C. muridarum*.

Despite confirmation of expression of transposase from the transposon delivery vector pNiggHimar in *E. coli*, it was not possible to recover transformants in *C. muridarum*. The transformation control, which involved the parent plasmid pGFP::Nigg successfully transformed Nigg P- each time. Therefore, it was reasoned that the inability to recover transformants was likely to be a result of premature transposition causing plasmid loss and potential lethal mutations.

Initial attempts to transform *C. trachomatis* with a similar inducible transposon system derived from plasmid pRPF215 was also unable to transform *C. trachomatis* (Skilton *et al.*, 2021). The authors hypothesised that premature transposition caused by basal expression of transposase from the tet promoter in the 'off-state' (uninduced) was behind the inability to recover transformants in *C. trachomatis*. This was confirmed by the relatively straight forward recovery of transformants carrying transposition-negative vectors that contained either a functioning transposase without the transposon element or vice versa. However, the same was not true for *C. muridarum*. Neither the transposon knockout plasmid pNiggHimar_GFP_ΔTn nor the transposase knockout plasmid pNiggHimar_GFP_ΔTpase were recovered in *C. muridarum*. It was shown in the previous chapter of this thesis that plasmid pGFP::Nigg, which provides the backbone for these plasmids, is maintained at a very low copy number (≤ 1) in *C. muridarum*, much lower than is typical for *C. trachomatis* strains. It is extremely likely that this combined with the very low transformation efficiency are responsible for the failure to recover transformants of *C. muridarum* carrying either transposition negative constructs.

Immunodetection of transposase expression in the induced cultures containing pNiggHimar and not the uninduced cultures, cannot rule out the possibility of premature transposition caused by transposase expression from the tet promoter in the uninduced state. The antisera itself was approximately 30 years old and likely to have been degraded over that time. In addition, the

sensitivity of the transposase for the wild type *Himar1* transposase enzyme was not known. The total protein measured in the induced and uninduced cultures for Q358/pNiggHimar at the 1-hour point were comparable, so the inability to detect the basal expression of transposase in the uninduced cultures show that recovery of transposition-negative vectors is, at the minimum, required to show that the Tet-system was leaky for plasmid pNiggHimar. Furthermore, it is highly likely that species-differences also undermine the ability to recover the vectors in *C. muridarum* such that recovery of the transposition-negative plasmids was always unlikely.

Several features distinguish the vector designed for inducible transposon mutagenesis for *C. trachomatis* recently published by Skilton et al (2021) from the inducible vector designed for *C. muridarum* in this study. These include a backbone, derived from *E. coli-C. trachomatis* shuttle vector pGFP::SW2, the use of the hyperactive form of the *Himar1* transposase in place of the wild type gene and the *bla* gene in place of the *ermB* marker. However, the most significant difference that renders *C. muridarum* typically less genetically tractable than *C. trachomatis* is the very low copy number combined with the poor transformation efficiency. The minimal gene set for a stably replicating vector in *C. muridarum* was shown to exclude plasmid genes *CDS5* and *CDS6*, with a plasmid copy number roughly 4-times higher than that of pGFP::Nigg, in chapter 4 of this thesis. With plasmid copy numbers of ~4 per bacterial cell, these overlap with reported copy numbers for *C. trachomatis* strains (Pickett et al., 2005). Therefore, it is possible that swapping the pGFP::Nigg backbone with pNiggCDS56Del could improve the chances of recovering the transposition-negative control plasmids.

5.5 Conclusions

It was hypothesised that the generation of near-saturation mutants libraries may be possible with the expansion of the transformant population carrying a transposon delivery vector prior to the induction of transposon transposition (Skilton et al., 2021). This required a replication-proficient vector that could be stably passaged in cell culture. The inducible *Himar1* transposon system containing an *ermB*-transposon was cloned from plasmid pRPF215 into *E. coli-C. muridarum* shuttle vector pGFP::Nigg which was previously shown to stably replicate at a low copy number (<1) in *C. muridarum* Nigg P- to generate a replication-proficient and inducible transposon delivery vector called pNiggHimar.

The conditions for use of *ermB* as a selectable maker in *C. muridarum* were optimised and confirmation of functioning *bla* and *ermB* markers as well as fluorescent reporter GFP from pNiggHimar were verified in *E. coli*. Additionally, the wild type transposase from plasmid pRPF215 was shown to be inducible in *E. coli* and therefore highly likely to functional in *C. muridarum*. Despite these findings, plasmid pNiggHimar was unable to be recovered in *C. muridarum*. This was

also the case for an *C. trachomatis* inducible vector using the Tet-system to control transposition (Skilton et al., 2021), except that transposition-negative plasmids were recovered in *C. trachomatis* demonstrating that a basal expression of transposase from the tet promoter was likely to be responsible for the inability to recover the plasmid carrying both transposon and transposase. The inability to recover the transposition—negative plasmids derived from pNiggHimar in *C. muridarum* are highly suggestive that species-specific factors such as the very low plasmid copy number combined with the low transformation efficiency further undermines the ability to recover these vectors in *C. muridarum*.

Chapter 6 Final discussion

The overall strategic aim of this project was to develop a plasmid-based tool for inducible transposon mutagenesis in *C. muridarum*. Since work began in October 2017, the first tools for transposon mutagenesis of any *Chlamydia* species were reported using a suicide vector approach (LaBrie et al., 2019; Wang et al., 2019). Such systems, although inefficient at generating the numbers of unique mutants required for the discovery of essential genes using transposon-sequencing techniques, demonstrated the functionality of the hyperactive variant of the *Himar1* transposase in both *C. trachomatis* and *C. muridarum*. To reach saturation mutagenesis, an alternative approach has been proposed for *C. trachomatis* using an inducible transposon system (Skilton et al., 2021). The application of such an approach to *C. muridarum* was the focus of the work presented in this thesis.

The application of an inducible transposon mutagenesis in *C. muridarum* first required the characterisation of *in vitro* plasmid loss in this species using available replication-proficient vectors for the identification of a stably replicating plasmid and potentially a mechanism for plasmid elimination, which is required for the removal of the transposase gene post transposition. This was followed by the optimisation of an inducible transposon mutagenesis protocol for *C. muridarum* and demonstration of a functional inducible transposon mutagenesis system that could be maintained and expanded in *C. muridarum* in cell culture prior to transposition. The development of a robust and reproducible plasmid stability assay for *Chlamydia* is presented in chapter 3, which was used to test the stability of a range of available replicating vectors in chapter 4 to identify an appropriate backbone for a transposon delivery vector. An inducible transposon vector system was constructed and tested in *E. coli* with attempts made at recovering transformants in *C. muridarum*, presented in chapter 5.

Standardisation of a plasmid stability assay for *Chlamydia* requires the ability to generate standard inocula where every cell contained a plasmid with which to measure plasmid loss over generations of EBs. This was achieved using the limited available antibiotic resistance markers for the positive selection of transformants available for use in *Chlamydia* and was first demonstrated with the *E. coli*-*C. muridarum* shuttle vector pGFP::Nigg (containing the complete native *C. muridarum* plasmid) using bactericidal concentrations of chloramphenicol. High concentrations of chloramphenicol are effective at killing sensitive bacteria, as demonstrated by maintenance of a plasmid copy number of ~ 1 over passage. However, plasmid-derivatives of pGFP::Nigg lacking certain plasmid-genes previously considered to be not-essential for maintenance, were incapable of expansion under these conditions. Previously undefined MICs for chloramphenicol in *C. muridarum* at sub-inhibitory concentrations were sufficient for generation of standard inocula for

these plasmids, which, in concordance with published data for similar gene-deletion constructs, had higher copy numbers under any test condition than the parent plasmid pGFP::Nigg.

The measurement of plasmid loss from EBs in *Chlamydia* previously relied upon indirect methods alone that quantified the proportion of plasmid-free inclusions recognised as either lacking glycogen or loss of fluorescent reporters expressed from a plasmid over serial passage (Russell et al., 2011; Shima et al., 2018). Furthermore, plasmid stability was assumed to be based upon the ability to recover transformants in *Chlamydia* without a quantitative measure of plasmid loss (Gong et al., 2013; Liu et al., 2014a; Song et al., 2013). Plasmid stability without antibiotic selection had previously never been investigated. The assay design optimised in chapter 3 sought to improve the accuracy and sensitivity of measuring plasmid loss in *Chlamydia* by combining both direct molecular and indirect approaches, adaptable for any species or selectable antibiotic resistance marker that may become available for use in genetic studies in the future.

Direct molecular approaches have been widely adopted to measure plasmid copy number in free-living bacteria (Dell'anno et al., 1998; Projan et al., 1983), but never had change in plasmid copy number been used to investigate plasmid stability in *Chlamydia*. Using the only other available selectable marker, *bla*, plasmid loss frequency (the proportion of plasmid-free inclusions) and changes in plasmid copy number were measured for four different replicating vectors under selection with penicillin and without selection over serial passage. No true linear relationship was found between plasmid copy number and the plasmid loss frequency indicating that higher plasmid copy number does not indicate plasmid instability contrary to models developed in high copy number plasmids (Million-Weaver and Camps, 2014). These findings were significant for accurately interpreting changes in copy number and plasmid loss frequency as separate but complementary strategies. Decreases in plasmid copy number and an increase in the plasmid loss frequency over serial passage indicated unstable plasmids.

The presence of plasmid-free inclusions, indicated by the loss of expression of GFP, was always present under any test condition except for plasmid pGFP::Nigg grown under bactericidal concentrations of chloramphenicol, and was therefore not itself an indicator of plasmid instability. This was expected for such low copy number plasmids (≤ 4), especially as plasmid copy number is measured as the average across the total bacterial population, and shown to mask the variation in distribution of plasmids (Werbowy et al., 2017). Plasmid loss frequencies ranged between 0 and 12% in concordance with published findings in *C. muridarum* (Russell et al., 2011), but never increased above ~4% for stable plasmids.

The ability to control the degree of heterogeneity in a bacterial population is an invaluable strategy for genetic studies that ideally require a homogeneous genetic background to make more accurate assumptions about the function of genes. The ability to generate standard inocula for

transformants in *C. muridarum* was important, not just for a reproducible means to assess plasmid stability but to demonstrate a means by which bacterial cells carrying the transposon delivery vector can be optimally expanded in cell culture prior to the induction of transposition. However, the ideal transposon mutagenesis approach would have a mechanism for eliminating the plasmid post transposition from all plasmid-carrying cells which reduces the likelihood of secondary transposition events.

A potential novel mechanism for the elimination of the plasmid in *C. muridarum* was observed when bactericidal concentrations of chloramphenicol were removed from the growth media for plasmid pGFP::Nigg resulting in the collapse of plasmid copy number that was unable to recover with further passaging under positive selection. Chloramphenicol is a potent inhibitor of transcription and translation of chlamydial genes used at high concentrations (Scidmore et al., 1996) therefore it could be hypothesised that this phenomenon was likely to be a result of the degree at which chloramphenicol inhibited transcription and translation of an early gene product that was responsible for plasmid maintenance thus allowing for the expansion of the plasmid-free population upon its removal. However, further investigation is required to understand the potential mechanism behind this and to replicate the findings of the single assay performed in this study. The development of a robust plasmid stability assay provides a framework for investigating candidate genes involved in plasmid maintenance in *Chlamydia* however this was outside of the scope of this study.

The stability of available replication-proficient plasmids in *C. muridarum* were investigated in chapter 4. Plasmid pSW2NiggCDS2 was hypothesised to be unstable because it contains a *C. trachomatis*-derived backbone and presence of plasmid-free inclusions had been previously observed in cell culture under penicillin selection (Wang et al., 2014). But, as the data showed, the simple presence of plasmid-free inclusions does not itself indicate an unstable plasmid in *C. muridarum*. The hypothesis that this plasmid was unstable was supported, however, by the findings that plasmid copy number decreased by ~2-fold upon removal of selection and that the plasmid loss frequency increased over passage without antibiotic selection. In addition, plasmid-free inclusions were present in the same amount in cultures selected for with penicillin and without selection. Thus, plasmid pSW2NiggCDS2 would not be considered an appropriate vector choice for the backbone of a stable replicating vector for transposon mutagenesis in *C. muridarum*.

Additionally, the stability of plasmid-gene-deletion mutants missing non-essential genes for plasmid maintenance (pNiggCDS56Del and pNiggCDS567Del) were investigated. This was to determine the minimal gene-set that could be adapted to carry the largest gene cassettes without compromising transformation efficiency and plasmid maintenance. Plasmid copy number was

increased ~4-fold for both plasmids compared to the parent plasmid pGFP::Nigg. Where plasmid pNiggCDS56Del exhibited stable maintenance regardless of test conditions with or without positive selection for the plasmid. In contrast, plasmid pNiggCDS567Del that differs to plasmid pNiggCDS56Del only in the absence of *CDS7*, was shown to be inherently unstable without selection. The plasmid copy number increased upon removal of selection for plasmid pNiggCDS56Del whereas it stayed the same for plasmid pNiggCDS567Del. It was therefore hypothesised that the gene product for *CDS7* could have a role in the positive regulation of plasmid copy number and highlights the importance of more sensitive quantitative approaches for determining the role of genes involved in mechanisms of plasmid maintenance in *Chlamydia*. To prove a role for plasmid-gene *CDS7* in control of plasmid copy number would require a repeat of these investigations using the single-gene deletion mutant in pGFP::Nigg.

Plasmid pGFP::Nigg was chosen for the backbone of a stably replicating inducible transposon delivery vector because it exhibited stable maintenance and a potential mechanism for plasmid elimination upon removal of selection. An inducible *Himar1* transposase system under tet promoter control optimised for use in *C. diff* was hypothesised to be functional in *C. muridarum* based upon the evidence that the *Himar1* hyperactive variant of transposase was shown to be functional in *C. muridarum* and that the tet promoter is known to be functional and tightly regulated in *Chlamydia* (LaBrie et al., 2019; Wang et al., 2019; Wickstrum et al., 2013). Therefore, this system was cloned into plasmid pGFP::Nigg to generate plasmid pNiggHimar; a potentially inducible transposon mutagenesis system for *C. muridarum*. Functionality of the antibiotic resistance genes carried on the transposon (*ermB*) and the plasmid backbone (*cat* and *bla*), as well as fluorescent reporter gene expression was confirmed in *E. coli* as well as inducible expression of the wild type transposase. However, transformants carrying pNiggHimar were not recovered in *C. muridarum*. This was consistent with the findings in *C. trachomatis* that also placed both transposon and transposase under tet promoter control on the same vector (Skilton et al., 2021).

Failure to recover transformants in *C. trachomatis* were hypothesised to be the result of weak tet promoter control over transposase expression resulting in premature transposition and loss of the plasmid. The relatively easy recovery of transposition-negative constructs supported this hypothesis, albeit that the corresponding constructs derived from pNiggHimar in this study also failed to be recovered in *C. muridarum*. These suggest that species-specific factors, in addition to a potential issue with regulation over transposase expression, were limiting the ability to recover transformants in *C. muridarum*. These are most likely to be the extremely low copy number (<0.5) that plasmid pGFP::Nigg is maintained in *C. muridarum* in addition to the low transformation efficiency. To improve the chances of recovering the transposition-negative constructs, the backbone of pNiggHimar could be swapped with pNiggCDS56Del, that stably replicated with a

plasmid copy number of ~4 per cell. This copy number is more comparable to those reported in *C. trachomatis* strains (Pickett et al., 2005). Additional changes to improve repression of transposase in the uninduced state using the tet promoter system would be required to facilitate the recovery of a single inducible transposon delivery vector in *C. muridarum*.

A solution to this problem was very recently demonstrated in *C. trachomatis*. The approach incorporated translational control over transposase expression with the addition of a riboswitch resulting in the successful recovery of a single inducible transposon delivery vector and the generation of transposon mutants in *C. trachomatis* (O'Neill et al., 2021). With this system, control over transposition has been demonstrated, in a protocol that induced transposition in mature inclusions at 24 hpi enabling the generation of mutant libraries at scale. The degree of saturation of the genome achieved in this proof of principle study has yet to be determined. Given that this system has been shown to be functional in *C. trachomatis* it is highly likely that the tet promoter with the addition of the riboswitch for control of both transcription and translation would also result in a successful inducible transposon mutagenesis approach with the right vector backbone in *C. muridarum*. Yet, a means to eliminate the vector post transposition is still required for the *C. trachomatis* system. It is possible that chloramphenicol used at bactericidal concentrations and then removed from the growth media could offer a suitable approach for plasmid destabilisation in *C. trachomatis* as well as *C. muridarum*. This would avoid the addition of further exogenous gene components that could interfere with transformation efficiency or plasmid stability.

6.1 Further Work

This project has opened avenues for further work in the field of plasmid biology and genetics in *Chlamydia* research. The development of a robust plasmid stability assay provides a means to investigate mechanisms of plasmid maintenance which includes regulation of copy number control and plasmid replication. To date, very little is known of the mechanisms governing these processes in any species of *Chlamydia*, therefore, this direction of research could yield further insights into the importance of the plasmid, a known virulence factor, in infection and why some strains are prone to plasmid loss *in vitro*, where others are not. Furthermore, this approach has the potential to be adapted for use in other important pathogenic intracellular bacteria, where a standardised means to assess plasmid stability also does not exist.

The discovery that plasmid gene *CDS7* has a putative role in the regulation of plasmid copy number in *C. muridarum* suggests that there may be the potential to alter the plasmid copy number through codon optimisation of this gene. This would be beneficial for any plasmid-based technology in this species that is reliant on maintenance of the plasmid for mutagenesis.

Chapter 6

Additionally, the translated protein product of this gene could be a potential target to destabilise the plasmid with the potential for generating less virulent strains. This would first require the functional characterisation of this protein to determine how its' function may be altered during live infection.

The finding that translational control over the *Himar1* transposase expression alone was not adequate for the recovery of transformants in *C. muridarum* was no surprise, given that the same outcome was observed in *C. trachomatis* in work recently published by this group (O'Neill et al., (2021)). Tighter control over the expression of the *Himar1* transposase with the addition of a riboswitch to improve translational control as well as fine tuning the activity of this enzyme facilitated the recovery of transformants and their expansion over serial passage while maintaining the transposon delivery vector. This facilitated the generation of a transposon mutant library. These findings indicate that a balance between transposase activity and the ability to maintain the vector are critical. In *C. muridarum*, the plasmid copy number is much lower than that of *C. trachomatis*, which in addition to the low transformation efficiency are a further challenge. Therefore, the next logical step to achieving the same in *C. muridarum* would be to test the various forms of the *Himar1* transposase enzyme that have higher levels of activity than the wild type used in this project in the presence of the riboswitch, but also to change the backbone of the vector to increase the plasmid copy number through deletion of the non-essential plasmid genes.

Appendix A qPCR data

A.1 Standard curves

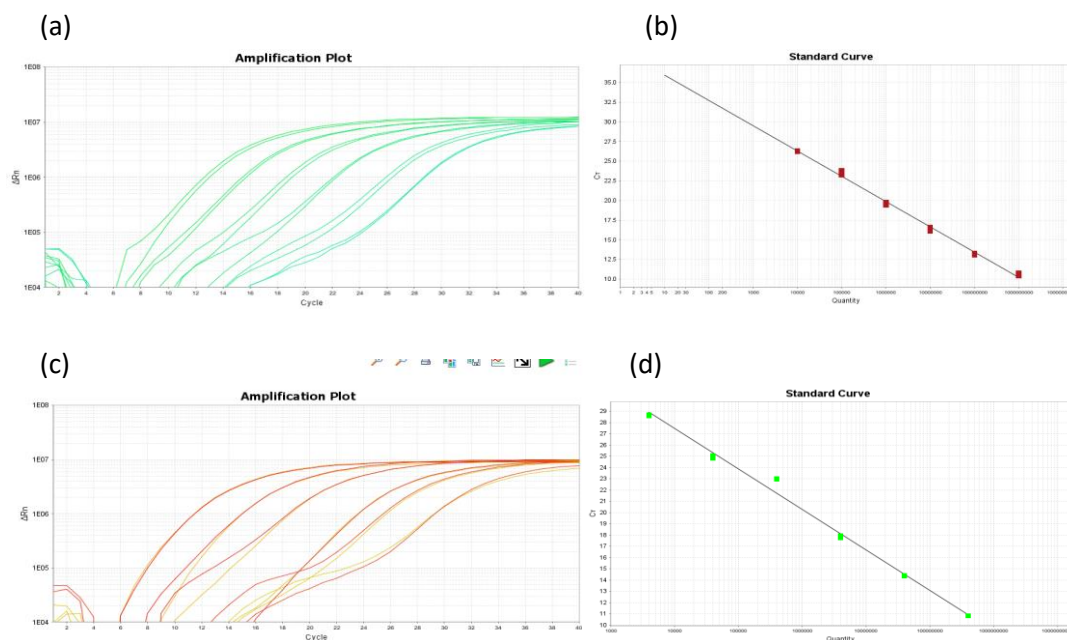


Figure A-1 Amplification plot and standard curve generated for qPCR to quantify copies of plasmids (*CDS2*) and chromosomes (*omcB*) in *C. muridarum* Nigg P+

(a) Amplification plot of *C. muridarum CDS2* (plasmid) assay using the pSW2NiggCDS2 standard. (b) Standard curve derived from (a). (c) Amplification plot of the *C. muridarum omcB* assay using the pSRP1A standard. (d) Standard curve derived from (c) Serial, tenfold dilutions of purified plasmid DNA from 10^{-4} to 10^{-8} were used as template. The amplification plots shown were generated for quantification of plasmids and chromosomes for Nigg P- transformed with shuttle vector pGFP::Nigg grown under penicillin (10Uml^{-1}) for three passages. The quantity of DNA molecules was calculated for samples using the Cq set for standard curves: 0.059 for genomes and 0.131 for plasmids. Standard reactions were performed in duplicate.

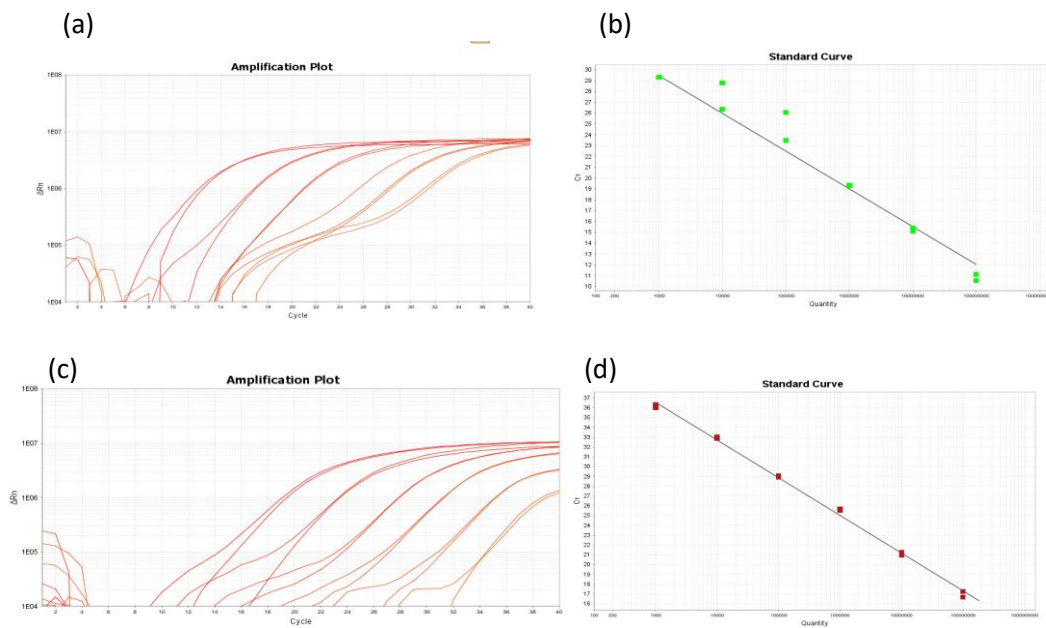


Figure A-2 Amplification plot and standard curve generated for qPCR to quantify copies of plasmids (*CDS2*) and chromosomes (*omcB*) in Nigg P-/pGFP::Nigg

(a) Amplification plot of *C. muridarum CDS2* (plasmid) assay using the pSW2NiggCDS2 standard. (b) Standard curve derived from (a). (c) Amplification plot of the *C. muridarum omcB* assay using the pSRP1A standard. (d) Standard curve derived from (c). Serial, tenfold dilutions of purified plasmid DNA from 10^{-4} to 10^{-8} were used as template. The amplification plots shown were generated for quantification of plasmids and chromosomes for Nigg P- transformed with shuttle vector pGFP::Nigg grown under penicillin (10Uml^{-1}) and without selection for three passages. The quantity of DNA molecules was calculated for samples using the Cq set for standard curves: 0.059 for genomes and 0.131 for plasmids. Standard reactions were performed in duplicate.

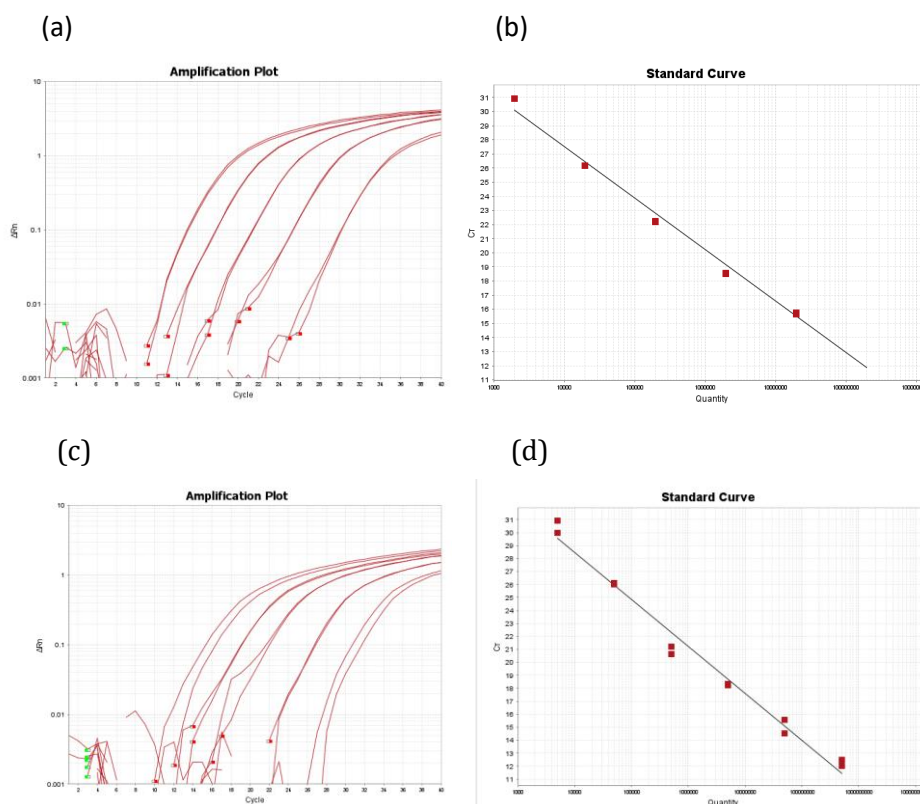


Figure A-3 Amplification plot and standard curve generated for qPCR to quantify copies of plasmids (*CDS2*) and chromosomes (*omcB*) in Nigg P-/pGFP::*Nigg*

(a) Amplification plot of *C. muridarum CDS2* (plasmid) assay using the pSW2NiggCDS2 standard. (b) Standard curve derived from (a). (c) Amplification plot of the *C. muridarum omcB* assay using the pSRP1A standard. (d) Standard curve derived from (c) Serial, tenfold dilutions of purified plasmid DNA from 10^{-4} to 10^{-8} were used as template. The amplification plots shown were generated for quantification of plasmids and chromosomes for Nigg P- transformed with shuttle vector pGFP::*Nigg* grown under chloramphenicol ($0.4\mu\text{gml}^{-1}$), and with penicillin selection (10Uml^{-1}) and without selection. The quantity of DNA molecules was calculated for samples using the Cq set for standard curves: 0.059 for genomes and 0.131 for plasmids. Standard reactions were performed in duplicate.

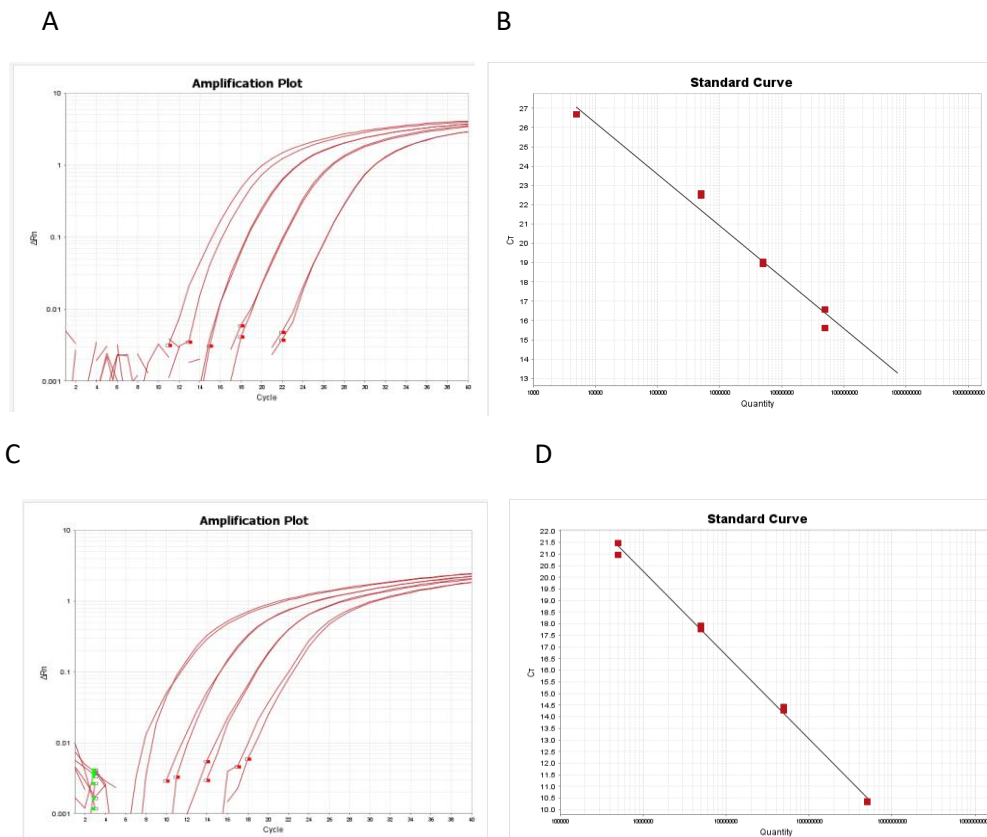


Figure A-4 Amplification plot and standard curve generated for qPCR to quantify copies of plasmids (*CDS2*) and chromosomes (*omcB*) in Nigg P-/pSW2NiggCDS2, Nigg P-/pNiggCDS56Del and Nigg P-/pNiggCDS567Del

(a) Amplification plot of *C. muridarum* *CDS2* (plasmid) assay using the pSW2NiggCDS2 standard. (b) Standard curve derived from (a). (c) Amplification plot of the *C. muridarum* *omcB* assay using the pSRP1A standard. (d) Standard curve derived from (c)

Serial, tenfold dilutions of purified plasmid DNA from 10^{-4} to 10^{-7} were used as template. The amplification plots shown were generated for quantification of plasmids and chromosomes for Nigg P- transformed with shuttle vector pSW2NiggCDS2, and plasmid-gene deletion mutants pNiggCDS56Del and pNiggDS567Del grown under chloramphenicol ($0.4\mu\text{gml}^{-1}$), and with penicillin selection (10Uml^{-1}) and without selection. The quantity of DNA molecules was calculated for samples using the Cq set for standard curves: 0.059 for genomes and 0.131 for plasmids. Standard reactions were performed in duplicate.

Appendix B Project amendment and approval

B.1 Project amendment



AMENDMENT, CESSATION OR TRANSFER OF A PROJECT INVOLVING WORK WITH GENETICALLY MODIFIED ORGANISMS

This form should be used to identify changes to any pre- approved GM project or to notify the GMBSO of a change of PI or closure of the project.

Completed forms must be sent to the University Biological Safety Adviser for submission to the GMBSO.

According to University of Southampton Policy, it is the responsibility of the person directing the research (i.e. the Principal Investigator) to ensure that all these requirements are complied with and that this risk assessment remains valid.

PERSON RESPONSIBLE FOR THIS WORK (THE PRINCIPAL INVESTIGATOR)

| | | |
|-------------------|--------------------|---------------------|
| Name: Ian Clarke | Staff ID: 1133624 | Position: Professor |
| Faculty: Medicine | Academic Unit: CES | |
| Campus: SGH | | |

PROJECT DETAILS

| |
|--|
| Title: The genetic transformation of Chlamydiae |
| Original Approval Date: 6 th August 2010 |
| GMBSO Reference Number (Assigned originally by GMBSO): GMBSO/ see attached application - this was one of the first CL2 applications approved by Dr Stewart Clarke - no number was assigned |

| Current Containment Level | | | Current Activity Classification | | |
|----------------------------|---------------------------------------|----------------------------|---------------------------------|---------------------------------------|----------------------------|
| 1 <input type="checkbox"/> | 2 <input checked="" type="checkbox"/> | 3 <input type="checkbox"/> | 1 <input type="checkbox"/> | 2 <input checked="" type="checkbox"/> | 3 <input type="checkbox"/> |

| Will the changes affect the original Containment Level of the project? | | Will the changes affect the original Activity Classification of the project? | |
|--|--|--|--|
| Yes <input type="checkbox"/> | No <input checked="" type="checkbox"/> | Yes <input type="checkbox"/> | No <input checked="" type="checkbox"/> |

| If yes, what is the new Activity Classification? | | | If 'Yes', what is the new Containment Level? | | |
|--|----------------------------|----------------------------|--|----------------------------|----------------------------|
| 1 <input type="checkbox"/> | 2 <input type="checkbox"/> | 3 <input type="checkbox"/> | 1 <input type="checkbox"/> | 2 <input type="checkbox"/> | 3 <input type="checkbox"/> |

Uncontrolled if printed

1 REVISIONS**Complete all relevant sections****1.1 HEALTH SURVEILLANCE**

1.1.1 *If the class of this project has changed, is Occupational Health advice required?*

| | |
|------------------------------|--|
| Yes <input type="checkbox"/> | No <input checked="" type="checkbox"/> |
|------------------------------|--|

1.1.2 *Do any new personnel to this project need to be incorporated into the Health surveillance programme(s)*

| | |
|------------------------------|--|
| Yes <input type="checkbox"/> | No <input checked="" type="checkbox"/> |
|------------------------------|--|

1.2 SCIENTIFIC CHANGES

1.2.1 *Summarise the proposed changes and state how they differ from the original proposal.*

Be as detailed as possible.

Since conception of the original proposal, successful development of a robust transformation protocol for Chlamydiae has been achieved involving the use of shuttle vectors containing both markers for chloramphenicol and penicillin. This facilitated genetic studies to elucidate the role of the native plasmid in chlamydial infection. Chlamydia muridarum (C. muridarum), the mouse pathogen, serves as a model of urogenital infection with Chlamydia trachomatis (C. trachomatis). Chloramphenicol is a useful antibiotic for selection of transformants in C. muridarum, however, our new work will require a second antibiotic for the selection of transposon mutants. Plasmid stability was poor under penicillin selection (data not published). Consequently penicillin has been excluded as a suitable resistance marker in transformants of C. muridarum. Therefore, alternative markers for selection for use in genetic studies of C. muridarum are needed. Erythromycin (ERY), a macrolide class of antibiotic, has a bacteriostatic mode of action by inhibiting normal ribosomal function. Preliminary work by the group has shown the minimum inhibitory concentration as defined by the lowest concentration of ERY fully inhibiting inclusion formation to be 0.03µg/ml in wild type C. muridarum strain Nigg while displaying low levels of toxicity to McCoy cells in culture thus making it an ideal candidate as a selection marker in this system.

It is our intention to insert the erythromycin resistance gene, erm(B), into a C. muridarum based shuttle vector, cloned from a standard E. coli plasmid vector, for transformation of C. muridarum strains only. C. muridarum is not transmissible to humans and therefore classified as a hazard group 1 microorganism. However, ERY is a second line therapy recommended to treat C. trachomatis in humans, in which there is no known natural resistance. Therefore, as a precaution all work conducted with a C. muridarum strain containing erm(B) including handling and storage will be contained in a separate laboratory (LC73) to where work with C. trachomatis is conducted. This will eliminate any possibility of interactions with a C. trachomatis transforming plasmid vector.

1.2.2 *Identify any new agents or material being introduced to the project.*

| New Host | New Vector | New Insert |
|--------------|---|-------------------------------------|
| C. muridarum | no new vector - all based on the chlamydial plasmid | ermB - erythromycin resistance gene |

1.2.3 *If this change involves the addition of a new animal or plant, please detail this addition.*

This Amendment Form can not be used for the addition of a genetically modified animal host if this is the first use of an animal host in this project. GM Animals Risk Assessment must be completed.

| Species | Parent strain(s) | Genetic Modification | Effect of Modification | Name of GM Animal or Plant <input type="checkbox"/> |
|---------|------------------|----------------------|------------------------|---|
| | | | | |
| | | | | |
| | | | | |

1.3 OTHER CHANGES

Uncontrolled if printed

1.3.1 Change of location

Will this research be conducted solely within University of Southampton managed facilities? If yes, proceed to 1.4.2. If no, please provide details of the non-UoS facility, including location, reciprocation agreements, biosafety management arrangements in place, local codes of practice and contact details of lab manager responsible for the venue.

| | |
|--|-------------------|
| Details of non-UoS venue: Not applicable - research conducted with existing facility | |
| Contact Name: | Contact Position: |
| Contact Telephone: | Contact E-mail: |

1.3.2 Details of University of Southampton venue

| Room(s) | Building | Campus | Person in control of area |
|---------|-------------|--------|---------------------------|
| LC73 | South Block | SGH | Prof Ian Clarke |
| | | | |
| | | | |

1.3.3 Change of Principal Investigator

| Current Principle Investigator | |
|--------------------------------|-----------|
| Name: | Position: |
| Reason for transfer to new PI: | |
| New Principle Investigator | |
| Name: | Position: |

2 CLOSURE OF PROJECT

To be completed by the Principle Investigator responsible for this project.

By ticking this box I confirm that the above project has been closed, all work has ceased and all GM material associated with this project has been destroyed.

| Principle Investigator | |
|------------------------|-----------|
| Name: | Position: |

3 DECLARATION

To be completed by the Principle Investigator responsible for this project.

By ticking this box I confirm that all information contained in this notification meets the requirements of the University's Biological Safety Policy and is correct and up to date.

I also undertake to ensure that no work will be carried out until the original risk assessment has been suitably and sufficiently revised and approved by the GMBSC and that all necessary control measures are in place. Also, I accept that a statutory notification period may be required before work can commence.

Uncontrolled if printed

| Principle Investigator | |
|------------------------|--|
| Name: Ian Clarke | Position: Professor of Virology/Molecular Microbiology |

4 HSE NOTIFICATION

The BSA will inform the PI if the project amendment will require notification to the HSE. All notifications MUST be made by the BSA and MUST NOT be made by the individual Faculties/Academic Units or Principal Investigators. If notification is required the correct forms will be supplied by the BSA once all other approvals have been obtained.

5 TO BE COMPLETED BY THE BSA

Is HSE notification required for any aspect of this project? Such notification must only be carried out by Safety and Occupational Health.

| | |
|------------------------------|-----------------------------|
| Yes <input type="checkbox"/> | No <input type="checkbox"/> |
| Date HSE consent was given: | HSE reference: |

Is DEFRA notification required under SAPO 2008? Such notification must only be carried out by Safety and Occupational Health.

| | |
|-------------------------------|-----------------------------|
| Yes <input type="checkbox"/> | No <input type="checkbox"/> |
| Date DEFRA consent was given: | DEFRA reference: |

Is Home Office notification required under ATCSA 2001? Such notification must only be carried out by Safety and Occupational Health.

| | |
|------------------------------|-----------------------------|
| Yes <input type="checkbox"/> | No <input type="checkbox"/> |
| Date Home Office notified: | |

Date of the GMBSC meeting where this amendment was reviewed

| |
|--|
| |
|--|

Uncontrolled if printed

B.2 Confirmation of approval for amendment

From: [Lockey R.W.](#)
To: [Clarke I.N.](#)
Subject: Amendment GBSC/00FD - The genetic transformation of [Chlamydiae](#)
Date: 11 January 2019 09:16:50

Dear Professor Clarke

The amendment to your project *The genetic transformation of [Chlamydiae](#)* was reviewed at the GBSC Committee meeting on 8/1/19. I am pleased to inform you that this has been approved. Please keep a copy of this email for your records.

Thank [you](#)

[Richard](#)

[Richard Lockey](#)
Biological Safety Adviser
Health, Safety and Risk Directorate
University of Southampton
26 University Road,
Highfield Campus
Southampton, SO17 1BJ
Tel: +44 (0)23 8059 6850
[Mob:+44 \(0\)7785451952](#)

List of References

- Abdelsamed, H., Peters, J., Byrne, G.I., 2013. Genetic variation in *Chlamydia trachomatis* and their hosts: Impact on disease severity and tissue tropism. *Future Microbiol.*
<https://doi.org/10.2217/fmb.13.80>
- Agaisse, H., Derré, I., 2013. A *C. trachomatis* Cloning Vector and the Generation of *C. trachomatis* Strains Expressing Fluorescent Proteins under the Control of a *C. trachomatis* Promoter. *PLoS One* 8, e57090. <https://doi.org/10.1371/journal.pone.0057090>
- Alagumaruthanayagam, A., Pavankumar, A.R., Vasanthamallika, T.K., Sankaran, K., 2009. Evaluation of solid (disc diffusion)- and liquid (turbidity)-phase antibiogram methods for clinical isolates of diarrheagenic *E. coli* and correlation with efflux. *J. Antibiot. (Tokyo)*. 62, 377–384. <https://doi.org/10.1038/ja.2009.45>
- Alberts, B., Johnson, A., Lewis, J., Raff, M., Roberts, K., Walter, P., 2002. *How Genetic Switches Work.*
- An, Q., Radcliffe, G., Vassallo, R., Buxton, D., O'Brien, W.J., Pelletier, D.A., Weisburg, W.G., Klinger, J.D., Olive, D.M., 1992. Infection with a plasmid-free variant chlamydia related to *Chlamydia trachomatis* identified by using multiple assays for nucleic acid detection. *J. Clin. Microbiol.* 30, 2814–2821. <https://doi.org/10.1128/jcm.30.11.2814-2821.1992>
- Andremont, A., Gerbaud, G., Courvalin, P., 1986. Plasmid-Mediated High-Level Resistance to Erythromycin in *Escherichia coli*, *ANTIMICROBIAL AGENTS AND CHEMOTHERAPY.*
- Barquist, L., Boinett, C.J., Cain, A.K., 2013. Approaches to querying bacterial genomes with transposon-insertion sequencing. *RNA Biol.* 10, 1161–9. <https://doi.org/10.4161/rna.24765>
- Barron, A.L., White, H.J., Rank, R.G., Soloff, B.L., Moses, E.B., 1981. A New Animal Model for the Study of *Chlamydia trachomatis* Genital Infections: Infection of Mice with the Agent of Mouse Pneumonitis. *J. Infect. Dis.* 143, 63–66. <https://doi.org/10.1093/infdis/143.1.63>
- Bastidas, R.J., Valdivia, R.H., 2016. Emancipating *Chlamydia*: Advances in the Genetic Manipulation of a Recalcitrant Intracellular Pathogen. *Microbiol. Mol. Biol. Rev.* 80, 411–27. <https://doi.org/10.1128/MMBR.00071-15>
- Bauler, L.D., Hackstadt, T., 2014. Expression and Targeting of secreted proteins from *Chlamydia trachomatis*. *J. Bacteriol.* 196, 1325–1334. <https://doi.org/10.1128/JB.01290-13>
- Beare, P.A., Howe, D., Cockrell, D.C., Omsland, A., Hansen, B., Heinzen, R.A., 2009.

List of References

- Characterization of a *Coxiella burnetii* ftsZ mutant generated by Himar1 transposon mutagenesis. *J. Bacteriol.* 191, 1369–1381. <https://doi.org/10.1128/JB.01580-08>
- Belland, R.J., Zhong, G., Crane, D.D., Hogan, D., Sturdevant, D., Sharma, J., Beatty, W.L., Caldwell, H.D., 2003. Genomic transcriptional profiling of the developmental cycle of *Chlamydia trachomatis*. *Proc. Natl. Acad. Sci. U. S. A.* 100, 8478–83. <https://doi.org/10.1073/pnas.1331135100>
- Black, L.A., Higgins, D.P., Govendir, M., 2015. In vitro activity of chloramphenicol, florfenicol and enrofloxacin against *Chlamydia pecorum* isolated from koalas (*Phascolarctos cinereus*). *Aust. Vet. J.* 93, 420–423. <https://doi.org/10.1111/AVJ.12364>
- Bouuaert, C.C., Tellier, M., Chalmers, R., 2014. One to rule them all. *Mob. Genet. Elements* 4, e28807. <https://doi.org/10.4161/mge.28807>
- Brantl, S., 2015. Antisense-RNA mediated control of plasmid replication - pIP501 revisited. *Plasmid* 78, 4–16. <https://doi.org/10.1016/j.plasmid.2014.07.004>
- Brantl, S., 2014. Plasmid Replication Control by Antisense RNAs. *Microbiol. Spectr.* 2. <https://doi.org/10.1128/microbiolspec.plas-0001-2013>
- Brantl, S., 2002. Antisense RNAs in plasmids: control of replication and maintenance. *Plasmid* 48, 165–173. [https://doi.org/10.1016/S0147-619X\(02\)00108-7](https://doi.org/10.1016/S0147-619X(02)00108-7)
- Brunham, R.C., Rey-Ladino, J., 2005. Immunology of *Chlamydia* infection: Implications for a *Chlamydia trachomatis* vaccine. *Nat. Rev. Immunol.* <https://doi.org/10.1038/nri1551>
- Cain, A.K., Barquist, L., Goodman, A.L., Paulsen, I.T., Parkhill, J., van Opijnen, T., 2020. A decade of advances in transposon-insertion sequencing. *Nat. Rev. Genet.* <https://doi.org/10.1038/s41576-020-0244-x>
- Campbell, J., Huang, Y., Liu, Y., Schenken, R., Arulanandam, B., Zhong, G., 2014. Bioluminescence Imaging of *Chlamydia muridarum* Ascending Infection in Mice. *PLoS One* 9. <https://doi.org/10.1371/journal.pone.0101634>
- Carpenter, V., Chen, Y.-S., Dolat, L., Valdivia, R.H., 2017. The Effector TepP Mediates Recruitment and Activation of Phosphoinositide 3-Kinase on Early *Chlamydia trachomatis* Vacuoles. *mSphere* 2. <https://doi.org/10.1128/msphere.00207-17>
- Ceovic, R., Jerkovic Gulin, S., 2015. Lymphogranuloma venereum: diagnostic and treatment challenges. *Infect. Drug Resist.* 8, 39. <https://doi.org/10.2147/IDR.S57540>
- Cheng, C., Nair, A.D.S., Indukuri, V. V, Gong, S., Felsheim, R.F., Jaworski, D., Munderloh, U.G.,

- Ganta, R.R., 2013. Targeted and random mutagenesis of *Ehrlichia chaffeensis* for the identification of genes required for in vivo infection. *PLoS Pathog.* 9, e1003171. <https://doi.org/10.1371/journal.ppat.1003171>
- Choudhary, E., Thakur, P., Pareek, M., Agarwal, N., 2015. Gene silencing by CRISPR interference in mycobacteria. *Nat. Commun.* 6, 1–11. <https://doi.org/10.1038/ncomms7267>
- Claeys Bouuaert, C., Chalmers, R., 2017. A single active site in the mariner transposase cleaves DNA strands of opposite polarity. *Nucleic Acids Res.* 45, 11467–11478. <https://doi.org/10.1093/nar/gkx826>
- Clewell, D.B., 1972. Nature of Col E1 Plasmid Replication in *Escherichia coli* in the Presence of Chloramphenicol. *J. Bacteriol.* 110, 667. <https://doi.org/10.1128/jb.110.2.667-676.1972>
- Cohen, S.N., Chang, A.C., Hsu, L., 1972. Nonchromosomal antibiotic resistance in bacteria: genetic transformation of *Escherichia coli* by R-factor DNA. *Proc. Natl. Acad. Sci. U. S. A.* 69, 2110–2114. <https://doi.org/10.1073/pnas.69.8.2110>
- Collingro, A., Tischler, P., Weinmaier, T., Penz, T., Heinz, E., Brunham, R.C., Read, T.D., Bavoil, P.M., Sachse, K., Kahane, S., Friedman, M.G., Rattei, T., Myers, G.S.A., Horn, M., 2011. Unity in variety-the pan-genome of the chlamydiae. *Mol. Biol. Evol.* 28, 3253–3270. <https://doi.org/10.1093/molbev/msr161>
- Cortina, M.E., Ende, R.J., Bishop, R.C., Bayne, C., Derré, I., 2019. *Chlamydia trachomatis* and *Chlamydia muridarum* spectinomycin resistant vectors and a transcriptional fluorescent reporter to monitor conversion from replicative to infectious bacteria. *PLoS One* 14, e0217753. <https://doi.org/10.1371/journal.pone.0217753>
- Dejesus, M.A., Gerrick, E.R., Xu, W., Park, S.W., Long, J.E., Boutte, C.C., Rubin, E.J., Schnappinger, D., Ehrst, S., Fortune, S.M., Sassetti, C.M., Ioerger, T.R., 2017. Comprehensive essentiality analysis of the *Mycobacterium tuberculosis* genome via saturating transposon mutagenesis. *MBio* 8. <https://doi.org/10.1128/mBio.02133-16>
- Dell'anno, A., Fabiano, M., Duineveld, G.C.A., Kok, A., Danovaro, R., 1998. Nucleic Acid (DNA, RNA) Quantification and RNA/DNA Ratio Determination in Marine Sediments: Comparison of Spectrophotometric, Fluorometric, and HighPerformance Liquid Chromatography Methods and Estimation of Detrital DNA. *Appl. Environ. Microbiol.* 64, 3238. <https://doi.org/10.1128/aem.64.9.3238-3245.1998>
- Dembek, M., Barquist, L., Boinett, C.J., Cain, A.K., Mayo, M., Lawley, T.D., Fairweather, N.F., Fagan, R.P., 2015. High-throughput analysis of gene essentiality and sporulation in

List of References

- Clostridium difficile*. MBio 6. <https://doi.org/10.1128/mBio.02383-14>
- Desjardins, M., Delgaty, K.L., Ramotar, K., Seetaram, C., Toye, B., 2004. Prevalence and Mechanisms of Erythromycin Resistance in Group A and Group B Streptococcus: Implications for Reporting Susceptibility Results. *J. Clin. Microbiol.* 42, 5620. <https://doi.org/10.1128/JCM.42.12.5620-5623.2004>
- Detels, R., Green, A.M., Klausner, J.D., Katzenstein, D., Gaydos, C., Handsfield, H.H., Pequegnat, W., Mayer, K., Hartwell, T.D., Quinn, T.C., 2011. The incidence and correlates of symptomatic and asymptomatic chlamydia trachomatis and neisseria gonorrhoeae infections in selected populations in five countries. *Sex. Transm. Dis.* 38, 503–509. <https://doi.org/10.1097/OLQ.0b013e318206c288>
- Elwell, C., Mirrashidi, K., Engel, J., 2016. Chlamydia cell biology and pathogenesis. *Nat. Rev. Microbiol.* 14, 385–400. <https://doi.org/10.1038/nrmicro.2016.30>
- Everett, K.D.E., Bush, R.M., Andersen, A.A., 1999. Emended description of the order Chlamydiales, proposal of Parachlamydiaceae fam. nov. and Simkaniaceae fam. nov., each containing one monotypic genus, revised taxonomy of the family Chlamydiaceae, including a new genus and five new species, and standards for the identification of organisms. *Int. J. Syst. Bacteriol.* 49, 415–440. <https://doi.org/10.1099/00207713-49-2-415>
- Felsheim, R.F., Herron, M.J., Nelson, C.M., Burkhardt, N.Y., Barbet, A.F., Kurtti, T.J., Munderloh, U.G., 2006. Transformation of *Anaplasma phagocytophilum*. *BMC Biotechnol.* 6, 42. <https://doi.org/10.1186/1472-6750-6-42>
- Ferreira, R., Borges, V., Nunes, A., Borrego, M.J., Gomes, J.P., 2013. Assessment of the load and transcriptional dynamics of *Chlamydia trachomatis* plasmid according to strains' tissue tropism. *Microbiol. Res.* 168, 333–339. <https://doi.org/10.1016/J.MICRES.2013.02.001>
- Fields, K.A., Fischer, E.R., Mead, D.J., Hackstadt, T., 2005. Analysis of putative *Chlamydia trachomatis* chaperones Scc2 and Scc3 and their use in the identification of type III secretion substrates. *J. Bacteriol.* 187, 6466–6478. <https://doi.org/10.1128/JB.187.18.6466-6478.2005>
- Fields, K.A., Hackstadt, T., 2002. THE CHLAMYDIAL INCLUSION: Escape from the Endocytic Pathway 1. *Annu. Rev. Cell Dev. Biol.* 18, 221–45. <https://doi.org/10.1146/annurev.cellbio.18.012502.105845>
- Fischer, A., Harrison, K.S., Ramirez, Y., Auer, D., Chowdhury, S.R., Prusty, B.K., Sauer, F., Dimond, Z., Kisker, C., Hefty, P.S., Rudel, T., 2017. *Chlamydia trachomatis*-containing vacuole serves as deubiquitination platform to stabilize Mcl-1 and to interfere with host defense. *Elife* 6.

<https://doi.org/10.7554/eLife.21465>

- Fox, J.G., Davisson, M.T., Quimby, F.W., Barthold, S.W., Newcomer, C.E., Smith, A.L., 2006. The Mouse in Biomedical Research , 2 nd Edition, Vol.II Diseases 776.
- Gaydos, C.A., Quinn, T.C., Willis, D., Weissfeld, A., Hook, E.W., Martin, D.H., Ferrero, D. V, Schachter, J., 2003. Performance of the APTIMA Combo 2 assay for detection of Chlamydia trachomatis and Neisseria gonorrhoeae in female urine and endocervical swab specimens. *J. Clin. Microbiol.* 41, 304–9.
- Geelen, T.H., Rossen, J.W., Beerens, A.M., Poort, L., Morr e, S.A., Ritmeester, W.S., Van Kruchten, H.E., Van De Pas, M.M., Savelkoul, P.H.M., 2013. Performance of cobas[®] 4800 and m2000 real-time[™] assays for detection of Chlamydia trachomatis and Neisseria gonorrhoeae in rectal and self-collected vaginal specimen. *Diagn. Microbiol. Infect. Dis.* 77, 101–105. <https://doi.org/10.1016/j.diagmicrobio.2013.06.020>
- Geisler, W.M., Suchland, R.J., Whittington, W.L.H., Stamm, W.E., 2003. The relationship of serovar to clinical manifestations of urogenital Chlamydia trachomatis infection. *Sex. Transm. Dis.* 30, 160–165. <https://doi.org/10.1097/00007435-200302000-00013>
- Ghosh, S., Ruelke, E.A., Ferrell, J.C., Bodero, M.D., Fields, K.A., Jewett, T.J., 2020. Fluorescence-Reported Allelic Exchange Mutagenesis-Mediated Gene Deletion Indicates a Requirement for Chlamydia trachomatis Tarp during In Vivo Infectivity and Reveals a Specific Role for the C Terminus during Cellular Invasion . *Infect. Immun.* 88. <https://doi.org/10.1128/iai.00841-19>
- Giraldo, R., Fern andez-Tresguerres, M.E., 2004. Twenty years of the pPS10 replicon: Insights on the molecular mechanism for the activation of DNA replication in iteron-containing bacterial plasmids. *Plasmid.* <https://doi.org/10.1016/j.plasmid.2004.06.002>
- Gondek, D.C., Olive, A.J., Stary, G., Starnbach, M.N., 2012. CD4 + T Cells Are Necessary and Sufficient To Confer Protection against Chlamydia trachomatis Infection in the Murine Upper Genital Tract . *J. Immunol.* 189, 2441–2449. <https://doi.org/10.4049/jimmunol.1103032>
- Gong, S., Yang, Z., Lei, L., Shen, L., Zhong, G., 2013. Characterization of Chlamydia trachomatis plasmid-encoded open reading frames. *J. Bacteriol.* 195, 3819–26. <https://doi.org/10.1128/JB.00511-13>
- Goryshin, I.Y., Reznikoff, W.S., 1998. Tn5 in vitro transposition. *J. Biol. Chem.* 273, 7367–7374. <https://doi.org/10.1074/jbc.273.13.7367>
- Hackstadt, T., Rockey, D.D., Heinzen, R.A., Scidmore, M.A., 1996. Chlamydia trachomatis

List of References

- interrupts an exocytic pathway to acquire endogenously synthesized sphingomyelin in transit from the Golgi apparatus to the plasma membrane. *EMBO J.* 15, 964–977.
<https://doi.org/10.1002/j.1460-2075.1996.tb00433.x>
- Hackstadt, T., Scidmore-Carlson, M.A., Shaw, E.I., Fischer, E.R., 1999. The Chlamydia trachomatis IncA protein is required for homotypic vesicle fusion. *Cell. Microbiol.* 1, 119–130.
<https://doi.org/10.1046/j.1462-5822.1999.00012.x>
- Han, Y., Derré, I., 2017. A Co-infection Model System and the Use of Chimeric Proteins to Study Chlamydia Inclusion Proteins Interaction. *Front. Cell. Infect. Microbiol.* 7, 79.
<https://doi.org/10.3389/fcimb.2017.00079>
- Harding-Esch, E.M., Cousins, E.C., Chow, S.L.C., Phillips, L.T., Hall, C.L., Cooper, N., Fuller, S.S., Nori, A. V., Patel, R., Thomas-William, S., Whitlock, G., Edwards, S.J.E., Green, M., Clarkson, J., Arlett, B., Dunbar, J.K., Lowndes, C.M., Sadiq, S.T., 2018. A 30-Min Nucleic Acid Amplification Point-of-Care Test for Genital Chlamydia trachomatis Infection in Women: A Prospective, Multi-center Study of Diagnostic Accuracy. *EBioMedicine* 28, 120–127.
<https://doi.org/10.1016/j.ebiom.2017.12.029>
- Harding-Esch, E.M., Holland, M.J., Schémann, J.F., Sillah, A., Sarr, B., Christerson, L., Pickering, H., Molina-Gonzalez, S., Sarr, I., Andreasen, A.A., Jeffries, D., Grundy, C., Mabey, D.C.W., Herrmann, B., Bailey, R.L., 2019. Impact of a single round of mass drug administration with azithromycin on active trachoma and ocular Chlamydia trachomatis prevalence and circulating strains in the Gambia and Senegal. *Parasites and Vectors* 12.
<https://doi.org/10.1186/s13071-019-3743-x>
- Harris, S.R., Clarke, I.N., Seth-Smith, H.M.B., Solomon, A.W., Cutcliffe, L.T., Marsh, P., Skilton, R.J., Holland, M.J., Mabey, D., Peeling, R.W., Lewis, D.A., Spratt, B.G., Unemo, M., Persson, K., Bjartling, C., Brunham, R., Vries, H.J.C. de, Morré, S.A., Speksnijder, A., Bébéar, C.M., Clerc, M., Barbeyrac, B. de, Parkhill, J., Thomson, N.R., 2012. Whole genome analysis of diverse Chlamydia trachomatis strains identifies phylogenetic relationships masked by current clinical typing. *Nat. Genet.* 44, 413. <https://doi.org/10.1038/NG.2214>
- Hatt, C., Ward, M.E., Clarke, I.N., 1988. Analysis of the entire nucleotide sequence of the cryptic plasmid of Chlamydia trachomatis serovar L1. Evidence for involvement in DNA replication. *Nucleic Acids Res.* 16, 4053–67. <https://doi.org/10.1093/nar/16.9.4053>
- Hayes, F., 2003. Transposon-Based Strategies for Microbial Functional Genomics and Proteomics. *Annu. Rev. Genet.* <https://doi.org/10.1146/annurev.genet.37.110801.142807>
- Heap, J.T., Pennington, O.J., Cartman, S.T., Minton, N.P., 2009. A modular system for Clostridium

- shuttle plasmids. *J. Microbiol. Methods* 78, 79–85.
<https://doi.org/10.1016/J.MIMET.2009.05.004>
- Hoffman, L.M., Jendrisak, J.J., Meis, R.J., Goryshin, I.Y., Reznikoff, W.S., 2000. Transposome insertional mutagenesis and direct sequencing of microbial genomes, *Genetica*.
- Huang, Y., Zhang, Q., Yang, Z., Conrad, T., Liu, Y., Zhong, G., 2015. Plasmid-encoded Pgp5 is a significant contributor to *Chlamydia muridarum* induction of hydrosalpinx. *PLoS One*.
<https://doi.org/10.1371/journal.pone.0124840>
- Hybiske, K., Stephens, R.S., 2007. Mechanisms of host cell exit by the intracellular bacterium *Chlamydia*. *Proc. Natl. Acad. Sci. U. S. A.* 104, 11430–11435.
<https://doi.org/10.1073/pnas.0703218104>
- Illingworth, M., Hooppaw, A.J., Ruan, L., Fisher, D.J., Chen, L., 2017. Biochemical and genetic analysis of the *Chlamydia* GroEL chaperonins. *J. Bacteriol.* 199.
<https://doi.org/10.1128/JB.00844-16>
- Jahn, M., Vorpahl, C., Türkowsky, D., Lindmeyer, M., Bühler, B., Harms, H., Müller, S., 2014. Accurate determination of plasmid copy number of flow-sorted cells using droplet digital PCR. *Anal. Chem.* 86, 5969–5976.
https://doi.org/10.1021/AC501118V/SUPPL_FILE/AC501118V_SI_005.PDF
- Jeffrey, B.M., Suchland, R.J., Quinn, K.L., Davidson, J.R., Stamm, W.E., Rockey, D.D., 2010. Genome Sequencing of Recent Clinical *Chlamydia trachomatis* Strains Identifies Loci Associated with Tissue Tropism and Regions of Apparent Recombination. *Infect. Immun.* 78, 2544–2553.
<https://doi.org/10.1128/IAI.01324-09>
- Johnson, C.M., Fisher, D.J., 2013. Site-Specific, Insertional Inactivation of *incA* in *Chlamydia trachomatis* Using a Group II Intron. *PLoS One* 8, 83989.
<https://doi.org/10.1371/journal.pone.0083989>
- Jones, C.A., Hadfield, J., Thomson, N.R., Cleary, D.W., Marsh, P., Clarke, I.N., O’neill, C.E., 2020. The nature and extent of plasmid variation in *chlamydia trachomatis*. *Microorganisms* 8.
<https://doi.org/10.3390/microorganisms8030373>
- K, R., AM, G., E, T., S, H., JH, N., SG, M., L, K., RP, M., DE, N., 2015. Mutational Analysis of the *Chlamydia muridarum* Plasticity Zone. *Infect. Immun.* 83, 2870–2881.
<https://doi.org/10.1128/IAI.00106-15>
- Kannan, R.M., Gérard, H.C., Mishra, M.K., Mao, G., Wang, S., Hali, M., Whittum-Hudson, J.A., Hudson, A.P., 2013. Dendrimer-enabled transformation of *Chlamydia trachomatis*. *Microb.*

List of References

- Pathog. 65, 29–35. <https://doi.org/10.1016/j.micpath.2013.08.003>
- Kari, L., Goheen, M.M., Randall, L.B., Taylor, L.D., Carlson, J.H., Whitmire, W.M., Virok, D., Rajaram, K., Endresz, V., McClarty, G., Nelson, D.E., Caldwell, H.D., 2011. Generation of targeted *Chlamydia trachomatis* null mutants. *Proc. Natl. Acad. Sci. U. S. A.* 108, 7189–93. <https://doi.org/10.1073/pnas.1102229108>
- Kari, L., Southern, T.R., Downey, C.J., Watkins, H.S., Randall, L.B., Taylor, L.D., Sturdevant, G.L., Whitmire, W.M., Caldwell, H.D., 2014. *Chlamydia trachomatis* polymorphic membrane protein D is a virulence factor involved in early host-cell interactions. *Infect. Immun.* 82, 2756–2762. <https://doi.org/10.1128/IAI.01686-14>
- Karn, J., Brenner, S., Barnett, L., Cesareni, G., 1980. Novel bacteriophage X cloning vector (genome coverage/spi phenotype/in vitro packaging/unc-54 gene) 77, 5172.
- Keb, G., Fields, K.A., 2019. Markerless gene deletion by floxed cassette allelic exchange mutagenesis in *Chlamydia trachomatis*. *J. Vis. Exp.* 2020. <https://doi.org/10.3791/60848>
- Keb, G., Hayman, R., Fields, K.A., 2018. Floxed-Cassette Allelic Exchange Mutagenesis Enables Markerless Gene Deletion in *Chlamydia trachomatis* and Can Reverse Cassette-Induced Polar Effects. *J. Bacteriol.* 200. <https://doi.org/10.1128/JB.00479-18>
- Kokes, M., Dunn, J.D., Granek, J.A., Nguyen, B.D., Barker, J.R., Valdivia, R.H., Bastidas, R.J., 2015. Integrating chemical mutagenesis and whole-genome sequencing as a platform for forward and reverse genetic analysis of *Chlamydia*. *Cell Host Microbe* 17, 716–25. <https://doi.org/10.1016/j.chom.2015.03.014>
- LaBrie, S.D., Dimond, Z.E., Harrison, K.S., Baid, S., Wickstrum, J., Suchland, R.J., Hefty, P.S., 2019. Transposon Mutagenesis in *Chlamydia trachomatis* Identifies CT339 as a ComEC Homolog Important for DNA Uptake and Lateral Gene Transfer. *MBio* 10, e01343-19. <https://doi.org/10.1128/MBIO.01343-19>
- Lambowitz, A.M., Zimmerly, S., 2004. Mobile Group II Introns. *Annu. Rev. Genet.* 38, 1–35. <https://doi.org/10.1146/annurev.genet.38.072902.091600>
- Lampe, D.J., Akerley, B.J., Rubin, E.J., Mekalanos, J.J., Robertson, H.M., 1999. Hyperactive transposase mutants of the Himar1 mariner transposon, *Genetics*.
- Lampe, D.J., Churchill, M.E., Robertson, H.M., 1996. A purified mariner transposase is sufficient to mediate transposition in vitro. *EMBO J.* 15, 5470–9.
- Lander, E.S., Linton, L.M., Birren, B., Nusbaum, C., Zody, M.C., Baldwin, J., Devon, K., Dewar, K.,

Doyle, M., FitzHugh, W., Funke, R., Gage, D., Harris, K., Heaford, A., Howland, J., Kann, L., Lehoczy, J., LeVine, R., McEwan, P., McKernan, K., Meldrim, J., Mesirov, J.P., Miranda, C., Morris, W., Naylor, J., Raymond, Christina, Rosetti, M., Santos, R., Sheridan, A., Sougnez, C., Stange-Thomann, N., Stojanovic, N., Subramanian, A., Wyman, D., Rogers, J., Sulston, J., Ainscough, R., Beck, S., Bentley, D., Burton, J., Clee, C., Carter, N., Coulson, A., Deadman, R., Deloukas, P., Dunham, A., Dunham, I., Durbin, R., French, L., Grafham, D., Gregory, S., Hubbard, T., Humphray, S., Hunt, A., Jones, M., Lloyd, C., McMurray, A., Matthews, L., Mercer, S., Milne, S., Mullikin, J.C., Mungall, A., Plumb, R., Ross, M., Shownkeen, R., Sims, S., Waterston, R.H., Wilson, R.K., Hillier, L.W., McPherson, J.D., Marra, M.A., Mardis, E.R., Fulton, L.A., Chinwalla, A.T., Pepin, K.H., Gish, W.R., Chissoe, S.L., Wendl, M.C., Delehaunty, K.D., Miner, T.L., Delehaunty, A., Kramer, J.B., Cook, L.L., Fulton, R.S., Johnson, D.L., Minx, P.J., Clifton, S.W., Hawkins, T., Branscomb, E., Predki, P., Richardson, P., Wenning, S., Slezak, T., Doggett, N., Cheng, J.-F., Olsen, A., Lucas, S., Elkin, C., Uberbacher, E., Frazier, M., Gibbs, R.A., Muzny, D.M., Scherer, S.E., Bouck, J.B., Sodergren, E.J., Worley, K.C., Rives, C.M., Gorrell, J.H., Metzker, M.L., Naylor, S.L., Kucherlapati, R.S., Nelson, D.L., Weinstock, G.M., Sakaki, Y., Fujiyama, A., Hattori, M., Yada, T., Toyoda, A., Itoh, T., Kawagoe, C., Watanabe, H., Totoki, Y., Taylor, T., Weissenbach, J., Heilig, R., Saurin, W., Artiguenave, F., Brottier, P., Bruls, T., Pelletier, E., Robert, C., Wincker, P., Rosenthal, A., Platzer, M., Nyakatura, G., Taudien, S., Rump, A., Smith, D.R., Doucette-Stamm, L., Rubenfield, M., Weinstock, K., Lee, H.M., Dubois, J., Yang, H., Yu, J., Wang, J., Huang, G., Gu, J., Hood, L., Rowen, L., Madan, A., Qin, S., Davis, R.W., Federspiel, N.A., Abola, A.P., Proctor, M.J., Roe, B.A., Chen, F., Pan, H., Ramser, J., Lehrach, H., Reinhardt, R., McCombie, W.R., de la Bastide, M., Dedhia, N., Blöcker, H., Hornischer, K., Nordsiek, G., Agarwala, R., Aravind, L., Bailey, J.A., Bateman, A., Batzoglu, S., Birney, E., Bork, P., Brown, D.G., Burge, C.B., Cerutti, L., Chen, H.-C., Church, D., Clamp, M., Copley, R.R., Doerks, T., Eddy, S.R., Eichler, E.E., Furey, T.S., Galagan, J., Gilbert, J.G.R., Harmon, C., Hayashizaki, Y., Haussler, D., Hermjakob, H., Hokamp, K., Jang, W., Johnson, L.S., Jones, T.A., Kasif, S., Kasprzyk, A., Kennedy, S., Kent, W.J., Kitts, P., Koonin, E. V., Korf, I., Kulp, D., Lancet, D., Lowe, T.M., McLysaght, A., Mikkelsen, T., Moran, J. V., Mulder, N., Pollara, V.J., Ponting, C.P., Schuler, G., Schultz, J., Slater, G., Smit, A.F.A., Stupka, E., Szustakowki, J., Thierry-Mieg, D., Thierry-Mieg, J., Wagner, L., Wallis, J., Wheeler, R., Williams, A., Wolf, Y.I., Wolfe, K.H., Yang, S.-P., Yeh, R.-F., Collins, F., Guyer, M.S., Peterson, J., Felsenfeld, A., Wetterstrand, K.A., Myers, R.M., Schmutz, J., Dickson, M., Grimwood, J., Cox, D.R., Olson, M. V., Kaul, R., Raymond, Christopher, Shimizu, N., Kawasaki, K., Minoshima, S., Evans, G.A., Athanasiou, M., Schultz, R., Patrinos, A., Morgan, M.J., 2001. Initial sequencing and analysis of the human genome. *Nature* 409, 860–921. <https://doi.org/10.1038/35057062>

List of References

- Langridge, G.C., Phan, M.-D., Turner, D.J., Perkins, T.T., Parts, L., Haase, J., Charles, I., Maskell, D.J., Peters, S.E., Dougan, G., Wain, J., Parkhill, J., Turner, A.K., 2009. Simultaneous assay of every *Salmonella Typhi* gene using one million transposon mutants. *Genome Res.* 19, 2308–16. <https://doi.org/10.1101/gr.097097.109>
- Lanham, Stuart, Herbert, A., Basarab, A., Watt, P., 2001. Detection of Cervical Infections in Colposcopy Clinic Patients. *J. Clin. Microbiol.* 39, 2946. <https://doi.org/10.1128/JCM.39.8.2946-2950.2001>
- Lanham, S., Herbert, A., Watt, P., 2001. HPV detection and measurement of HPV-16, telomerase, and survivin transcripts in colposcopy clinic patients. *J. Clin. Pathol.* 54, 304–308. <https://doi.org/10.1136/JCP.54.4.304>
- Last, A.R., Roberts, C.H., Cassama, E., Nabicassa, M., Molina-Gonzalez, S., Burr, S.E., Mabey, D.C.W., Bailey, R.L., Holland, M.J., 2014. Plasmid copy number and disease severity in naturally occurring ocular chlamydia trachomatis infection. *J. Clin. Microbiol.* 52, 324–327. <https://doi.org/10.1128/JCM.02618-13>
- Lau, B.T.C., Malkus, P., Paulsson, J., 2013. New quantitative methods for measuring plasmid loss rates reveal unexpected stability. *Plasmid* 70, 353. <https://doi.org/10.1016/J.PLASMID.2013.07.007>
- Li, C.-H., Cheng, Y.-W., Liao, P.-L., Yang, Y.-T., Kang, J.-J., 2010. Chloramphenicol causes mitochondrial stress, decreases ATP biosynthesis, induces matrix metalloproteinase-13 expression, and solid-tumor cell invasion. *Toxicol. Sci.* 116, 140–50. <https://doi.org/10.1093/toxsci/kfq085>
- Li, X.-Z., Plésiat, P., Nikaido, H., 2015. The challenge of efflux-mediated antibiotic resistance in Gram-negative bacteria. *Clin. Microbiol. Rev.* 28, 337–418. <https://doi.org/10.1128/CMR.00117-14>
- Li, Z., Chen, D., Zhong, Y., Wang, S., Zhong, G., 2008. The chlamydial plasmid-encoded protein *pgp3* is secreted into the cytosol of *Chlamydia*-infected cells. *Infect. Immun.* 76, 3415–28. <https://doi.org/10.1128/IAI.01377-07>
- Liu, Y., Chen, C., Gong, S., Hou, S., Qi, M., Liu, Q., Baseman, J., Zhong, G., 2014a. Transformation of *Chlamydia muridarum* reveals a role for *Pgp5* in suppression of plasmid-dependent gene expression. *J. Bacteriol.* 196, 989–98. <https://doi.org/10.1128/JB.01161-13>
- Liu, Y., Huang, Y., Yang, Z., Sun, Y., Gong, S., Hou, S., Chen, C., Li, Z., Liu, Q., Wu, Y., Baseman, J., Zhong, G., 2014b. Plasmid-encoded *Pgp3* is a major virulence factor for *Chlamydia*

- muridarum to induce hydrosalpinx in mice. *Infect. Immun.* 82, 5327–35.
<https://doi.org/10.1128/IAI.02576-14>
- Lobato-Márquez, D., 2020. Measuring Plasmid Stability in Gram-Negative Bacteria, in: *Methods in Molecular Biology*. Humana Press Inc., pp. 223–233. https://doi.org/10.1007/978-1-4939-9877-7_16
- Lohe, A.R., Hartl, D.L., 1996. Autoregulation of mariner transposase activity by overproduction and dominant-negative complementation. *Mol. Biol. Evol.* 13, 549–555.
<https://doi.org/10.1093/oxfordjournals.molbev.a025615>
- Low, N., 2007. Screening programmes for chlamydial infection: When will we ever learn? *Br. Med. J.* 334, 725–728. <https://doi.org/10.1136/bmj.39154.378079.be>
- Lowden, N.M., Yeruva, L., Johnson, C.M., Bowlin, A.K., Fisher, D.J., 2015. Use of aminoglycoside 3' adenylyltransferase as a selection marker for *Chlamydia trachomatis* intron-mutagenesis and in vivo intron stability. *BMC Res. Notes* 8, 570. <https://doi.org/10.1186/s13104-015-1542-9>
- Maloy, S.R., Nunn, W.D., 1981. Selection for loss of tetracycline resistance by *Escherichia coli*. *J. Bacteriol.* 145, 1110.
- Masek, B.J., Arora, N., Quinn, N., Aumakhan, B., Holden, J., Hardick, A., Agreda, P., Barnes, M., Gaydos, C.A., 2009. Performance of three nucleic acid amplification tests for detection of *Chlamydia trachomatis* and *Neisseria gonorrhoeae* by use of self-collected vaginal swabs obtained via an Internet-based screening program. *J. Clin. Microbiol.* 47, 1663–7.
<https://doi.org/10.1128/JCM.02387-08>
- McKuen, M.J., Mueller, K.E., Bae, Y.S., Fields, K.A., 2017. Fluorescence-Reported Allelic Exchange Mutagenesis Reveals a Role for *Chlamydia trachomatis* TmeA in Invasion That Is Independent of Host AHNAK. *Infect. Immun.* 85. <https://doi.org/10.1128/IAI.00640-17>
- Million-Weaver, S., Camps, M., 2014. Mechanisms of plasmid segregation: have multicopy plasmids been overlooked? *Plasmid* 0, 27. <https://doi.org/10.1016/J.PLASMID.2014.07.002>
- Morré, S.A., Lyons, J.M., Ito, J., Morrison, R.P., 2000. Murine models of *chlamydia trachomatis* genital tract infection: Use of mouse pneumonitis strain versus human strains [1]. *Infect. Immun.* <https://doi.org/10.1128/IAI.68.12.7209-7211.2000>
- Mueller, K.E., Wolf, K., Fields, K.A., 2017. *Chlamydia trachomatis* Transformation and Allelic Exchange Mutagenesis. *Curr. Protoc. Microbiol.* 45, 11A.3.1-11A.3.15.
<https://doi.org/10.1002/cpmc.31>

List of References

- Mueller, K.E., Wolf, K., Fields, K.A., 2016. Gene Deletion by Fluorescence-Reported Allelic Exchange Mutagenesis in *Chlamydia trachomatis*. *MBio* 7, e01817-15.
<https://doi.org/10.1128/mBio.01817-15>
- Naorem, S.S., Han, J., Zhang, S.Y., Zhang, J., Graham, L.B., Song, A., Smith, C. V., Rashid, F., Guo, H., 2018. Efficient transposon mutagenesis mediated by an IPTG-controlled conditional suicide plasmid. *BMC Microbiol.* 18, 1–11. <https://doi.org/10.1186/s12866-018-1319-0>
- Nguyen, B.D., Valdivia, R.H., 2012. Virulence determinants in the obligate intracellular pathogen *Chlamydia trachomatis* revealed by forward genetic approaches. *Proc. Natl. Acad. Sci. U. S. A.* 109, 1263–8. <https://doi.org/10.1073/pnas.1117884109>
- Nigg, C., 1942. AN UNIDENTIFIED VIRUS WHICH PRODUCES PNEUMONIA AND SYSTEMIC INFECTION IN MICE. *Science* 95, 49–50. <https://doi.org/10.1126/science.95.2454.49-a>
- Nigg, C., Eaton, M.D., 1944. ISOLATION FROM NORMAL MICE OF A PNEUMOTROPIC VIRUS WHICH FORMS ELEMENTARY BODIES. *J. Exp. Med.* 79, 497–510.
<https://doi.org/10.1084/jem.79.5.497>
- Nwokolo, N.C., Dragovic, B., Patel, S., Tong, C.Y.W., Barker, G., Radcliffe, K., 2016. 2015 UK national guideline for the management of infection with *Chlamydia trachomatis* 27, 251–267. <https://doi.org/10.1177/0956462415615443>
- O’Connell, C.M., Ferone, M.E., 2016. *Chlamydia trachomatis* Genital Infections. *Microb. cell (Graz, Austria)* 3, 390–403. <https://doi.org/10.15698/mic2016.09.525>
- O’Connell, C.M., Ingalls, R.R., Andrews, C.W., Scurlock, A.M., Darville, T., 2007. Plasmid-deficient *Chlamydia muridarum* fail to induce immune pathology and protect against oviduct disease. *J. Immunol.* 179, 4027–34. <https://doi.org/10.4049/JIMMUNOL.179.6.4027>
- O’Connell, C.M., Nicks, K.M., 2006. A plasmid-cured *Chlamydia muridarum* strain displays altered plaque morphology and reduced infectivity in cell culture. *Microbiology* 152, 1601–1607.
<https://doi.org/10.1099/mic.0.28658-0>
- O’Neill, C.E., Skilton, R.J., Forster, J., Cleary, D.W., Pearson, S.A., Lampe, D.J., Thomson, N.R., Clarke, I.N., 2021. An inducible transposon mutagenesis approach for the intracellular human pathogen *Chlamydia trachomatis*. *Wellcome Open Res.* 2021 6312 6, 312.
<https://doi.org/10.12688/wellcomeopenres.16068.1>
- Opperman, T., Ling, L.L., Moir, D.T., 2003. Microbial pathogen genomes - New strategies for identifying therapeutic and vaccine targets. *Expert Opin. Ther. Targets.*
<https://doi.org/10.1517/14728222.7.4.469>

- Ouellette, S.P., 2018. Feasibility of a Conditional Knockout System for Chlamydia Based on CRISPR Interference. *Front. Cell. Infect. Microbiol.* 8, 59. <https://doi.org/10.3389/fcimb.2018.00059>
- Panja, S., Saha, S., Jana, B., Basu, T., 2006. Role of membrane potential on artificial transformation of *E. coli* with plasmid DNA. *J. Biotechnol.* 127, 14–20. <https://doi.org/10.1016/j.jbiotec.2006.06.008>
- Pankey, G.A., Sabath, L.D., 2004. Clinical Relevance of Bacteriostatic versus Bactericidal Mechanisms of Action in the Treatment of Gram-Positive Bacterial Infections. *Clin. Infect. Dis.* 38, 864–870. <https://doi.org/10.1086/381972>
- Parks, K.S., Dixon, P.B., Richey, C.M., Hook, E.W., 1997. Spontaneous clearance of chlamydia trachomatis infection in untreated patients. *Sex. Transm. Dis.* 24, 229–235. <https://doi.org/10.1097/00007435-199704000-00008>
- Parrett, C.J., Lenoci, R. V., Nguyen, B., Russell, L., Jewett, T.J., 2016. Targeted disruption of *Chlamydia trachomatis* invasion by in trans expression of dominant negative tarp effectors. *Front. Cell. Infect. Microbiol.* 6, 84. <https://doi.org/10.3389/fcimb.2016.00084>
- Perutka, J., Wang, W., Goerlitz, D., Lambowitz, A.M., 2004. Use of Computer-designed Group II Introns to Disrupt *Escherichia coli* DExH/D-box Protein and DNA Helicase Genes. *J. Mol. Biol.* 336, 421–439. <https://doi.org/10.1016/j.jmb.2003.12.009>
- Pickett, M.A., Everson, J.S., Pead, P.J., Clarke, I.N., 2005. The plasmids of *Chlamydia trachomatis* and *Chlamydophila pneumoniae* (N16): Accurate determination of copy number and the paradoxical effect of plasmid-curing agents. *Microbiology* 151, 893–903. <https://doi.org/10.1099/mic.0.27625-0>
- Polard, P., Chandler, M., 1995. Bacterial transposases and retroviral integrases. *Mol. Microbiol.* <https://doi.org/10.1111/j.1365-2958.1995.tb02217.x>
- Projan, S.J., Carleton, S., Novick, R.P., 1983. Determination of plasmid copy number by fluorescence densitometry. *Plasmid* 9, 182–190. [https://doi.org/10.1016/0147-619X\(83\)90019-7](https://doi.org/10.1016/0147-619X(83)90019-7)
- Pudjiatmoko, Fukushi, H., Ochiai, Y., Yamaguchi, T., Hirai, K., 1998. In vitro susceptibility of *Chlamydia pecorum* to macrolides, tetracyclines, quinolones and β -lactam. *Microbiol. Immunol.* 42, 61–63. <https://doi.org/10.1111/J.1348-0421.1998.TB01971.X>
- Qin, A., Tucker, A.M., Hines, A., Wood, D.O., 2004. Transposon mutagenesis of the obligate intracellular pathogen *Rickettsia prowazekii*. *Appl. Environ. Microbiol.* 70, 2816–2822. <https://doi.org/10.1128/AEM.70.5.2816-2822.2004>

List of References

- Rahnama, M., Fields, K.A., 2018. Transformation of Chlamydia: current approaches and impact on our understanding of chlamydial infection biology. *Microbes Infect.* 20, 445–450. <https://doi.org/10.1016/j.micinf.2018.01.002>
- Read, T.D., Brunham, R.C., Shen, C., Gill, S.R., Heidelberg, J.F., White, O., Hickey, E.K., Peterson, J., Utterback, T., Berry, K., Bass, S., Linher, K., Weidman, J., Khouri, H., Craven, B., Bowman, C., Dodson, R., Gwinn, M., Nelson, W., DeBoy, R., Kolonay, J., McClarty, G., Salzberg, S.L., Eisen, J., Fraser, C.M., 2000. Genome sequences of *Chlamydia trachomatis* MoPn and *Chlamydia pneumoniae* AR39. *Nucleic Acids Res.* 28, 1397–406. <https://doi.org/10.1093/nar/28.6.1397>
- Richardson, J.M., Colloms, S.D., Finnegan, D.J., Walkinshaw, M.D., 2009. Molecular Architecture of the Mos1 Paired-End Complex: The Structural Basis of DNA Transposition in a Eukaryote. *Cell* 138, 1096–1108. <https://doi.org/10.1016/j.cell.2009.07.012>
- Richardson, J.M., Dawson, A., O'Hagan, N., Taylor, P., Finnegan, D.J., Walkinshaw, M.D., 2006. Mechanism of Mos1 transposition: Insights from structural analysis. *EMBO J.* 25, 1324–1334. <https://doi.org/10.1038/sj.emboj.7601018>
- Russell, M., Darville, T., Chandra-Kuntal, K., Smith, B., Andrews, C.W., O'Connell, C.M., O'Connell, C.M., 2011. Infectivity acts as in vivo selection for maintenance of the chlamydial cryptic plasmid. *Infect. Immun.* 79, 98–107. <https://doi.org/10.1128/IAI.01105-10>
- S, C., M, L., RC, R., SL, C., 2017. Direct and convenient measurement of plasmid stability in lab and clinical isolates of *E. coli*. *Sci. Rep.* 7. <https://doi.org/10.1038/S41598-017-05219-X>
- SA, B., V, B., JA, G., J, Hellems, J, Huggett, M, K., R, M., T, N., MW, P., GL, S., J, V., CT, W., 2009. The MIQE guidelines: minimum information for publication of quantitative real-time PCR experiments. *Clin. Chem.* 55, 611–622. <https://doi.org/10.1373/CLINCHEM.2008.112797>
- SanMiguel, P., Tikhonov, A., Jin, Y.K., Motchoulskaia, N., Zakharov, D., Melake-Berhan, A., Springer, P.S., Edwards, K.J., Lee, M., Avramova, Z., Bennetzen, J.L., 1996. Nested retrotransposons in the intergenic regions of the maize genome. *Science* 274, 765–8.
- Schwarz, S., Kehrenberg, C., Doublet, B., Cloeckert, A., 2004. Molecular basis of bacterial resistance to chloramphenicol and florfenicol. *FEMS Microbiol. Rev.* 28, 519–542. <https://doi.org/10.1016/J.FEMSRE.2004.04.001>
- Scidmore-Carlson, M.A., Shaw, E.I., Dooley, C.A., Fischer, E.R., Hackstadt, T., 1999. Identification and characterization of a *Chlamydia trachomatis* early operon encoding four novel inclusion membrane proteins. *Mol. Microbiol.* 33, 753–765. <https://doi.org/10.1046/j.1365-2958.1999.01523.x>

- Scidmore, M.A., Hackstadt, T., 2001. Mammalian 14-3-3 β associates with the *Chlamydia trachomatis* inclusion membrane via its interaction with IncG. *Mol. Microbiol.* 39, 1638–1650. <https://doi.org/10.1046/j.1365-2958.2001.02355.x>
- Scidmore, M.A., Rockey, D.D., Fischer, E.R., Heinzen, R.A., Hackstadt, T., 1996. Vesicular interactions of the *Chlamydia trachomatis* inclusion are determined by chlamydial early protein synthesis rather than route of entry. *Infect. Immun.* 64, 5366–5372. <https://doi.org/10.1128/iai.64.12.5366-5372.1996>
- Sengupta, M., Austin, S., 2011. Prevalence and significance of plasmid maintenance functions in the virulence plasmids of pathogenic bacteria. *Infect. Immun.* 79, 2502–9. <https://doi.org/10.1128/IAI.00127-11>
- Seth-Smith, H.M., Harris, S.R., Persson, K., Marsh, P., Barron, A., Bignell, A., Bjartling, C., Clark, L., Cutcliffe, L.T., Lambden, P.R., Lennard, N., Lockey, S.J., Quail, M.A., Salim, O., Skilton, R.J., Wang, Y., Holland, M.J., Parkhill, J., Thomson, N.R., Clarke, I.N., 2009. Co-evolution of genomes and plasmids within *Chlamydia trachomatis* and the emergence in Sweden of a new variant strain. *BMC Genomics* 10, 239. <https://doi.org/10.1186/1471-2164-10-239>
- Seth-Smith, H.M.B., Harris, S.R., Skilton, R.J., Radebe, F.M., Golparian, D., Shipitsyna, E., Duy, P.T., Scott, P., Cutcliffe, L.T., O'Neill, C., Parmar, S., Pitt, R., Baker, S., Ison, C.A., Marsh, P., Jalal, H., Lewis, D.A., Unemo, M., Clarke, I.N., Parkhill, J., Thomson, N.R., 2013. Whole-genome sequences of *Chlamydia trachomatis* directly from clinical samples without culture. *Genome Res.* 23, 855–866. <https://doi.org/10.1101/gr.150037.112>
- Shaw, A.C., Gevaert, K., Demol, H., Hoorelbeke, B., Vandekerckhove, J., Larsen, M.R., Roepstorff, P., Holm, A., Christiansen, G., Birkelund, S., 2002. Comparative proteome analysis of *Chlamydia trachomatis* serovar A, D and L2. *Proteomics* 2, 164–186. [https://doi.org/10.1002/1615-9861\(200202\)2:2<164::AID-PROT164>3.0.CO;2-U](https://doi.org/10.1002/1615-9861(200202)2:2<164::AID-PROT164>3.0.CO;2-U)
- Shaw, E.I., Dooley, C.A., Fischer, E.R., Scidmore, M.A., Fields, K.A., Hackstadt, T., 2000. Three temporal classes of gene expression during the *Chlamydia trachomatis* developmental cycle. *Mol. Microbiol.* 37, 913–925. <https://doi.org/10.1046/j.1365-2958.2000.02057.x>
- Shen, L., Li, M., Zhang, Y.-X., 2004. *Chlamydia trachomatis* 28 recognizes the *fliC* promoter of *Escherichia coli* and responds to heat shock in chlamydiae. *Microbiology* 150, 205–215. <https://doi.org/10.1099/mic.0.26734-0>
- Shima, K., Wanker, M., Skilton, R.J., Cutcliffe, L.T., Schnee, C., Kohl, T.A., Niemann, S., Geijo, J., Klinger, M., Timms, P., Rattei, T., Sachse, K., Clarke, I.N., Rupp, J., 2018. The Genetic Transformation of *Chlamydia pneumoniae*. *mSphere* 3.

List of References

- <https://doi.org/10.1128/mSphere.00412-18>
- Shintani, M., Sanchez, Z.K., Kimbara, K., 2015. Genomics of microbial plasmids: Classification and identification based on replication and transfer systems and host taxonomy. *Front. Microbiol.* <https://doi.org/10.3389/fmicb.2015.00242>
- Silva, F., Queiroz, J.A., Domingues, F.C., 2012. Evaluating metabolic stress and plasmid stability in plasmid DNA production by *Escherichia coli*. *Biotechnol. Adv.* <https://doi.org/10.1016/j.biotechadv.2011.12.005>
- Sixt, B.S., Bastidas, R.J., Finethy, R., Baxter, R.M., Carpenter, V.K., Kroemer, G., Coers, J., Valdivia, R.H., 2017. The *Chlamydia trachomatis* Inclusion Membrane Protein CpoS Counteracts STING-Mediated Cellular Surveillance and Suicide Programs. *Cell Host Microbe* 21, 113–121. <https://doi.org/10.1016/j.chom.2016.12.002>
- Sixt, B.S., Valdivia, R.H., 2016. Molecular Genetic Analysis of *Chlamydia* Species. *Annu. Rev. Microbiol.* 70, 179–198. <https://doi.org/10.1146/annurev-micro-102215-095539>
- Skerman, V.B.D., McGowan, V., Sneath, P.H.A., 1980. Approved lists of bacterial names. *Int. J. Syst. Bacteriol.* 30, 225–420. <https://doi.org/10.1099/00207713-30-1-225>
- Skilton, R.J., Cutcliffe, L.T., Pickett, M.A., Lambden, P.R., Fane, B.A., Clarke, I.N., 2007. Intracellular parasitism of chlamydiae: specific infectivity of chlamydiophage Chp2 in *Chlamydia abortus*. *J. Bacteriol.* 189, 4957–9. <https://doi.org/10.1128/JB.00235-07>
- Skilton, R.J., O'Neill, C., Thomson, N.R., Lampe, D.J., Clarke, I.N., 2021. Progress towards an inducible, replication-proficient transposon delivery vector for *Chlamydia trachomatis*. *Wellcome Open Res.* 6, 82. <https://doi.org/10.12688/wellcomeopenres.16665.1>
- Skilton, R.J., Wang, Y., O'Neill, C., Filardo, S., Marsh, P., Bénard, A., Thomson, N.R., Ramsey, K.H., Clarke, I.N., 2018. The *Chlamydia muridarum* plasmid revisited : new insights into growth kinetics. *Wellcome Open Res.* 3, 25. <https://doi.org/10.12688/wellcomeopenres.13905.1>
- Śliwa-Dominiak, J., Suszyńska, E., Pawlikowska, M., Deptuła, W., 2013. *Chlamydia* bacteriophages. *Arch. Microbiol.* <https://doi.org/10.1007/s00203-013-0912-8>
- Song, L., Carlson, J.H., Whitmire, W.M., Kari, L., Virtaneva, K., Sturdevant, D.E., Watkins, H., Zhou, B., Sturdevant, G.L., Porcella, S.F., McClarty, G., Caldwell, H.D., 2013. *Chlamydia trachomatis* plasmid-encoded Pgp4 is a transcriptional regulator of virulence-associated genes. *Infect. Immun.* 81, 636–44. <https://doi.org/10.1128/IAI.01305-12>
- Song, L., Carlson, J.H., Zhou, B., Virtaneva, K., Whitmire, W.M., Sturdevant, G.L., Porcella, S.F.,

- McClarty, G., Caldwell, H.D., 2014. Plasmid-mediated transformation tropism of chlamydial biovars. *Pathog. Dis.* 70, 189–93. <https://doi.org/10.1111/2049-632X.12104>
- Sriprakash, K.S., Macavoy, E.S., 1987. Characterization and sequence of a plasmid from the trachoma biovar of *Chlamydia trachomatis*. *Plasmid* 18, 205–214. [https://doi.org/10.1016/0147-619X\(87\)90063-1](https://doi.org/10.1016/0147-619X(87)90063-1)
- Standley, M.S., Million-Weaver, S., Alexander, D.L., Hu, S., Camps, M., 2019. Genetic control of ColE1 plasmid stability that is independent of plasmid copy number regulation. *Curr. Genet.* 65, 179. <https://doi.org/10.1007/S00294-018-0858-0>
- Stephens, R.S., Kalman, S., Lammel, C., Fan, J., Marathe, R., Aravind, L., Mitchell, W., Olinger, L., Tatusov, R.L., Zhao, Q., Koonin, E. V., Davis, R.W., 1998. Genome sequence of an obligate intracellular pathogen of humans: *Chlamydia trachomatis*. *Science* (80-.). 282, 754–759. <https://doi.org/10.1126/science.282.5389.754>
- Sturdevant, G.L., Kari, L., Gardner, D.J., Olivares-Zavaleta, N., Randall, L.B., Whitmire, W.M., Carlson, J.H., Goheen, M.M., Selleck, E.M., Martens, C., Caldwell, H.D., 2010. Frameshift mutations in a single novel virulence factor alter the in vivo pathogenicity of *Chlamydia trachomatis* for the female murine genital tract. *Infect. Immun.* 78, 3660–3668. <https://doi.org/10.1128/IAI.00386-10>
- Suchland, R.J., Geisler, W.M., Stamm, W.E., 2003. Methodologies and Cell Lines Used for Antimicrobial Susceptibility Testing of *Chlamydia* spp. *Antimicrob. Agents Chemother.* 47, 636. <https://doi.org/10.1128/AAC.47.2.636-642.2003>
- Tam, J.E., Davis, C.H., Thresher, R.J., Wyrick, P.B., 1992. Location of the origin of replication for the 7.5-kb *Chlamydia trachomatis* plasmid. *Plasmid* 27, 231–6.
- Tam, J.E., Davis, C.H., Wyrick, P.B., 1994. Expression of recombinant DNA introduced into *Chlamydia trachomatis* by electroporation. *Can. J. Microbiol.* 40, 583–91.
- Thomas, N.S., Lusher, M., Storey, C.C., Clarke, I.N., 1997. Plasmid diversity in *Chlamydia*. *Microbiology* 143, 1847–1854. <https://doi.org/10.1099/00221287-143-6-1847>
- Thompson, C.C., Griffiths, C., Nicod, S.S., Lowden, N.M., Wigneshweraraj, S., Fisher, D.J., McClure, M.O., 2015. The Rsb Phosphoregulatory Network Controls Availability of the Primary Sigma Factor in *Chlamydia trachomatis* and Influences the Kinetics of Growth and Development. *PLoS Pathog.* 11, e1005125. <https://doi.org/10.1371/journal.ppat.1005125>
- Thomson, V.J., Bhattacharjee, M.K., Fine, D.H., Derbyshire, K.M., Figurski, D.H., 1999. Direct selection of IS903 transposon insertions by use of a broad-host-range vector: Isolation of

List of References

- catalase-deficient mutants of *Actinobacillus actinomycetemcomitans*. *J. Bacteriol.* 181, 7298–7307. <https://doi.org/10.1128/jb.181.23.7298-7307.1999>
- Tomizawa, J. ichi, Som, T., 1984. Control of *colE1* plasmid replication: Enhancement of binding of RNA I to the primer transcript by the *rom* protein. *Cell* 38, 871–878. [https://doi.org/10.1016/0092-8674\(84\)90282-4](https://doi.org/10.1016/0092-8674(84)90282-4)
- Torrone, E., Papp, J., Weinstock, H., Centers for Disease Control and Prevention (CDC), 2014. Prevalence of *Chlamydia trachomatis* genital infection among persons aged 14-39 years--United States, 2007-2012. *MMWR. Morb. Mortal. Wkly. Rep.* 63, 834–8.
- Valdivia, R.H., Bastidas, R.J., 2018. The Expanding Molecular Genetics Tool Kit in *Chlamydia*. *J. Bacteriol.* 200, e00590-18. <https://doi.org/10.1128/JB.00590-18>
- van de Laar, M.J., Morré, S.A., 2007. *Chlamydia*: a major challenge for public health. *Eurosurveillance* 12, 1–2. <https://doi.org/10.2807/esm.12.10.00735-en>
- Van Opijnen, T., Bodi, K.L., Camilli, A., 2009. Tn-seq; high-throughput parallel sequencing for fitness and genetic interaction studies in microorganisms.
- Van Opijnen, T., Camilli, A., 2013. Transposon insertion sequencing: A new tool for systems-level analysis of microorganisms. *Nat. Rev. Microbiol.* 11, 435–442. <https://doi.org/10.1038/nrmicro3033>
- Vos, T., Abajobir, A.A., Abate, K.H., Abbafati, C., Abbas, K.M., Abd-Allah, F., Abdulkader, R.S., Abdulle, A.M., Abebo, T.A., Abera, S.F., Aboyans, V., Abu-Raddad, L.J., Ackerman, I.N., Adamu, A.A., Adetokunboh, O., Afarideh, M., Afshin, A., Agarwal, S.K., Aggarwal, R., Agrawal, A., Agrawal, S., Ahmadieh, H., Ahmed, M.B., Aichour, M.T.E., Aichour, A.N., Aichour, I., Aiyar, S., Akinyemi, R.O., Akseer, N., Al Lami, F.H., Alahdab, F., Al-Aly, Z., Alam, K., Alam, N., Alam, T., Alasfoor, D., Alene, K.A., Ali, R., Alizadeh-Navaei, R., Alkerwi, A., Alla, F., Allebeck, P., Allen, C., Al-Maskari, F., Al-Raddadi, R., Alsharif, U., Alsowaidi, S., Altirkawi, K.A., Amare, A.T., Amini, E., Ammar, W., Amoako, Y.A., Andersen, H.H., Antonio, C.A.T., Anwari, P., Ärnlöv, J., Artaman, A., Aryal, K.K., Asayesh, H., Asgedom, S.W., Assadi, R., Atey, T.M., Atnafu, N.T., Atre, S.R., Avila-Burgos, L., Avokphako, E.F.G.A., Awasthi, A., Bacha, U., Badawi, A., Balakrishnan, K., Banerjee, A., Bannick, M.S., Barac, A., Barber, R.M., Barker-Collo, S.L., Bärnighausen, T., Barquera, S., Barregard, L., Barrero, L.H., Basu, S., Battista, B., Battle, K.E., Baune, B.T., Bazargan-Hejazi, S., Beardsley, J., Bedi, N., Beghi, E., Béjot, Y., Bekele, B.B., Bell, M.L., Bennett, D.A., Bensenor, I.M., Benson, J., Berhane, A., Berhe, D.F., Bernabé, E., Betsu, B.D., Beuran, M., Beyene, A.S., Bhala, N., Bhansali, A., Bhatt, S., Bhutta, Z.A., Biadgilign, S., Bicer, B.K., Bienhoff, K., Bikbov, B., Birungi, C., Biryukov, S., Bisanzio, D., Bizuayehu, H.M.,

Boneya, D.J., Boufous, S., Bourne, R.R.A., Brazinova, A., Brugha, T.S., Buchbinder, R., Bulto, L.N.B., Bumgarner, B.R., Butt, Z.A., Cahuana-Hurtado, L., Cameron, E., Car, M., Carabin, H., Carapetis, J.R., Cárdenas, R., Carpenter, D.O., Carrero, J.J., Carter, A., Carvalho, F., Casey, D.C., Caso, V., Castañeda-Orjuela, C.A., Castle, C.D., Catalá-López, F., Chang, H.-Y., Chang, J.-C., Charlson, F.J., Chen, H., Chibalabala, M., Chibueze, C.E., Chisumpa, V.H., Chitheer, A.A., Christopher, D.J., Ciobanu, L.G., Cirillo, M., Colombara, D., Cooper, C., Cortesi, P.A., Criqui, M.H., Crump, J.A., Dadi, A.F., Dalal, K., Dandona, L., Dandona, R., das Neves, J., Davitoliu, D. V, de Courten, B., De Leo, D. De, Defo, B.K., Degenhardt, L., Deiparine, S., Dellavalle, R.P., Deribe, K., Des Jarlais, D.C., Dey, S., Dharmaratne, S.D., Dhillon, P.K., Dicker, D., Ding, E.L., Djalalinia, S., Do, H.P., Dorsey, E.R., dos Santos, K.P.B., Douwes-Schultz, D., Doyle, K.E., Driscoll, T.R., Dubey, M., Duncan, B.B., El-Khatib, Z.Z., Ellerstrand, J., Enayati, A., Endries, A.Y., Ermakov, S.P., Erskine, H.E., Eshrati, B., Eskandarieh, S., Esteghamati, A., Estep, K., Fanuel, F.B.B., Farinha, C.S.E.S., Faro, A., Farzadfar, F., Fazeli, M.S., Feigin, V.L., Fereshtehnejad, S.-M., Fernandes, J.C., Ferrari, A.J., Feyissa, T.R., Filip, I., Fischer, F., Fitzmaurice, C., Flaxman, A.D., Flor, L.S., Foigt, N., Foreman, K.J., Franklin, R.C., Fullman, N., Fürst, T., Furtado, J.M., Futran, N.D., Gakidou, E., Ganji, M., Garcia-Basteiro, A.L., Gebre, T., Gebrehiwot, T.T., Geleto, A., Gemechu, B.L., Gesesew, H.A., Gething, P.W., Ghajar, A., Gibney, K.B., Gill, P.S., Gillum, R.F., Ginawi, I.A.M., Giref, A.Z., Gishu, M.D., Giussani, G., Godwin, W.W., Gold, A.L., Goldberg, E.M., Gona, P.N., Goodridge, A., Gopalani, S.V., Goto, A., Goulart, A.C., Griswold, M., Gughani, H.C., Gupta, Rahul, Gupta, Rajeev, Gupta, T., Gupta, V., Hafezi-Nejad, N., Hailu, G.B., Hailu, A.D., Hamadeh, R.R., Hamidi, S., Handal, A.J., Hankey, G.J., Hanson, S.W., Hao, Y., Harb, H.L., Hareri, H.A., Haro, J.M., Harvey, J., Hassanvand, M.S., Havmoeller, R., Hawley, C., Hay, S.I., Hay, R.J., Henry, N.J., Heredia-Pi, I.B., Hernandez, J.M., Heydarpour, P., Hoek, H.W., Hoffman, H.J., Horita, N., Hosgood, H.D., Hostiuc, S., Hotez, P.J., Hoy, D.G., Htet, A.S., Hu, G., Huang, H., Huynh, C., Iburg, K.M., Igumbor, E.U., Ikeda, C., Irvine, C.M.S., Jacobsen, K.H., Jahanmehr, N., Jakovljevic, M.B., Jassal, S.K., Javanbakht, M., Jayaraman, S.P., Jeemon, P., Jensen, P.N., Jha, V., Jiang, G., John, D., Johnson, S.C., Johnson, C.O., Jonas, J.B., Jürisson, M., Kabir, Z., Kadel, R., Kahsay, A., Kamal, R., Kan, H., Karam, N.E., Karch, A., Karema, C.K., Kasaeian, A., Kassa, G.M., Kassaw, N.A., Kassebaum, N.J., Kastor, A., Katikireddi, S.V., Kaul, A., Kawakami, N., Keiyoro, P.N., Kengne, A.P., Keren, A., Khader, Y.S., Khalil, I.A., Khan, E.A., Khang, Y.-H., Khosravi, A., Khubchandani, J., Kiadaliri, A.A., Kielsing, C., Kim, Y.J., Kim, D., Kim, P., Kimokoti, R.W., Kinfu, Y., Kisa, A., Kissimova-Skarbek, K.A., Kivimaki, M., Knudsen, A.K., Kokubo, Y., Kolte, D., Kopec, J.A., Kosen, S., Koul, P.A., Koyanagi, A., Kravchenko, M., Krishnaswami, S., Krohn, K.J., Kumar, G.A., Kumar, P., Kumar, S., Kyu, H.H., Lal, D.K., Lalloo, R., Lambert, N., Lan, Q., Larsson, A., Lavados, P.M., Leasher, J.L., Lee, P.H., Lee, J.-T., Leigh, J., Leshargie, C.T., Leung, J., Leung, R., Levi, M., Li, Yichong, Li, Yongmei, Li Kappe, D., Liang, X., Liben, M.L., Lim, S.S., Linn, S., Liu, P.Y., Liu, A., Liu, S., Liu, Y., Lodha, R.,

List of References

Logroscino, G., London, S.J., Looker, K.J., Lopez, A.D., Lorkowski, S., Lotufo, P.A., Low, N., Lozano, R., Lucas, T.C.D., Macarayan, E.R.K., Magdy Abd El Razek, H., Magdy Abd El Razek, M., Mahdavi, M., Majdan, M., Majdzadeh, R., Majeed, A., Malekzadeh, R., Malhotra, R., Malta, D.C., Mamun, A.A., Manguerra, H., Manhertz, T., Mantilla, A., Mantovani, L.G., Mapoma, C.C., Marczak, L.B., Martinez-Raga, J., Martins-Melo, F.R., Martopullo, I., März, W., Mathur, M.R., Mazidi, M., McAlinden, C., McGaughey, M., McGrath, J.J., McKee, M., McNellan, C., Mehata, S., Mehndiratta, M.M., Mekonnen, T.C., Memiah, P., Memish, Z.A., Mendoza, W., Mengistie, M.A., Mengistu, D.T., Mensah, G.A., Meretoja, T.J., Meretoja, A., Mezgebe, H.B., Micha, R., Millear, A., Miller, T.R., Mills, E.J., Mirarefin, M., Mirrakhimov, E.M., Misganaw, A., Mishra, S.R., Mitchell, P.B., Mohammad, K.A., Mohammadi, A., Mohammed, K.E., Mohammed, S., Mohanty, S.K., Mokdad, A.H., Mollenkopf, S.K., Monasta, L., Montico, M., Moradi-Lakeh, M., Moraga, P., Mori, R., Morozoff, C., Morrison, S.D., Moses, M., Mountjoy-Venning, C., Mruts, K.B., Mueller, U.O., Muller, K., Murdoch, M.E., Murthy, G.V.S., Musa, K.I., Nachega, J.B., Nagel, G., Naghavi, M., Naheed, A., Naidoo, K.S., Naldi, L., Nangia, V., Natarajan, G., Negasa, D.E., Negoi, R.I., Negoi, I., Newton, C.R., Ngunjiri, J.W., Nguyen, T.H., Nguyen, Q. Le, Nguyen, C.T., Nguyen, G., Nguyen, M., Nichols, E., Ningrum, D.N.A., Nolte, S., Nong, V.M., Norrving, B., Noubiap, J.J.N., O'Donnell, M.J., Ogbo, F.A., Oh, I.-H., Okoro, A., Oladimeji, O., Olagunju, T.O., Olagunju, A.T., Olsen, H.E., Olusanya, B.O., Olusanya, J.O., Ong, K., Opio, J.N., Oren, E., Ortiz, A., Osgood-Zimmerman, A., Osman, M., Owolabi, M.O., PA, M., Pacella, R.E., Pana, A., Panda, B.K., Papachristou, C., Park, E.-K., Parry, C.D., Parsaeian, M., Patten, S.B., Patton, G.C., Paulson, K., Pearce, N., Pereira, D.M., Perico, N., Pesudovs, K., Peterson, C.B., Petzold, M., Phillips, M.R., Pigott, D.M., Pillay, J.D., Pinho, C., Plass, D., Pletcher, M.A., Popova, S., Poulton, R.G., Pourmalek, F., Prabhakaran, D., Prasad, N.M., Prasad, N., Purcell, C., Qorbani, M., Quansah, R., Quintanilla, B.P.A., Rabiee, R.H.S., Radfar, A., Rafay, A., Rahimi, K., Rahimi-Movaghar, A., Rahimi-Movaghar, V., Rahman, M.H.U., Rahman, M., Rai, R.K., Rajsic, S., Ram, U., Ranabhat, C.L., Rankin, Z., Rao, P.C., Rao, P.V., Rawaf, S., Ray, S.E., Reiner, R.C., Reinig, N., Reitsma, M.B., Remuzzi, G., Renzaho, A.M.N., Resnikoff, S., Rezaei, S., Ribeiro, A.L., Ronfani, L., Roshandel, G., Roth, G.A., Roy, A., Rubagotti, E., Ruhago, G.M., Saadat, S., Sadat, N., Safdarian, M., Safi, S., Safiri, S., Sagar, R., Sahathevan, R., Salama, J., Saleem, H.O.B., Salomon, J.A., Salvi, S.S., Samy, A.M., Sanabria, J.R., Santomauro, D., Santos, I.S., Santos, J.V., Santric Milicevic, M.M., Sartorius, B., Satpathy, M., Sawhney, M., Saxena, S., Schmidt, M.I., Schneider, I.J.C., Schöttker, B., Schwebel, D.C., Schwendicke, F., Seedat, S., Sepanlou, S.G., Servan-Mori, E.E., Setegn, T., Shackelford, K.A., Shaheen, A., Shaikh, M.A., Shamsipour, M., Shariful Islam, S.M., Sharma, J., Sharma, R., She, J., Shi, P., Shields, C., Shifa, G.T., Shigematsu, M., Shinohara, Y., Shiri, R., Shirkoobi, R., Shirude, S., Shishani, K., Shrimme, M.G., Sibai, A.M., Sigfusdottir, I.D., Silva, D.A.S., Silva, J.P., Silveira, D.G.A., Singh, J.A., Singh, N.P., Sinha, D.N., Skiadaresi, E., Skirbekk, V., Slepak, E.L.,

- Sligar, A., Smith, D.L., Smith, M., Sobaih, B.H.A., Sobngwi, E., Sorensen, R.J.D., Sousa, T.C.M., Sposato, L.A., Sreeramareddy, C.T., Srinivasan, V., Stanaway, J.D., Stathopoulou, V., Steel, N., Stein, M.B., Stein, D.J., Steiner, T.J., Steiner, C., Steinke, S., Stokes, M.A., Stovner, L.J., Strub, B., Subart, M., Sufiyani, M.B., Sunguya, B.F., Sur, P.J., Swaminathan, S., Sykes, B.L., Sylte, D.O., Tabarés-Seisdedos, R., Taffere, G.R., Takala, J.S., Tandon, N., Tavakkoli, M., Taveira, N., Taylor, H.R., Tehrani-Banihashemi, A., Tekelab, T., Terkawi, A.S., Tesfaye, D.J., Tessema, B., Thamsuwan, O., Thomas, K.E., Thrift, A.G., Tiruye, T.Y., Tobe-Gai, R., Tollanes, M.C., Tonelli, M., Topor-Madry, R., Tortajada, M., Touvier, M., Tran, B.X., Tripathi, S., Troeger, C., Truelsen, T., Tsoi, D., Tuem, K.B., Tuzcu, E.M., Tyrovolas, S., Ukwaja, K.N., Undurraga, E.A., Uneke, C.J., Updike, R., Uthman, O.A., Uzochukwu, B.S.C., van Boven, J.F.M., Varughese, S., Vasankari, T., Venkatesh, S., Venketasubramanian, N., Vidavalur, R., Violante, F.S., Vladimirov, S.K., Vlassov, V.V., Vollset, S.E., Wadilo, F., Wakayo, T., Wang, Y.-P., Weaver, M., Weichenthal, S., Weiderpass, E., Weintraub, R.G., Werdecker, A., Westerman, R., Whiteford, H.A., Wijeratne, T., Wiysonge, C.S., Wolfe, C.D.A., Woodbrook, R., Woolf, A.D., Workicho, A., Xavier, D., Xu, G., Yadgir, S., Yaghoubi, M., Yakob, B., Yan, L.L., Yano, Y., Ye, P., Yimam, H.H., Yip, P., Yonemoto, N., Yoon, S.-J., Yotebieng, M., Younis, M.Z., Zaidi, Z., Zaki, M.E.S., Zegeye, E.A., Zenebe, Z.M., Zhang, X., Zhou, M., Zipkin, B., Zodpey, S., Zuhlke, L.J., Murray, C.J.L., 2017. Global, regional, and national incidence, prevalence, and years lived with disability for 328 diseases and injuries for 195 countries, 1990–2016: a systematic analysis for the Global Burden of Disease Study 2016. *Lancet* 390, 1211–1259. [https://doi.org/10.1016/S0140-6736\(17\)32154-2](https://doi.org/10.1016/S0140-6736(17)32154-2)
- Wang, Y., Cutcliffe, L.T., Skilton, R.J., Persson, K., Bjartling, C., Clarke, I.N., 2013a. Transformation of a plasmid-free, genital tract isolate of *Chlamydia trachomatis* with a plasmid vector carrying a deletion in CDS6 revealed that this gene regulates inclusion phenotype. *Pathog. Dis.* 67, 100–3. <https://doi.org/10.1111/2049-632X.12024>
- Wang, Y., Cutcliffe, L.T., Skilton, R.J., Ramsey, K.H., Thomson, N.R., Clarke, I.N., 2014. The genetic basis of plasmid tropism between *Chlamydia trachomatis* and *Chlamydia muridarum*. *Pathog. Dis.* 72, 19–23. <https://doi.org/10.1111/2049-632X.12175>
- Wang, Y., Kahane, S., Cutcliffe, L.T., Skilton, R.J., Lambden, P.R., Clarke, I.N., 2011. Development of a Transformation System for *Chlamydia trachomatis*: Restoration of Glycogen Biosynthesis by Acquisition of a Plasmid Shuttle Vector. <https://doi.org/10.1371/journal.ppat.1002258>
- Wang, Y., Kahane, S., Cutcliffe, L.T., Skilton, R.J., Lambden, P.R., Persson, K., Bjartling, C., Clarke, I.N., 2013b. Genetic Transformation of a Clinical (Genital Tract), Plasmid-Free Isolate of *Chlamydia trachomatis*: Engineering the Plasmid as a Cloning Vector. *PLoS One* 8, e59195. <https://doi.org/10.1371/journal.pone.0059195>

List of References

- Wang, Y., LaBrie, S.D., Carrell, S.J., Suchland, R.J., Dimond, Z.E., Kwong, F., Rockey, D.D., Hefty, P.S., Hybiske, K., 2019. Development of transposon mutagenesis for *Chlamydia muridarum*. *J. Bacteriol.* <https://doi.org/10.1128/jb.00366-19>
- Weber, M.M., Bauler, L.D., Lam, J., Hackstadt, T., 2015. Expression and localization of predicted inclusion membrane proteins in *Chlamydia trachomatis*. *Infect. Immun.* 83, 4710–4718. <https://doi.org/10.1128/IAI.01075-15>
- Weber, M.M., Noriega, N.F., Bauler, L.D., Lam, J.L., Sager, J., Wesolowski, J., Paumet, F., Hackstadt, T., 2016. A functional core of IncA is required for *Chlamydia trachomatis* inclusion fusion. *J. Bacteriol.* 198, 1347–1355. <https://doi.org/10.1128/JB.00933-15>
- Weinmaier, T., Hoser, J., Eck, S., Kaufhold, I., Shima, K., Strom, T.M., Rattei, T., Rupp, J., 2015. Genomic factors related to tissue tropism in *Chlamydia pneumoniae* infection. *BMC Genomics* 16, 268. <https://doi.org/10.1186/s12864-015-1377-8>
- Werbowsky, O., Werbowsky, S., Kaczorowski, T., 2017. Plasmid stability analysis based on a new theoretical model employing stochastic simulations. <https://doi.org/10.1371/journal.pone.0183512>
- Wickstrum, J., Sammons, L.R., Restivo, K.N., Hefty, P.S., 2013. Conditional gene expression in *Chlamydia trachomatis* using the tet system. *PLoS One* 8, e76743. <https://doi.org/10.1371/journal.pone.0076743>
- Williams, D.M., Schachter, J., Drutz, D.J., Sumaya, C. V., 1981. Pneumonia due to chlamydia trachomatis in the immunocompromised (Nude) mouse. *J. Infect. Dis.* 143, 238–241. <https://doi.org/10.1093/infdis/143.2.238>
- Xu, S., Battaglia, L., Bao, X., Fan, H., 2013. Chloramphenicol acetyltransferase as a selection marker for chlamydial transformation. *BMC Res. Notes* 6, 377. <https://doi.org/10.1186/1756-0500-6-377>
- Yang, C., Kari, L., Lei, L., Carlson, J.H., Ma, L., Couch, C.E., Whitmire, W.M., Bock, K., Moore, I., Bonner, C., McClarty, G., Caldwell, H.D., 2020. *Chlamydia trachomatis* plasmid gene protein 3 is essential for the establishment of persistent infection and associated immunopathology. *MBio* 11, 1–12. <https://doi.org/10.1128/mBio.01902-20>
- Yang, Z., Tang, L., Shao, L., Zhang, Y., Zhang, T., Schenken, R., Valdivia, R., Zhonga, G., 2016. The chlamydia-secreted protease CPAF promotes chlamydial survival in the mouse lower genital tract. *Infect. Immun.* 84, 2697–2702. <https://doi.org/10.1128/IAI.00280-16>
- Yu, H., Karunakaran, K.P., Jiang, X., Shen, C., Andersen, P., Brunham, R.C., 2012. *Chlamydia*

- muridarum T cell antigens and adjuvants that induce protective immunity in mice. *Infect. Immun.* 80, 1510–1518. <https://doi.org/10.1128/IAI.06338-11>
- Yu, H., Lin, H., Xie, L., Tang, L., Chen, J., Zhou, Z., Ni, J., Zhong, G., 2019. *Chlamydia muridarum* induces pathology in the female upper genital tract via distinct mechanisms. *Infect. Immun.* 87. <https://doi.org/10.1128/IAI.00145-19>
- Zhong, G., 2009. Killing me softly: chlamydial use of proteolysis for evading host defenses. *Trends Microbiol.* <https://doi.org/10.1016/j.tim.2009.07.007>
- Zuck, M., Sherrid, A., Suchland, R., Ellis, T., Hybiske, K., 2016. Conservation of extrusion as an exit mechanism for *Chlamydia*. *Pathog. Dis.* 74. <https://doi.org/10.1093/femspd/ftw093>